UNIVERSITY OF SIENA

DEPARTMENT OF MEDICAL BIOTECHNOLOGIES

PhD Program in Medical Biotechnology

Section of Microbiology and Vaccines

XXIX Cycle

Host-pathogen interaction: study of Toscana virus

Supervisor:

Prof.ssa Maria Grazia Cusi

PhD student:

Claudia Gandolfo

2017

Acknowledgment

I would like to express my sincere gratitude to my supervisor Prof.ssa Maria Grazia Cusi for her continuous support to my PhD study and for conveying to me the enthusiasm for the research.

I want to thank all the people who contributed to the realization of this work, starting from Gianni, Chiara, Shibily, my friend Giulia, my love Simone and all my colleagues I had work with.

Foreword

This thesis is divided in eight sections: abstract; introduction; aim of PhD project; materials and methods; results; conclusions; bibliography and annexes.

The annexes include the related paper that has been published in relation to the thesis work and other five papers published before and during the PhD period, but not related to this work.

Contents

Abstract

The *Bunyaviridae* is a large family of RNA viruses distributed worldwide, transmitted to vertebrate hosts by arthropods (arbo-bunyaviruses) which can cause severe pathologies in humans and livestock (Léger & Lozach 2015). Due to climate changes and diffusion of competent arthropods worldwide, arbo-bunyaviruses have become pathogens of major medical importance (Briant et al. 2014). While the majority of arbo-bunyavirus infections do not lead to neuroinvasive forms of disease, they are among the most severe infectious risks to the health of the human central nervous system (CNS) (Salimi et al. 2016). Yet transmission, tropism, receptors and cell entry remain poorly characterized (Léger & Lozach 2015). Nowadays, Toscana virus (TOSV) a *Phlebovirus* belonging to the *Bunyaviridae* family, is considered an emergent pathogen associated with acute neurological disease, such as meningitis, meningoencephalitis and encephalitis, occurring in the Mediterranean countries (principally Italy, Spain, France) during the summer months (Valassina et al. 2003 a; Valassina et al. 2003 b; Charrel et al. 2005; Sanbonmatsu –Gàmez et al. 2009; Cusi et al. 2010). The cellular receptors employed by TOSV, for host-cell entry, have not been identified so far, and the paucity of information on virus host interactions during the first stages of infection may limit therapeutic and preventive approaches (Hofmann & Pohlmann 2011).

During natural transmission, TOSV is introduced into the skin through bites of infected arthropods. In this PhD project, we determined the role of dermal dendritic cells and their influence in the activation of humoral response after TOSV infection. Moreover, by *in vitro* and *in vivo* studies we investigated the role of endothelial cells in the maintenance of viremia and their involvement in viral neuroinvasion.

Finally, to better understand the mechanisms of virus-host interaction, we focused our attention on viral glycoproteins. In this field, studies on immunological response and immunological memory of subjects infected by TOSV, could be useful to identify the correlates of protection. In particular, we tried to identify the viral glycoproteins' epitopes recognized by neutralizing antibodies. By immortalization of human memory B cells (Traggiai et al. 2004) and the "high throughput method", we were able to identify specific antibodies reacting with different epitopes of the viral envelope glycoproteins.

The identification and characterization of neutralizing antibodies against TOSV envelope proteins could suggest promising viral targets for vaccine formulation.

Chapter 1

Toscana virus: an emerging *Phlebovirus*

1.1 Arbovirus: emerging viruses of serious infectious diseases

"*Vector-borne diseases are among the most complex of all infectious diseases to prevent and control*" (CDC, Division of Vector-borne Disease, 2016).

Arthropod borne virus (arbovirus) represent a global problem in the setting of public health and agriculture productivity with a worldwide distribution (Léger & Lozach, 2015). Although some arboviral infections are asymptomatic or cause mild influenza-like illness, many arboviruses are important human and veterinary pathogens causing serious illness ranging from rash and arthritis to encephalitis and hemorrhagic fever (Hollidge et al 2010).

Arboviruses are transmitted to vertebral hosts during blood feedings by mosquitoes, ticks, biting flies, mites and nits (Salimi et al. 2016). Biological transmission can be vertical, involving the passage of the virus from an infected female vector to both male and female offspring. Horizontal transmission can be venereal, from a vertically infected male directly to a female vector, as well as oral from a vector to a vertebrate host via the saliva during blood feeding (Weaver and Reisen 2010). Usually the dissemination of arbovirus is linked to the natural geographic distribution of the vector, nowday climate changing, increasing globalization and habitat modification facilitate the spreading of arboviruses to new geographic location. Consequently, the exposure of nonimmune populations to pathogenic arboviruses and outbreak episodes seem inevitable (Léger & Lozach 2015).

Arboviruses are found in various viral families, including *Togaviridae* (genus *Alphavirus*); *Bunyaviridae* (genera *Hantavirus*, *Nairovirus*,*Orthobunyavirus*, *Phlebovirus*, and *Tospovirus*); *Flaviviridae* (genus *Flavivirus*); *Rhabdoviridae* (genus *Vesiculovirus*); *Orthomyxoviridae* (genus *Thogotovirus*); *Reoviridae* (genus *Orbivirus*); and *Asfarviridae* (genus *Asfarvirus*) (Weaver and Reisen 2010).

The *Bunyaviridae* family with more than 350 viruses, is one of the largest families of RNA virus. Except for the hantaviruses, which are transmitted by rodent excreta through areosol, bunyaviruses are carried and transmitted by arthropods, primarily mosquitoes, ticks, sandflies or thrips (Schmaljohn & Elliott 2014). The *Bunyaviridae* family includes viruses with global distribution and the capacity to infect a wide range of hosts, including plants, invertebrates and vertebrates.

Our attention is focused on an emerging *Phlebovirus*, Toscana virus (TOSV), associated with acute neurological disease, such as meningitis, meningoencephalitis and encephalitis, occurringin most of the Western European and Mediterranean countries (principally Italy, Spain, France) during the summer months (Valassina et al. 2003a; Valassina et al. 2003b; Charrel et al. 2005; Sanbonmatsu –Gàmez et al. 2009; Cusi et al. 2010).

1.2 *Bunyaviridae* family

Structure and viral genes coding strategies

Bunyaviruses are enveloped viruses included in the family of *Bunyaviridae* and share spherical or pleomorphic virions with 80 to 120 nm in diameter; they display surface glycoprotein projections of 5 to 10 nm, which are embedded in a lipid bilayered envelope approximately 5 to 7 nm thick (Schmaljohn & Elliott 2014). The glycoproteins interact to form surface morphologic units that vary among viruses in different genera. Viruses in the *Phlebovirus* genus (e.g., Rift Valley fever, Punta Toro, Sandfly Fever Sicilian, Toscana and Uukuniemi viruses) have round, closely packed morphologic units (Ellis et al. 1988; Martin et al. 1985). Virions contain three single-stranded RNA genome segments designated as large (L), medium (M), and small (S), that share similar overall segment length and a generally common expression strategy for their encoded protein products (Schmaljohn & Nichol 2006). The three viral RNA segments code for a minimum of four structural proteins in a negative-sense orientation. The L and M segments have negative polarity and code for the polymerase L and a polyprotein precursor spanning the two glycoproteins and the nonstructural protein NSm, respectively. The S segment uses anambisense coding strategy: the nucleocapsid protein N is thereby translated from an mRNA that is directly transcribed from the genomic S segment, whereas the nonstructural protein NSs mRNA is transcribed from the antigenomic S segment (Figure 1) (Wuerth & Weber 2016). The genome segments further contain conserved complementary oligonucleotide sequences at their 5'- and 3'-ends (NTRs), allowing the formation of "panhandle" structures and noncovalently closed circular RNAs (Schmaljohn & Elliott 2014). This terminal nucleotide sequences, which surround a single transcriptional unit, are highly conserved among viruses within a genus, but differ from those of viruses in other genera. These structures seem to be important for transcription mechanisms and genome replication, or for genome packaging and for virion assembly (Valassina et al. 2003). The RNA segments are packaged into individual ribonucleoprotein particles (RNPs) by the nucleocapsid protein N and associated with the RNA-dependent RNA polymerase (RdRp) L, to form a single virion. The N protein thus has an important role in the protection of the viral genetic information from degradation (Léger & Lozach 2015). A major difference between bunyaviruses from other enveloped viruses is that the virions are devoid of any classical matrix or capsid protein (Spiegel et al. 2016). The matrix function is performed by the cytoplasmic tail of Gn, one of the two glycoprotein, that not only contains a Golgi localization signal but is also involved in the initiation of the budding process and the packaging of ribonucleoproteins (RNPs) into virus particles (Spiegel et al. 2016).

The S segment (1869 nucleotides) of all bunyaviruses encodes the nucleocapsid (N) protein, whose primary role is to encapsidate the viral RNA-replication products and form the ribonucleoprotein (RNP) complex. The N protein is the most abundant viral product in virions and infected cells. The S segments of most members of the genera *Orthobunyavirus*, *Tospovirus* and *Phlebovirus* also encode a non-structural protein called NSs, that shows a low conservation across the *Phlebovirus* genus compared to other viral proteins, with sequence similarities ranging only from approximately 10% to 30% (Bichaud et al. 2016; Yu et al. 2011). The NSs protein is an important virulence determinant, acting as an inhibitor of the antiviral type I IFN system of the mammalian host (Boshra et al. 2011; Weber et al. 2014 a; Weber et al. 2014 b). Hantaviruses and Nairoviruses use the negative-sense coding RNA to express a single protein N from their virion complementary-sense RNA (cRNA) (Schmaljohn& Hooper 2001). The N and NSs proteins of Orthobunyaviruses are translated from the same mRNA encoded by the S segment genome, whereas the phlebovirus and tospovirus N and NSs proteins are translated from separate mRNAs transcribed from the genomic and antigenomic strands, respectively (ambisense gene expression) (Walter & Barr 2011). In particular, a viral complementary, subgenomic mRNA corresponding to the 3' half of the viral S RNA codes for the N protein, and the viral subgenomic mRNA corresponding to the 5' half of the viral S RNA codes for the NSs proteins. Among phleboviruses, there is a short intergenic region (IR) (Valassina et al. 2003), a sequence stretch that is proposed to form an irregular double-stranded RNA (dsRNA) structure in the region between the two ORFs (Boshra et al. 2011). Formation of the RNP (ribonucleoprotein) depends on the association of viral RNA with multiple copies of the N protein so that the RNA becomes encapsidated along its entire length (Walter & Barr 2011). Whilst the primary role of the N protein is to provide structural uniformity to the RNA genome, the additional roles include interaction with membrane glycoproteins (Hepojoki et al. 2010; Overby et al. 2007; Ribeiro et al. 2009; Shi et al. 2007; Snippe et al. 2007 b) and interaction with the viral RNA-dependent RNA polymerase (RdRp) to allow access to the RNP during RNA synthesis (Walter & Barr 2011).

The M segment (ranging from 3,600 to 4,900 nucleotides) of all members of the *Bunyaviridae* family encodes, in a single open reading frame (ORF) of cRNA, a polyprotein precursor, that is processed into the glycoproteins Gn and Gc (referring to the amino-terminal or carboxy-terminal coding of the proteins) (Walter & Barr 2011). The Gn/Gc precursor is translocated, due to a signal sequence preceding Gn, from the cytoplasm into the membrane of the endoplasmic reticulum (ER), where it is cleaved into Gn and Gc components by host-cell proteases (Schmaljohn & Elliott 2014). In the ER, Gn and Gc are decorated with N-linked glycans (Kuismanen et al. 1984; Matsuoka et al. 1988) ofthe high-mannose type, which can be processed into hybrid and complex forms upon import of the two glycoproteins into the Golgi apparatus (Kuismanen et al. 1984;

Matsuoka et al. 1988; Madoff et al. 1982; Shi et al. 2005). By virtue of a retention signal, the heavily glycosylated Gn– Gc heterodimer is retained in the Golgi, where it associates with RNPs to mediate assembly and budding of mature virus particles, that are released from infected cells by exocytosis. The Gn–Gc heterodimer performs critical roles in mediating virus assembly, formation of the virus particle and attachment to new target cells (Schmaljohn & Nichol 2006). Most members of the genera *Orthobunyavirus*, *Phlebovirus* and *Tospovirus* also encode an NSm protein. The tospovirus NSm protein is translated from a separate mRNA encoded by the antigenome, whereas the orthobunyavirus and phlebovirus NSm is cleaved by cellular proteases from the same polyprotein precursor that yields the Gn and Gc proteins (Walter & Barr 2011). Bunyavirus NSm protein is thought to play a role in virus assembly (Shi et al. 2007). In contrast, the phlebovirus NSm has been shown to be non-essential (Gerrard et al. 2007), but may play accessory roles in the regulation of apoptosis (Won et al. 2007). The M segment of tospoviruses uses an ambisense coding strategy. The cRNA has a gene order of 5'-Gn-Gc-3', and the vRNA encodes NSm. There are separate, subgenomic messages for the Gc–Gn precursor and for NSm (Law et al. 1992; Kormelink et al. 1992). Hantaviruses have an M segment cRNA gene order of 5'-Gc-Gn-3' (Schmaljohn et al. 1987), while a gene order of 5'-Gn-Gc-3' was determined for the nairovirus (Marriott et al. 1992). The M segment gene order and the coding strategy varies among viruses in the Phlebovirus genus (Schmaljohn& Elliott 2014). For Rift Valley fever virus (RVFV) and Toscana virus (TOSV), the cRNA gene order of M fragment is 5'-NSm-Gn-Gc-3' (Collett et al. 1985; Valassina et al. 2003). In general, M-segment gene products have a cysteine content of approximately 4% to 7%. Positions of these residues are highly conserved in the M-segment products of related viruses, suggesting that the positions may be crucial for determining correct polypeptide folding. In the case of TOSV, there are nine sites of glycosilation (Valassina et al. 2003). The secondary structure of the proteins is also involved in immunogenicity, as indicated by the finding that neutralizing or protective epitopes are often nonlinear. All M-segment polyproteins display variable numbers of predicted transmembrane regions, and a hydrophobic sequence at the carboxy-terminus, indicative of a membrane anchor region. Therefore, the M-segment translation products of viruses in the *Bunyaviridae* family are typical class I membrane proteins, with the amino terminus exposed on the surface of the virion and the carboxy-terminus anchored in the membrane (Schmaljohn & Elliott 2014).

The L segment (range in size from about 237kD for phleboviruses, to 459 kD for nairoviruses) contains a single open reading frame (ORF) that encodes the viral polymerase. The L ORF is expressed via a viral-complementary mRNA (Valassina M. et al. 2003). All L segments of viruses of the family use conventional negative sense coding strategies (Schmaljohn & Elliott 2014). Bunyavirus L proteins perform several complex functions that together result in the generation of

RNA-replication and mRNA-transcription products from their respective viral templates (Walter & Barr 2011). Primary transcription of negative-sense vRNA to mRNA is initiated by interaction of the virion-associated polymerase (L) and the three viral RNA templates (Bouloy & Hannoun 1976; Ranki & Pettersson 1975). Members of the *Bunyaviridae* family use primers cleaved from cytoplasmic host-cell mRNAs for extension. Cleavage of the capped primers is accomplished by endonucleolytic activity associated with virions (Patterson JL. et al. 1984). Alignments with homologues of other members of the *Bunyaviridae* family indicate that L protein- associated endonuclease domain is well-conserved, containing metal-binding and catalytic lysine residues, and shows a high degree of sequence similarity to putative endonuclease motifs of L proteins from other segmented, negative-stranded RNA viruses such as arenaviruses, emaraviruses and tenuiviruses (Walter & Barr 2011).

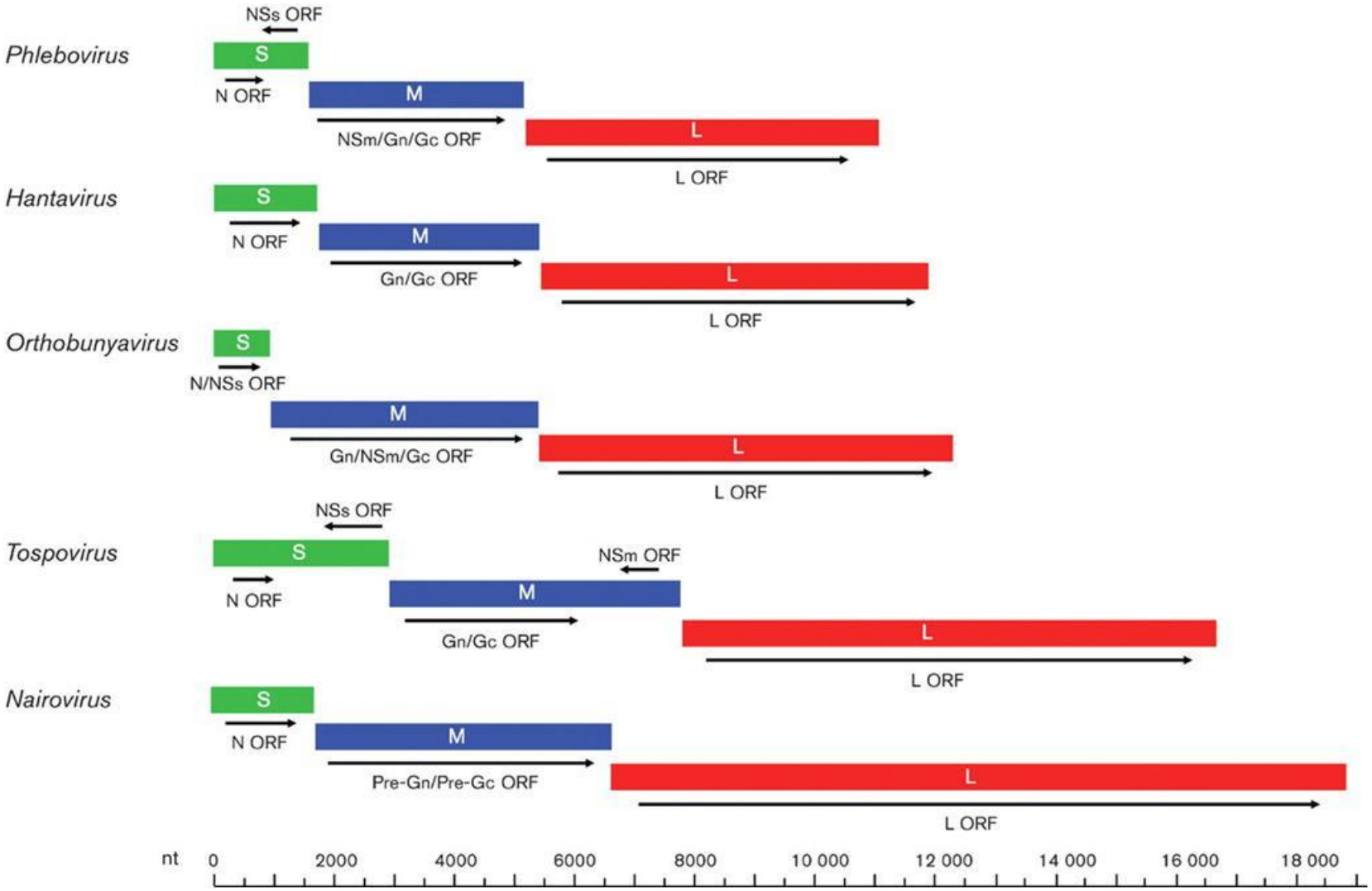

Figure 1. Schematic representation of genomic RNAs belonging to prototypic members of the five genera classified within the family *Bunyaviridae* (Walter & Barr 2011).

Replicative cycle

The *Bunyaviridae* family gains access to the host cell with a similar mechanism reported for many other enveloped viruses. The first step involves an interaction between cell surface receptors and viral glycoproteins, Gn and/or Gc. In the case of phleboviruses and hantaviruses, probably, it is possible that dimerization of both glycoproteins can promote a conformational changes leading to their activation and viral attachment (Schmaljohn & Elliott 2014). Many studies are focused on the glycoprotein Gc. It belongs to the group of class II membrane fusion proteins and seems to be involved in the primary recognition and/or fusion on cell mebrane (Valentini et al. 2008). However, there are various questions concerning the global interactions of the glycoproteins Gn and Gc at the surface of virus particles (Rusu et al. 2012). To this extent, the X-ray structure of Gn is still lacking (Léger & Lozach 2015).

After attachment, viruses of the *Phlebovirus* and *Nairovirus* genera are observed in phagocytic vacuoles (Ellis et al. 1988; Rwambo et al. 1996). After endocytosis, acidification of the endocytic vesiclesis thought to promote a conformational change in Gn and/or Gc that facilitates fusion of the viral and cellular membranes, thereby allowing the viral genome and polymerase access to the cytoplasm. For orthobunyaviruses, the Gc glycoprotein is involved in endosomic membrane fusion (Schmaljohn & Elliott 2014). After uncoating of viral genomes, the virion-associated L protein, which is an RNA-dependent RNA polymerase (RdRp), starts the transcription of negative-sense vRNA to mRNA, by interaction with the three viral ribonucleocapsids (Schmaljohn & Elliott 2014). L protein, with endonuclease activity, cleaves host cell mRNAs from 12 to 18 nucleotides to prime transcription on the virion-encapsidated RNAs (vRNAs). Transcription products are extended at their 5' ends by the capped oligoribonucleotide sequestered (Walter & Barr 2011). A result of this mRNA transcription is the presence of 5' terminal extensions of approximately 10 to 20 heterogeneous nucleotides that are not found in vRNA (Bishop et al. 1983). The capped oligonucleotides prime transcription of viral mRNA from negative-sense genes to yield mRNAs nearly as long as the vRNA template. Analysis of the L mRNAs of the hantavirus Sin Nombre virus (SNV) (Hutchinson et al. 1996) and RVFV and TOSV phleboviruses (Bird & Nichol 2007) showed they were co-terminal with the L vRNA template, suggesting L mRNA synthesis terminates by run-off of the RNA template (Schmaljohn & Elliott 2014). Analysis of M segment mRNA termination sites for three phleboviruses (RVFV, TOSV, and (SFSV) Sandfly fever Sicilian virus) showed that termination occurred immediately following a C-rich domain in the template (Bird & Nichol 2007). Detailed mapping of mRNA termination sitesfor the N and NSs mRNA of RVFV, TOSV, and SFSV phleboviruses showed that the 3’ ends of the mRNAs contained most of the intergenic sequence and indeed overlapped each other.This termination signal is also critical for packaging of all three segments L, M, and S and appear to be independent for each other (Schmaljohn & Elliott 2014).

Ambisense genes (S segments of phleboviruses and tospoviruses, and M segments of tospoviruses) are copied to yield mRNAs complementary to the 3' portion of the vRNA template. Replication involves primer-independent synthesis of complementary RNA (cRNA) from vRNA templates followed by primer-independent synthesis of progeny vRNA from cRNA templates. For viruses that use ambisense coding strategies to express nonstructural proteins (NSs of phleboviruses and tospoviruses and NSm of tospoviruses), the cRNA also serves as template for mRNA synthesis. As in primary transcription, capped, host-derived oligonucleotides prime synthesis of the ambisense mRNAs, and transcription termination occurs at a predicted hairpin structure (Schmaljohn & Hooper 2001). The 5' end of the replication product is fundamentally different from that of mRNAs, which implies that they are the products of different pathways and also the added capped host sequences on the 5' ends of viral messangers may somehow prevent encapsidation (Walter & Barr 2011).Viral polypeptides are synthesized shortly after infection, with S and L mRNAs translated on free ribosomes, and M mRNAs translated on membrane-bound ribosomes. Indeed the viral Gc and Gn envelope glycoproteins, processed through the Golgi, allow virus particles to bud from the Golgi apparatus to be released from the host cell by extocytosis, as viral particles with full infectivity (Walter & Barr 2011).

1.3 Toscana virus

Within the *Bunyaviridae* family (Table 1), *Phlebovirus* genus contains more than 80 viruses, with about half classified into nine antigenic complexes that are regarded as species, whereas 33 are considered as tentative species in the genus. The viruses of the genus *Phlebovirus* are present throughout the world and their name is associated with their principal vector, *phlebotomine sandflies*, however there are prominent exceptions, such as RVFV which is primarily associated with *Aedes* species mosquitoes and Uukuniemi virus (UUKV), which is associated with the tick *Ixodesricinus* (Schmaljohn & Elliott 2014).

Indeed, phleboviruses are currently divided into two groups, the sandfly fever group, members of which are all transmitted by mosquitoes and flies, and the tick-borne Uukeniemi-like virus group (Elliott & Brennan 2014).

Except for Toscana virus (TOSV), which has a marked tropism for central and peripheral neurological systems, sandfly fever viruses cause moderately severe disease (Alkan et al. 2013).

Sandfly fever was first clinically described by Alois Pick in 1886, after the discovery of febbrile illness among soldiers who had recently arrived in endemic regions. For this reason most of the

literature on sandfly fever has been published in military journals, where the disease was named “pappataci fever’’or ‘‘phlebotomus fever’’ or ‘‘three-day fever’’ (Alkan et al. 2013).

Among the sandfly fever viruses, the Naples serocomplex and the Sicilian serocomplex are the two main serocomplexes associated with human diseases (Charrel et al. 2012). TOSV is a serotype of the species *Sandfly fever Naples virus* that currently includes also Sabin, Tehran and Karimabad viruses. Recently, novel phleboviruses (Massilia virus, Granada virus, Punique virus) closely related to, but clearly distinct from TOSV, have been discovered and are likely to belong to this species (Alkan et al. 2013).

Toscana virus was isolated in the first time in 1971, in Monte Argentario (Grosseto province, central Italy) from two different species of sandflies, *Phlebotomus perniciosus* (*P. perniciosus*) and *Phlebotomus perfiliewi* (*P. perfiliewi*) (Verani et al. 1988; Verani et al. 1982; Verani et al. 1984). After the demonstration of its involvement in central nervous system (CNS) infection of Swedishand and US citizens returning from Portugal and Italy, respectively (Chalisher et al.1989; Ehrnst et al 1985), TOSV was isolated in the first time from a woman with aseptic meningitis, thus confirming it as a major cause of CNS infection in Central Italy (Nicoletti et al. 1991). Many case reports in travelers, clinical research and epidemiologic studies conducted around the Mediterranean regions (Italy,Spain, France, Cyprus, Portugal, Greece, Turkey, Tunisia) confirmed that TOSV has a tropism for the CNS and is a major cause of meningitis and encephalitis in countries in which its vector circulates (principlly from May to October) (Charrel et al. 2012). In particular, TOSV has been reported as the leading cause of summertime CNS infections in Italy in the 1990’s (Alkan et al. 2013).

Studies based on the L and M segments demonstrated a co-circulation of two major viral lineages in the Mediterranean areas: genotypes A and B. The geographic distribution may be different for each TOSV virus genotype. TOSV A genotype circulates in Italy, France, and Portugal; the TOSV B genotype circulates in Spain, Portugal, and France (Collao et al. 2009). Recently, a studied carried out in Croatia demonstrates the presence of new geographical lineage inside TOSV serotype, called C, that has similar homology to TOSV sequences from lineage A an B (75-82%) (Punda-Polić et al. 2012).

In the countries where TOSV is detected, it is the most prevalent virus causing meningitis during the warm season, togheter with enteroviruses and herpesviruses (Cusi et al. 2010; Charrel et al. 2012). However, asymptomatic infections and infections without CNS involvement (about 60 %) have also been described (Braito et al. 1997).

Despite the important role played by TOSV in CNS infections, it remains a neglected agent and is rarely considered by physicians, despite it should be considered an emergent pathogen (Charrel et al. 2012).

Genus	Species	Notable virus	Geographic distribution	Principal vector	Disease
Orthobunyavirus	*Acara virus*	Acara virus	SA/ NA	Mosquitoes	
	Akabane virus	Akabane virus	Africa, Asia, Australia	Mosquitoes, culicoid flies	Cattle
	Alajuela virus	Alajuela virus	NA	Mosquitoes	
	Anopheles A virus	Anopheles A virus	SA	Mosquitoes	
	Anopheles B virus	Anopheles B virus	SA	Mosquitoes	
	Bakau virus	Bakau virus	Asia	Mosquitoes	
	Batama virus	Batama virus	Africa	N.D.	
	Benevides virus	Benevides virus	SA	Mosquitoes	
	Bertioga virus	Bertioga virus	SA	N.D.	
	Bimiti virus	Bimiti virus	SA	Mosquitoes	
	Botambi virus	Botambi virus	Africa	Mosquitoes	
	Bunyamwera virus	Bunyamwera virus	Africa	Mosquitoes	Human
		Batai virus	Asia, Europe	Mosquitoes	Human
		Cache Valley virus	NA	Mosquitoes	Sheep, Cattle,
	California encephalitis virus	California encephalitis virus	NA	Mosquitoes	Human
		Inkoo virus	Europe	Mosquitoes	Human
		Jamestown Canyon virus	NA	Mosquitoes	Human
		La Crosse virus	NA	Mosquitoes	Human
		Lumbo virus	Africa	Mosquitoes	Human
		Snowshoe hare virus	NA	Mosquitoes	Human
		Tahyna virus	Europe	Mosquitoes	Human
	Capim virus	Capim virus	SA	Mosquitoes	
	Caraparu virus	Caraparu virus	SA, NA	Mosquitoes	Human
		Apeu virus	SA	Mosquitoes	Human
		Ossa virus	NA	Mosquitoes	Human
Hantavirus	*Andes virus*	Andes virus	SA	*Oligoryzomys longicaudatus*	Human
		Bermejo virus	SA	*Oligoryzomys chacoensis*	Human
		Lechiguanas virus	SA	*Oligoryzomys flavescens*	Human
		Maciel virus	SA	*Bolomys obscurus*	
		Oran virus	SA	*Oligoryzomys longicaudatus*	Human
		Pergamino virus	SA	*Akodon azarae*	
	Bayou virus	Bayou virus	NA	*Oryzomys palustris*	Human
	Black Creek Canal virus	Black Creek Canal virus	NA	*Sigmodon hispidus*	Human
	Cano Delgadito virus	Cano Delgadito virus	SA	*Sigmodon alstoni*	
	Dobrava-Belgrade virus	Dobrava virus	Europe	*Apodemus flavicollis*	Human
	El Moro Canyon virus	El Moro Canyon virus	NA	*Reithrodontomys megalotis*	
	Hantaan virus	Hantaan virus	Asia	*Apodemus agrarius coreae*	Human
	Isla Vista virus	Isla Vista virus	NA	*Microtus californicus*	
	Khabarovsk virus	Khabarovsk virus	Asia	*Microtus maximowiczii, Microtus fortis*	
	Sin Nombre virus	Blue River virus	NA	*Peromyscus leucopus*	
		Monongahela virus	NA	*Peromyscus maniculatus*	Human
		Sin Nombre virus	NA	*Peromyscus maniculatus*	Human
	Thailand virus	Thailand virus	Asia	*Bandicota indica*	
	Thottapalayam virus	Thottapalayam virus	India	*Suncus murinus*	
	Topografov virus	Topografov virus	Asia, Europe	*Lemmus sibiricus*	
	Tula virus	Tula virus	Europe	*Microtus arvalis, M. rossiaemeridionalis*	

Genus	Species	Notable virus	Geographic distribution	Principal vector	Disease
Nairovirus	*Crimean-Congo hemorrhagic fever virus*	Crimean-Congo hemorrhagic fever virus	Africa, Asia, Europe	Culicoid flies, ticks	Human
		Hazara virus	Asia	Ticks	
	Dera Ghazi Khan virus	Dera Ghazi Khan virus	Asia	Ticks	
	Dugbe virus	Dugbe virus	Africa	Ticks	Human, cattle
		Nairobi sheep disease virus (Ganjam virus)	Africa, Asia	Ticks, culicoid flies, mosquitoes	Human, cattle
	Hughes virus	Hughes virus	NA, SA	Ticks	Seabirds
	Qalyub virus	Qalyub virus		Ticks	
	Sakhalin virus	Sakhalin virus	Asia	Ticks	
	Thiafora virus	Erve virus	Europe	N.D.	Human
Phlebovirus	*Bujaru virus*	Bujaru virus	SA	N.D.	
	Candiru virus	Alenquer virus	SA	N.D.	Human
		Candiru virus	SA	N.D.	Human
	Chilibre virus	Chilibre virus		Phlebotomines	
	Frijoles virus	Frijoles virus		Phlebotomines	
	Punta Toro virus	Punta Toro virus	NA, SA	Phlebotomines	Human
	Rift Valley fever virus	Rift Valley fever virus	Africa	Mosquitoes	Human, cattle
	Salehabad virus	Salehabad virus	Asia	Phlebotomines	
	Sandfly fever Naples virus	Sandfly fever Naples virus	Europe, Africa, Asia	Phlebotomines	Human
		Sandfly fever Sicilian virus	Europe	Phlebotomines	Human
		Toscana virus	Europe	Phlebotomines	Human
	Uukuniemi virus	Uukuniemi virus	Europe	Ticks	Seabirds
Tospovirus	*Groundnut bud necrosis virus*	Groundnut bud necrosis virus (Peanut bud necrosis virus)	Asia	*Frankliniella schultzei, Thrips palmi*	Plant
	Groundnut ringspot virus	Groundnut ringspot virus	SA, Africa	*F. occidentalis, F. schultzei, F. gemina*	Plant
	Groundnut yellow spot virus	Groundnut yellow spot virus (Peanut yellow spot virus)	Asia	N.D.	
	Impatiens necrotic spot virus	Impatiens necrotic spot virus	NA, Europe	*F. occidentalis*	Plant
	Tomato spotted wilt virus	Tomato spotted wilt virus	Worldwide	*F. bispinosa, F. cephalica F. gemina, F. fusca, F. intonsa, F. occidentalis, F. schultzei, F. setosus, T. tabaci*	Plant
	Watermelon silver mottle virus	Watermelon silver mottle virus	Asia	*T. palmi*	Plant
	Zucchini lethal chlorosis virus	Zucchini lethal chlorosis virus	SA	*F. zucchini*	Plant

Table 1. Species in the family *Bunyaviridae* (Adapted from Bunyaviridae. In Fields Virology, 6th Edition. Vol 1)

Epidemiology and viral vectors

Increase globalization, climate changes, intensive deforestation, and overpopulation induce several modification in the geographic distribution of arbo-bunyavirus vectors, favoring the exposure of nonimmune populations to these pathogenic viruses (Léger & Lozach 2015). Arbo-bunyaviruses have provided many examples of new emerging viruses, like Schmallenberg virus (SBV) which emerged in Europe in 2011, and some known bunyaviruses like Rift Valley Fever Virus (RVFV), Crimean-Congo hemorrhagic fever (CCHF) viruses, that continue to emerge in new geographical locations (Elliott & Brennan 2014).

In this setting, Toscana Virus (TOSV) represents an important emerging pathogen in Europe and Northen Africa (Charrel et al. 2012). TOSV is the major cause of aseptic meningitis (95%) and meningoencephalitis (4.5%) and influenza-like illness during the summer season (Hemmersbach-Miller et al. 2004; Sanbonmatsu –Gàmez et al. 2009), especially in July, August and September when the maximum activity of the sandfly vector occurs. TOSV is transmitted to humans by *Phlebotomus*, *Sergentomyia* and *Lutzomya* genera, in particular by *Phlebotomus perniciosus* and *Phlebotomus perfiliewi* (Cusi et al. 2010). Like other arbo-bunyavirus, diffusion of TOSV is evolving with thegeographic distribution of its vector, leading to a higher pathogenicity in non exposed populations, outside areas of current prevalence (Mediterranean Basin) (Collao et al. 2009). TOSV was detected both in male and in female pools of phlebotomine sandflies. The detection of virus in pools of male flies suggests vertical and/or sexual transmission of TOSV among phlebotomine sandflies. Transovarial transmission of TOSV in sandflies has been demonstrated in laboratory experiment and by virus isolation from male phlebotomine flies. Venereal transmission from infected male to uninfected female has also been demonstrated (Charrel et al. 2012). The reservoir of TOSV is most likely the vector, indeed its animal reservoir has not yet been identified although serological studied have found specific antibodies against TOSV in some animal species (Navarro-Marí et al. 2011), indicating that it can also infect these animals. Although a number of phleboviruses have been isolated from the blood of sick persons and from wild animals, the role of vertebrates in the maintenance of the transmission cycle of these viruses remains unclear. Transient and low-level viremia is present after phlebovirus infection in humans and in susceptible laboratory animals (Bartelloni et al. 1976; Cusi et al. 2005). Moreover, sandflies must ingest a large quantity of virus to become infected (Ciufolini et al. 1985).

TOSV presence is being investigated in several European countries on the Mediterranean basin, including Italy, France, Spain, Portugal, Cyprus (Cusi et al.2010), Greece, North Africa (Tunisia, Algeria and Morocco), Turkey and Kosovo (Charrel et al. 2012). The A genotype is circulating mainly in Italy, but also in France and Portugal; the TOSV B genotype is circulating in Spain, France and Portugal, probably related to the vector geographic distribution. Furthermore, a novel

genotype, tentatively called as genotype C, is identified in patients from Croatia (Punda-Polić et al. 2012). In Italy, clinical and epidemiological studies have demonstrated human infection by TOSV in Tuscany (Braito et al. 1998; Nicoletti et al. 1991; Terrosi et al. 2009; Valassina et al. 2003; Cusi et al. 2010; Valassina et al.1996), Marches (Nicoletti et al. 1991), Sicily (Amodio et al. 2012; Calamusa et al. 2012; Colomba et al. 2012; Valassina et al. 1996), Emilia Romagna (Portolani et al. 2002; Vocale et al. 2012), Piedmont (Valassina et al. 2003), Umbria (Baldelli et al. 2004; Francisci et al. 2003),Campania (Di Nicuolo et al. 2005), Sardinia (Venturi et al. 2007), Elba island (Gabriel et al. 2010; Sonderegger et al. 2009), and Calabria (Greco et al. 2012). Generally, people living in endemic areas have an asymptomatic infection, instead, travelers often develop the disease. In this setting, surveillance studies should be improved in order to prevent the spread of TOSV in new areas (Cusi et al. 2011). Despite the important role played by TOSV in CNS infections, it remains aneglected agent and is rarely considered by physicians in the diagnosis of CNS infections and febrile illness during summer months (Charrel et al. 2012).

Clinical manifestations

TOSV is the only sandfly-transmitted phlebovirus with neurotropic activity. It was recognized as a causative agent of neurological disease in humans only in 1983, when it was isolated for the first time from a young woman with lymphocytic meningitis (Nicoletti et al. 1991). The most documented clinical form of TOSV infection consists of neuro-invasive cases which are generally hospitalized (Charrel et al. 2012).

A wider clinical spectrum of TOSV-associated diseases is now documented, including asymptomatic or mild disease without CNS involvement, such as febrile erythema or influenza-like illness, as well as unusual clinical manifestations or severe sequelae of the neurological infection (Bartels et al. 2011; Brisbarre et al. 2011; Serata et al. 2011). The clinical manifestations of meningitis from TOSV is quite similar to that caused by other viral agents; however Verani *et al*. (2015), found that levels of anti-inflammatory and antiviral mediators were significantly higher in cerebro spinal fluid (CSF) of TOSV-infected patients as compared to patients with other infectious or noninfectious neurological diseases. In any case, it is not possible to define a characteristic symptomatology for neurological infections caused by TOSV (Dionisio et al. 2003). Generally, incubation period is influenced by the virus load, ranging from few days to 2 weeks. Disease onset is intense with headache (100%, 18 h–5 days), fever (76%–97%), nausea and vomiting (67%–88%), and myalgias (18%). Physical examination may show neck rigidity (53%–95%), Kernig signs (87%), poor levels of consciousness (12%), tremors (2.6%), paresis (1.7%), nystagmus (5.2%). In most

cases CSF contained more than 5–10 cells with normoglycorrachia and normoproteinorrachia (Charrel et al. 2012). It is also possible to have abnormal CT or MRI (Rinaldi et al. 2011). Blood samples may show leukocytosis (29%) or leukopenia (6%) (Charrel et al. 2005). The mean duration of the disease is 7 days, and the outcome is usually favorable (Charrel et al. 2012). Although TOSV infection consists of a mild disease with a favorable outcome in most cases, an outcome with severe complications is possible, but only a small number of severe cases have been reported in the literature. Two young brothers and a sister living in Umbria experienced TOSV infection in the form of severe meningoencephalitis with stiff neck, deep coma, maculopapular rash, diffuse lymphadenopathy, hepatosplenomegaly, renal involvement, skin rash with lamellar desquamation, a tendency to bleed, and diffuse intravascular coagulopathy. CNS manifestations occurred after 3 weeks of fever (Baldelli et al. 2004). One case of meningitis, complicated by abducens nerve palsy, was reported (Schwarz et al. 1995). Two cases of ischemic complication followed diagnosis of TOSV infection were reported (Klugman et al. 2009). A case of deafness as a sequela of TOSV infection was also described (Martínez-García et al. 2008). A case in which lymphadenopathy was the main clinical finding at the presentation of symptoms and preceded the onset of meningitis was documented (Rinaldi et al. 2011). Recently a case of psychiatric sequelae following encephalitis due to TOSV infection was reported in a patient without personal or family psychiatric history (Serata et al. 2011). Severe and lethal encephalitis was also reported (Bartels & Boni 2012).

It was also postulated a correlation between nucleotide sequence of M segment of TOSV and pathological manifestation. Valentini *et al.* (2008) analyzed the genetic variability of TOSV M segment in several strains isolated from patients with meningitis from 1998 to 2004 in the region of Tuscany. Results revealed some changes in amino acids, particularly in the Gc protein, that is probably involved in recognition and binding to the cell receptor. But a strict correlation between the severity of the pathology with a peculiar nucleotide sequence was not found. In this setting, it is necessary to further investigate on other possible viral features correlated to TOSV neurovilunce.

Antigenic determinants: role of glycoproteins

Phleboviruses and other bunyaviruses use their envelope proteins, Gn and Gc, for entry into target cells and for assembly progeny particles in infected cells. Once inside the target cell, exposure to endosomal low pH induces Gc-driven fusion of the viral envelope and the vesicle membranes, leading the release of viral genome in the cytoplasm where the replication cycle can

starts. Moreover, Gn and Gc facilitate also virion incorporation of the viral genome via their intracellular domains. These glycoproteins represent a target for neutralizing antibodies and possible antigenic determinants. Despite their important role in bunyavirus entry and release, biogenesis and biological activities of Gn and Gc proteins are incompletely understood (Spiegel et al. 2016). Usually, the neutralizing activity is a property of the anti Gn-Gc antibodies, as shown for other viruses of this family like RVFV, La Crosse virus (LACV) and Hantaan virus (HTNV) (Saluzzo et al. 1989a,b; Gonzalez-Scarano et al. 1982; Grady & Kinch 1985; Arikawa et al. 1989). In the case of TOSV, previous studies focused the attention on the identification of the immunodominant antigen in the human immune response. Results showed the N protein as the immunodominant antigent, with a partial neutralizing activity of anti-N antibodies (Cusi et al. 2001) while the anti-glycoprotein response is short lived (Cusi et al. 2002; Di Bonito et al. 2002). This suggest an important role of N in human infection as demonstrated by the strong cytotoxic T cell response specific for N protein, found in patients affected by virus-associated meningitis (Cusi et al. 2002).

However, it was observed that a combination of recombinant TOSV structural protein N-Gc, used as vaccine, induces a specific and protective immune response upon viral infection in 100% of inoculated mice (Gori Savellini et al. 2008).

The mechanisms of protection against TOSV natural infection are not known, however it could be supposed that a virus-neutralizing antibody response against viral glycoproteins would be useful to block the first stages of infection. For these reason, we decided to focus our attention not only on N protein, but also on both viral glycoproteins and to identify possible conserved epitopes target by using human monoclonal antibodies.

There are different methods to isolate monoclonal antibody: from immune individuals, from immunized mice or from synthetic antibody libraries. The isolation of antibodies from immune donors offer the advantage that the human immune system is exposed to all the relevant antigens displayed by an infecting agent that consequently activated a broad response to most, if not all, these epitopes (Lanzavecchia et al. 2007). This approach is based on the isolation of specific monoclonal antibodies produced by memory B cells obtained from frozen PBMCs of patient infected by the pathogen. Antigen-specific memory B cells are immortalized by EBV and TLR9 agonist CpG (Traggiai et al. 2004) (Figure 3). These B cell clones, once activated, start the production of pathogen-specific antibodies that are released in the supernatant and analyzed by the use of automated liquid handling devices that allow high throughput screening of these antibodies, using functional assays such as binding and neutralization assay (Corti et al. 2011). The analysis of the human immune response and the isolation of neutralizing antibodies offer a good solution to study pathogen complexity and variability (Lanzavecchia et al. 2007), as the case of glycoproteins, possibly modified by antigenic drift events.

This approach has been employed to isolate specific monoclonal antibodies against different viruses, such as SARS coronavirus (Rockx et al. 2008), H5N1 (Simmons et al. 2007), HIV-1 (Corti D et al. 2010), human Cytomegalovirus (Macagno et al. 2010), Norovirus (Lindesmith et al. 2012) and Dengue virus (Beltramello et al. 2010).

In this way, it is possible to screen antibody repertoire of patients infected with TOSV in order to isolate finally potent and neutralizing monoclonal antibodies against conserved epitopes of the glycoproteins.

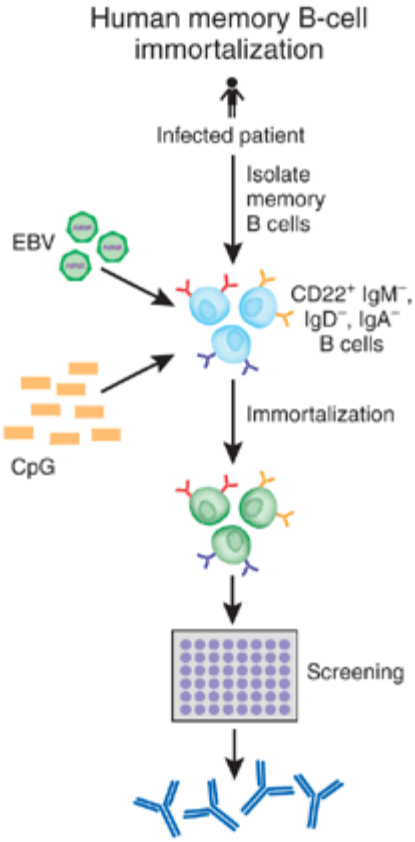

Figure 3. Memory B-cell immortalization. Memory B cells ($CD22^+$ IgM^-, IgD^-, IgA^-) are isolated from peripheral blood mononuclear cells (PBMCs). They are immortalized by EBV in the presence of a CpG. The culture supernatants are then screened directly for specific antibodies. Positive cultures are further cloned by limiting dilution and fully human mAbs can then be produced from the cloned B cells (Adapted from Marasco & Sui 2007).

Toscana virus infection: serological and molecular detection

Vaccine against TOSV is not yet available, although a study carried out on mouse model, reported that a combination of recombinant TOSV proteins, N-Gc protected 100% of mice infected with a lethal, neurovirulent strain of TOSV (Gori Savellini et al. 2008).

Both molecular detection of viral genome and seroconversion are important information to have a complete view of the state of the patient. Cusi (2011) gives a complete overview of the current molecular and serological techniques routinely employed in diagnostic laboratories. The serological investigation, by detection of IgG and IgM are important to understand the stage of infection when low level viremia is present. These analysis have been performed using ELISA, immunoflorescence (IFA) and/or neutralization tests. An ELISA test, based on recombinant nucleoprotein gene, was developed and is now commercialized (Soldateschi et al. 1999). However, cross-reactivity exists between phleboviruses. This is particularly critical among viruses that are antigenically related to TOSV, such as the other members of the *Sandfly fever Naples virus* species (Tehran, Naples, Sabin) and the viruses for which close relationships have been demonstrated, such as Massilia, Punique and Granada viruses (Charrel et al. 2009; Collao et al. 2010; Zhioua et al. 2010).

Direct diagnosis can be performed with virus isolation or molecular detection of the viral genome from cerebrospinal fluid samples and blood samples (Ergünay et al. 2011). The isolation of the virus from susceptible cell cultures is possible but not routinely used due to the long time required (Cusi &Gori Savellini 2011). The first attempts to isolate the virus from biological samples were carried out *in vivo*, by intracranial injection of specimens in mice (Gonzales-Scarano & Nathanson 1990). Successively, TOSV has been grown in cell culture where the virus can efficiently replicate. Numerous mammalian cells line, such as Vero, BHK-21, CV-1, SW13, are good substrates for TOSV replication with lytic cytopathic effect within a few days (Verani et al. 1984; Karabatsos et al. 1985). But, during the acute phase of the infection, there is the necessity of a tempestive diagnosis. For this reason, nucleic acids amplification techniques, linked to their rapidity and sensitivity, are the methods of choice to diagnose viral meningitis. The Real-time PCR is considered the best choice to perform a rapid and correct diagnosis, since it is less time-consuming and it reduces the risk of contamination (Cusi & Gori Savellini 2011). In the first time, the target of Real-time PCR amplification was the 3’ final portion of N gene, in the S segment (Pérez-Ruiz et al.2007), subsequently, this method was adapted and improved with more specific couples of primers and probe against another conserved portion of N gene (Weidmann et al. 2008).

Due to the improvement of the techniques used for TOSV diagnosis and to a better awareness, a higher number of TOSV infections has been recorded, solving many undiagnosed cases of summer meningitis or encephalitis in the Mediterranean countries (Charrel et al. 2012).

Chapter 2

Phlebovirus- host cell interactions

2.1 From arthropod vector to mammalian host

In contrast to vertebrate hosts, there is no clear evidence of pathology or lethal outcomes following arbo-bunyaviruses infection in arthropod hosts, that is usually asymptomatic, predominantly persistent and necessary for efficient propagation to other hosts (Léger & Lozach 2015). Complete lifecycle of an arbo-bunyavirus consists of two essential interdependent phases: the transmission cycle between, and within, non-vertebrate and vertebrate host populations; and the productive cycle in the host cells. The arthropod-to-mammal switch, results in important changes like molecular composition of glycan motifs, composition of lipid membrane and the capacity to survive at different temperatures (Léger & Lozach 2015). These modifications allow arbo-bunyaviruses to cause a productive infection also in the mammalian host. The viral particles transmitted by arthropods to mammals are covered by a glycan coat principally composed of mannose residues (Schiller et al. 2013). After mammalian host infection, arbo-bunyaviruses lose their high mannose coat to gain a more complex glycosylation, with the attachment of N-linked oligosaccharides during the steps of maturation through the ER and the Golgi apparatus (Butler et al. 2014). These modifications promote also the correct folding of viral glycoproteins, that once on the surface of the mature virion, influence the interaction with mammalian receptors in a positive way, mediating virus binding with cell surface lectin receptors and allowing the escape from the host humoral immune response, thus influencing viral replication and infectivity (Vigerust & Shepherd 2007).

There are substantial differences between insect and mammalian cells in terms of fatty acid transport, metabolism and lipid composition (Canavoso et al. 2001; Stanley-Samuelson et al. 1988). It has been postulated that lipids derived from arthropod cells, contribute to a stronger protection of the RNPs to the particle envelope, and indirectly, a higher infectivity of the virions compared with those originating from mammalian cells (Léger & Lozach 2015).

Also, the capacity to infect hosts with different body temperatures is another point to consider. Arbo-bunyaviruses are able to infect both arthropods, whose body temperature is the same of the environment, and mammalian cells, whose temperature is around 37°C, in a productive way, with functional proteins correctly folded (Léger & Lozach 2015).

Whit all these changes, arbo-bunyaviruses, once in mammalian host, are able to positively infect and replicate, promoting subsequent progression of the disease.

2.2 Arbovirus infection: first stages of pathogenesis

Little is known about the first stages of pathogenesis; in particular the role of the skin and its components during the early stage of infection must be clarified.

Linked to its structure, the skin constitutes a physical and immune barrier. It is composed of the epidermis, attached to a basement membrane, under which the dermis and a subcutaneous fatty region are present (Heath & Carbone 2013 a).The epidermis and dermis are, in turn, populated by a variety of cell types that together form a first line of defense against invading pathogens: keratinocytes in the upper layer of epidermidis, the resident fibroblasts and more specific immune cells: macrophages and dendritic cells (DCs) in the dermis (Bernard et al. 2015). Beneath the dermis, the lowest layer consists of adipocytes surrounded by fibroblasts, nerves and blood vessels (Briant et al. 2014). All these immuno-cells, in the presence of a pathogen, are activated through membrane receptors, the Toll-like receptors (Toll-like receptors or TLRs) and other recognition receptors (PRR: Pattern Recognition Receptors), and start the secretion of inflammatory cytokines, chemokines and antimicrobial peptides. Together all these cells coordinate the human defense, starting the response against microbial injury (Nestle et al. 2009).

During the natural transmission, arboviruses are introduced into the skin through bites, by the blood meal of an infected female arthropod. They are released from the arthropod saliva directly into the dermis layer and then spread in blood vessels, capillary beds, and lymphatics (Léger & Lozach 2015). Arthropod saliva components have the capacity to modulate skin cell responses by enhancing initial viral replication, thus allowing the establishment of systemic infection (Briant et al. 2014). Once in the skin, arboviruses can infect different subsets of immune cells or vessels endothelial cells, thus with an initial phase of replication, viruses can jump into the blood vessels or lymphatics (Léger & Lozach 2015) and reach visceral organs, including the spleen and the kidney (Salimi et al. 2016). This was also observed during TOSV infection in animal model; with subcutaneous viral injection in mice, virus, after a first replication in the endothelial cells, could reach the spleen (Gori Savellini et al. 2008) as a probably location for secondary viral replication, because of its vascular structure. Afterwards, the virus can reach CNS by different ways analysed in this thesis. In general, shortly after viremia, arboviruses enter the CNS via several mechanisms, depending on host and viral factors (Salimi et al. 2016).

2.3 First line of defence: dendritic cells and DC-SIGN

Dendritic cells and viral infections

DCs play a major role in immune defense against viral infections via innate and adaptive immune mechanisms since the activation state of the DC determines the type of immune response that gets triggered (Cunningham et al. 2010). DCs are a rare population of cells comprising only about 1% of lymphoid cells. They form an extensive interweaving network under epithelial surfaces that are the key sites of pathogen entry to the host (Belz et al. 2009). DCs are crucial participants in maintaining immune surveillance of the periphery and initiating primary immune responses within the draining lymph nodes (Johnson & Jackson 2014).

DCs can perform multiple immunogenic tasks such as the cross-presentation of exogenous antigens in the context of MHC class I molecules to CD8 + T lymphocytes, in addition to presentation of MHC class II-restricted peptides; the expression of special co-stimulatory surface molecules to induce the priming of naïve T cells and the capacity to polarize naïve T cells to various Th phenotypes (Freer & Matteucci 2009). Due to different origin, tissue distribution, and expression of surface receptors, DCs have been divided into conventional (cDCs) or myeloid (mDCs) and plasmacytoid DCs (pDCs); they differ in immunomodulatory functions and preferentially react to distinct microbial stimuli. cDCs, $CD11c^{+}$ MHC class II^{+}, include migratory cells and lymphoid-resident cells that cooperate and are essential to one another to turn on a T cell response (Freer & Matteucci 2009). cDCs are found predominantly in tissues such as the skin and mucosal surfaces, where they enter in contact with environment pathogens (Johnson &Jackson 2014). Indeed, cDCs are mostly devoted to taking up antigen in their steady state and presenting it to T cells in their activated or mature state. In this setting, early antigen presentation by lymphoid-resident DCs initiates activation and trapping of antigen-specific T lymphocytes in the draining lymph node, while migratory DCs interact with such T cells to induce clonal expansion (Allenspach et al. 2008). Once infected, cDCs can recognize cytoplasmic viral RNA by endosomal Toll-like receptor (TLR)-3, binding double-stranded RNA (Alexopoulou et al. 2001), and cytoplasmic receptors such as retinoic-acid-inducible protein I (RIG-I) and melanoma-differentiation-associated gene 5 (MDA5) and start type I IFN production (Kato et al. 2005; Kato et al. 2006; Pichlmair et al. 2006). The second less abundant subset of DCs are the plasmacitoid dendritic cells (pDCs). pDCs, $CD11c^{low}$ MHC class II^{low}, are the first line of defense against viral and intracellular parasite replication: they express endosomal nucleic-acid sensing TLR-7, TLR-8, and TLR-9, that, once triggered, are mostly responsible for the release of type I IFN by these cells (Heil et al. 2004). Therefore, pDCs are also able to quickly prime CD8+ cytotoxic activity upon interaction with viruses (Di Pucchio et al. 2008). pDCs accumulate mainly in the blood and

lymphoid tissue and are thought to enter lymph nodes via postcapillary high endothelial venules (Johnson & Jackson 2014).

With their maturation, DCs acquired the ability to migrate to lymph nodes, as well as to express co-stimulatory molecules responsible for activating naïve T cells in germinal centers. Upon maturation, DCs become professional antigen-presenting cells, with an altered chemokine receptor repertoire, an increased motility and responsiveness to lymph tropic chemokines (Sallusto et al. 1998). A large variety of pro-inflammatory stimuli can induce maturation, however, most stimuli appear to act through tumour necrosis factor-α (TNF-α) and IL-1β (Enk et al. 1992; Enk et al. 1993; Cumberbatch et al. 1995). Maturation also leads to the expression of different surface molecules; one of the best markers for human DC maturation is CD83, which is highly expressed by mature DCs both in a membrane-bound and in a soluble secreted form (Freer & Matteucci 2009).

DC-SIGN as a receptor for Phlebovirus

Recent evidence indicates that phleboviruses, including TOSV, are capable to infect cells that express DC-SIGN, a type II transmembrane protein (Lozach et al. 2011). Due to its highly restricted expression, DC-SIGN is considered a dendritic cell -specific phenotypic marker (Urban & Anderluh 2010). DC-SIGN is abundantly expressed on immature DCs (iDCs); in particular it is present on dermal DCs, interstitial DCs, a subset of blood DCs (Urban & Anderluh 2010). It is also found, albeit down-regulated, on mature or activated DCs (mDCs), in lymphoid tissues such as lymph nodes, tonsils and spleen (Geijtenbeek et al. 2000), in macrophages and Houfbauer cells in the placenta (Soilleux et al. 2001) and macrophages in the lungs (Soilleux et al. 2002). However, it is not expressed on certain DCs-types such as follicular DCs or on skin-resident Langerhans DCs (Urban & Anderluh 2010). The lectin DC-SIGN (CD209) is a type II transmembrane protein with an N-terminal cytoplasmic domain, with recycling and internalization motifs, followed by a neckdomain and a C-terminal carbohydrate recognition domain (CRD). DC-SIGN is an antigen capturing receptor (Figure 4) (Zhang et al. 2014). The lectin domain facilitates binding to mannose and fucose containing ligands, as those of phlebovirus Gn and/or Gc glycoproteins, in a calcium-dependent (C-type) way. High-avidity ligand-binding depends on DC-SIGN tetramerization, which is catalyzed by the neck domain. Clustering of DC-SIGN is thought to improve binding to viral particles with multivalent binding sites, by providing high-avidity binding platforms, as show by Lozach *et al.* (2011) for the Uukuniemi virus (UUKV). Bound ligands can be internalized due to specific sequences in the DC-SIGN cytoplasmic domain, a di-leucine (LL) motif which triggers its

endocytosis (Hofmann & Pohlmann 2011). DC-SIGN contains an additional tri-acidic cluster (EEE or DDD) in its cytoplasmic tail, important for targeting to proteolytic compartments (Urban & Anderluh 2010). Indeed, a dual role has been indicated for acidic motif as a sorting signal in the secretory pathway and a lysosomal targeting signal in the endocytic pathway (Azad et al. 2008). Accordingly, DC-SIGN-ligand complexes are targeted to late endosomal or lysosomal compartments (Mahnke et al. 2000). In MHC class II-positive late endosomes, DC-SIGN-ligand complexes are processed for MHC class II presentation to T cells. Otherwise, DC-SIGN-ligand complexes are targeted to classical early endosome, where low pH induces release of virions from DC-SIGN. Upon release of ligand, DC-SIGN is likely recycled to the cell surface, while virions are trafficked into late endosomes/lysosomes (Mahnke et al. 2000). The increased acidification of late endosomes triggers viral fusion of Gc glycoprotein with the endosomal membrane. As a consequence, viral proteins and nucleic acids are released into the host-cell cytoplasm to start the replicative cycle (Hofmann & Pohlmann 2011).

Evidence from literature underlines the role of DC-SIGN as antigen receptor in many phatogenic conditions. It can capture antigens for processing and presentation, such as those for human immunodeficiency virus type 1 (HIV-1) (Geijtenbeek et al. 2000; Auwerx et al. 2009; Bashirova et al. 2001), hepatitis C virus (HCV) (Li et al. 2009; Gardner et al. 2003; Pohlmann et al. 2003; Lai et al. 2006), Dengue virus (Tassaneetrithep et al. 2003), Ebola virus (Gramberg et al. 2008), SARS-CoV (Marzi et al. 2004; Chan et al. 2006), Lassa virus (Shimojima et al. 2012), *Mycobacterium tuberculosis* (Tailleuxet al. 2003), *Helicobacter pylori* (Bergman et al. 2004), *Neisseria meningitidis* (Steeghs et al. 2006), *Candida albicans*(Cambi et al. 2003), *Aspergillus fumigatus* (Serrano-Gomez et al. 2004), *Schistosoma mansoni* (Meyer et al. 2005) and *Leishmania* parasites (Colmenareset al. 2002).

It is also observed that DC-SIGN is involved in the process of DCs migration across endothelium. It mediates adhesion and rolling of DCs on primary human umbilical vein endothelial cells (HUVEC) through Le^{Y}antigen expressed on ICAM-2 (Garcia-Vallejo et al. 2008).

The expression of this C type lectin on immature dermal DCs, that are present in the anatomical site of virus transmission, suggest a concrete role of these cells as target cells in the pathogenesis of arbo-bunyaviruses infections (Varani et al. 2015). In addition, DC-SIGN expression was sufficient to render cell lines susceptible to phlebovirus entry (Lozach et al. 2011; Hofmann et al. 2013). There are various examples of arbo-bunyaviruses that recognize DC-SIGN; among them RVFV, UUKV, Punta Toro (PTV) and TOSV (Lozach et al. 2011) but also LACV and severe fever with thrombocytopenia syndrome virus (SFTSV) (Hofmann et al. 2013). For all of these reasons, interactions between DC-SIGN and phleboviruses are thought to be one on the first steps during phlebovirus pathogenesis (Léger & Lozach 2015).

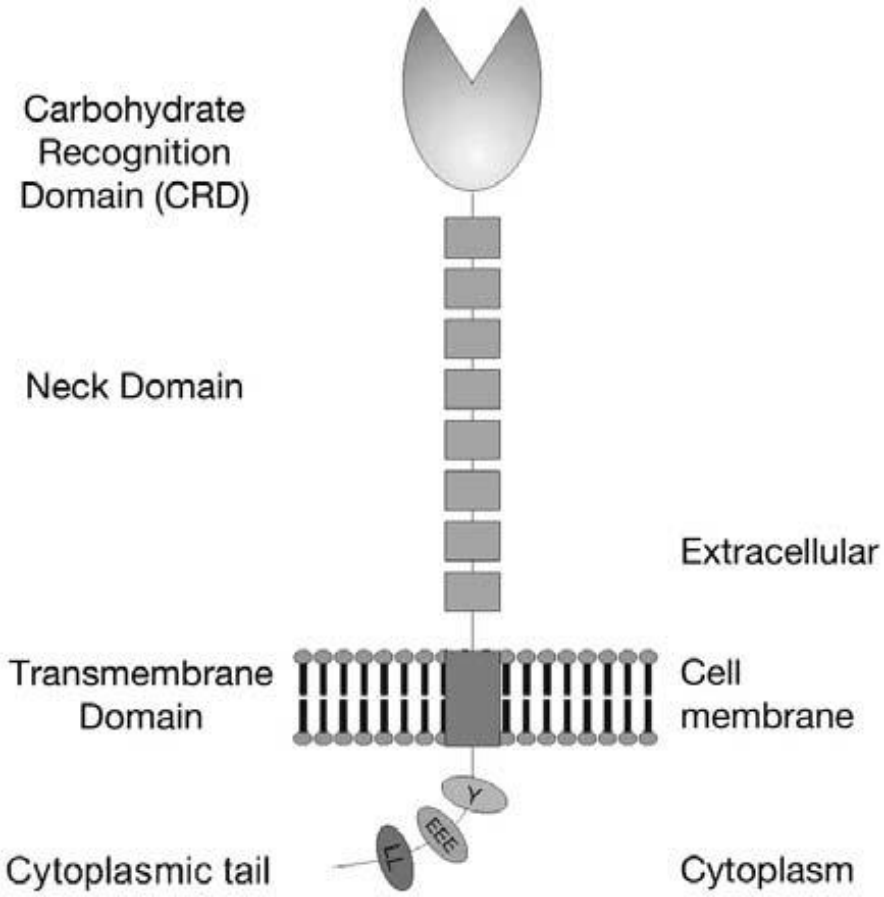

Figure 4. Structure of DC-SIGN. The C-type lectins DC-SIGN is type II transmembrane proteins. Its cytoplasmic tails contain internalization signals (di-leucine, tyrosine, and tri-acidic) which are involved in internalization of the lectin. The extracellular domain is composed of a carbohydrate recognition domain (CRD) and a neck domain implicated in the oligomerization of these lectins. (Lozach et al. 2007).

2.4 Spreading through the host: role of endothelial cells and L-SIGN

Activation of Endothelium

Blood vessels and capillary beds are spread throughout the dermis. Draining lymphatic vessels in the dermis cross the deeper layers of the skin to eventually access the lymph nodes (Heath & Carbone 2013b).

Afferent lymphatic capillaries in peripheral tissue are composed of interdigitating endothelial cells, with junctions stabilized by the adherens junction protein, vascular endothelial cadherin (VE-cadherin), the tight junction-associated proteins such as occludin, claudin-5, zonula occludens- 1 (ZO-1), the junctional adhesion molecule-A (JAM-A), the endothelial cell selective adhesion molecule (ESAM), and the endothelial cell adhesion molecule CD31 (Baluk et al. 2007). These molecules are differentially distributed at the base and tops of distinctive structures that form discontinuous endothelial junctions in the initial lymphatic vessels and continuous junctions in the larger collecting vessels (Johnson & Jackson 2014).

Detection of a microbial infection or tissue damage by the host is one of the earliest events in the inflammatory response mediated by dendritic cells, macrophages, mast cells and vascular endothelial cells (Staros et al. 2005; Arancibia et al. 2007). Exposure of these cells to stimuli such as pathogen-associated molecular pattern (PAMP) induces secretion of pro-inflammatory cytokines, including interleukin-1β (IL-1β), IL-6, and tumour necrosis factor-α (TNF-α) and a range of different chemokines (Takeuchi et al. 2010; McDonald et al. 2010). In response to the release of these inflammatory mediators, the adjacent vascular endothelium becomes activated, thus inducing profound changes in gene expression, structural organization and functions that allow the endothelial cells to participate in various inflammatory processes. Upon activation, the endothelial cells present a new profile of chemokine and colony stimulating factors secretion, in parallel with the change in chemokine receptor repertoire expressed by DCs upon maturation (Johnson & Jackson 2014). It has been observed the up-regulation of adhesion molecules on the luminal surface including VCAM-1, ICAM-1 and ICAM-2, that support increased DC transmigration and transit to the draining lymph nodes, through interactions with their DC-expressed integrin ligands (Johnson et al. 2006; Teoh et al. 2009). Other molecules are implicated in the endothelial cells activation, such as the adhesion molecules L1 (Maddaluno t al. 2009), JAM-A (Cera et al. 2004), ALCAM (Iolyeva et al. 2013), CD31 and CD99 (Torzicky et al. 2012); the TNF receptor family member CD137 (TNFRSF9) (Teijeira et al. 2012); the lipid mediator sphinosine-1-phosphate (Czeloth et al. 2005; Pham et al. 2010); podoplanin (Acton et al. 2012); and semaphorin 3A (Takamatsu et al. 2010).

Role of L-SIGN in Phlebovirus infection

L-SIGN, also known as CD209L, CD299 or DC-SIGNR, is a type II membrane protein that binds high mannose *N*-glycans, including many viral glycoproteins (Pustylnikov et al. 2014; , Mitchell et al. 2001), through its C-terminal carbohydrate recognition domain (CRD) (Guo et al. 2004). The gene coding for L-SIGN is located on chromosome 19p13.3 and forms a lectin gene cluster containing DC-SIGN, DC-SIGNR, CD23 and LSECtin (Soilleux et al. 2000; Liu et al. 2004). L-SIGN shares 77% amino acid sequence and 73% nucleotide sequence homology with DC-SIGN (Zhang et al. 2016). It is expressed on the endothelial cells of the lymph node sinuses (Engering et al 2004), liver sinus endothelial cells (Pohlmann et al. 2001; Engering et al 2004), capillary endothelial cells of the placenta (Pohlmann et al. 2001), pulmonary endothelial cells (Chan et al. 2006, Jeffers et al. 2004) and the endothelium of the gastrointestinal tract (Jameson et al. 2002).The N-terminal tail of DC-SIGNR, like DC-SIGN, is located in the cytoplasm, it contains several internalization motifs and is responsible for receptor signaling, for the binding and intra-cellular trafficking of ligand molecules (Zhang et al. 2014). The transmembrane domain of L-SIGN consists of approximately 22 amino acids (Soilleux et al. 2000; Liu et al. 2004). The extra-cellular portion of the receptor, like DC-SIGN, is characterized by the presence of a C-type carbohydrate-recognition domain (CRD) and a neck domain. The CRD domain of L-SIGN may interact with high-mannose carbohydrates, and the neck domains of these proteins contain23-amino acid sequence repeats that support the CRD and may influence the multimerization and the ligand-binding properties of these lectins (Figure 5) (Soilleux et al. 2000;Koppel et al. 2005). Hydrodynamic studies found that the C-terminal portion of the neck domain of the receptors adjacent to the CRD are important in dimer formation, whereas portions near the N terminus are important for stabilizing the tetramers (Feinberg et al. 2005). These portions are conserved despite the variation in the length of the neck domain between DC-SIGN and L-SIGN (Zhang et al. 2014). Also, L-SIGN may facilitate interactions with lymphocytes allowing their migration across endothelium (Engering et al. 2004). Previous studies showed that L-SIGN can recognize *N*-glycans structures of HIV-1 (Auwerx et al. 2009;Bashirova et al. 2001), HCV (Li et al. 2009; Gardner et al. 2003; Pohlmann et al. 2003; Lai et al. 2006), SARS-CoV (Chan et al. 2006; Jeffers et al. 2004), *M. tuberculosis* (Carroll et al. 2010) and influenza A viruses (Londrigan et al. 2011). The expression of L-SIGN on endothelial cells and its capacity to bind *N*-glycans on viral glycoproteins make this lectin a possible candidate receptor responsible for phlebovirus dissemination into the host trough infecting endothelial cells. It has been proposed that besides pleboviruses, members of the flavi- and alphavirus families, have found a way to use L-SIGN for attachment, viral entry and infection (Pustylnikov et al. 2014; Van Breedam et al. 2014). Studies by Léger *et al.*(2016), showed that L-SIGN can markedly augment phlebovirus entry into cell lines otherwise barely susceptible, after transfection of this receptor gene. In contrast to

DC-SIGN, that is an endocytic receptor, L-SIGN mainly promotes viral attachment but not uptake into cells (Guo et al. 2004). Thus, it is conceivable that L-SIGN promotes phlebovirus entry by concentrating virions onto the cell surface, thereby increasing interactions with a so far unidentified receptor. The presence of such receptor(s) is suggested by the broad cell tropism of several phleboviruses and the relatively low cell and tissue expression of the lectins (Spiegel et al. 2016).

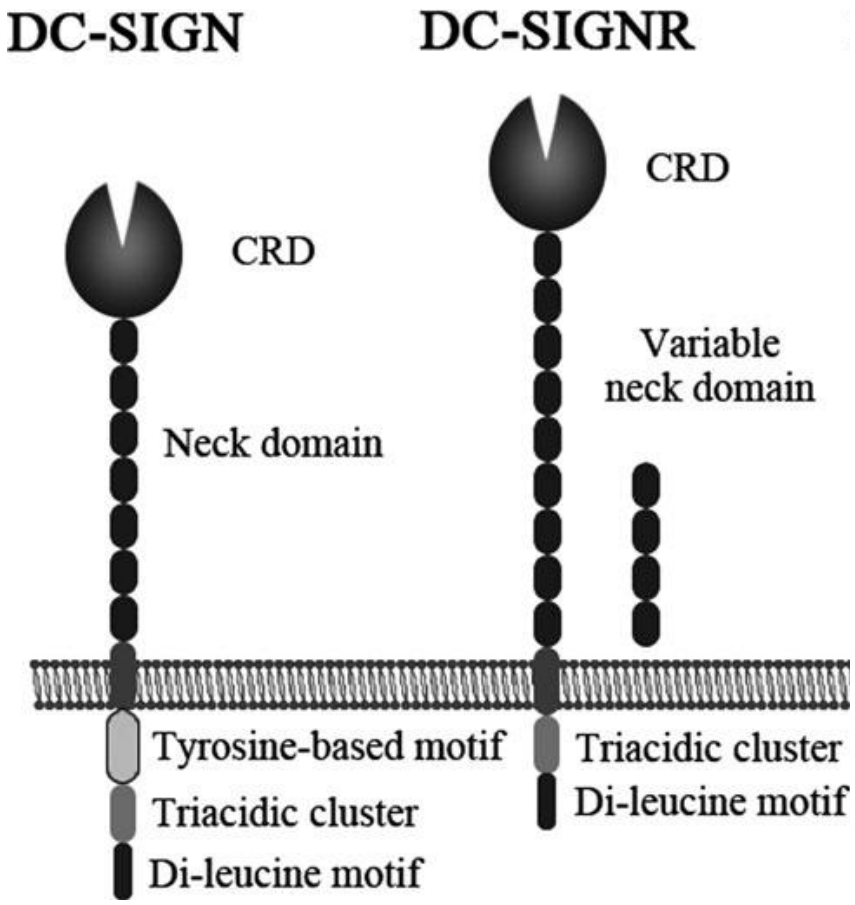

Figure 5. DC-SIGN, DC-SIGNR are trans-membrane proteins. Each contains an intra-cellular domain, a trans-membrane domain and an extra-cellular domain (Adapted from Zhang et al. 2014).

2.5 Phleboviruses and the Central Nervous System

While the majority of arbo- bunyaviral infections do not lead to neuroinvasive forms of disease, they are among the most severe infectious risks to the health of the human central nervous system (CNS) (Salimi et al. 2016).

There are several arbovirus families, such as *Togaviridae*, *Bunyaviridae, Flaviviridae and Reoviridae*, that cause neuroinvasive disease in vertebrate hosts thus, with their worldwide distribution, contributing to systemic and neurologic infections in a variety of geographical locations (Salimi et al. 2016). Viral CNS infections can be very difficult to treat, due to the rapid onset of severe disease symptoms that can occur (Furr & Marriott 2012). Shortly after viremia, arboviruses enter the CNS via several mechanisms and linked to host and viral factors, cause severe, persisting neurologic deficits or death (Table 2).

Following CNS infection, inflammation can arise in distinct anatomical regions such as the meninges (meningitis), brain (encephalitis), and spinal cord (myelitis), or simultaneously in multiple regions (meningoencephalitis, encephalomyelitis) (Swanson & McGavern 2015). However, one additional source of CNS damage comes from the immune response that develops following CNS viral infection, indeed experimental animal models have revealed that the antiviral immune response can also, under certain conditions, be an active contributor to disease (Swanson & McGavern 2015).

CNS is protected by a highly complex barrier system. Three barrier layers limit and regulate molecular exchange at the interfaces between the blood and the neural tissue or its fluid spaces: the choroid plexus epithelium between blood and ventricular CSF (blood-cerebrospinal fluid); the arachnoid epithelium between blood and subarachnoid CSF and the blood brain- barrier (BBB) formed by the cerebrovascular endothelial cells between blood and brain interstitial fluid (ISF)(Abbott et al.2004).

Despite years of intensive research, the exact mechanisms by which arboviruses enter the CNS remain unclear (Salimi et al. 2016). Arboviruses that enter through the skin after an insect bite are uptaken by immune cells like mDCs, which then migrate to the draining lymph nodes (Wu et al. 2000;Fernandez-Garcia et al. 2009), from where viruses are often shed into the blood stream, resulting in systemic infection; or they directly infect vascular endothelial cell in order to reach CNS across the blood brain barrier (BBB) (Verma et al. 2009; Moses et al 1993). Pathways of direct viral transit across the BBB include: (1) spread of viruses across brain microvascular endothelial cells (BMEC) tight junctions, due to high levels of viremia and inflammation (Daniels et al. 2014); (2) direct infection of BMECs and transport of new generated viruses across basolateral membranes (Dittmar et al. 2008). Infected hematopoietic cells can also be used as 'Trojan horses'

to transport virus into the CNS via the blood supply (Clay et al. 2007; Tabor-Godwin et al. 2010). Finally, systemic viral infection can lead to inflammation-induced breakdown of the BBB (Eugenin et al. 2006) allowing viruses to enter into the CNS.

As a second major route of CNS entry, some viruses infect and migrate through peripheral nerves. Arboviral infections typically occur in highly innervated dermis, which may lead viral entry to the CNS through peripheral neurons. Both *in vitro* and *in vivo* studies have shown that WNV can spread along neurons via retrograde axonal microtubule-mediated transport (Samuel et al. 2007; Wang et al. 2009). Also, CNS invasion via olfactory bulb has been demonstrated for several encephalitic arboviruses such us LACV (Bennett et al. 2008).

It has been postulated that TOSV could invade CNS crossing the BBB either by passive diffusion or by replication in BMECs (Sahni 2001), causing meningitis, meningoencephalitis or encephalitis.

Brain microvascular endothelial cells (BMECs) are the major component of the BBB and represent the tightest vasculature in the body (Combes et al. 2012). These cells display unique features such as tight junctions that are not found in endothelia from other vascular beds (Chan-Ling et al. 2004). There is a functional polarity on the morphology of the brain microvascular endothelium. This polarity is evidenced by asymmetric distribution of the majority of the transport-related enzymes and carriers, present in the luminal and abluminal ECs plasma membranes, indicating that apical and basolateral membranes of these cells are functionally distinct (Farellet al. 1991; Vorbrodtet al. 1993). During pathological events, such as virus infections, the BBB is capable of modulating its own cyto-architecture, increasing permeability while retaining structural integrity, and hence protecting the brain and maintaining homeostasis; however, this function may be lost under extreme conditions. Indeed, many of the cell types associated with brain microvessels, including microglia and astrocytes, and nerve terminals adjacent to the endothelial extracellular matrix/basal lamina release vasoactive agents and cytokines which can modify tight junctions assembly and barrier permeability (Abbott et al. 2006), which in turn lead decreased neuronal function and brain damage (Correale & Villa 2009).

It is possible that TOSV, like other neurotropic arboviruses, could infect the microvascular endothelial cells and cause BBB alterations with modifications in the cell-cell contacts and reach the CNS. The conditions that increase permeability between cells, affecting the organization of adherens junctions (AJs), in particular, influencing the activity of VE-cadherin (Dejanaet al. 2008). In this way, is possible that this protein may have a role during TOSV infection, modifying the strength of the contact between BMECs, thus influencing the permeability and allowing the passage of the virus through the BBB.

Family	Virus	Vector	Geographical distribution	Systemic illnesses	Neurologic diseases
Togaviridae	EEEV	Mosquito (*Culiseta*, *Aedes*)	Eastern and Gulf coasts of USA, Caribbean islands, Central America, north-east South America	Flu-like illness with nausea and vomiting	Meningoencephalitis, coma
	WEEV	Mosquito (*Culiseta*, *Culex*)	Mid-west and western USA, Canada	Febrile illness	Encephalitis
	VEEV	Mosquito (*Culex*, *Aedes*)	South and Central Americas, south-east and south-west USA	Flu-like illness	Encephalitis
	CHIKV	Mosquito (*Aedes*)	Africa, India, Southeast Asia, Caribbean islands, south-east USA	Fever, rash, arthralgias, myalgias	Rare encephalitis, GBS
Flaviviridae	SLEV	Mosquito (*Culex*)	North, Central, and South America	Flu-like illness with nausea	Meningitis, encephalitis, coma
	JEV	Mosquito (*Culex*)	Japan, North-East, South-East, and Central Asia, Indian subcontinent	–	Meningoencephalitis with seizures
	WNV	Mosquito (*Culex*)	Africa, Mediterranean region, Central Asia, India, Europe, North, Central, and South Americas	Flu-like illness	Meningitis, flaccid paralysis, encephalitis
	ZIKV	Mosquito (*Aedes*), sexual transmission	Africa, India, South-East Asia, Caribbean islands, Central, North, and South Americas	Flu-like illness with arthralgias, conjunctivitis	Meningoencephalitis, ADEM, GBS, IUGR, microcephaly
	DENV	Mosquito (*Aedes*)	Asia, tropical and subtropical regions of the world	Fever, rash, headache, myalgias, hemorrhagic fever	Encephalopathy, rare encephalitis
	MVEV	Mosquito (*Culex*, *Aedes*)	Australia, New Zealand, New Guinea	Flu-like illness with nausea	Encephalitis
Bunyaviridae	CEV	Mosquito (*Aedes*)	Western USA	Flu-like illness with nausea and vomiting	Meningoencephalitis with seizures
	LACV	Mosquito (*Aedes*)	Mid-west and eastern USA	–	Meningoencephalitis with seizures
	TOSV	Sandfly (*Phlebotomus*)	Europe, North Africa	–	Meningitis
	RVFV	Mosquito (*Culex*, *Aedes*)	East and South Africa, Saudi Arabia	Fever, hepatitis, hemorrhagic fever	Encephalitis
Reoviridae	CTFV	Ticks (Dermacentor)	Rocky Mountains of the USA	Flu-like illness with nausea, vomiting, hepatitis, rash, hemorrhagic fever	Meningitis, encephalitis

Table 2. Arbovirus families: vectors, geographical distribution, and the illnesses they cause. EEEV = eastern equine encephalitis virus; WEEV = western equine encephalitis virus; VEEV = Venezuelan equine encephalitis virus; CHIKV = Chikungunya virus; GBS = Guillain-Barré syndrome; SLEV = Saint Louis encephalitis virus; JEV = Japanese encephalitis virus; WNV = West Nile virus; ZIKV = Zika virus; ADEM = acute demyelinating encephalomyelitis; IUGR = intrauterine growth retardation; DENV = Dengue virus; MVEV = Murray Valley encephalitis virus; CEV = California encephalitis virus; LACV = La Crosse virus; TOSV = Toscana virus; RVFV = Rift Valley fever virus; CTFV = Colorado tick fever virus. (Salimi et al. 2016).

Chapter 3

Aim of the project

Toscana virus (TOSV) pathogenesis is still largely unclear. Most of the attention is focused on the identification of factors involved in the first steps of infection and the progression of the disease caused by this virus.

An intriguing aspect is the understanding of the mechanisms involved in the virus spreading to the central nervous system (CNS), analyzing which cell types can be infected by TOSV after the virus has entered into the host. To this aim we wanted to analyze the susceptibility of two types of cells that the virus encounters once in the host. We examined DCs susceptibility to TOSV infection and the role of endothelial cells in the viral neuroinvasive process, evaluating the TOSV capability to infect endothelial cells *in vitro* and *in vivo*.

Additionally, we investigated the role of viral glycoproteins, Gn and Gc, as antigenic determinants for humans. By studying the immunological memory of a patient with meningitis infected by TOSV, our aim was to isolate and characterize human neutralizing monoclonal antibodies directed to conserved glycoprotein epitopes. The identification of these regions could consequently suggest the most promising viral targets for vaccine formulation.

Chapter 4

Materials and Methods

Viruses and cells

Human humbelical vein endothelial cells (HUVECs) (Cambrexcorp.,Walkersville, MD) were cultured and subcultured in endothelial basal medium (EBM-2) (Cambrex. Cp) supplemented with 10 % FCS, hydrocortisone (1 mg/ml), human epidermal growth factor (EGF) (0.1 mg/ml) and bovine brain extract (BBE) (1 mg/ml) in 5 % CO2 at 37 °C. PBMCs were isolated from a buffy coat of TOSV seronegative healthy donors, upon informed consent, by Ficoll-Hypaque gradient separation and resuspended in RPMI 1640 medium (Hyclone, Cramligton, UK) supplemented with 10 % FCS (Life Technologies, Milan, Italy) and IL-2 (50 UI/ml) (CHIRON, Emervylle, CA, USA).Vero (ATCC CCL-81) cells were grown as a monolayer in Dulbecco's modified Eagle's medium (DMEM) (Lonza,Milan, Italy) supplemented with 5% heat-inactivated fetal calf serum(FCS) (Lonza) and 100 U/ml penicillin-streptomycin (HyClone Europe,Milan, Italy) at 37°C. Human embryonic kidney (HEK)-Lenti-X 293 cells (Clontech,Milan, Italy) were grown as a monolayer in DMEM (Lonza,Milan, Italy) supplemented with 10% heat-inactivated FCS (Lonza), 100U/ml penicillin-streptomycin (HyClone Europe) at 37°C. Spodoptera frugiperda cells (Sf9) were propagated in SF-900II medium (GIBCO InVitrogen, Milan, ITALY) containing streptomycin (100 mg/ml; Life Technologies), and penicillin (100 UI/ml; Life Technologies). Toscana virus, strain 1812(TOSV) (isolated from a clinical specimen in the Virology laboratory of S.Maria delle Scotte Hospital, Siena, Italy), was plaque purified and propagated on Vero cells. Sandfly Fever Naples virus (SFNV strain Sabin, provided by ISS), Punique virus (PUNV, strain P1_B4_2008, isolated from sandflies pool collected in Tunisia) and Sandfly Fever Sicilian virus (SFSV, strain Sabin, provided by ISS) were grown on Vero cells at the Virology laboratory, University of Siena.

Human PBMCs isolation

PBMCs were isolated from human blood, diluted in an equal volume of phosphate buffered saline (PBS) and further separated on Ficoll-Hypaque gradient by centrifugation at 1800 rpm for 20 minutes at RT. Cells were collected from the plasma/Ficoll interface and resuspended in PBS and centrifuged at 1300 rpm for 10 min. at RT. Cells were finally resuspended in RPMI 1640 medium (Hyclone, Cramligton, UK) and counted.

Generation of human monocyte-derived dendritic cells

Monocyte-derived dendritic cells (moDCs) were generated by culturing human PBMCs in the presence of granulocyte–macrophage-colony stimulating factor (GM-CSF) (50 ng/ml) and IL-4 (for 0.5 ng/ml) (R & D Minneapolis, MN, USA) for 7 days, as described elsewhere (Bell et al. 1999). To estimate immature monocyte-derived dendritic cells phenotype, cultures were examined for the expression of CD11c and CD83 (Chemicon, Germany) as described below.

TOSV infection of endothelial and dendritic cells *in vitro*

HUVECs and moDCs were seeded in 6-well culture plates at a density of 5×10^5 and 1×10^6 cells per well, respectively, and incubated at 37 °C in 5 % CO_2 atmosphere. Cells were then infected with TOSV at a multiplicity of infection (MOI) of 1, 3 or 5 and, after 90 min at 37 °C, washed with medium. 24, 48, 72 and 96 h later, cells were collected and assayed by indirect immunofluorescence assay (IFA). Briefly, cells were spotted on slides and fixed for 10 min at room temperature with cold methanol/acetone. Cells were then incubated for 1 h at 37 °C with anti-TOSV N protein (provided by DIESSE Srl, Siena, Italy; diluted at 1:200). After washing with PBS, fluorescein-labelled anti-mouse IgG (Sigma, Milan, Italy) was added for 1 h at 37 °C. Immunofluorescence was visualised using a Diaplan microscope (Leica Microsystems, Milan, Italy). Infected moDCs were also analysed by cytofluorimetric analysis, as described elsewhere (Lozach et al. 2011). After fixation and permeabilization with phosphate buffered saline (PBS) containing 0.5 % saponin and 2 % FCS, cells were stained with anti- TOSV N protein monoclonal antibody (diluted at 1:50) for 30 min on ice. After two washing steps, cells were incubated with FITC-conjugated anti-mouse IgG (Sigma, Milan, Italy, diluted at 1:100) and anti-hCD4-PE mAb (Sigma, Milan, Italy, diluted at 1:10) or anti-hCD8-PerCy5 mAb (Chemicon, Germany, diluted at 1:10), anti-hCD11c-PE mAb (Chemicon, Germany, diluted at 1:10), anti-hCD14-PE mAb (Chemicon, Germany, diluted at 1:10), anti-hCD19-PE mAb (Chemicon, Germany, diluted at 1:10), or anti CD83 (Chemicon, diluted 1: 50). Stained cells were washed in PBS and analysed using a FACSCalibur with CellQuest software (BD Biosciences, San Jose, CA). The supernatant of infected HUVECs and moDCs was collected 1, 2, 3,and 4 days after infection for virus titration.

TOSV titration

Briefly, the supernatant of infected cells was diluted tenfold and titrated by plaque assay on a 6-well plate of Vero cells and incubated at 37 °C in 5 % CO_2 for 1 h (Hemmersbach-Miller et al. 2004). The medium was then removed, and 3.5 ml of overlay medium containing 3 % purified agar (Oxoid, Milan, Italy) was added. After 5 days, the cell sheet was stained with neutral red, and the viral titre was determined as plaque forming units/ml (PFU/ml). Mock-infected cells were included in each experiment as controls. All experiments were repeated three times.

Cytokine assay

Supernatants of HUVECs and moDCs collected 24, 48, 72 and 96 h after TOSV infection were tested for the presence of interleukin-6 (IL-6) and tumour necrosis factor-α (TNF-α) by ELISArray (SABiosciences Corp. Frederick, MD, USA) following the manufacturer's instructions. To determine interferon-β (IFN-β), the supernatant was assayed at the same time points using the human IFN-β ELISA kit (PBL Interferon Source, Piscataway, NJ, USA) according to the manufacturer's protocol.

Permeability assay

Permeability assays were performed on 24-well plates with polycarbonate filters (3 µm pore and 6 mm diameter (Corning Life Sciences, The Netherlands) coated with HUVECs (5×10^4 cells per cm^2) in 300 µl of complete EBM2 medium (upper compartment) and cultured until confluence (2 days). Lower compartments contained 700 µl of medium. Before the permeability assay, HUVECs were washed with medium and transferred to a new plate. Cells were then infected in triplicate with TOSV at an MOI of 1 and incubated at 37°C for 5 h. Human PBMCs (2×10^4), previously isolated as described, were then added to each well coated with infected HUVECs and incubated at 37 °C for 24 h. Finally, FITC-dextran (4 KDamolwt, Sigma, Milan, Italy) (0.5 mg/ml) was added to the upper chamber of the filter, and after 3 h, the fluorescence intensity of transmigrated FITC-dextran was measured in the upper and lower chambers using a Perkin-Elmer fluorimeter (490-nm excitation, 530 nm emission). Uninfected HUVECs, uninfected HUVECs + PBMCs and TOSV-infected HUVECs were used as controls. In order to monitor TOSV infections, endothelial cell monolayers in 96-well plates were infected at the same MOI as the Transwell plates. At 24 h post-infection, cells were fixed and tested for the presence of virus by immunofluorescence. The assay was repeated three times. The FITC dextran transmigrated across the membrane was calculated as the ratio of fluorescence units/ml in the upper and lower chambers for all experimental samples. A t test for *in vitro* permeability assay was performed using a SigmaStat (San Jose, California), and p values of <0.05 were considered significant.

Animal infection

Four-week-old female BALB/c mice (Charles River, Milan, Italy) were used for TOSV infection. Groups of four mice were subcutaneously (sc.) injected with 200 µl of TOSV 1812 V (3×10^6 PFU/ml) (Cusi et al. 2005). Blood was drawn from mice 24 h and 3 and 6 days after infection for viral genome detection. Mouse blood samples were centrifuged at 1600g for 5 min. Plasma was recovered, while the buffy coat and erythrocytes were mixed with an equal volume of phosphate buffered saline and further separated by Ficoll-Hypaque gradient for purifying peripheral blood mononuclear cells. Moreover, pieces of mouse epidermis and brain were removed and processed for histology. Each experiment was repeated three times in order to assess the reproducibility of results. All animal experiments were approved by the local Ethics Committee and carried out in strict compliance with the Institutional Animal Care and Use Committee (IACUC) guidelines and in accordance with the 2010/63/EU Directive (http://eurlex.europa.eu/LexUriServ/LexUriServ.do?uri= OJ:L:2010:276:0033:0079:EN:PDF) of the European Parliament and the Council for the Protection of Animals Used for Scientific Purposes.

Histological and immunohistochemical analysis of tissues

After removal, organs were post-fixed in phosphate buffered 10 % formalin. After fixation, fragments of epidermis and coronal slices of brain were embedded in paraffin. Serial sections from each organ slice were partly stained with haematoxylin and eosin (HE), thionin, Bielschowski and luxol fast blue (Klüver-Barrera) and

partly processed for immunohistochemistry or immunofluorescence. A commercial kit (Super Sensitive Bioptica, Milan, Italy) was used to perform immunohistochemistry in order to detect virus antigen distribution and to identify the infected cell types. After deparaffinization, sections were washed in Tris–HCl buffer (pH 7.6) and incubated for 8 min with UltraV Block. After washing, the anti-N TOSV mAb (diluted 1:400) was applied for 1 h, and a secondary biotinylated goat anti-mouse antibody (NeoMarkers, BioOptica, Milan, Italy) was applied for 20 min at room temperature. Sections were washed again and then incubated for 20 min with Streptavidin Alk-Phos or streptavidin-HRP (NeoMarkers) at room temperature. Conjugates were visualised with brown staining, using a diaminobenzidine solution (NeoMarkers) as chromogen, after 8 min incubation. Haematoxylin was used for counterstaining. In order to colocalize TOSV and endothelial cells, a double immunofluorescence stain was performed in tissue sections treated with mouse FITC-labelled anti-TOSV mAb (DIESSE, srl, diluted 1/200) and rabbit Alexa Fluor 647 labelled anti-mouse CD31 (diluted 1/200; BioLegend, Milan, Italy). The nuclei were counterstained by incubating sections for 10 min with 4,6-diamidino-2-phenylindole (DAPI) as described elsewhere (Tini et al. 2015). Images were acquired and analysed with a Leica AFCTR6500HS microscope (Leica Microsystems, Milan, Italy).

RT-PCR

Separated blood components (plasma, PBMCs) or whole blood of infected mice were subjected to RNA extraction using a total RNA isolation kit (Promega, Mannheim, Germany). Total RNA was amplified by RT-PCR; reverse transcription was performed at 37 °C for 30 s, followed by 35 cycles of amplification (94 °C for 1 min, 52 °C for 30 s and 72 °C for 40 s), as previously described (Cusi et al. 2005).

Immortalization of human memory B cells

Peripheral blood mononuclear cell (PBMC) and plasma samples were obtained, upon informed consent, from a patient with meningitis, infected by TOSV, during the acute phase and one year after the infection. At the Institute for Research in Biomedicine (Bellinzona Switzerland), frozen peripheral blood mononuclear cells (PBMCs) were thawed and IgG^+ memory B cell were isolated and immortalized, using EBV in the presence of CpG, as previously described (Traggiai et al. 2004). Culture supernatants were harvested after 14 days and assayed by Intellicyt Cytometer against VERO cells infected with TOSV. Positive cultures were collected, expanded and cell culture supernatants, containing mAbs, were send to our laboratory for subsequent screening.

ELISA α-N TOSV

Microtiter plates (Labsystem, Helsinki, Finland) were coated with TOSV purified recombinant N protein (1 µg/ml), (100 µl/well) in 0.1 M carbonate buffer (pH 9.6) overnight at 4 °C. After three washing steps with phosphate buffer solution (PBS) containing 0.05% Brij, 100 µl of undiluted mAbs were added to the wells in

duplicate and the plates were incubated at 37°C for 1h. After washing, 100 µl of peroxidase-conjugated anti-human IgG (diluted 1:75,000; Sigma-Aldrich) was added and the plates were incubated at 37°C for 1 h. Finally, the plates were washed as described above and the immunocomplex formation was developed by adding 100 µl of 3,3',5,5'-tetramethylbenzidine (Sigma-Aldrich) for 15 min. Then, the reaction was stopped by adding 1 NH_2SO_4 solution and the plates were read at 450 nm. Negative and positive controls were included in each test.

Neutralization test

Virus neutralization was carried out on Vero cells in a 96 wellmicroplate. Briefly, two-fold serial dilutions (25µl) of mAbs or human positive sera were added to an equal volume of a TOSV dilution containing 200 $TCID_{50}$ and incubated for 90 min at 37 °C, then 30 min at 4 °C. Fifty µl of cells (10^6/ml) were suspended in MEM (InVitrogen, Milan, Italy) with 5% FCS and added to each well. Five days after incubation at 37 °C, the cultures were examined microscopically for the presence of cytophatic effect. The 50% end point titre of the serum neutralizing dose was calculated using the Reed and Muench method (Reed & Muench 1938).

Plasmid

Viral RNA was extracted from TOSV-infected Vero cells using a QIAamp viral RNAminikit (Qiagen). The Gn coding gene (GenBank accession no.JF330280) was amplified by reverse transcriptase PCR (RT-PCR) from purified viral RNA with sense (nt 831 to 854) 5'-GGATCCATGAGAAACCATGTGCGTAGACCA-3' and antisense (nt 2470 to 2445) 5'-CTCGAGTTATTTAGCCCCTGGAGCTCCTCCTGT-3' primers (Sigma-Aldrich, Milan, Italy). The reaction was carried out using the SuperScript III one-step RT-PCR mix (Invitrogen) by one cycle of reverse transcription at 50°C for 30 min and 94°C for 2 min, followed by 40 cycles of PCR (15 min at 94°C, 30 s at 56°C, and 1 min at 68°C) and 5 min at 68°C. The gene was cloned in pcDNA3.1 (+) plasmid (Invitrogen) at the BamHI-XhoI unique site. This resulted in plasmid GC-182.

Reactivity evaluation of human monoclonal antibodies to TOSV Gn and Gc proteins

Recombinant baculovirus expressing the ectodomains of TOSV Bac-Gn and Bac-Gc were kindly provided by P. Di Bonito from Istituto Superiore di Sanità in Rome (Di Bonito et al. 2002). Sf9 cells were infected with Bac-Gn and Bac-Gc at a multiplicity of infection (MOI) of 0.1, as described elsewhere (Di Bonito et al. 1997), collected five dayspost-infection and tested for protein expression by immunofluorescence (IFA) using a mouse polyclonal anti-Gn or anti-Gc serum (Di Bonito et al. 1997).

Transfections of Lenti-X HEK293 were performed using the GeneJuice reagent (Merck-Millipore, Milan, Italy) by following the manufacturer's instructions. Cells were seeded in a 6-well culture plate at a density of $1x10^6$cells per well and incubated at 37°C in a 5% CO_2 atmosphere. Cell monolayers were transfected with 1 µg of Gn-expressing plasmids. Forty-eight hours post-transfection, cells were collected and assayed for indirect immunofluorescence (IFA).

Briefly, both types of cells expressing the recombinant proteins were analyzed by IFA with undiluted human mAbs and with mouse anti-Gc or anti-Gn for the positive controls. A negative control represented by a pool of human TOSV seronegative sera was also included in the assay. Immunofluorescence was visualized by a Diaplan microscope (Leica Microsystems, Milan, Italy).

SPOT peptide synthesis

A set of 82 overlapping peptides of 15 aa, shifted by five residues, spanning aa 1–416 of TOSV Gn glycoprotein (GenBank accession no: AEM36009.1 from aa 308–834) was synthesized as an array on derivatized cellulose-based membranes in Prof L. Bracci's Lab, Department of Medical Biotechnologies, University of Siena, using SPOT technology (Hilpert et al. 2007; Winkler & Campbell, 2008). In the sequence, the cysteines were replaced by serine. The membrane immobilized peptides were first saturated in MBS (pH 7.0) containing 2% of milk power, 0,05% Tween 20 in TBS o/n at 4°C. After three washing steps with TBS containing 0,05% Tween 20 (T-TBS), peptides were probed with each individual mAb at a concentration of 5 μg/ml in MBS for 90 minutes at 37°C. Following other three washing steps, membrane was incubated with HRP-conjugated goat antimouse IgG (Sigma) at 1 : 8000 dilution and, after three washing steps, an enhanced chemiluminescent substrate kit was used for detection of HRP development (Thermo SCIENTIFIC), according to the manufacturer's instructions. The spots were evaluated with a gray scale of intensity, after imagine acquisition by using ImageQuantTL, as described (Lin et al. 2010).

Statistical analysis

All experiments were carried out in triplicate; mean differences were statistically analysed using Stat View statistical software (Abacus Concepts, Berkeley, CA). Differences of P values ≤ 0.05 were considered significant.

Chapter 5

Results

Part I

5.1 Toscana virus pathogenesis: a way to reach the Central Nervous System

Related Pubblication:

Toscana virus infect dendritic and endothelial cells opening the way for the central nervous system

Maria Grazia Cusi[1], Claudia Gandolfo[1], Chiara Terrosi[1], Gianni Gori Savellini[1], Giuseppe Belmonte[2], Clelia Miracco[2]

In this first section we focus our attention on the identification of TOSV cell targets relying on *in vitro* and *in vivo* studies. The aim is to provide a description of possible mechanisms involved in TOSV spreading into the host.

TOSV infection: in vitro studies

We observed that dendritic cells (DCs) and endothelial cells were susceptible to viral infection without any sign of cytopatic effect. Both monocyte-derived DCs (moDCs) and HUVECs support viral replication as confirmed by virus titration in their medium, with a peak titre at 48 h post-infection (Figure 6). Endothelial cells were more susceptible to TOSV infection than DCs. In fact, while HUVECs, infected with 1 MOI resulted positive by immunofluorescence 24 h post- infection (Figure 7), moDCs, infected with the same virus amount, showed positivity only by a more sensitive FACS analysis. A clear result was obtained at 48 h with higher MOI (29,8% with 5 MOI), indicating that the infection was multiplicity dependent. We also realized that the infection induced DC activation, as demonstrated by FACS analysis, with the increase of expression of the CD83 activation marker (Figure 8).

To evaluate the effect of TOSV infection on endothelial permeability, we used a standard permeability assay, based on the evaluation of the FITC-dextran passage across the endothelial monolayer, in a transwell-system, in the presence or absence of PBMCs. Compared with the controls, only the addition of PBMCs, 5 h post endothelium infection, increased endothelium permeability (Figure 9).

Since exposure of DCs and vascular endothelial cells to pathogen stimuli, induces secretion of pro-inflammatory cytokines, such as interleukin-1β (IL-1β), IL-6, and tumour necrosis factor-α (TNF-α) (Takeuchi et al. 2010; McDonald et al. 2010), we investigated the presence of these inflammatory cytokines in the supernatant of infected moDCs and HUVECs. Only IL-6 was produced by HUVECs, reaching a peak (3365 ± 183 pg/ml) at 72 h post infection. On the contrary, moDCs constantly produced IL-6 throughout the experiment, and TNF-α at high level, with a peak at 96 h post-

infection (1553 ±201 pg/ml). The supernatant of these cells was also analyzed by ELISA, to evaluate the presence of IFN-β in order to determine the activation of the innate immune response. HUVECs produced a high amount of IFN-β at 48 h post-infection (165 ± 1,7 pg/ml), while moDcs produced it at a lower amount in the first 3 days post- infection (7 to 10 pg/ml).

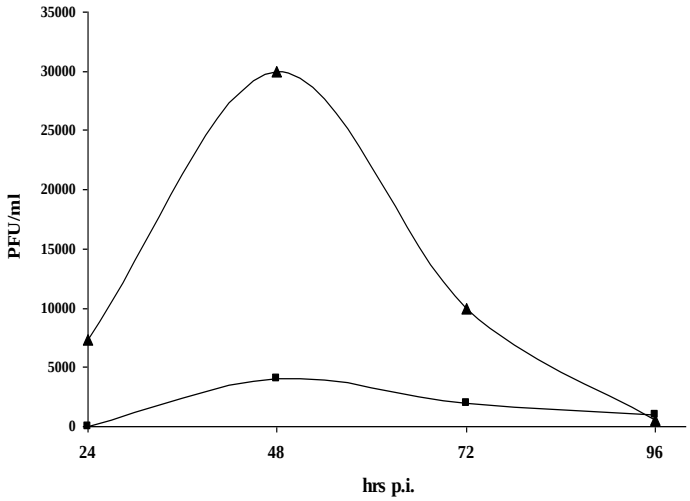

Figure 6. Titration of TOSV in cell culture supernatant. Cell culture supernatants were collected from HUVECs (—▲—) or moDCs (—■—) infected with TOSV at an MOI of 3 at 24–96 h p.i. for virus titration. Titer values, expressed as PFU/ml, represent the average of at least three independent infections.

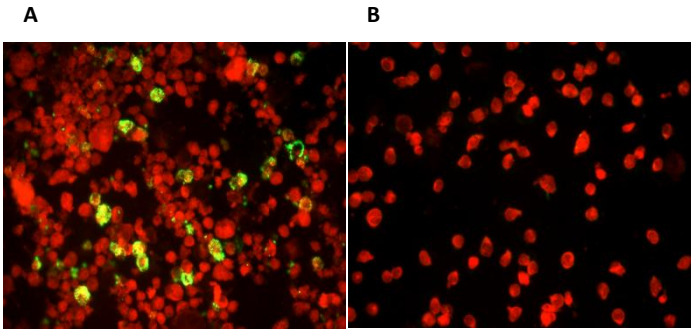

Figure 7. Immunofluorescence assay on HUVECs infected by TOSV (MOI 1) and observed at 24 h p.i. (400x).
The cells were fixed and stained with anti TOSV mabs (DIESSE).(A) TOSV infected HUVECs or (B) mock-infected cells.

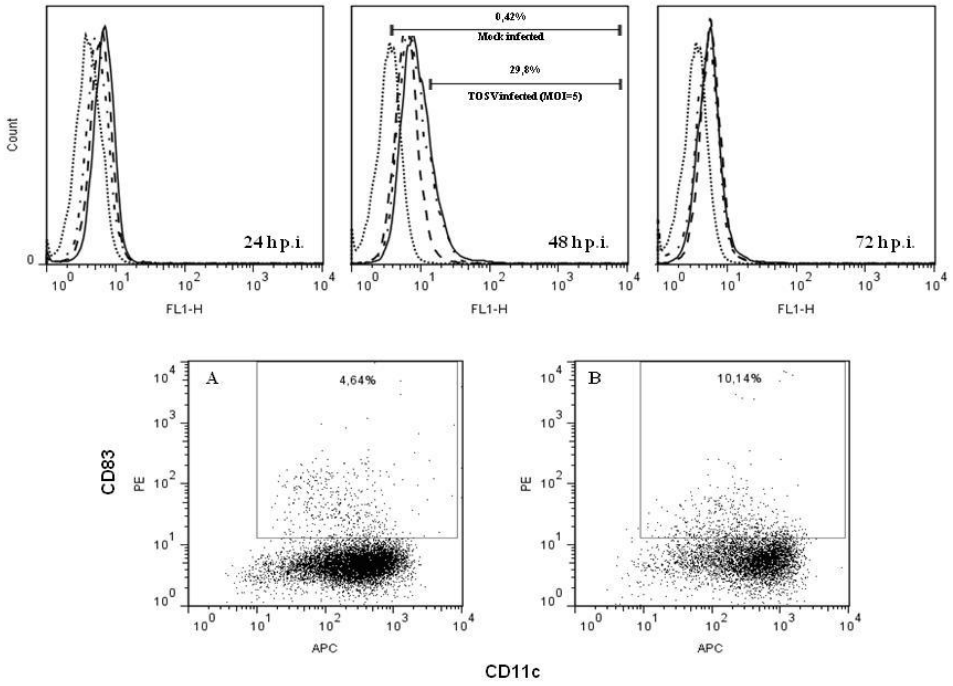

Figure 8. Quantification of fluorescence in TOSV-infected moDCs by FACS analysis, as described in Experimental procedures. Histograms show uninfected control cells (…) and TOSV-infected cells with 5 MOI (—), 3 MOI (—■—), and 1 MOI (— —) at 24, 48 and 72 h p.i., as indicated. FL1-H is the measurement of fluorescence intensity. Human moDCs were also analysed for CD11c+ (APC) and CD83+ (PE) cells. A Mock-infected moDCs, B TOSV-infected moDCs.

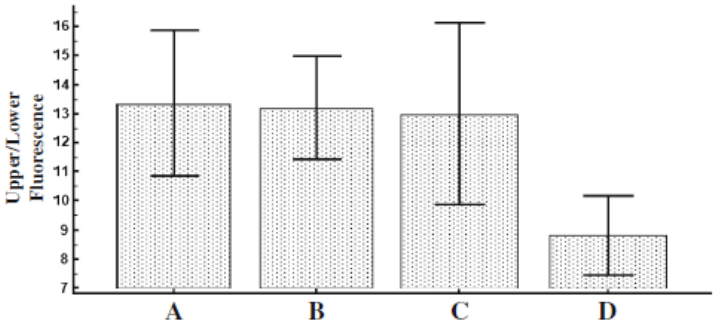

Figure 9. FITC-dextran permeability assay on HUVECs after TOSV infection. The assay was performed at 24 h p.i. A. mock-infected HUVECs, B. TOSV-infected HUVECs, C. HUVECs+PBMC, D. TOSV infected HUVECs+PBMC. FICT-dextran emission was measured and reported as the ratio of the fluorescence units/µl in the upper and lower chamber. The data are representative of three independent experiments.

TOSV infection: in vivo studies

In order to understand how TOSV disseminates through the host, we analyzed blood samples taken 1, 3 and 6 days after infection from mice sc. inoculated with TOSV. Whole blood, plasma and PBMCs were analyzed by RT-PCR in order to find viral genome. The virus genome was revealed only in the whole blood and in the plasma but not in PBMCs, (Figure 10), underling that the virus can circulate in the blood as free virus. It has been *in vitro* demonstrated that moDCs and endothelial cells are infected by TOSV. Next aim was to evaluate this cell infection also *in vivo.* Histological analysis of skin biopsies of infected mice revealed TOSV presence in endothelial cells of sub-cutaneous post-capillary venulae (Figure 11 A, G-I). It was also possible to high light a leakage in endothelium with an alterated elastic lamina and an inflammatory infiltrate (Figure 11 B), mainly CD8+ T lymphocytes, in some tissue sections of the epidermis (Figure 11 C). Also brain sections of these mice showed the presence of TOSV in the endothelium of venulae, but, in this area, without inflammatory cells (Figure 11 D), suggesting that virus, when inoculated by the natural route (subcutaneously) can reach CNS, without causing serious damage in mouse, which is not the natural host.

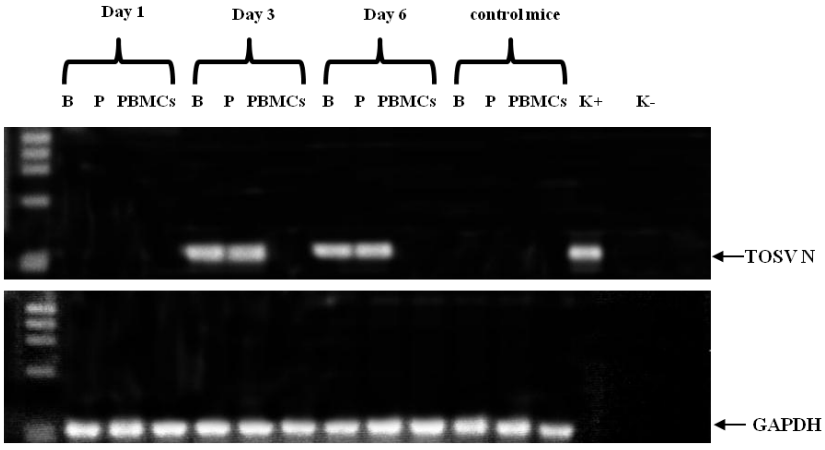

Figure 10. TOSV detection in infected mice. The presence of TOSV genomic RNA was investigated by RT nested-PCR on whole blood (B), plasma (P) or peripheral-blood mononuclear cells (PBMCs) samples collected from mice at 1, 3 and 6 days after infection. The same samples drawn from mock-infected mice (control mice) were assayed at the 3rd day p.i. A positive control (K+) and blank (K−) were included in the assay (upper panel). All the samples were tested for GAPDH (glyceraldehyde-3 phosphate dehydrogenase) as internal control (lower panel).

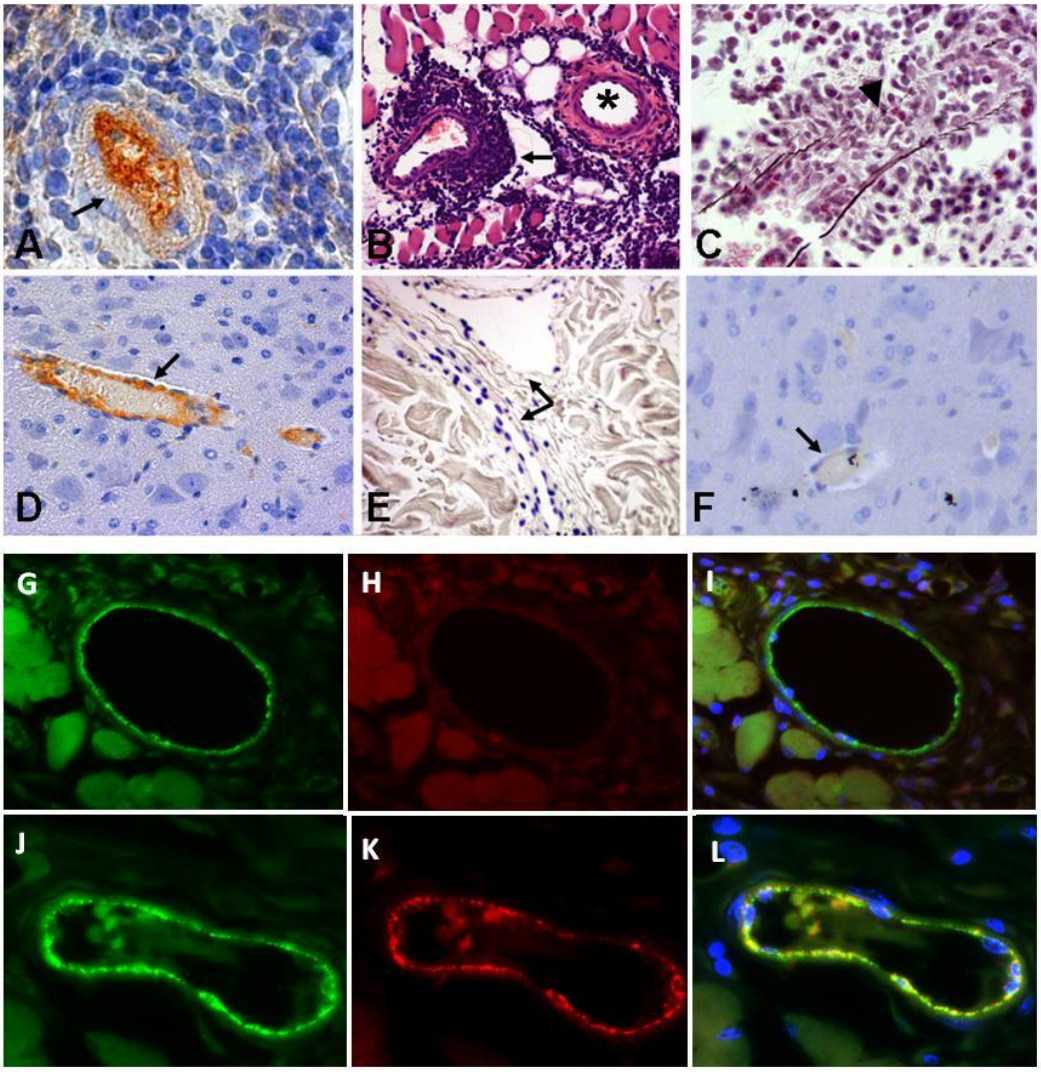

Figure 11. Immunohistochemistry and IF of tissues of TOSV-inoculated mice. Virus immunohistochemistry of skin (A) and brain (D) tissues drawn from mice sc. inoculated with TOSV. Brown-stained endothelial cells of cutaneous (A) and brain (D) venulae (arrow), positive for TOSV. Lymphocyte infiltrate of a cutaneous venula wall (B, arrow). Vasculitis does not affect arteriolae (B, the asterisk indicates the lumen of an arteriole) and partly destroys venular elastic lamina (C, arrow head). Skin (E) and brain tissue (F) of a mock-infected mouse (the arrows indicate TOSV-negative vessels). A, D, E, F Immunohistochemistry; original magnification (OM): A, D, F ×400; E ×200; B haematoxylin and eosin;OM×200; C Orcein-Giemsa stain,OM×200. Immunofluorescence of TOSV and CD31 on endothelial cells of the skin of a sc. Infected mouse: positivity to CD31 (J) and TOSV (K); l the merged image shows co-localization of CD31 and TOSV. G–I IFA performed with the same antibodies on the skin of a negative control mouse (magnification ×630).

In conclusion, we investigated which type of cells were infected by the virus once into the host. Previous studies demonstrated that TOSV doesn't infect peripheral blood mononuclear cells, such as B and T lymphocytes (Lozach et al 2010, 2011), but during the infection, the virus encounters other subsets of cells, such as dendritic cells (DCs) and endothelial cells, which can be infected. We have demonstrated that TOSV is able to infect and replicate in moDCs and endothelial cells before entering the bloodstream, where it is free to move as revealed by the absence of viral genome in any blood cell population. We observed that DCs infection is dose dependent, and induces DCs maturation leading to the activation of innate and adaptive immune response. Indeed, the production of high amount of TNF-α by TOSV infected DCs, is probably involved in the process of antigen presentation and in the activation of a local inflammatory response, thus mediating leukocytes migration across endothelium.

Endothelial cells are more susceptible to TOSV infection than DCs. Viral infection induces the activation of the innate immune response, as confirmed by the high amount of IFN-β produced by these cells just after 48 h post infection. Moreover, the production of IL-6 in the supernatant of infected HUVECs suggests that leukocytes migration is activated during TOSV and is also responsible for the increased endothelial permeability, as confirmed by the permeability assay.

In vivo studies confirmed that TOSV is able to reach the CNS without causing particular vessel damage. The virus probably crosses the BBB, altering the barrier function at endothelium level, thus causing the infiltration of leukocytes, such as CD8+ lymphocytes.

Results

Part II

5.2 Identification of TOSV Gn glycoprotein epitopes: epitope mapping by using human monoclonal antibodies

In this second section, we investigated the role of TOSV glycoproteins as targets for neutralizing monoclonal antibodies obtained from a patient infected by TOSV. With the immortalization of patient IgG^+ memory B cells, a high amount of monoclonal antibodies obtained were analyzed by pepscan analysis, in order to select neutralizing monoclonal antibodies directed to TOSV glycoproteins, and identify those epitopes recognized by these monoclonal antibodies.

Isolation and screening of a panel of TOSV human monoclonal antibodies

A patient affected with meningitis, selected for serological positivity ($IgM^+$and IgG^+) to TOSV infection was used in this study. This patient's PBMCs and serum were collected during the acute phase and one year post infection. IgG^+ memory B cells were obtained from frozen PBMCs and immortalized with EBV in the presence of CpG according to a previously described method (Traggiai et al. 2004). To detect antibodies recognizing TOSV antigens, B cell culture supernatants were screened by high throughput FACS analysis using VERO cells infected with TOSV.

Based on this first screening, 112 mAbs positively reactive against TOSV infected cells, were selected. Among them, 7 antibodies were derived from PBMCs of the acute phase (identified as TVA mAbs), while 105 were from PBMCs collected one year post infection (TVB mAbs). Whole mAbs were firstly screened against recombinant TOSV N protein by ELISA test (Table 3). Two mAbs of the acute phase and 52 mAbs of the convalescent phase were positive to N protein, while 58 mAbs that did not react with the N protein, were screened with the envelope glycoproteins, in order to isolate a representative panel of TOSV-neutralizing antibodies. These mAbs were screened by neutralization assay with TOSV strain 1812 (Table 4).We did not find any monoclonal antibody with neutralizing activity in the acute phase, although the serum had a neutralizing titre of 1:161. On the contrary, mAbs derived from the convalescent phase had a high neutralizing activity. Afterwards, both negative and neutralizing mAbs were analyzed by immunofluorescence with Sf9 cells infected with the recombinant baculovirus, Bac-Gn or Bac-Gc, expressing the ectodomains of TOSV Gn and Gc proteins respectively (Figure 12). We also included in the test, two mAbs, positive to the N protein (TVB 38 and TVB 39), as negative control. Thirteen out of 58 mAbs, were positive to Sf9-Gn, 2 showed an uncertain positivity to Sf9-Gn and 5 showed positivity to Sf9-Gc, 38 resulted negative to both the proteins (Table 5). It is possible that some of these negative mAbs recognized epitopes present in the extracellular region near

the transmembrane domain of the glycoproteins that was not expressed by recombinant Baculovirus in Sf9 cells. For this reason, we analysed only those mAbs, having a neutralization titre≥ 1:128, by IFA with Lenti-X HEK293 cells, transfected with plasmids expressing the whole glycoproteins. Our attention was first addressed to the Gn glycoprotein, because all the mAbs with a high neutralization titre were positive to the Gn glycoprotein (Table 5). In addition, we noticed that some mAbs, previously negative by IFA on Sf9-Gn cells, were, instead positive on Lenti-X HEK293-Gn, suggesting that the region near the transmembrane domain could include same epitopes recognized by neutralizing antibodies.

Table 3. Results of ELISA using recombinant TOSV N protein. The highlighted values are considered positive, comparing with the value of the negative controls.

Acute phase		1 year post infection					
mAbs ID	ELISA α-N	mAbs ID	ELISA α-N	mAbs ID	ELISA α-N	mAbs ID	ELISA α-N
TVA 49	0,145	TVB 2	0,05	TVB 88	0,377	TVB179	0,017
TVA 73	0,049	TVB 10	0,044	TVB 89	0,787	TVB181	0,485
TVA 81	0,512	TVB 11	0,024	TVB 93	0,482	TVB182	0,014
TVA 83	0,024	TVB 22	0,018	TVB 95	0,203	TVB183	0,017
TVA 96	0,011	TVB 25	0,026	TVB 97	0,541	TVB184	0,325
TVA 106	0,029	TVB27	0,012	TVB 98	0,021	TVB185	0,313
TVA 128	0,349	TVB 28	0,012	TVB 101	0,338	TVB187	0,018
		TVB 30	0,673	TVB 102	0,444	TVB190	0,683
		TVB 31	0,036	TVB 103	0,013	TVB191	0,022
		TVB 35	0,563	TVB105	0,017	TVB193	0,029
		TVB 36	0,363	TVB110	0,463	TVB197	0,062
		TVB 37	0,254	TVB112	0,384	TVB202	0,589
		TVB 38	0,359	TVB117	0,014	TVB207	0,633
		TVB 39	0,71	TVB120	0,456	TVB208	1,148
		TVB 40	0,446	TVB122	0,43	TVB211	0,047
		TVB 41	0,023	TVB124	0,847	TVB213	0,032
		TVB 43	0,014	TVB125	0,603	TVB215	1,176
		TVB 53	0,431	TVB127	0,01	TVB216	0,03
		TVB 56	0,416	TVB132	0,716	TVB218	0,026
		TVB 57	0,017	TVB134	0,429	TVB219	0,02
		TVB 59	0,23	TVB139	0,466	TVB220	0,021
		TVB 61	0,484	TVB140	0,015	TVB226	0,018
		TVB 63	0,011	TVB147	0,043	TVB227	0,471
		TVB 71	0,016	TVB150	0,027	TVB230	0,586
		TVB 73	0,013	TVB161	0,026	TVB237	0,021
		TVB 74	0,363	TVB162	0,728	TVB241	0,898
		TVB 76	0,449	TVB164	0,032	TVB242	1,057
		TVB 77	0,013	TVB165	0,13	TVB246	1,162
		TVB 78	0,017	TVB167	0,367	TVB247	1,067
		TVB 79	0,414	TVB169	0,034	TVB248	1,164
		TVB 80	0,011	TVB170	0,153	TVB250	0,592
		TVB 81	0,478	TVB173	0,022	TVB254	0,044
		TVB 82	0,807	TVB174	0,11	TVB257	0,631
		TVB 84	0,017	TVB176	0,419	TVB259	0,521
		TVB 86	0,47	TVB177	0,416	TVB262	0,039

Table 4. Results of the neutralization assay with mAbs and sera, using TOSV strain 1812.

Acute phase		1 year post infection					
mAbs ID	**NT titre**	**mAbs ID**	**NT titre**	**mAbs ID**	**NT titre**	**mAbs ID**	**NT titre**
TVA 49	-	TVB 2	-	TVB 80	1:181	TVB179	-
TVA 73	-	TVB 10	-	TVB 84	-	TVB182	1:512
TVA 83	-	TVB 11	-	TVB 95	-	TVB183	-
TVA 96	-	TVB 22	-	TVB 98	-	TVB187	-
TVA 106	-	TVB 25	1:512	TVB 103	>1:512	TVB191	1:203
		TVB27	1:161	TVB105	>1:512	TVB193	1:645
		TVB 28	-	TVB117	-	TVB197	1:16
		TVB 31	1:645	TVB127	-	TVB211	1:4
		TVB 37	-	TVB140	-	TVB213	-
		TVB 41	-	TVB147	1:645	TVB216	-
		TVB 43	1:181	TVB150	>1:512	TVB218	-
		TVB 57	>1:512	TVB161	1:645	TVB219	1:4
		TVB 59	-	TVB164	1:6	TVB220	1:323
		TVB 63	1:128	TVB165	1:8	TVB226	-
		TVB 71	-	TVB169	1:32	TVB237	1:645
		TVB 73	>1:512	TVB170	-	TVB254	1:4
		TVB 77	>1:512	TVB173	1:128	TVB262	-
		TVB 78	-	TVB174	-		

NT titre	
Serum Acute phase	1:161
Serum 1 year later	1:323

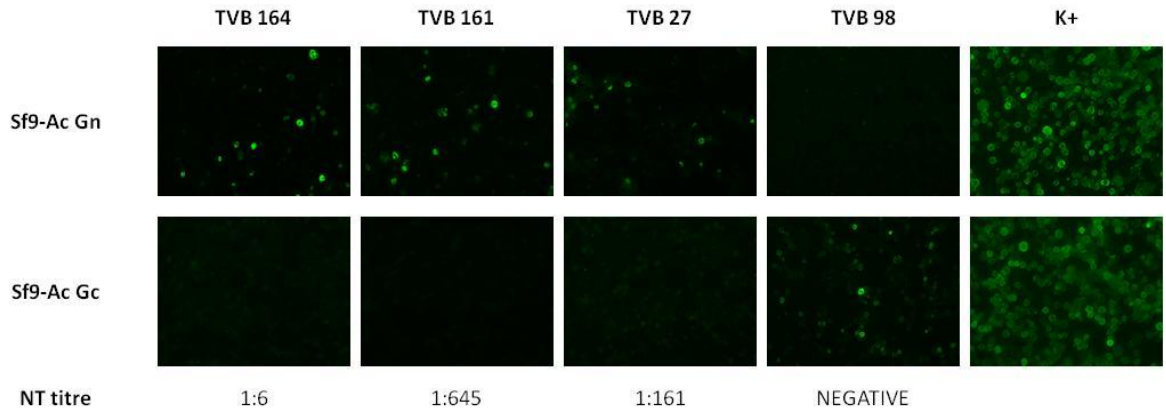

Figure 12. Immunofluorescence with Sf9-Gn and Sf9-Gc cells with human mAbs and with a mouse polyclonal anti-Gn or anti-Gc serum for the positives controls (200x).

Table 5. Immunofluorescence assay of mAbs with Sf9 and Lenti-X HEK293 cells expressing recombinant proteins.

	mAbs ID	NT Titre	Sf9-Gn	Sf9-Gc	Lenti-X HEK293- Gn
Acute phase	TVA 49	-	-	-	
	TVA 73	-	+	-	+
	TVA 83	-	-	-	
	TVA 96	-	-	-	
	TVA 106	-	-	-	
1 year post infection	TVB 2	-	+	-	
	TVB 10	-	-	-	
	TVB 11	-	-	-	
	TVB 22	-	+	-	
	TVB 25	1:512	+/-	-	+
	TVB27	1:161	+/-	-	+
	TVB 28	-	+	-	
	TVB 31	1:645	-	-	+
	TVB 37	-	-	-	
	TVB 41	-	-	-	
	TVB 43	1:181	-	-	+
	TVB 57	>1:512	-	-	+
	TVB 59	-	-	-	
	TVB 63	1:128	-	-	+
	TVB 71	-	+	-	
	TVB 73	1:512	+	-	+
	TVB 77	>1:512	-	-	+
	TVB 78	-	-	-	
	TVB 80	1:181	-	-	+
	TVB 84	-	-	-	
	TVB 95	-	-	-	
	TVB 98	-	-	+	
	TVB 103	>1:512	-	-	-
	TVB105	>1:512	+	-	+
	TVB117	-	-	-	
	TVB127	-	-	-	
	TVB140	-	-	-	
	TVB147	1:645	+	-	+
	TVB150	>1:512	-	-	+
	TVB161	1:645	+	-	+
	TVB164	1:6	+	-	
	TVB165	1:8	-	-	
	TVB169	1:32	-	-	
	TVB170	-	-	-	
	TVB173	1:128	+	-	+
	TVB174	-	-	-	
	TVB179	-	+	-	
	TVB182	1:512	-	-	+
	TVB183	-	-	+	
	TVB187	-	-	+	
	TVB191	1:203	-	-	+
	TVB193	1:645	-	-	+
	TVB197	1:16	-	-	
	TVB211	1:4	+	-	
	TVB213	-	-	-	
	TVB216	-	-	-	
	TVB218	-	-	-	
	TVB219	1:4	-	-	
	TVB220	1:323	-	-	+
	TVB226	-	-	+	
	TVB237	1:645	-	-	+
	TVB254	1:4	-	-	
	TVB262	-	-	+	

Identification of neutralizing TOSV Gn epitopes by pepscan analysis

SPOT peptide synthesis (Frank 2002) was used to generate membranes of 82 spots of 15 aa–long peptides shifted by 5 residues, covering Gn glycoprotein of TOSV from aa 1 to aa 416 (GenBank accession no: AEM36009.1 from aa 308–834) (Figure 13; Table 6).

These membranes were used to identify Gn epitopes recognized by previously selected neutralizing mAbs reacting to Gn glycoprotein. In the first screening we tested both patient sera, one mAbs positive to Gc glycoprotein (TVB 98) and two non neutralizing mAbs, one mAb of the acute phase (TVA 73) and one of the convalescent phase (TVB 71) as negative controls and five mAbs with a neutralization titre> 1: 512. To set the background, we probed the membrane with only the secondary antibody (Figure 14).

We identified the same three regions of the Gn protein recognized by most of the neutralizing mAbs tested (Table6). Two of these linear peptides were localized in the first half of the protein, one was instead close to the transmembrane region of the glycoprotein (Figure 15), leading us to suppose that it could concern a larger conformational epitope. We noticed that those mAbs reacting with the soluble form of Gn showed a lower reactivity than those reacting with the whole protein, thus it seems that the epitope (close to the transmembrane region) present only in the whole protein could affect the strength of the binding. The three regions identified by the neutralizing mAbs are also recognized by both sera with a higher reactivity, confirming the results obtained with mAbs. Studies are in course, in order to analyse and, possibly, measure the affinity strength of these mAbs. Furthermore, the serum drawn during the convalescent phase showed a higher reactivity against the spotted peptides, compared with the serum of the acute phase. This result is probably due to an effect of the activation of the immune system with the production of more specific mAbs with a higher affinity.

Since cross-reactivity of sera among Phleboviruses is quite common, we decided to analyze the capacity of some TOSV glycoproteins mAbs to neutralize viruses of the same genus of TOSV, such as Sandfly Fever Naples Virus (SFNV), Sandfly Fever Sicilian Virus (SFSV), and Punique Virus (PUNV). A preliminary screening on some mAbs, detected one anti TOSV mAb able to neutralize SFNV. Unfortunately, because of a low amount of patient sera, we could not test them against other phleboviruses. On the contrary, mAbs screened with SFSV and PUNV were all negative (Table 8). However, these data must be confirmed on a larger number of samples.

```
  1 NHLLNWPGNG AYTLSDFAES TCTLAYGSEC KSWEHQLDEL SFPFFHSNLD KYSMLEAATE
 61 TIPILNKSSA VCTISPSTHS SNACGREASL IKKKCGSDMS AFFYVNLAGQ ITVVKCDTNH
121 VLSNDCGNCI SKTLSGQKIY TPVQDMFCQK GWSESIPSTR YSKDLCSIGL HTVKECKIGT
181 TNFERVGFIV VKGRKMYIEQ MKMRSRQEFS EDQFLCYKSE GSSGSSVKLK KVKVESCKGV
241 TTSSASKCSG DEYFCSRYPC ETANVEAHCI LRRHSAVIEV NVNGVWVVPR CIGYEEVLVR
301 RTSLKVEDTS SRECDTCLWE CGKNKLIVKT HGPKIVYATA CSHGSCKSVM QKPATFVYLP
361 YPGNSEIVGG DIGVHMTEES SPSNIHMVAH CPAKDSCEVS SCLFCVHGLL NYQCHTLFSA
421 LLISTTVMSI LTLLLLLVKG AKDLVKRLFY WLITPLCWLS VFCGWMIRSW KKRVGSAISR
481 TNDTIGWRDN SRRGQDIERA QYTGGAPGAK YSFYGVMILG LLGNVHS
```

Figure 13. TOSV Gn glycoprotein (GenBank accession no: AEM36009.1 from aa 308–834), aa 1–416 were used to generate membranes of 82 spots.

Overlapping peptides							
1	^{1}NHLLNWPGNGAYTLS^{15}	**25**	^{121}VLSNDSGNSISKTLS^{135}	**49**	^{241}TTSSASKSSGDEYFS^{255}	**73**	^{361}YPGNSEIVGGDIGVH^{375}
2	^{6}WPGNGAYTLSDFAES^{20}	**26**	^{126}SGNSISKTLSGQKIY^{140}	**50**	^{246}SKSSGDEYFSSRYPS^{260}	**74**	^{366}EIVGGDIGVHMTEES^{380}
3	^{11}AYTLSDFAESTSTLA^{25}	**27**	^{131}SKTLSGQKIYTPVQD^{145}	**51**	^{251}DEYFSSRYPSETANV^{265}	**75**	^{371}DIGVHMTEESSPSNI^{385}
4	^{16}DFAESTSTLAYGSES^{30}	**28**	^{136}GQKIYTPVQDMFSQK^{150}	**52**	^{256}SRYPSETANVEAHSI^{270}	**76**	^{376}MTEESSPSNIHMVAH^{390}
5	^{21}TSTLAYGSESKSWEH^{35}	**29**	^{141}TPVQDMFSQKGWSES^{155}	**53**	^{261}ETANVEAHSILRRHS^{275}	**77**	^{381}SPSNIHMVAHSPAKD^{395}
6	^{26}YGSESKSWEHQLDEL^{40}	**30**	^{146}MFSQKGWSESIPSTR^{160}	**54**	^{266}EAHSILRRHSAVIEV^{280}	**78**	^{386}HMVAHSPAKDSSEVS^{400}
7	^{31}KSWEHQLDELSFPFF^{45}	**31**	^{151}GWSESIPSTRYSKDL^{165}	**55**	^{271}LRRHSAVIEVNVNG^{285}	**79**	^{391}SPAKDSSEVSSSLFS^{405}
8	^{36}QLDELSFPFFHSNLD^{50}	**32**	^{156}IPSTRYSKDLSSIGL^{170}	**56**	^{276}AVIEVNVNGVWVVPR^{290}	**80**	^{396}SSEVSSSLFSVHGLL^{410}
9	^{41}SFPFFHSNLDKYSML^{55}	**33**	^{161}YSKDLSSIGLHTVKE^{175}	**57**	^{281}NVNGVWVVPRSIGYE^{295}	**81**	^{401}SSLFSVHGLLNYQSH^{415}
10	^{46}HSNLDKYSMLEAATE^{60}	**34**	^{166}SSIGLHTVKESKIGT^{180}	**58**	^{286}WVVPRSIGYEEVLVR^{300}	**82**	^{406}SLFSVHGLLNYQSHT^{420}
11	^{51}KYSMLEAATETIPIL^{65}	**35**	^{171}HTVKESKIGTTNFER^{185}	**59**	^{291}SIGYEEVLVRRTSLK^{305}		
12	^{56}EAATETIPILNKSSA^{70}	**36**	^{176}SKIGTTNFERVGFIV^{190}	**60**	^{296}EVLVRRTSLKVEDTS^{310}		
13	^{61}TIPILNKSSAVSTIS^{75}	**37**	^{181}TNFERVGFIVVKGRK^{195}	**61**	^{301}RTSLKVEDTSSRESD^{315}		
14	^{66}NKSSAVSTISPSTHS^{80}	**38**	^{186}VGFIVVKGRKMYIEQ^{200}	**62**	^{306}VEDTSSRESDTSLWE^{320}		
15	^{71}VSTISPSTHSSNASG^{85}	**39**	^{191}VKGRKMYIEQMKMRS^{205}	**63**	^{311}SRESDTSLWESGKNK^{325}		
16	^{76}PSTHSSNASGREASL^{90}	**40**	^{196}MYIEQMKMRSRQEFS^{210}	**64**	^{316}TSLWESGKNKLIVKT^{330}		
17	^{81}SNASGREASLIKKKS^{95}	**41**	^{201}MKMRSRQEFSEDQFL^{215}	**65**	^{321}SGKNKLIVKTHGPKI^{335}		
18	^{86}REASLIKKKSGSDMS^{100}	**42**	^{206}RQEFSEDQFLSYKSE^{220}	**66**	^{326}LIVKTHGPKIVYATA^{340}		
19	^{91}IKKKSGSDMSAFFYV^{105}	**43**	^{211}EDQFLSYKSEGSSGS^{225}	**67**	^{331}HGPKIVYATASSHGS^{345}		
20	^{96}GSDMSAFFYVNLAGQ^{110}	**44**	^{216}SYKSEGSSGSSVKLK^{230}	**68**	^{336}VYATASSHGSSKSVM^{350}		
21	^{101}AFFYVNLAGQITVVK^{115}	**45**	^{221}GSSGSSVKLKKVKVE^{235}	**69**	^{341}SSHGSSKSVMQKPAT^{355}		
22	^{106}NLAGQITVVKSDTNH^{120}	**46**	^{226}SVKLKKVKVESSKGV^{240}	**70**	^{346}SKSVMQKPATFVYLP^{360}		
23	^{111}ITVVKSDTNHVLSND^{125}	**47**	^{231}KVKVESSKGVTTSSA^{245}	**71**	^{351}QKPATFVYLPYPGNS^{365}		
24	^{116}SDTNHVLSNDSGNSI^{130}	**48**	^{236}SSKGVTTSSASKSSG^{250}	**72**	^{356}FVYLPYPGNSEIVGG^{370}		

Table 6. 82 peptides 15 aa–long shifted by 5 residues, covering TOSV Gn glycoprotein aa 1–416 (GenBank accession no: AEM36009.1 from aa 308–723).

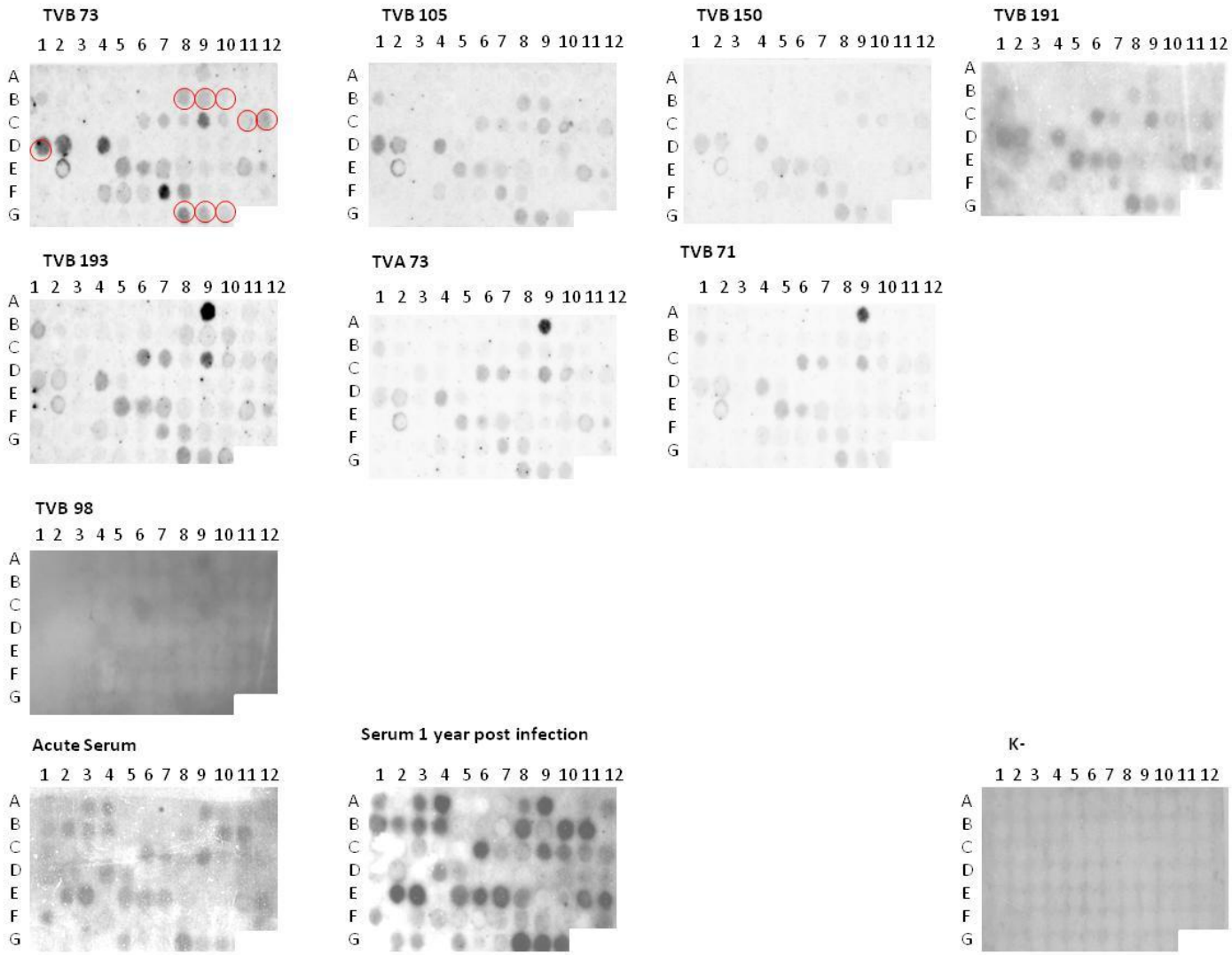

Figure 14. Membrane probed with: mAbs with a neutralization titre> 1: 512; patient sera (acute and 1 year post-infection); one mAbs positive to Gc glycoprotein (TVB 98); two non neutralizing mAbs positive to Gn, one mAb of the acute phase (TVA 73) and one of the convalescent phase (TVB 71) and only the secondary antibody (K-). The circles indicate the three regions of interest.

Table 7. Analysis of spots reactivity.

				Reactivity	0%	<25%	25-50%	>50-75%	>75%				
			mAbs										
		NT Titre	**>1:512**	**>1:512**	**>1:512**	**>1:512**	**1:645**	**NEG**	**NEG**	**NEG**	**1:161**	**1:323**	
		Overlappingpeptides	**TVB 73**	**TVB 105**	**TVB 150**	**TVB 191**	**TVB 193**	**TVB 71**	**TVA 73**	**TVB 98**	**Acute Serum**	**Serum 1 year later infection**	
A1	1	^{1}NHLLNWPGNGAYTLS^{15}										+	
A2	2	^{6}WPGNGAYTLSDFAES^{20}											
A3	3	^{11}AYTLSDFAESTSTLA^{25}									+	+	
A4	4	^{16}DFAESTSTLAYGSES^{30}									+	+	
A5	5	^{21}TSTLAYGSESKSWEH^{35}											
A6	6	^{26}YGSESKSWEHQLDEL^{40}											
A7	7	^{31}KSWEHQLDELSFPFF^{45}											
A8	8	^{36}QLDELSFPFFHSNLD^{50}				+						+	
A9	9	^{41}SFPFFHSNLDKYSML^{55}	+				+	+	+	+	+	+	
A10	10	^{46}HSNLDKYSMLEAATE^{60}									+		
A11	11	^{51}KYSMLEAATETIPIL^{65}									+		
A12	12	^{56}EAATETIPILNKSSA^{70}										+	
B1	13	^{61}TIPILNKSSAVSTIS^{75}	+	+		+	+	+	+		+	+	
B2	14	^{66}NKSSAVSTISPSTHS^{80}									+	+	
B3	15	^{71}VSTISPSTHSSNASG^{85}									+	+	
B4	16	^{76}PSTHSSNASGREASL^{90}									+	+	
B5	17	^{81}SNASGREASLIKKKS^{95}											
B6	18	^{86}REASLIKKKSGSDMS^{100}											
B7	19	^{91}IKKKSGSDMSAFFYV^{105}											
B8	20	^{96}GSDMSAFFYVNLAGQ^{110}	+	+	+	+	+				+	+	*
B9	21	^{101}AFFYVNLAGQITVVK^{115}	+	+	+	+	+						* REGION 1
B10	22	^{106}NLAGQITVVKSDTNH^{120}					+				+	+	*
B11	23	^{111}ITVVKSDTNHVLSND^{125}									+	+	
B12	24	^{116}SDTNHVLSNDSGNSI^{130}											
C1	25	^{121}VLSNDSGNSISKTLS^{135}									+		
C2	26	^{126}SGNSISKTLSGQKIY^{140}											
C3	27	^{131}SKTLSGQKIYTPVQD^{145}										+	
C4	28	^{136}GQKIYTPVQDMFSQK^{150}											
C5	29	^{141}TPVQDMFSQKGWSES^{155}											
C6	30	^{146}MFSQKGWSESIPSTR^{160}	+	+		+	+	+	+	+	+	+	
C7	31	^{151}GWSESIPSTRYSKDL^{165}	+	+		+	+	+	+		+	+	
C8	32	^{156}IPSTRYSKDLSSIGL^{170}	+	+								+	
C9	33	^{161}YSKDLSSIGLHTVKE^{175}	+	+	+	+	+	+	+	+	+	+	
C10	34	^{166}SSIGLHTVKESKIGT^{180}	+		+		+	+	+			+	
C11	35	^{171}HTVKESKIGTTNFER^{185}	+									+	*
C12	36	^{176}SKIGTTNFERVGFIV^{190}	+	+	+	+						+	* REGION 2
D1	37	^{181}TNFERVGFIVVKGRK^{195}	+	+	+	+	+	+	+				*
D2	38	^{186}VGFIVVKGRKMYIEQ^{200}	+	+	+	+	+		+				
D3	39	^{191}VKGRKMYIEQMKMRS^{205}											
D4	40	^{196}MYIEQMKMRSRQEFS^{210}	+	+	+	+	+	+	+	+	+	+	
D5	41	^{201}MKMRSRQEFSEDQFL^{215}									+	+	

D6	42	^{206}RQEFSEDQFLSYKSE^{220}											
D7	43	^{211}EDQFLSYKSEGSSGS^{225}											
D8	44	^{216}SYKSEGSSGSSVKLK^{230}											
D9	45	^{221}GSSGSSVKLKKVKVE^{235}											
D10	46	^{226}SVKLKKVKVESSKGV^{240}											+
D11	47	^{231}KVKVESSKGVTTSSA^{245}											+
D12	48	^{236}SSKGVTTSSASKSSG^{250}											+
E1	49	^{241}TTSSASKSSGDEYFS^{255}											
E2	50	^{246}SKSSGDEYFSSRYPS^{260}				+						+	+
E3	51	^{251}DEYFSSRYPSETANV^{265}										+	+
E4	52	^{256}SRYPSETANVEAHSI^{270}											
E5	53	^{261}ETANVEAHSILRRHS^{275}	+	+	+	+	+	+	+		+	+	
E6	54	^{266}EAHSILRRHSAVIEV^{280}	+	+	+	+	+	+	+		+	+	
E7	55	^{271}LRRHSAVIEVNVNG^{285}	+	+	+	+	+	+	+		+	+	
E8	56	^{276}AVIEVNVNGVWVVPR^{290}		+									+
E9	57	^{281}NVNGVWVVPRSIGYE^{295}											
E10	58	^{286}WVVPRSIGYEEVLVR^{300}											
E11	59	^{291}SIGYEEVLVRRTSLK^{305}	+	+	+	+	+	+					+
E12	60	^{296}EVLVRRTSLKVEDTS^{310}	+									+	+
F1	61	^{301}RTSLKVEDTSSRESD^{315}										+	+
F2	62	^{306}VEDTSSRESDTSLWE^{320}											
F3	63	^{311}SRESDTSLWESGKNK^{325}											+
F4	64	^{316}TSLWESGKNKLIVKT^{330}	+	+	+			+					+
F5	65	^{321}SGKNKLIVKTHGPKI^{335}	+										
F6	66	^{326}LIVKTHGPKIVYATA^{340}	+										
F7	67	^{331}HGPKIVYATASSHGS^{345}	+	+	+	+	+	+	+				
F8	68	^{336}VYATASSHGSSKSVM^{350}	+	+	+		+	+	+				+
F9	69	^{341}SSHGSSKSVMQKPAT^{355}											+
F10	70	^{346}SKSVMQKPATFVYLP^{360}											
F11	71	^{351}QKPATFVYLPYPGNS^{365}											
F12	72	^{356}FVYLPYPGNSEIVGG^{370}										+	+
G1	73	^{361}YPGNSEIVGGDIGVH^{375}											
G2	74	^{366}EIVGGDIGVHMTEES^{380}											+
G3	75	^{371}DIGVHMTEESSPSNI^{385}											+
G4	76	^{376}MTEESSPSNIHMVAH^{390}											
G5	77	^{381}SPSNIHMVAHSPAKD^{395}										+	+
G6	78	^{386}HMVAHSPAKDSSEVS^{400}											
G7	79	^{391}SPAKDSSEVSSSLFS^{405}											+
G8	80	^{396}SSEVSSSLFSVHGLL^{410}	+	+	+	+	+	+	+	+	+	+	*
G9	81	^{401}SSLFSVHGLLNYQSH^{415}	+	+	+	+	+	+	+		+	+	* REGION 3
G10	82	^{406}SLFSVHGLLNYQSHT^{420}	+	+	+	+	+	+	+		+	+	*

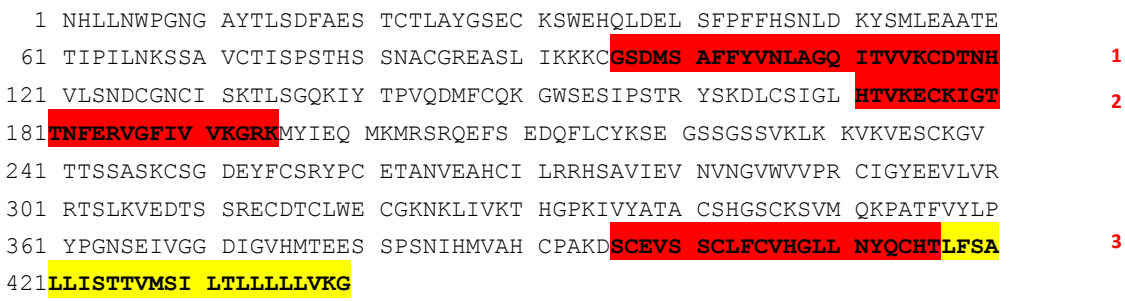

Figure 15. In red, the three regions identified by pepscan analysis. In yellow, the transmembrane region of TOSV Gn glycoprotein (LFSALLISTTVMSILTLLLLLVK), (aa 724–746 of TOSV polyprotein).

Table 8. Neutralization assay with SFNV,PUNV and SFSV.

mAbs ID	NT CPE 50%			
1 year post infection	**TOSV**	**SFNV**	**PUNV**	**SFNV**
TVB27	1:161	1:25	-	-
TVB73	>1:512	-	-	-
TVB 98	-	-	-	-
TVB147	1:645	-	-	-
TVB161	1:645	-	-	-
TVB164	1:6	-	-	-

By using an improved memory B cells immortalization method (Traggiai et al. 2004), combined with parallel high throughput screening for TOSV antigens, we could isolate a panel of human mAbs which we characterized with regard to epitope specificity and neutralizing activity.

We demonstrated that most of the neutralizing antibodies are directed to TOSV glycoproteins and they mature with time, in fact they were all obtained from PBMCs of the convalescent phase serum. Focusing on Gn glycoprotein, an important neutralizing epitope is probably present near the transmembrane region, as demonstrated by some neutralizing mAbs that resulted reactive against Gn only when expressed on the surface of Lenti-X HEK293.

These data are in agreement with pepscan analysis which showed an antibody reactivity with the peptides present in the first half and near the transmembrane region of the protein, leading us to hypothesize that these sequences are part of a conformational epitope. The specificity of these regions were also confirmed by membrane probed with both patient's sera. Furthermore, a higher reactivity of the convalescent serum was observed in comparison with that of the serum drawn at the acute phase, either for intensity and number of spots. This is in line with the increase specificity that was acquired after the activation of the immune response and also confirm the results obtained with the neutralization screening where no mAbs of the acute phase have neutralizing activity while all neutralizing mAbs were derived from the convalescent phase.

Finally we evaluated the possible serological cross-reactivity of some TOSV mAbs to viruses belonging to the same Phlebovirus genus. We found, among 6 mAbs tested by neutralization assay for SFNV, SFSV and PUNV, only one (TVB 27) showed reactivity with SFNV. This is only a preliminary screening and a larger analysis must be carried out. It could be interesting to detect epitopes shared by other phleboviruses that could be exploited for a potential vaccine protecting against several sandfly viruses.

Chapter 6

Conclusions

In the recent years, several arboviruses have become increasingly important human pathogens causing neurologic disease. Among them, Toscana virus (TOSV) belonging to the *Bunyaviridae* family, is considered an emergent phlebovirus, etiologic agent of acute neurological disease, such as meningitis, meningoencephalitis and encephalitis, occurring in the Mediterranean countries (principally Italy, Spain, France) during the summer months (Valassina et al. 2003a; Valassina et al. 2003b; Charrel et al. 2005; Sanbonmatsu –Gàmez et al. 2009; Cusi et al. 2010). TOSV is transmitted to humans by sandflies of Phlebotomus species, in particular *Phlebotomus perniciosus* and *Phlebotomus perfiliewi.* Changes in the natural distribution and density of these arthropod vectors, influenced by climate change and environmental modifications, can allow the spread of this phlebovirus to new geographic areas and may facilitate the transmission to humans, leading frequently to disease that is not diagnosed by physicians.

Aim of this PhD project was to understand the basis of TOSV pathogenesis, with the identification of permissive cells where viral replication occurs, allowing TOSV to reach the CNS; subsequently with the characterization of envelope glycoproteins as pathogenic determinants, we tried to identify conserved epitopes targeted by human specific neutralizing monoclonal antibodies.

In the first part of results, we have demonstrated that TOSV, before entering the bloodstream, is able to infect and replicate both in moDCs and in endothelial cells. TOSV, indeed, is free to move in the blood and it is not vehiculated by specific blood mononuclear cells, as revealed by the absence of viral genome in specific blood cells. These results were *in vivo* confirmed using mouse as animal model. Mice were subcutaneously infected by TOSV, in order to reproduce the natural route of human infection. The virus migrated from the skin, infecting DCs causing their activation, to the draining lymph nodes and, after replication in the endothelial cells, it reached the spleen (Gori Savellini G. et al. 2008) where, probably, a secondary virus replication occurred. Further, through unidentified mechanisms, TOSV could enter the central nervous system (CNS) and cause neurological disease. We have noticed in *in vivo* experiments that the endothelial cells in the brain sections of infected mice were positive to TOSV antigen few days after infection, providing the proof of concept that the virus can reach the CNS without causing disease. In these infected mice, at the vascular level (particularly the venulae in derma), we noticed the presence of inflammatory cell infiltrates, monocytes and, particularly, CD8+ lymphocytes, probably involved in the alteration of vascular permeability. In fact, as previously demonstrated, dysregulation of the blood-brain barrier (BBB) is a hallmark feature of numerous viral neurologic disorders (Koyuncu et al. 2013), and CD8+ cells are a cell population that can promote vascular permeability in these conditions. These data were also confirmed *in vitro* by testing supernatants of infected DCs and endothelial cells. A high amount of

TNF-α was detected in the supernatant of TOSV infected DCs, indicating an activation of the immune system. Moreover, a significant increase of IL-6, an inflammatory cytokine involved in vascular damage or inflammation of the vascular wall, was detected in the supernatant of infected HUVECs. Its presence led us to suppose that it could have an important role in the modulation of brain endothelium structure during TOSV infection. The virus, in this way, might indirectly act by triggering the release of proinflammatory lymphokines, inducing leukocyte activation, that in turn, would activate or damage endothelial cells themselves. Due to these changes, the virus could cross the BBB either destroying the lining of the endothelium or by passive passage through the endothelial cells. Crossing the endothelium, the virus may enter the cerebrospinal fluid (CSF). Thus, once in the CSF, TOSV may remain limited to the meninges, causing meningitis or meningoencephalitis or it may enter the brain parenchyma, causing the neurological disease. All these data could partly provide an explanation to some events described as serious manifestations of this infectious disease, such as ischemic complication and lethal encephalitis (Sanbonmatsu –Gàmez S. et. al 2009). These results also, indicate that replication in the endothelium may be important either for the maintainance of viremia and as a grow- through mechanism for neuroinvasion.

Future prospects will focus on a better understanding of the molecular mechanisms of virus neuroinvasion. However, we better defined the role of inflammatory cell infiltrates, mainly CD8+ lymphocytes, in the alteration of vascular permeability of the infected tissues. Finally, the role of L-SIGN molecule is under investigation as possible TOSV candidate receptor on endothelial cells, since some studies have recognized this molecule as receptor for other phleboviruses (Pustylnikov et al. 2014; Van Breedam et al. 2014; Léger et al. 2016).

In the second section, we investigated TOSV glycoproteins as targets for neutralizing monoclonal antibodies. Despite their important role in viral entry and release, biological activities of TOSV Gn and Gc glycoproteins are incompletely understood. The glycoproteins mediate the first step in phlebovirus replication cycle and are targets for neutralizing antibodies (Spiegel et al. 2016). The analysis of the human immune response with the isolation of neutralizing antibodies offer a solution to identify conserved epitopes within viral glycoproteins. To this aim, we selected a patient with menininigitis diagnosed with TOSV infection. Memory B cells obtained from PBMCs during the acute phase and convalescent phase were immortalized for the isolation of B cell clones producing monoclonal antibodies. The antibodies secreted in the culture supernatants were examined against TOSV antigens in order to characterize their specificity and to select those with neutralizing activity. We excluded mAbs reactive to TOSV N-protein and we focused on mAbs reacting with TOSV glycoproteins. Among the viral glycoproteins binding antibodies, we selected those having

neutralizing activity. The high prevalence of antibodies reactive against TOSV Gn allowed us to first characterize Gn sites reacting with neutralizing mAbs, using pepscan analysis. Overlapping peptides covering the Gn aminoacidic sequence, excluding the transmembrane region, were spotted on cellulose-based membranes and probed with neutralizing mAbs. Three different aminoacidic regions were identified as reacting to the mAbs, but they were not overlapping. This feature let us to hypothesize that these regions are part of a larger conformational epitope that can be recognized when exposed on the viral envelope. These peptides are also recognized by both sera, with a higher reactivity of the serum drawn one year before infection. These results are justified by the selection, during the maturation of the immune response, of antibodies with increased affinity produced after specific B lymphocytes clonal expansion, class switch and somatic hypermutation (Rajewsky 1996).

Finally, we tested mAbs cross-reactivity to other phleboviruses related to TOSV (Charrel RN et al. 2009; Collao X et al. 2010 Zhioua E et al. 2010). A preliminary neutralization test of some human mAbs against SFNV, PUNV and SFSV, highlighted only one mAb cross-reactive to SFNV. However, these are very preliminary data and a higher number of mAbs are under analysis.

The next step will be to characterize other specific Gn mAbs with pepscan analysis, in order to confirm or identify new neutralizing epitopes, then to broaden the study, we will start to characterize the Gc glycoprotein mAbs. Moreover, it is worthy to note that these results were based only on the screening of mAbs derived from one patient. Thus, this study will be opened to other TOSV positive patients, to characterize further antibodies and enlarge the spectrum of functional epitopes. Additionally, selected mAbs will be analyzed for their cross-reactivity to antigens related TOSV virus and other phleboviruses, with the aim to isolate mAbs able to confer cross-protection to viruses of the same species. In the future, based on these findings, it would be ideal to formulate a cocktail of two to three antibodies with broadly neutralizing activity, thus providing broad protection against TOSV and serological related viruses (Traggiai et al. 2008; Rockx et al. 2008). Finally, the characterization of these conserved epitopes could give important clues for a vaccine design against Phleboviruses.

Chapter 7

Bibliography

Abbott, N. J. (2004). Evidence for bulk flow of brain interstitial fluid: significance for physiology and pathology. Neurochem. Int. 45, 545–552.

Abbott, N.J., Rönnbäck, L., Hansson, E., (2006).Astrocyte–endothelial interactions at the blood–brain barrier. Nature Rev. Neurosci. 7, 41–53.

Acton SE, Astarita JL, Malhotra D, Lukacs-Kornek V, Franz B, Hess PR, Jakus Z, Kuligowski M, Fletcher AL, Elpek KG, Bellemare- Pelletier A, Sceats L, Reynoso ED, Gonzalez SF, Graham DB, Chang J, Peters A, Woodruff M, Kim YA, Swat W, Morita T, Kuchroo V, Carroll MC, Kahn ML, Wucherpfennig KW, Turley SJ (2012) Podoplanin-rich stromal networks induce dendritic cell motility via activation of the C-type lectin receptor CLEC-2. Immunity 37(2):276–289.

Albarino CG, Bird BH, Nichol ST. A shared transcription termination signal on negative and ambisense RNA genome segments of Rift Valley fever, sandly fever Sicilian, and Toscana viruses. J Virol 2007;81:5246–5256.

Alexopoulou L, Holt AC, Medzhitov R, Flavell RA (2001) Recognition of double-stranded RNA and activation of NF-kB by Toll-like receptor 3. Nature 413: 732–738.

Allenspach EJ, Lemos MP, Porrett PM, Turka LA, Laufer TM (2008) Migratory and lymphoid-resident dendritic cells cooperate to efficiently prime naive CD4 T cells. Immunity 29: 795–806.

Amodio, E., Cusi, M.G., Valenti, R.M., Valentini, M., Mammina, C., Gori-Savellini, G., Vitale, F., Romano, N., Goedert, J.J., Calamusa, G., 2012. Immunoglobulin M seropositivity for Toscana virus in a random population sample in Sicily. Int. J. Infect Dis. 16, e633–e635.

Arancibia SA, Beltran CJ, Aguirre IM, Silva P, Peralta AL, Malinarich F, et al. Toll-like receptors are key participants in innate immune responses. Biol Res 2007;40:97–112.

Arikawa, J., Schmaljohn, A.L., Dalrymple, J.M., Schmaljohn, C.S., 1989. Characterization of Hantaan virus envelope glycoprotein antigenic determinants defined by monoclonal antibodies. J. Gen. Virol. 70, 615–624.

Auwerx J, Franc¸ois KO, Vanstreels E, et al. Capture and transmission of HIV-1 by the C-type lectin L-SIGN (DC-SIGNR) is inhibited by carbohydrate-binding agents and polyanions. Antiviral Res 2009;83(1):61–70.

Azad AK, Torrelles JB, Schlesinger LS. Mutation in the DC-SIGN cytoplasmic triacidic cluster motif markedly attenuates receptor activity for phagocytosis and endocytosis of mannose-containing ligands by human myeloid cells. J Leukoc Biol. 2008;84(6):1594-1603.

Baldelli F, Ciufolini MG, Francisci D, Marchi A, Venturi G, Fiorentini C, Luchetta ML, Bruto L, Pauluzzi S. Unusual presentation of life-threatening Toscana virus meningoencephalitis. Clin Infect Dis 2004; 38: 515-520

Baluk P, Fuxe J, Hashizume H, Romano T, Lashnits E, Butz S, Vestweber D, Corada M, Molendini C, Dejana E, McDonald DM (2007) Functionally specialized junctions between endothelial cells of lymphatic vessels. J Exp Med 204(10):2349–2362.

Bartelloni PJ, Tesh RB. Clinical and serologic responses of volunteers infected with phlebotomus fever virus (Sicilian type) (1976). Am J Trop Med Hyg.;25:456–62.

Bartels S., De Boni L., Kretzschmar H.A., Heckmann J.G. (2011). Lethal encephalitis caused by the Toscana virus in an elderly patient. J. Neurol. Jun 9.

Bashirova AA, Geijtenbeek TB, van Duijnhoven GC, et al. A dendritic cell-specific intercellular adhesion molecule 3-grabbing nonintegrin (DC-SIGN)-related protein is highly expressed on human liver sinusoidal endothelial cells and promotes HIV-1 infection. J ExpMed 2001;193(6):671–678.

Bell D, Young JW, Banchereau J (1999) Dendritic cells. Adv Immunol 72:255–324.

Beltramello M, Williams KL, Simmons CP, Macagno A, Simonelli L, Quyen NTH, Sukupolvi-Petty S, Navarro-Sanchez E, Young PR, de Silva AM, Rey FA, Varani L, Whitehead SS, Diamond MS, Harris E, Lanzavecchia A, Sallusto F. 2010. The human immune response to Dengue virus is dominated by highly cross-reactive antibodies endowed with neutralizing and enhancing activity. Cell Host Microbe 8:271–283.

Belz G, Mount A, Masson F. Dendritic cells in viral infections. Handb Exp Pharmacol. 2009;188:51-77.

Bennett RS, Cress CM, Ward JM, Firestone C-Y, Murphy BR,Whitehead SS. La Crosse virus infectivity, pathogenesis, and immunogenicity in mice and monkeys. Virol J 2008;5:25.

Bergman MP, Engering A, Smits HH, et al. Helicobacter pylorimodulates the T helper cell 1/T helper cell 2 balance through phase-variable interaction between lipopolysaccharide and DC-SIGN. J Exp Med 2004;200(8):979–990.

Bernard Q, Jaulhac B, Boulanger N. Skin and arthropods: an effective interaction used by pathogens in vector-borne diseases. 2015;25(April):18-22. doi:10.1684/ejd.2015.2550.

Bichaud, L.; Dachraoui, K.; Alwassouf, S.; Alkan, C.; Mensi, M.; Piorkowski, G.; Sakhria, S.; Seston, M.; Fares, W.; de Lamballerie, X.; et al. Isolation, full genomic characterization and neutralization-based human seroprevalence of Medjerda Valley virus, a novel sandfly-borne phlebovirus belonging to the

Salehabad virus complex in northern Tunisia. J. Gen. Virol. 2016, 97, 602–610.

Bishop D, Gay M, Matsuoko Y. (1983). Nonviral heterogeneous sequences are present at the 5' ends of one species of snowshoe hare bunyavirus S complementary RNA. Nucleic Acids Res;11:6409–6419.

Boshra, H.; Lorenzo, G.; Busquets, N.; Brun, A. Rift Valley fever: Recent insights into pathogenesis and prevention. J. Virol. 2011, 85, 6098–6105.

Bouloy M, Hannoun C. (1976). Studies on lumbo virus replication I. RNA-dependent RNA polymerase associated with virions. Virology;69:258–264.

Braito A, Ciufolini MG, Pippi L, Corbisiero R, Fiorentini C, Gistri A, Toscano L. Phlebotomus-transmitted toscana virus infections of the central nervous system: a seven-year experience in Tuscany. Scand J Infect Dis 1998; 30: 505-508.

Braito A, Corbisiero R, Corradini S, Fiorentini C, Ciufolini MG. Toscana virus infections of the central nervous system in children: a report of 14 cases. J Pediatr 1998; 132: 144-148.

Braito, A., Corbisiero, R., Corradini, S., Marchi, B., Sancasciani, N., Fiorentini, C. & Ciufolini, M. G. (1997). Evidence of Toscana virus infections without central nervous system involvement: a serological study. Eur J Epidemiol 13, 761–764.

Briant L, Desprès P, Choumet V, Missé D. Role of skin immune cells on the host susceptibility to mosquito-borne viruses. Virology. 2014;464-465(1):26-32.

Brisbarre N., Attoui H., Gallian P., Di Bonito P., Giorgi C., Cantaloube J.F., et al. (2011). Seroprevalence of Toscana virus in blood donors, France, 2007. Emerg. Infect. Dis. 17, 941-943.

Butler M, Spearman M. The choice of mammalian cell host and possibilities for glycosylation engineering. Curr. Opin. Biotechnol. 30C, 107–112 (2014).

Calamusa, G., Valenti, R.M., Vitale, F., Mammina, C., Romano, N., Goedert, J.J., Gori- Savellini, G., Cusi, M.G., Amodio, E., 2012. Seroprevalence of and risk factors for Toscana and Sicilian virus infection in a sample population of Sicily (Italy). J. Infect. 64, 212–217.

Cambi A,Gijzen K,de Vries IJ, et al.TheC-type lectin DC-SIGN(CD209) is an antigen-uptake receptor for Candida albicans on dendritic cells. Eur J Immunol 2003;33(2):532–538.

Canavoso LE, Jouni ZE, Karnas KJ, Pennington JE, Wells MA. Fat metabolism in insects. Annu. Rev. Nutr. 21, 23–46 (2001).

Carroll MV, Sim RB, Bigi F, et al. Identification of four novel DC-SIGN ligands on Mycobacterium bovis BCG. Protein Cell 2010;1(9):859–870.

Centre of Disease Control and Prevention, CDC, Division of Vector-borne.Disease http://www.cdc.gov/ncezid/dvbd/index.html [Page last updated:April 2, 2016]

Cera MR, Del Prete A, Vecchi A, Corada M, Martin-Padura I, Motoike T, Tonetti P, Bazzoni G, Vermi W, Gentili F, Bernasconi S, Sato T, Mantovani A, Dejana E (2004) Increased DC trafficking to lymph nodes and contact hypersensitivity in junctional adhesion molecule-A-deficient mice. J Clin Investig 114(5):729–738.

Chan VS, Chan KY, Chen Y, et al. Homozygous L-SIGN (CLEC4M) plays a protective role in SARS coronavirus infection. Nat Genet 2006;38(1):38–46.

Chan-Ling T, McLeod DS, Hughes S, et al. Astrocyte-endothelial cell relationships during human retinal vascular development. Invest Ophthalmol Vis Sci. 2004;45(6):2020-2032.

Charrel Rèmi N. , Gallian Pierre , Navarro-Mari Josè-Maria, Nicoletti Loredana , Papa Anna, Sànchez Seco Màaria Paz, Tenorio Antonio, e de Lambelleire Xavier (2005). Emergency of Toscana Virus in Europe. Emergency Infection Diseas , Vol.11,No.11, November 2005.

Charrel RN, Bichaud L, Lamballerie X De. Emergence of Toscana virus in the mediterranean area. 2012;1(5):135-141.

Charrel RN, Moureau G, Temmam S, Izri A, Marty P, Parola P, da Rosa AT, Tesh RB, de Lamballerie X. Massilia virus, a novel Phlebovirus (Bunyaviridae) isolated from sandflies in the Mediterranean. Vector Borne Zoonotic Dis 2009; 9: 519-530.

Ciufolini MG, Maroli M, Verani P. Growth of two phleboviruses after experimental infection of their suspected sand fly vector, Phlebotomus perniciosus (Diptera: Psychodidae). Am J Trop Med Hyg 1985; 34: 174-179.

Clay CC, Rodrigues DS, Ho YS, Fallert BA, Janatpour K, Reinhart TA, Esser U: Neuroinvasion of fluorescein-positive monocytes in acute simian immunodeficiency virus infection. J Virol 2007, 81:12040-12048.

Collao X, Palacios G, de Ory F, Sanbonmatsu S, Pérez-Ruiz M, Navarro JM, Molina R, Hutchison SK, Lipkin WI, Tenorio A, Sánchez-Seco MP. Granada virus: a natural phlebovirus reassortant of the sandfly fever Naples serocomplex with low seroprevalence in humans. Am J Trop Med Hyg 2010; 83: 760-765.

Collao X, Palacios G, Sanbonmatsu-Gámez S, et al. Genetic diversity of Toscana virus. Emerg Infect Dis 2009; 15: 574-7

Collao X, Palacios G, Sanbonmatsu-gámez S, et al. of Toscana Virus. 2009;15(4):574-577.

Collett MS, Purchio AF, Keegan K, et al. (1985). Complete nucleotide sequence of the M RNA segment of Rift Valley fever virus. Virology 144:228–245.

Colmenares M, Puig-Kr¨oger A, Pello OM, et al. Dendritic cell (DC)-specific intercellular adhesion molecule 3 (ICAM-3)-grabbing nonintegrin (DC-SIGN, CD209), a C-type surface lectin in human DCs, is a receptor for Leishmania amastigotes. J Biol Chem 2002;277(39):36766–36769.

Colomba, C., Saporito, L., Ciufolini, M.G., Marchi, A., Rotolo, V., De Grazia, S., Titone, L., Giammanco, G.M., 2012. Prevalence of Toscana sandfly fever virus antibodies in neurological patients and control subjects in Sicily. New Microbiol. 35, 161– 165.

Combes V,Guillemin GJ,Chan-Ling T,Hunt NH,Grau GE. (2012). The crossroads of neuroinflammation in infectious diseases: endothelial cells and astrocytes. Trends Parasitol. 28(8):311-9.

Corti D, Langedijk JPM, Hinz A, Seaman MS, Vanzetta F, Fernandez- Rodriguez BM, Silacci C, Pinna D, Jarrossay D, Balla-Jhagjhoorsingh S, Willems B, Zekveld MJ, Dreja H, O'Sullivan E, Pade C, Orkin C, Jeffs SA, Montefiori DC, Davis D, Weissenhorn W, McKnight A, Heeney JL, Sallusto F, Sattentau QJ, Weiss RA, Lanzavecchia A. 2010. Analysis of memory B cell responses and isolation of novel monoclonal antibodies with neutralizing breadth from HIV-1-infected individuals. PLoS One 5:e8805.

Corti D, Sallusto F, Lanzavecchia A. High throughput cellular screens to interrogate the human T and B cell repertoires. Curr Opin Immunol. 2011;23(3):430-435.

Cumberbatch M, Kimber I (1995) Tumour necrosis factor-alpha is required for accumulation of dendritic cells in draining lymph nodes and for optimal contact sensitization. Immunology 84(1):31–35.

Cunningham AL, Donaghy H, Harman AN, Kim M, Turville SG. Manipulation of dendritic cell function by viruses. Curr Opin Microbiol. 2010;13(4):524-529.

Cusi M.G.,Gori Savellini G.,Zanelli G. (2010) Toscana virus epidemiology :from Italy to beyond. The open virology Journal 4:22-28.

Cusi MG, Gori Savellini G, Terrosi C, Di Genova G, Valassina M, Valentini M, Bartolommei S, Miracco C. Development of a mouse model for the study of Toscana virus pathogenesis. Virology 2005; 333: 66-73.

Cusi, M.G., Valensin, P.E., Donati, M., Valassina, M., 2001. Neutralization of Toscana virus is partially mediated by antibodies to the nucleocapsid protein. J. Med. Virol. 63, 72–75.

Cusi, M.G., Valentini, M., Valensin, P.E., Valassina, M., 2002. Immune response to the neurotropic Toscana virus infection: preliminary data. 1st SIV International Workshop on Neurovirology. Alghero, June 23–25, Italy.

Czeloth N, Bernhardt G, Hofmann F, Genth H, Forster R (2005) Sphingosine-1-phosphate mediates migration of mature dendritic cells. J Immunol 175(5):2960–2967.

Daniele Serata, Chiara Rapinesi, Antonio Del Casale, Alessio Simonetti,Lorenzo Mazzarini, Elisa Ambrosi, Giorgio D. Kotzalidis, Claudio Fensore, Paolo Girardi & Roberto Tatarelli (2011) Personality Changes After Toscana Virus (TOSV) Encephalitis in a 49-Year-Old Man: A Case Report, International Journal of Neuroscience, 121:3, 165-169.

Daniels BP, Holman DW, Cruz-Orengo L, Jujjavarapu H, Durrant DM, Klein RS: Viral pathogen-associated molecular patterns regulate blood–brain barrier integrity via competing innate cytokine signals. mBio 2014:5.

De Haan, P. et al., 1990. The S RNA segment of tomato spotted wilt virus has an ambisense character. Journal of General Virology, 71(5), pp.1001–1007.

Dejana, E., Orsenigo, F., and Lampugnani, M.G. (2008). The role of adherens junctions and VE-cadherin in the control of vascular permeability. J. Cell Sci. 121, 2115–2122.

Di Bonito, P., Bosco, S., Mochi, S., Accardi, L., Ciufolini, M.G., Nicoletti, L., Giorgi, C., 2002. Human antibody response to Toscana virus glycoproteins expressed by recombinant baculovirus. J. Med.Virol. 68, 615–619.

Di Bonito, P., Mochi, S., Gro, M.C., Fortini, D., Giorgi, C., 1997. Organization of the M genomic segment of Toscana phlebovirus. J. Gen. Virol. 76, 77–81.

Di Nicuolo, G., Pagliano, P., Battisti, S., Starace, M., Mininni, V., Attanasio, V., Faella, F.S., 2005. Toscana virus central nervous system infections in southern Italy. J Clin Microbiol 43, 6186–6188.

Di Pucchio T, Chatterjee B, Smed-So¨rensen A, Clayton S, Palazzo A, et al. (2008) Direct proteasome-independent cross-presentation of viral antigen by plasmacytoid dendritic cells on major histocompatibility complex class I. Nat Immunol 9: 551–557.

Dionisio D, Esperti F, Vivarelli A, Valassina M. Epidemiological, clinical and laboratory aspects of sandfly fever. Curr Opin Infect Dis. 2003;16(5):383-388.

Dittmar S, Harms H, Runkler N, Maisner A, Kim KS, Schneider- Schaulies J: Measles virus-induced block of transendothelial migration of T lymphocytes and infection-mediated virus spread across endothelial cell barriers. J Virol 2008, 82:11273-11282.

Elliott, R.M.; Brennan, B. Emerging phleboviruses. Curr. Opin. Virol. 2014, 5, 50–57.

Ellis DS, Shirodaria PV, Fleming E, et al. Morphology and development of Rift Valley fever virus in Vero cell cultures. J Med Virol1988;24:161–174.

Emery, V.C. & Bishop, D.H.L., 1987. Characterization of Punta Toro S mRNA species and identification of an inverted complementary sequence in the intergenic region of Punta Toro phlebovirus ambisense S RNA that is involved in mRNA transcription termination. Virology, 156(1), pp.1–11.

Engering A, vanVliet SJ,HebedaK, et al.Dynamic populations of dendritic cell-specific ICAM-3 grabbing nonintegrin-positive immature dendritic cells and liver/lymph node-specific ICAM-3 grabbing nonintegrin-positive endothelial cells in the outer zones of the paracortex of human lymph nodes. Am J Pathol 2004;164(5):1587–1595.

Enk AH, Angeloni VL, Udey MC, Katz SI (1993) An essential role for Langerhans cell-derived IL-1 beta in the initiation of primary immune responses in skin. J Immunol 150(9):3698–3704.

Enk AH, Katz SI (1992) Early molecular events in the induction phase of contact sensitivity. Proc Nat Acad Sci USA 89:1398–1402.

Ergünay K, Saygan MB, Aydoğan S, Lo MM, Weidmann M, Dilcher M, Sener B, Hasçelik G, Pınar A, Us D. Sandfly fever virus activity in central/northern Anatolia, Turkey: first report of Toscana virus infections. Clin Microbiol Infect 2011; 17: 575-581.

Eugenin EA, Osiecki K, Lopez L, Goldstein H, Calderon TM, Berman JW: CCL2/monocyte chemoattractant protein-1 mediates enhanced transmigration of human immunodeficiency virus (HIV)-infected leukocytes across the blood–brain barrier: a potential mechanism of HIV-CNS invasion and NeuroAIDS. J Neurosci 2006, 26:1098-1106.

Farell CL, Pardridge WM (1991) Blood-brain-barrier glucose transporter is symmetrically distributed on brain capillary endothelial luminal and abluminal membranes: an electronic microscopic immunogold study. Proc Natl Acad Sci USA 88: 5779–5783.

Feinberg H, Guo Y, Mitchell DA, et al. Extended neck regions stabilize tetramers of the receptors DC-SIGN and DC-SIGNR. J Biol Chem 2005;280(2):1327–1335.

Fernandez-Garcia MD, Mazzon M, Jacobs M, Amara A. Pathogenesis of flavivirus infections: using and abusing the host cell. Cell Host Microbe 5(4), 318–328 (2009).

Francisci, D., Papili, R., Camanni, G., Morosi, S., Ferracchiato, N., Valente, M., Ciufolini, M.G., Baldelli, F., 2003. Evidence of Toscana virus circulation in Umbria: first report. Eur. J. Epidemiol. 18, 457 459.

Frank R (2002) The SPOT-synthesis technique: Synthetic peptide arrays on membrane supports—principles and applications. J Immunol Methods 267: 13–26.

Freer G, Matteucci D. Influence of dendritic cells on viral pathogenicity. PLoS Pathog. 2009;5(7).

Furr Samantha R. and Marriott Ian (2012). Viral CNS infections: role of glial pattern recognition receptors in neuroinflammation. Frontiers in Microbiology Vol 3 art. 201.

Gabriel, M., Resch, C., Gunther, S., Schmidt-Chanasit, J., 2010. Toscana virus infection imported from Elba into Switzerland. Emerg. Infect Dis. 16, 1034–1036.

Garcia-Vallejo J.J., van Liempt E., da Costa Martins P., Beckers C., van het Hof B., Gringhuis S.I., Zwaginga J.J., van Dijk W., Geijtenbeek T.B., van Kooyk Y., van Die I., Mol. Immunol. 45 (8) (2008) 2359.

Gardner JP, Durso RJ, Arrigale RR, et al. L-SIGN (CD 209L) is a liver-specific capture receptor for hepatitis C virus. Proc Natl Acad Sci USA 2003;100(8):4498–4503.

Geijtenbeek T.B., Krooshoop D.J., Bleijs D.A., van Vliet S.J., van Duijnhoven G.C., Grabovsky V., Alon R., Figdor C.G., van Kooyk Y., Nat. Immunol. 1 (4) (2000) 353.

Geijtenbeek TB, Kwon DS, Torensma R, et al. DC-SIGN, a dendritic cell-specific HIV-1-binding protein that enhances trans-infection of T cells. Cell 2000;100(5):587–597.

Gerrard, S. R., Bird, B. H., Albarin˜ o, C. G. & Nichol, S. T. (2007). The NSm proteins of Rift Valley fever virus are dispensable for maturation, replication and infection. Virology 359, 459–465.

Gonzales-Scarano F, Nathanson N. Bunyaviridae. In: Virology (Volume 1). Fields BN, Knipe DM, Howley PM (Eds). Raven Press, New York, NY, USA, 1195–1228 (1990).

Gonzalez-Mariscal, L., Tapia, R., and Chamorro, D. (2008). Crosstalk of tight junction components with signaling pathways. Biochim. Biophys. Acta 1778; 729–756.

Gonzalez-Scarano F, Janssen RS, Najjar JA, et al. An avirulent G1 glycoprotein variant of La Crosse bunyavirus with defective fusion function. J Virol 1985;54:757–763.

Gonzalez-Scarano, F., Shope, R.E., Calisher, C.E., Nathanson, N., 1982. Characterization of monoclonal antibodies against GN and N proteins of La Crosse and Tahyna, two California serogroup bunyaviruses. Virology 120, 42–53.

Gori Savellini, G., Di Genova, G., Terrosi, C., Di Bonito, P., Giorgi, C., Valentini, M.,Docquier, J.D., Cusi, M.G., 2008. Immunization with Toscana virus

N-Gc proteins protects mice against virus challenge. Virology 375, 521–528.

Grady, L., Kinch,W., 1985. Two monoclonal antibodies against La Crosse virus show host-dependent neutralizing activity. J. Gen. Virol. 66, 2773–2776.

Gramberg T, Soilleux E, Fisch T, et al. Interactions of LSECtin andDC-SIGN/DC-SIGNRwith viral ligands: differential pHdependence, internalization and virion binding. Virology 2008;373(1):189–201.

Greco, F., Mauro, M.V., Tenuta, R., Apuzzo, G., Giraldi, C., 2012. A new case of meningitis due to Toscana virus. New Microbiol. 35, 99–100.

Guo Y, Feinberg H, Conroy E, Mitchell DA, Alvarez R, Blixt O, Taylor ME, Weis WI, Drickamer K. Structural basis for distinct ligand-binding and targeting properties of the receptors DC-SIGN and DC-SIGNR. Nat Struct Mol Biol 2004;11:591–598.

Heath WR, Carbone FR. The skin-resident and migratory immune system in steady state and memory : innate lymphocytes , dendritic cells and T cells. 2013;14(10). doi:10.1038/ni.2680.

Heil F, Hemmi H, Hochrein H, Ampenberger F, Kirschning C, et al. (2004) Species-specific recognition of single-stranded RNA via Toll-like receptor 7 and 8. Science 303: 1526–1529.

Hemmersbach-Miller M, Parola P, Charrel RN, Paul Durand J, Brouqui P. (2004). Sandfly fever due to Toscana virus: an emerging infection in southern France. Eur J Intern Med; 15: 316-317.

Hepojoki, J., Strandin, T., Wang, H., Vapalahti, O., Vaheri, A. & Lankinen, H. (2010). Cytoplasmic tails of hantavirus glycoproteins interact with the nucleocapsid protein. J Gen Virol 91, 2341–2350.

Hessell AJ, Hangartner L, Hunter M, Havenith CE, Beurskens FJ, et al. (2007) Fc receptor but not complement binding is important in antibody protection against HIV. Nature 449: 101–104.

Hilpert, K., Winkler, D. F. & Hancock, R. E. (2007). Peptide arrays on cellulose support: SPOT synthesis, a time and cost efficient method for synthesis of large numbers of peptides in a parallel and addressable fashion. Nat Protoc 2, 1333–1349.

Hofmann H, Pohlmann S. 2011.DC-SIGN: access portal for sweet viral killers.Cell Host Microbe10:5–7.

Hofmann, H.; Li, X.; Zhang, X.; Liu, W.; Kuhl, A.; Kaup, F.; Soldan, S.S.; Gonzalez-Scarano, F.; Weber, F.; He, Y.; et al. Severe fever with thrombocytopenia virus glycoproteins are targeted by neutralizing antibodies and can use DC-SIGN as a receptor for pH-dependent entry into human and animal cell lines. J. Virol. 2013, 87, 4384–4394.

Hollidge BS, Gonzalez-Scarano F, Soldan SS. Arboviral encephalitides: transmission, emergence, and pathogenesis. J Neuroimmune Pharmacol. 2010;5(3):428-442.

Hutchinson KL, Peters CJ, Nichol ST. Sin Nombre virus mRNA synthesis. Virology 1996;224:139–149.

Iolyeva M, Karaman S, Willrodt AH, Weingartner S, Vigl B, Halin C (2013) Novel role for ALCAM in lymphatic network formation and function. FASEB J 27(3):978–990.

Jameson B, Baribaud F, P¨ohlmann S, et al. Expression ofDC-SIGN by dendritic cells of intestinal and genitalmucosae in humans and rhesusmacaques. J Virol 2002;76(4):1866–1875.

Jeffers SA, Tusell SM, Gillim-Ross L, et al. CD209L (L-SIGN) is a receptor for severe acute respiratory syndrome coronavirus. Proc Natl Acad Sci USA 2004;101(44):15748–15753.

Johnson LA, Clasper S, Holt AP, Lalor PF, Baban D, Jackson DG (2006) An inflammation-induced mechanism for leukocyte transmigration across lymphatic vessel endothelium. J Exp Med 203:2763–2777.

Johnson LA, Jackson DG. Control of dendritic cell trafficking in lymphatics by chemokines. Angiogenesis. 2014;17(2):335-345.

Karabatsos N. International Catalogue of Arboviruses Including Certain Other Viruses of Vertebrates, 3rd ed. San Antonio: American Society of Tropical Medicine and Hygiene, 1985.

Kato H, Sato S, Yoneyama M, Yamamoto M, Uematsu S, et al. (2005) Cell-type specific involvement of RIG-I in antiviral response. Immunity 23: 19–28.

Kato H, Takeuchi O, Sato S, Yoneyama M, Yamamoto M, et al. (2006) Differential roles of MDA5 and RIG-I helicases in the recognition of RNA viruses. Nature 441: 101–105.

Klugman KP, Astley M, Lipsitch M. Unusual Manifestation of Toscana Virus Sporadic Oropouche Virus Infection , Acre ,. 2009;15(2):347-348. doi:10.1086/591708.

Koppel EA, van Gisbergen KP, Geijtenbeek TB, van Kooyk Y. Distinct functions of DC-SIGN and its homologues L-SIGN (DC-SIGNR) and mSIGNR1 in pathogen recognition and immune regulation. CellMicrobiol 2005;7(2):157–165.

Kormelink R, de Haan P, Meurs C, et al. (1992)The nucleotide sequence of the M RNA segment of tomato spotted wilt virus, a bunyavirus with two ambisense RNA segments. J Gen Virol 73:2795–2804.

Koyuncu OO, Hogue IB, Enquist LW: Virus infections in the nervous system. Cell Host Microbe 2013, 13:379-393.

Kuismanen, E. Post translational processing of Uukuniemi virus glycoproteins G1 and G2. J. Virol. 1984, 51, 806–812.

Lai WK, Sun PJ, Zhang J, et al. Expression ofDC-SIGN andDC-SIGNR on human sinusoidal endothelium: a role for capturing hepatitis C virus particles. AmJ Pathol 2006;169(1):200–208.

Lanzavecchia A, Corti D, Sallusto F. Human monoclonal antibodies by immortalization of memory B cells.2007.

Law MD, Speck J, Moyer JW. (1992). The M RNA of impatiens necrotic spot tospovirus (Bunyaviridae) has an ambisense genomic organization. Virology 188:732–741.

Léger P, Lozach P-Y. Bunyaviruses: from transmission by arthropods to virus entry into the mammalian host first-target cells. Future Virol. 2015;10(7):859-881. doi:10.2217/fvl.15.52.1.

Li Y, Hao B, Kuai X, et al. C-type lectin LSECtin interacts with DC-SIGNR and is involved in hepatitis C virus binding.Mol Cell Biochem 2009;327(1–2):183–190.

Lin M, Mcrae H, Dan H, et al. High-resolution epitope mapping for monoclonal antibodies to the structural protein E rns of classical swine fever virus using peptide array and random peptide phage display approaches. 2010;138:2928-2940.

Lindesmith LC, Beltramello M, Donaldson EF, Corti D, Swanstrom J, Debbink K, Lanzavecchia A, Baric RS. 2012. Immunogenetic mechanisms driving norovirus GII.4 antigenic variation. PLoS Pathog 8:e1002705.

Liu W, Tang L, Zhang G, et al. Characterization of a novel C-type lectin-like gene, LSECtin: demonstration of carbohydrate binding and expression in sinusoidal endothelial cells of liver and lymph node. J Biol Chem 2004;279(18):18748–18758.

Londrigan SL, Turville SG, TateMD, et al. N-linked glycosylation facilitates sialic acid-independent attachment and entry of influenza A viruses into cells expressing DC-SIGN or L-SIGN. J Virol 2011;85(6):2990–3000.

Lozach P, Mancini R, Bitto D, Meier R, Oestereich L, Anna KO. Article Entry of Bunyaviruses into Mammalian Cells. 2010:488-499.

Lozach P-Y, Burleigh L, Staropoli I, Amara A. The C type lectins DC-SIGN and L-SIGN: receptors for viral glycoproteins. Methods Mol Biol. 2007;379:51-68.

Lozach, P.Y.; Kuhbacher, A.; Meier, R.; Mancini, R.; Bitto, D.; Bouloy, M.; Helenius, A. DC-SIGN as a receptor for phleboviruses. Cell Host Microbe 2011, 10, 75–88.

Macagno A, Bernasconi NL, Vanzetta F, Dander E, Sarasini A, Revello MG, Gerna G, Sallusto F, Lanzavecchia A. 2010. Isolation of human monoclonal antibodies that potently neutralize human cytomegalovirus infection by targeting different epitopes on the gH/gL/UL128- 131A complex. J Virol 84:1005–1013.

Maddaluno L, Verbrugge SE, Martinoli C, Matteoli G, Chiavelli A, Zeng Y, Williams ED, Rescigno M, Cavallaro U (2009) The adhesion molecule L1 regulates transendothelial migration and trafficking of dendritic cells. J Exp Med 206(3):623–635.

Madoff, D.H.; Lenard, J. A membrane glycoprotein that accumulates intracellularly: Cellular processing of the large glycoprotein of LaCrosse virus. Cell 1982, 28, 821–829.

Mahnke K, Guo M, Lee S, et al. The dendritic cell receptor for endocytosis, DEC-205, can recycle and enhance antigen presentation via major histocompatibility complex class II-positive lysosomal compartments. J Cell Biol. 2000;151(3):673-684.

Marasco W & Sui J. The growth and potential of human antiviral monoclonal antibody therapeutics. Nat Biotechnol. 2007;25(12):1421-1434.

Marriott AC, el Ghorr AA, Nuttall PA, et al. (1992). Dugbe nairovirus M RNA: Nucleotide sequence and coding strategy. Virology 190:606–615.

Martin ML, Regnery HL, Sasso DR, et al. (1985). Distinction between Bunyaviridae genera by surface structure and comparison with Hantaan virus using negative stain electron microscopy. Arch Virol 86:17–28.

Martínez-García FA, Moreno-Docón A, Segovia-Hernández M, Fernández-Barreiro A. Deafness as a sequela of Toscana virus meningitis. Med Clin (Barc) 2008; **130**: 639

Marzi A, Gramberg T, Simmons G, et al. DC-SIGN and DC-SIGNR interact with the glycoprotein of Marburg virus and the S protein of severe acute respiratory syndrome coronavirus. J Virol 2004;78(21):12090–12095.

Matsuoka, Y.; Ihara, T.; Bishop, D.H.; Compans, R.W. Intracellular accumulation of Punta Toro virus glycoproteins expressed from cloned cDNA. Virology 1988, 167, 251–260.

McDonald B, Pittman K,Menezes GB, Hirota SA, Slaba I, Waterhouse CC, et al. Intravascular danger signals guide neutrophils to sites of sterile inflammation. Science 2010;330:362–6.

Meyer S, van Liempt E, Imberty A, et al. DC-SIGN mediates binding of dendritic cells to authentic pseudo-LewisY glycolipids of Schistosoma mansoni cercariae, the first parasite-specific ligand ofDCSIGN. J Biol Chem 2005;280(45):37349–37359.

Mitchell DA, Fadden AJ, Drickamer K. A novel mechanism of carbohydrate recognition by the C-

type lectins DC-SIGN and DC-SIGNR. Subunit organization and binding to multivalent ligands. J Biol Chem 2001;276:28939–28945.

Moses AV, Bloom FE, Pauza CD, Nelson JA: Human immunodeficiency virus infection of human brain capillary endothelial cells occurs via a CD4/galactosylceramide- independent mechanism. Proc Natl Acad Sci U S A 1993, 90:10474-10478.

Navarro-Marí JM, Palop-Borrás B, Pérez-Ruiz M, Sanbonmatsu-Gámez S (2011) Serosurvey study of Toscana virus in domestic animals, Granada, Spain. Vector Borne Zoonotic Dis 11:583–587.

Nestle FO, Meglio P Di FO, Qin JZ, et al. Skin immune sentinels in health and disease. Nat Rev Immunol 2009; 9: 679-91.

Nicoletti L, Verani P, Caciolli S, Ciufolini MG, Renzi A, Bartolozzi D, Paci P, Leoncini F, Padovani P, Traini E. Central nervous system involvement during infection by Phlebovirus toscana of residents in natural foci in central Italy (1977-1988). Am J Trop Med Hyg 1991; 45: 429-434.

Overby, A. K., Pettersson, R. F. & Neve, E. P. (2007). The glycoprotein cytoplasmic tail of Uukuniemi virus (Bunyaviridae) interacts with ribonucleoproteins and is critical for genome packaging. J Virol 81, 3198–3205.

Patterson JL, Holloway B, Kolakofsky D. (1984). La Crosse virions contain a primer-stimulated RNA polymerase and a methylated cap-dependent endonuclease. J Virol 52:215–222.

Pérez-Ruiz M, Collao X, Navarro-Marí JM, Tenorio A. Reverse transcription, real-time PCR assay for detection of Toscana virus. J.Clin. Virol. 39, 276–281 (2007).

Pham TH, Baluk P, Xu Y, Grigorova I, Bankovich AJ, Pappu R, Coughlin SR, McDonald DM, Schwab SR, Cyster JG (2010) Lymphatic endothelial cell sphingosine kinase activity is required for lymphocyte egress and lymphatic patterning. J Exp Med 207(1):17–27.

Pichlmair A, Schulz O, Tan CP, Na¨slund TI, Liljestro¨m P, et al. (2006) RIG-Imediated antiviral responses to single-stranded RNA bearing 59-phosphates. Science 14: 997–1001.

Pohlmann S, Soilleux EJ, Baribaud F, et al.DC-SIGNR, a DC-SIGN homologue expressed in endothelial cells, binds to human and simianimmunodeficiency viruses and activates infection in trans. Proc Natl Acad Sci USA 2001;98(5):2670–2675.

Pohlmann S, Zhang J, Baribaud F, et al. Hepatitis C virus glycoproteins interact with DC-SIGN and DC-SIGNR. J Virol 2003;77(7):4070–4080.

Portolani, M., Sabbatini, A.M., Beretti, F., Gennari, W., Tamassia, M.G., Pecorari, M., 2002. Symptomatic infections by toscana virus in the Modena province in the triennium 1999–2001. New Microbiol. 25, 485–488.

Punda-Polic V, Mohar B, Duh D, Bradaric N, Korva M, Fajs L,Saksida A,Avsic-Zupanc T, 2012. Evidence of an autochthonous Toscana virus strain in Croatia. J Clin Virol 55: 4–7.

Pustylnikov S, Sagar D, Jain P, Khan ZK. Targeting the C-type lectins-mediated host-pathogen interactions with dextran. J Pharm Pharm Sci 2014;17:371–392.

Rajewsky K. Clonal selection and learning in the antibody system. Nature. 1996; 381:751–758.

Ranki M, Pettersson RF. (1975). Uukuneimi virus contains an RNA polymerase. J Virol 16:1420–1425.

Reed LJ, Muench H. A simple method of estimating fifty per cent endpoints. Am J Hyg 1938; 27: 493-497

Ribeiro, D., Borst, J. W., Goldbach, R. & Kormelink, R. (2009). Tomato spotted wilt virus nucleocapsid protein interacts with both viral glycoproteins Gn and Gc in planta. Virology 383, 121–130.

Rinaldi R., Goteri G., Biagetti S., Cusi M.G., Rossini S. (2011). Histological description of the lymphadenopathy related to Toscana virus infection. Report of a case. Pathol. Res. Pract. 207: 197-201.

Rockx B, Corti D, Donaldson E, Sheahan T, Stadler K, Lanzavecchia A, Baric R. 2008. Structural basis for potent cross-neutralizing human monoclonal antibody protection against lethal human and zoonotic severe acute respiratory syndrome coronavirus challenge. J Virol 82:3220 3235.

Rusu M, Bonneau R, Holbrook MR et al. An assembly model of rift valley Fever virus. Front. Microbiol. 3, 254 (2012).

Rwambo PM, Shaw MK, Rurangirwa FR, et al. (1996). Ultrastructural studies on the replication and morphogenesis of Nairobi sheep disease virus, a nairovirus. Arch Virol 141:1479–1492.

Salimi H, Cain MD, Klein RS.Encephalitic Arboviruses: Emergence, Clinical Presentation, and Neuropathogenesis.Neurotherapeutics. 2016 Jul;13(3):514-34.

Sallusto F, Schaerli P, Loetscher P, Schaniel C, Lenig D, Mackay CR, Qin S, Lanzavecchia A (1998) Rapid and coordinated switch in chemokine receptor expression during dendritic cell maturation. Eur J Immunol 28(9):2760–2769.

Saluzzo, J.F., Anderson Jr., G.W., Hodgson, L.A., Digoutte, J.P., Smith, J.F., 1989a. Antigenic and biological properties of Rift Valley fever virus isolated during the 1987 Mauritanian epidemic. Res. Virol. 140, 155–164.

Saluzzo, J.F., Anderson Jr., G.W., Smith, J.F., Fontenille, D., Coulanges, P., 1989b. Biological and antigenic relationship between Rift Valley fever virus strains isolated in Egypt and Madagascar. Trans. R. Soc. Trop. Med. Hyg. 83, 701.

Samuel MA, Wang H, Siddharthan V, Morrey JD, Diamond MS. Axonal transport mediates West Nile virus entry into the central nervous system and induces acute flaccid paralysis. Proc Natl Acad Sci U S A 2007;104:17140–17145.

Sanbonmatsu –Gàmez S. Pèrez –Ruiz m, Palop-Borràs B, Navarro-Marì JM. (2009). Unusual Manifestation of Toscana virus Infection, Spain. Emerg infect Dis;15:347-8;

Sánchez-Seco MP, Echevarría JM, Hernández L, Estévez D, Navarro-Marí JM, Tenorio A. Detection and identification of Toscana and other phleboviruses by RT-nested-PCR assays with degenerated primers. J. Med. Virol. 71, 140–149 (2003).

Schiller B, Hykollari A, Yan S, Paschinger K, Wilson IB. Complicated N-linked glycans in simple organisms. Biol. Chem. 393(8), 661–673 (2012).

Schmaljohn C. S., Hooper J. W. (2001). Bunyaviridae. In Fields Virology,4th Edition , vol 2, pp: 1293-1309. Edited by D. M. Knipe & P. M. Howley. Philadelphia, PA: Lippincott Williams & Wilkins.

Schmaljohn CS, Schmaljohn AL, Dalrymple JM. (1987). Hantaan virus M RNA: Coding strategy, nucleotide sequence, and gene order. Virology 157:31–39.

Schmaljohn, C. S. & Nichol, S. T. (2006). Bunyaviridae. In Fields Virology, 5th Edition, vol. 2, pp. 1741–1789. Edited by D. M. Knipe & P. M. Howley. Philadelphia, PA: Lippincott Williams & Wilkins.

Schmaljohn, C.; Elliott, R.M. Bunyaviridae. In Fields Virology, 6th Edition .; Knipe, D.M., Howley, P.M., Eds.; Lippincott Williams & Wilkins: Philadelphia, PA, USA, 2014; Volume 1, pp. 1244–1282.

Schwarz TF, Gilch S, Jäger G. Aseptic meningitis caused by sandfly fever virus, serotype Toscana. Clin Infect Dis 1995; 21: 669-671

Serata D., Rapinesi C., Del Casale A., Simonetti A., Mazzarini L., Ambrosi E., et al. (2011). Personality changes after Toscana virus (TOSV) encephalitis in a 49-year-old man: a case report. Int. J. Neurosci. 121, 165-169.

Serrano-Gomez D, Dom´ınguez-Soto A, Ancochea J, et al. Dendritic cell-specific intercellular adhesion molecule 3-grabbing nonintegrinmediates binding and internalization of Aspergillus fumigates conidia by dendritic cells andmacrophages. J Immunol 2004;173(9):5635–5643.

Shi X., Kohl A., Li P. & Elliott R. M. (2007). Role of the cytoplasmic tail domains of Bunyamwera orthobunyavirus glycoproteins Gn and Gc in virus assembly and morphogenesis. J Virol 81, 10151–10160.

Shi, X.; Brauburger, K.; Elliott, R.M. Role of N-linked glycans on bunyamwera virus glycoproteins in intracellular trafficking, protein folding, and virus infectivity. J. Virol. 2005, 79, 13725–13734.

Shimojima M, Str¨oher U, Ebihara H, et al. Identification of cell surface molecules involved in dystroglycan-independent Lassa virus cell entry. J Virol 2012;86(4):2067–2078.

Simmons CP, Bernasconi NL, Suguitan AL, Mills K, Ward JM, Chau NVV, Hien TT, Sallusto F, Ha DQ, Farrar J, de Jong MD, Lanzavecchia A, Subbarao K. 2007. Prophylactic and therapeutic efficacy of human monoclonal antibodies against H5N1 influenza. PLoS Med 4:e178.

Smith JF, Pifat DY. (1982). Morphogenesis of sandfly viruses (Bunyaviridae family). Virology 121:61–81.

Snippe, M., Willem Borst, J., Goldbach, R. & Kormelink, R. (2007b). Tomato spotted wilt virus Gc and N proteins interact in vivo. Virology 357, 115–123.

Soilleux EJ, Barten R, Trowsdale J. DC-SIGN; a related gene, DC-SIGNR; and CD23 forma cluster on 19p13. J Immunol 2000;165(6):2937–2942.

Soilleux EJ, Morris LS, Leslie G, et al. Constitutive and induced expression of DC-SIGN on dendritic cell and macrophage subpopulations in situ and in vitro. J Leukoc Biol 2002;71(3):445– 457.

Soilleux EJ,Morris LS, LeeB, et al. Placental expression of DC-SIGN may mediate intrauterine vertical transmission of HIV. J Pathol 2001;195(5):586–592.

Soldateschi D, Dal Maso GM, Valassina M, Santini L, Bianchi S, Cusi MG. Laboratory diagnosis of Toscana virus infection by enzyme immunoassay with recombinant viral nucleoprotein. J Clin Microbiol. 1999;37(3):649-652.

Sonderegger, B., Hachler, H., Dobler, G., Frei, M., 2009. Imported aseptic meningitis due to Toscana virus acquired on the island of Elba, Italy, August 2008. Euro Surveill 14.

Spiegel M, Plegge T, Pöhlmann S. The role of phlebovirus glycoproteins in viral entry, assembly and release. Viruses. 2016;8(7).

Stanley-Samuelson DW, Jurenka RA, Cripps C, Blomquist GJ, de Renobales M. Fatty acids in insects: Composition, metabolism, and biological significance. Arch. Insect. Biochem. Physiol. 9(1), 1–33 (1988).

Staros EB. Innate immunity: new approaches to understanding its clinical significance. Am J Clin Pathol 2005;123:305–12.

Steeghs L, van Vliet S, Uronen-Hansson H, et al. Neisseria meningitidis expressing lgtB lipopolysaccharide targets DC-SIGN and modulates dendritic cell function. Cell Microbiol 2006;8(2):316– 325.

Swanson PA II, McGavern DB: Viral diseases of the central nervous system. Curr Opin Virol 2015, 11:44-54.

Tabor-Godwin JM, Ruller CM, Bagalso N, An N, Pagarigan RR, Harkins S, Gilbert PE, Kiosses WB, Gude NA, Cornell CT et al.: A novel population of myeloid cells responding to coxsackievirus infection assists in the dissemination of virus within the neonatal CNS. J Neurosci 2010, 30:8676-8691.

Tailleux L, Schwartz O, Herrmann JL, Pivert E, Jackson M, Amara A, Legres L, Dreher D, Nicod LP, Gluckman JC, Lagrange PH, Gicquel B, Neyrolles O (2003) DC-SIGN is the major Mycobacterium tuberculosis receptor on human dendritic cells. J Exp Med 197:121–127.

Takamatsu H, Takegahara N, Nakagawa Y, Tomura M, Taniguchi M, Friedel RH, Rayburn H, Tessier-Lavigne M, Yoshida Y, Okuno T, Mizui M, Kang S, Nojima S, Tsujimura T, Nakatsuji Y, Katayama I, Toyofuku T, Kikutani H, Kumanogoh A (2010) Semaphorins guide the entry of dendritic cells into the lymphatics by activating myosin II. Nat Immunol 11(7):594–600.

Takeuchi O, Akira S. Pattern recognition receptors and inflammation. Cell 2010;140:805–20.

Tassaneetrithep B, Burgess TH, Granelli-Piperno A, et al. DC-SIGN (CD209) mediates dengue virus infection of human dendritic cells. J ExpMed 2003;197(7):823–829.

Teijeira A, Palazon A, Garasa S, Marre D, Auba C, Rogel A, Murillo O, Martinez-Forero I, Lang F, Melero I, Rouzaut A (2012) CD137 on inflamed lymphatic endothelial cells enhances CCL21-guided migration of dendritic cells. FASEB J 26(8):3380–3392.

Teoh D, Johnson LA, Hanke T, McMichael AJ, Jackson DG (2009) Blocking development of a CD8? T cell response by targeting lymphatic recruitment of antigen presenting cells. J Immunol 182(4):2425–2431.

Terrosi C., Olivieri R., Bianco C., Cellesi C., Cusi M.G., Age-dependent seroprevalence of Toscana virus in central Italy and correlation with the clinical profile. Clin Vaccine Immunol 2009; 16: 1251-2.

Tini P, Belmonte G, Toscano M, Miracco C, Palumbo S, Pastina P, Battaglia G, Nardone V, Butorano MA, Masucci A, Cerase A, Pirtoli L (2015) Combined epidermal growth factor receptor and beclin 1 autophagic protein expression analysis identifies different clinical presentations, responses to chemo- and radiotherapy, and prognosis in glioblastoma. Biomed Res 2015:208076

Torzicky M, Viznerova P, Richter S, Strobl H, Scheinecker C, Foedinger D, Riedl E (2012) Platelet endothelial cell adhesion molecule-1 (PECAM-1/CD31) and CD99 are critical in lymphatic transmigration of human dendritic cells. J Invest Dermatol 132(4):1149–1157.

Traggiai, E., S. Becker, K. Subbarao, L. Kolesnikova, Y. Uematsu, M. R. Gismondo, B. R. Murphy, R. Rappuoli, and A. Lanzavecchia. 2004. An efficient method to make human monoclonal antibodies from memory B cells: potent neutralization of SARS coronavirus. Nat. Med. 10:871–875.

Urban Š, Anderluh M. C-type lectin DC-SIGN : An adhesion , signalling and antigen-uptake molecule that guides dendritic cells in immunity. 2010;22:1397-1405. doi:10.1016/j.cellsig.2010.03.018.

Valassina M, Valentini M, Pugliese A, Valensin PE, Cusi MG. Serological Survey of Toscana Virus Infections in a High-Risk Population in Italy. 2003 (b).

Valassina M., Cusi M. G., Valensin P.E. 2003 (a). A Mediterranean arbovirus: The Toscana virus. Journal of NeuroVirology, 9:577-583.

Valassina, M., Cusi, M.G., Valensin, P.E., 1996. Rapid identification of Toscana virus by nested PCR during an outbreak in the Siena area of Italy. J. Clin. Microbiol. 34, 2500–2502.

Valentini M, Valassina M, Savellini GG, Cusi MG. Nucleotide variability of Toscana virus M segment in strains isolated from clinical cases. 2008;135:187-190. doi:10.1016/j.virusres.2008.01.016.

Van Breedam W, Pohlmann S, Favoreel HW, de Groot RJ, Nauwynck HJ. Bitter-sweet symphony: glycan-lectin interactions in virus biology. FEMS Microbiol Rev 2014;38:598–632.

Varani S, Gelsomino F, Bartoletti M, Pierluigi Viale , Antonio Mastroianni , Elisabetta Briganti , Patrizia Ortolani , Francesco Albertini , Carlo Calzetti , Francesca Prati , Patrizia Cenni , Gastone Castellani , Silvia Morini , Giada Rossini , Maria Paola Landini, Vittorio Sambri. Meningitis Caused by Toscana Virus Is Associated with Strong Antiviral Response in the CNS and Altered Frequency of Blood Antigen-Presenting Cells. 2015:5831-5843. doi:10.3390/v7112909.

Venturi, G., Madeddu, G., Rezza, G., Ciccozzi, M., Pettinato, M.L., Cilliano, M., Fiorentini, C., Mura, M.S., Ciufolini, M.G., 2007. Detection of Toscana virus central nervous system infections in Sardinia Island, Italy. J. Clin. Virol. 40, 90– 91.

Verani P, Ciufolini MG, Caciolli S, et al. Ecology of viruses isolated from sand flies in Italy and characterized of a new Phlebovirus (Arabia virus). Am J Trop Med Hyg. 1988;38(2):433-439.

Verani P, Ciufolini MG, Nicoletti L, et al. [Ecological and epidemiological studies of Toscana virus, an arbovirus isolated from Phlebotomus]. Ann Ist Super Sanita. 1982;18(3):397399.

Verani P, Nicoletti L, Ciufolini MG. Antigenic and biological characterization of Toscana virus, a new Phlebotomus fever group virus isolated in Italy. Acta Virol. 1984;28(1):39-47

Verma S, Lo Y, Chapagain M, Lum S, Kumar M, Gurjav U, Luo H, Nakatsuka A, Nerurkar VR: West Nile virus infection modulates human brain microvascular endothelial cells tight junction proteins and cell adhesion molecules: transmigration across the in vitro blood–brain barrier. Virology 2009, 385:425-433.

Vocale, C., Bartoletti, M., Rossini, G., Macini, P., Pascucci, M.G., Mori, F., Tampieri, A., Lenzi, T., Pavoni, M., Giorgi, C., Gaibani, P., Cavrini, F., Pierro, A., Landini, M.P., Viale, P., Sambri, V., 2012. Toscana virus infections in northern Italy: laboratory and clinical evaluation. Vector Borne Zoonotic Dis. 12, 526–529.

Vorbrodt AW (1993). Morphological evidence of the functional polarization of brain microvascular endothelium. In: Pardridge WM(ed) The blood-brain-barrier. Raven, New York, pp 137–164.

Wallez Y, Huber P. Endothelial adherens and tight junctions in vascular homeostasis, inflammation and angiogenesis. Biochim Biophys Acta Biomembr.2008;1778(3):794-809. doi:10.1016/j.bbamem.2007.09.003.

Walter CT, Barr JN. Recent advances in the molecular and cellular biology of bunyaviruses. 2011:2467-2484.

Wang H, Siddharthan V, Hall JO, Morrey JD. West Nile virus preferentially transports along motor neuron axons after sciatic nerve injection of hamsters. J Neurovirol 2009;15:293–299.

Weaver SC, Reisen WK. Present and Future Arboviral Threaths. Vol 85.; 2010. doi:10.1016/j.antiviral.2009.10.008.

Weber, M.; Weber, F. RIG-I-like receptors and negative-strand RNA viruses: RLRly bird catches some worms. Cytokine Growth Factor Rev. 2014 b, 25, 621–628.

Weber, M.;Weber, F. Segmented negative-strand RNA viruses and RIG-I: Divide (your genome) and rule. Curr. Opin. Microbiol. 2014 a, 20, 96–102.

Weidmann M, Sanchez-Seco MP, Sall AA et al. Rapid detection of important human pathogenic phleboviruses. J. Clin. Virol. 41, 138–142 (2008).

Winkler, D. F. & Campbell, W. D. (2008). The spot technique: synthesis and screening of peptide macroarrays on cellulose membranes. Methods Mol Biol 494, 47–70.

Won, S., Ikegami, T., Peters, C. J. & Makino, S. (2007). NSm protein of Rift Valley fever virus suppresses virus-induced apoptosis. J Virol 81, 13335–13345.

Wu SJ, Grouard-Vogel G, Sun W, Mascola JR, Brachtel E, Putvatana R, Louder MK, Filgueira L, Marovich MA, Wong HK et al.: Human skin Langerhans cells are targets of dengue virus infection. Nat Med 2000, 6:816-820.

Wuerth JD, Weber F. Phleboviruses and the Type I Interferon Response. 2016.

Yu, X.J.; Liang, M.F.; Zhang, S.Y.; Liu, Y.; Li, J.D.; Sun, Y.L.; Zhang, L.; Zhang, Q.F.; Popov, V.L.; Li, C.; et al. Fever with thrombocytopenia associated with a novel bunyavirus in China. N. Engl. J. Med. 2011, 364, 1523–1532.

Zhang Feng, Ren Shuangyi, Zuo Yunfei (2014) DC-SIGN, DC-SIGNR and LSECtin: C-Type Lectins for Infection, International Reviews of Immunology, 33:1, 54-66.

Zhioua E, Moureau G, Chelbi I, Ninove L, Bichaud L, Derbali M, Champs M, Cherni S, Salez N, Cook S, de Lamballerie X, Charrel RN. Punique virus, a novel phlebovirus, related to sandfly fever Naples virus, isolated from sandflies collected in Tunisia. J Gen Virol 2010; 91: 1275-1283.

Chapter 8

Annexes

OPEN

Citation: Cell Death Discovery (2016) 2, 16025; doi:10.1038/cddiscovery.2016.25

www.nature.com/cddiscovery

ARTICLE

Immune-modulating effects of bevacizumab in metastatic non-small-cell lung cancer patients

EC Martino[1], G Misso[2], P Pastina[1], S Costantini[3], F Vanni[1], C Gandolfo[4], C Botta[5], F Capone[3], A Lombardi[2], L Pirtoli[1], P Tassone[5], C Ulivieri[6], P Tagliaferri[5], MG Cusi[4], M Caraglia[2] and P Correale[1]

The mPEBev is an anticancer regimen which combines a chemotherapy doublet, based on cisplatin and oral etoposide (mPE), with bevacizumab (mPEBev), a mAb targeting the vasculo-endothelial growth factor (VEGF). In previous studies, this regimen showed powerful anti-angiogenetic effects and significant antitumor activity in metastatic non-small-cell lung cancer (mNSCLC) patients. We also recorded the best benefit in patients exhibiting low-systemic inflammatory profile at baseline. On these bases, we hypothesized that mPEBev antitumor activity could be partially related to bevacizumab-associated immunological effects. For this reason, we performed an immunological monitoring in 59 out of 120 stage IIIb-IV NSCLC patients enrolled in the BEVA2007 phase II trial, who received fractioned cisplatin (30 mg/sqm days 1-3q21) and oral etoposide (50 mg, days 1-15q21) (mPE doublet) ± bevacizumab. In this group of patients, 12 received the mPE doublet alone and 47 the doublet in combination with bevacizumab (5 mg/kg on the day 3q21; mPEBev regimen). Blood cell counts, serum analysis, multiplex cytokine assay and immunocytofluorimetric analysis, performed on baseline and post-treatment on blood samples from these patients, revealed that bevacizumab addition to the doublet decreased levels of pro-angiogenic (VEGF, Angiostatin-1 and Follistatin) and inflammatory cytokines (interferon (IFN)γ, IL4 and IL17), improved *in vivo* and *in vitro* cytotoxic T-lymphocytes (CTL) response and promoted dendritic cell activation. These results suggest that the mPEBev regimen improve the micro-environmental conditions for an efficient antigen-specific CTL response, making it a feasible candidate regimen to be assessed in combination with immune-checkpoint inhibitors in NSCLC patients.

Cell Death Discovery (2016) **2,** 16025; doi:10.1038/cddiscovery.2016.25; published online 3 October 2016

Non-small-cell lung cancer (NSCLC) is the most common malignancy and the leading cause of cancer death worldwide.[1] The majority of NSCLC patients who cannot undergo curative surgery and who are diagnosed with advanced disease, have a poor prognosis with a survival time that usually does not exceed 8–10 months.[2] The standard treatment for metastatic (m) NSCLC patients is based on doublets of platinum derivatives in combination with a second cytotoxic drug,[2,3] or molecular target-specific inhibitors for patients presenting activating EGFR mutations (Erlotinib, Gefitinib and Afatinib) or EML-ALK translocations (Crizotinib, etc.).[4,5] The efficacy of poly-chemotherapy in non-squamous NSCLC has been further improved by a multidrug combination with bevacizumab, a humanized IgG1 to the vascular endothelial growth factor (VEGF).[6,7] More recently, active immunotherapy and immune-checkpoint inhibitors are entering in the treatment of mNSCLC. In particular, two monoclonal antibodies (mAbs), Nivolumab and Pembrolizumab, have shown evidence of antitumor activity in these patients.[8–13] Nivolumab and Pembrolizumab are two mABs directed to the programmed cell death receptor (PD)1, commonly expressed on activated antigen-specific cytotoxic T lymphocytes (CTLs), residual of a pre-existing tumor-specific immune-response.[8–13] PD1 binding with its specific ligands (PDL-1 and 2) in tumor tissue, leads to the immediate deactivation of the effector cells[8–13] and, therefore, it represents a powerful inhibitory immune-checkpoint and a formidable mechanism of immune-escape for cancer cells.[8–13] In this context, it has been shown that the VEGF deprivation induced by bevacizumab may stimulate immunological alterations, which could contribute to enhance the efficacy of chemotherapy and the survival of cancer patients.[14–18] In fact, VEGF is a soluble dimeric protein family with multiple bio-regulative activities, mainly released in hypoxic and inflammatory conditions by mature granulocytes and platelets.[19–22] It is worldwide known for its ability in inducing endothelial proliferation, neo-vessel formation and normalization in cancer patients; however, its bio-regulative activity is very pleyotropic and complex, and also involves the anticancer immune-system. In fact, its effects are mediated throughout the binding to five different membrane receptors, which are, in turn, expressed on endothelial precursors and other cell lineages including myeloid precursors, dendritic cells (DCs), lymphocytes and mesencephalic neurons.[19–22] Therefore, VEGF release might exert multiple and different functions, including both neutrophils' and inhibitory myeloid cells' maturation, as well as inhibitory effects on DC maturation and CTL precursors' activation.[14–18] We have previously designed a phase I/II clinical trial (BEVA 2007 study) aimed to investigate the toxicity and the biological and antitumor activity of a novel metronomic bio-chemotherapy regimen (mPEBev) in mNSCLC patients. This regimen combined a previously described mPE doublet of cisplatin and oral etoposide, with bevacizumab (Bev). Our

[1]Radiotherapy Unit, Department of Oncology, Siena University Hospital, Siena, Italy; [2]Department of Biochemistry, Biophysics and General Pathology, Second Naples University, Naples, Italy; [3]CROM, Mercogliano, Italy; [4]Microbiology and Virology Unit, Department of Medical Biotechnology, Siena, Italy; [5]Medical Oncology Unit, 'Magna Graecia' University and AUO 'Materdomini', Catanzaro, Italy and [6]Department of Science of Life; University of Siena, Siena, Italy.
Correspondence: M Caraglia (michele.caraglia@unina2.it) or P Correale (correalep@yahoo.it)
Received 18 February 2016; accepted 2 March 2016; Edited by I Harris

preliminary results showed that the addition of bevacizumab to the metronomic doublet was safe and very active in term of antitumor activity.[23–26] We also found that the mPEBev administration was followed by a rapid decline in the primary tumor blood flux (perfusional CT scan)[25] paralleled by a significant decline in VEGF, angiopoietin-1, thrombospondin-1 serum levels[25] and systemic inflammatory markers (NLR, CRP, LDH and myeloperoxidase).[23–26] An additional study carried out by our group, demonstrated that the best advantage on progression-free survival and overall survival were recorded in patients who presented a lower systemic inflammatory profile before the beginning of the treatment.[27] These findings suggested that bevacizumab and, therefore, VEGF deprivation could synergize with the cytotoxic drug doublet through different mechanisms: (i) direct anticancer effects, (ii) anti-angiogenetic activity and (iii) immune-modulating activity. On these bases, with the present study we have evaluated immunological alterations in serum and peripheral blood mononuclear cells (PBMCs) derived from 59 patients who had received mPE doublet ± bevacizumab from September 2012 to May 2015. We also performed a fuctional *ex vivo* study on antigen-specific T-cell lines generated from patients' PBMCs isolated at baseline and after two and four treatment courses.

RESULTS

Demography

The BEVA2007 was a phase II trial, designed on translational bases and approved by the Siena University Ethical committee on March 2007. It was performed to assess toxicity, biological activity and antitumor activity of the mPE doublet ± bevacizumab in mNSCLC patients. One-hundred and fifteen, stage IIIb-IV NSCLC, patients signed an informant consent and were enrolled in the BEVA2007 trial since April 2007. All of them received the chemotherapy doublet, alone (30 patients; PE group) or combined with bevacizumab (85 patients; mPEBev group). We subsequently performed a pre-ordered immune-biological investigation, on the peripheral blood of 59 (51%) of these patients. Twelve out 59 patients had received the mPE doublet alone, whereas 47 had received the doublet combined with bevacizumab (mPEBev). Blood cell counts, serum analysis, multiplex assays and flow cytometry analysis were performed on blood samples isolated at baseline and after two and four treatment courses. The clinical features of these patients are shown in the Table 1.

Pro-angiogenic factors

Our multiplex assays detected a significant decline in the serum levels of multiple pro-angiogenic factors in the group of patients who received the mPEBev regimen, where it was found a significant decrease in VEGF (early event), angiopoietin-2 and follistatin (late events). For these patients, we were unable to demonstrate any significant change in the levels of other factors potentially involved in both tumorigenesis and neo-angiogenesis, such as HGF, PECAM-1, Leptin, PDGF-BB, G-CSF and IL8 (Figure 1).

Table 1. Patients enrolled in the BEVA2007 trial undergone the immune-biological monitoring

	mPE	*mPEBev*
Patient number	12	47
Age	69 (range 59–83)	62 (range 33–82)
Gender		
Male	10	37
Female	2	10
Hystology		
Adenocarcinoma	5	32
Squamous	4	6
Undifferentiated	2	4
Not specified	1	4

Inflammatory cytokine release

We performed, in the same patients, an additional multiplex assay to detect possible treatment-associated changes in serum levels of cytokines involved in different immunological and inflammatory profiles. We found a significant decrease of IFNγ (T_h1), IL4 (T_h2) and IL17 (T_h17) levels only in the group of patients who received the bevacizumab-based treatment and not in those who received the mPE doublet. The latter group of patients, conversely, showed a trend to increase IL8 and IFNγ levels, even though without reaching statistical significance. Finally, both groups of patients showed a trend to increase IL10 and G-CSF levels, also in this case, without reaching statistical significance (Figure 2).

Immunocytofluorimetric analysis

A multicolour flow cytometry study was carried out on the PBMCs from these patients, showing a parallel and coordinate increase in activated ($CD8^+CD62L^+$), central-memory ($CD8^+C45RA^-CCR7^+$; T_{cm}) and long-term memory ($CD8^+C45RA^-CCR7^+CD27^+$) CTLs; a trend to increase regulatory T cells (T_{reg}) was recorded only in patients who received the mPEBev regimen. On the other hand, patients who received the metronomic doublet alone; showed a significant increase in T_{cm}s (Figure 3a). In this set of patients, both treatment regimens did not induce significant changes in the levels of $CD3^+CD4^+$, $CD3^+CD8^+$ and natural killer cells ($CD3^-CD16^+CD56^+$;NK) cells ($P > 0.05$).

In PBMcs we also evaluated the effects of treatments on professional antigen-presenting cells, like DCs and myeloid derivative inhibitory cells (MDICs). We found that only mPEBev treatment, was associated with a significant increase in the

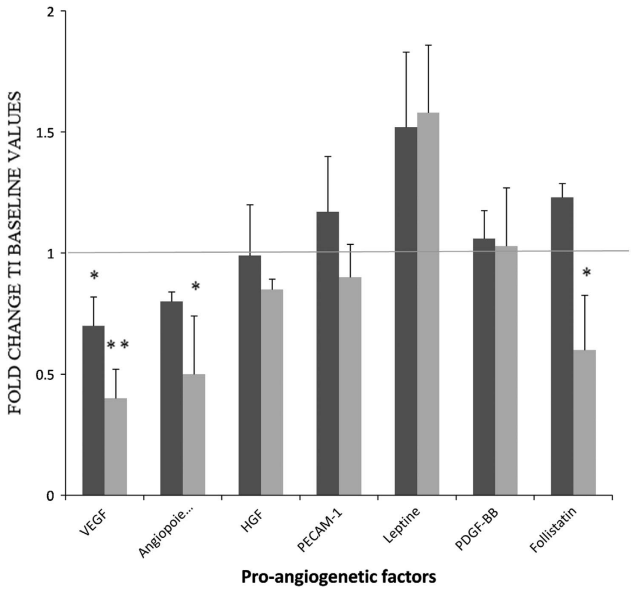

Figure 1. A multiplex analysis concerning the dosage of multiple pro-angiogenetic factors in the serum of mNSCLC patients enrolled in the BEVA2007 trial who have received the mPE doublet alone (■) or combined with bevacizumab (■). Results are expressed as fold induction relative to baseline indicated as 1 (± S.E.). Asterisks represent statistical significance to the correspondent baseline values (*$P < 0.05$; **$P < 0.01$).

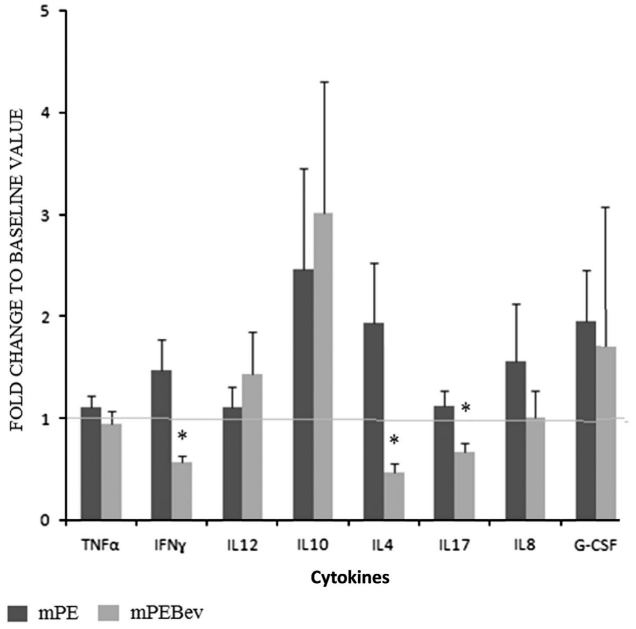

Figure 2. A multiplex analysis concerning the dosage of T_h1 (IFNγ, TNF*α* and IL12), T_h2 (IL4 and IL10), T_h17 and inflammatory cytokines (IL8 and G-CSF) in the serum of mNSCLC patients enrolled in the BEVA2007 trial who have received the mPE doublet alone (■) or combined with bevacizumab (■). Results are expressed as fold induction relative to baseline indicated as 1 (± S.E.). Asterisk represents statistical significance to the correspondent baseline values ($^*P < 0.05$).

percentage of activated DCs ($CD3^-CD19^-CD11c^+CD14^+CD15^-$), expressing either CD83 or CD80. Conversely, an increasing trend, even if not significant, was observed in the percentage of activated MDICs ($CD11b^+CD14^+CD15^+$) in both groups of patients (Figures 3b and 4).

Ex vivo characterization of patients-derived antigen-specific T-cell lines

We performed an *ex vivo* study on PBMCs isolated from patients at the baseline and after four treatment courses with mPE (four patients) or mPEBev (four patients), to verify whether these regimens were able to interfere with the generation of active antigen-specific CTLs. We evaluated multiple T-cell functions which could be potentially affected by the metronomic doublet ± bevacizumab. Thus we cyclically stimulated ex *vivo* PBMCs collected from patients with three antigens with completely different features: (i) streptococcal-B-superantigen (SEB), a bacterial antigen able to over-stimulate both $CD3^+CD8^+$ and $CD3^+CD4^+$ subsets;[28] (ii) immune-reconstituted influenza virosome (IRIV), an antigenic influenza virus membrane envelope, expressing high-immunogenic flow antigens and multiple T helper epitopes[29] and (iii) thymidylate synthase poly-epitope peptide vaccine (TSPP), a 27-mer peptide which assembles multiple class I-HLA restricted CTL epitopes of the thymidylate synthase, a tumor-associated enzyme commonly overexpressed in colo-rectal and NSCLC cancer patients.[30] TSPP was tested in previous preclinical studies showing the ability of generate an efficient antitumor *in vitro* CTL response, both in mice and in cancer patients.[31,32]

After multiple *in vitro* stimulations (IVSs), we evaluated the percentage of proliferative T cells ($CD3^+CD8^+Ki67^+$) and Th1/Th2 cytokine release in response to the three antigens. In our setting,

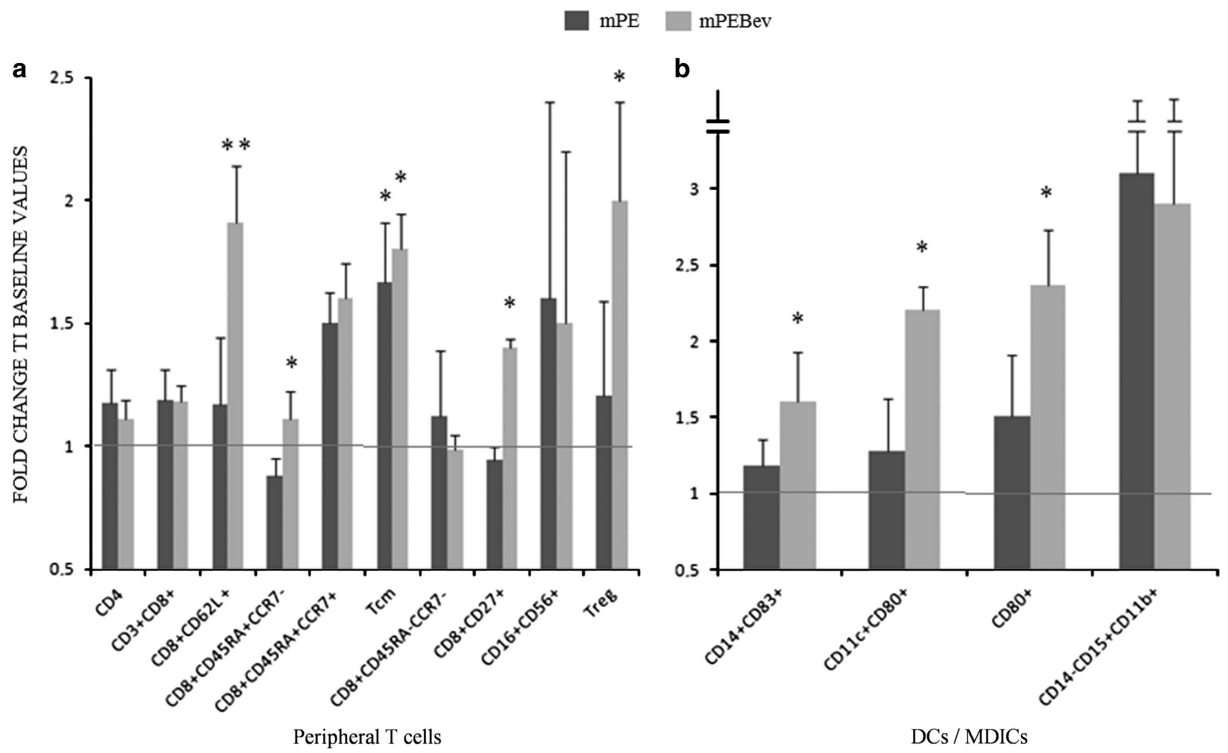

Figure 3. A flow cytometric analysis concerning the expression of (**a**) different T-cell subsets and (**b**) myeloid derivative cells (activated DCs and MDICs) in the PBMCs of mNSCLC patients enrolled in the BEVA2007 trial who have received the mPE doublet alone (■) or combined with bevacizumab (■). Results are expressed as fold induction relative to baseline indicated as 1 (± S.E.). Asterisks represent statistical significance to the correspondent baseline values ($^*P < 0.05$; $^{**}P < 0.01$).

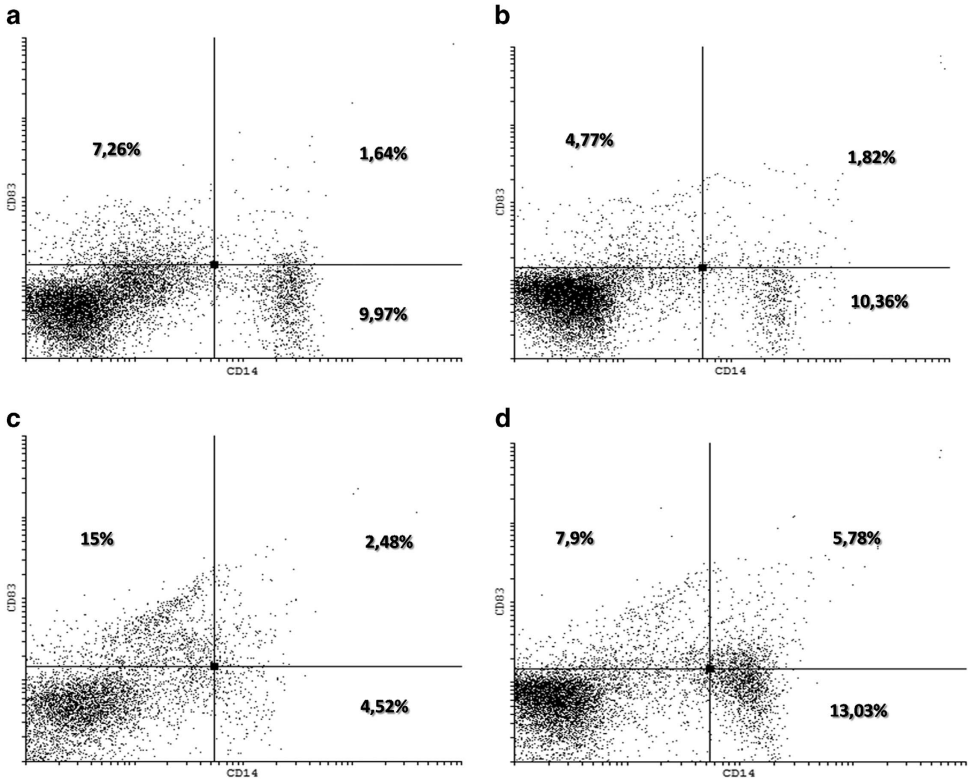

Figure 4. Flow cytometry dot plots of two representative patient PBMCs: activated DCs, isolated at the baseline (**a** and **b**) and after four treatment courses with mPE doublet and bevacizumab (**c** and **d**).

the T-cell lines derived from PBMCs isolated at the baseline, showed a minimal proliferative response to the three antigens (data not shown and Figure 5a). On the other hand, T-cell lines derived from PBMCs isolated after four treatments courses, showed a minimal proliferative response to TSPP and SEB (data not shown) and a higher response to IRIV (Figure 5a). Moreover, we observed a greater percentage of proliferative antigen-specific precursors in T-cell lines derived from patients receiving the mPEBev regimen, compared with the others (fold change to baseline values, mPE *versus* mPEBev = 2.2 (±0,55) *versus* 4. 1 (±0,4), $P = 0.049$; Figure 5a). The functional antigen-specific cytokine response of these T-cell lines also showed a powerful T_h1 response with parallel tumor necrosis factor (TNF)*a* and IFNγ release, only in T cells derived from both mPEBev-treated patients and normal donors. Furthermore, there was no different response to the three antigens used for each specific T-cell line *in vitro* sensitization (Figures 5b–d). These experiments also showed that T cells derived from the mPEBev-treated patients had a greater IL10 release in response to IRIV and TSPP. On the other hand, patients receiving the chemotherapy doublet alone, prevalently showed a non-cytotoxic T_h2 immune-response with an increased antigen-specific release of IL4 (Figures 5b–d).

DISCUSSION

In the present manuscript, we report the results of an immunological study performed on 59 patients, enrolled in the BEVA2007 trial, who received frontline treatment according to the mPE doublet ± bevacizumab. We show that the addition of the mAb to the chemotherapy in mNSCLC patients, as partially observed in our previous studies,[23–26] decreases their systemic inflammatory status and promotes anticancer immune-modulating effects. In fact, we found that the mPEBev regimen causes, in patient's serum, significant reduction in the levels of VEGF and other anti-angiogenetic factors, including Angiopietin 2 and Follistatin, an inhibitor of both TGF-β superfamily activin and FGF-2R angiogenesis inducer.[33] These events were paralleled by a progressive decline in NLR (data not shown),[26] and IFNγ, IL4 and IL17 serum levels. All together these cytokines are expression of cancer-associated systemic inflammation, that is paralleled by immune-suppression and neo-angiogenesis;[26,34–38] therefore, it is possible to hypothesize that a parallel and progressive reduction of pro-angiogenic factors can have a role in the ultimate antitumor effects of the mPEBev regimen. Bevacizumab is commonly considered an anti-angiogenic agent because it subtracts free VEGF that, in turn, promotes endothelial precursors' recruitment and neo-angiogenesis in tumor tissues. However, it has to be considered that VEGF effects are not limited to endothelial cells. In fact, VEGF is not produced only by tumor, but it is also transported to tumor tissues by platelets and inflammatory cells (i.e.: neutrophils and monocytes) during cancer-associated inflammation and hypoxic status.[18–22] VEGF, in addition, promotes activation and differentiation of neutrophils, monocytes and MDICs, and impairs the immune-system by affecting DCs and specific T-cell subsets.[18,22] These findings support the hypothesis that a systemic inflammation state at the baseline (before the beginning of treatment) is strongly predictive of poor prognosis in cancer patients receiving bevacizumab and/or other immunological-based treatments. Moreover, it has also been reported that IL17, a pro-inflammatory cytokine produced by T_h17 subsets upon stimulation by IFNγ, promotes immune-suppressive chronic inflammation that can be present in both auto-immune diseases and cancer. In fact, IL17 attracts neutrophils, myeloid derivative inhibitory cells and increases VEGF levels in tumor micro-environment. High IL17 levels are strictly involved in tumorigenesis, metastatization and in promotion of VEGF-independent neo-angiogenesis in different malignant diseases. In the case of lung cancer development, IL17 serum levels

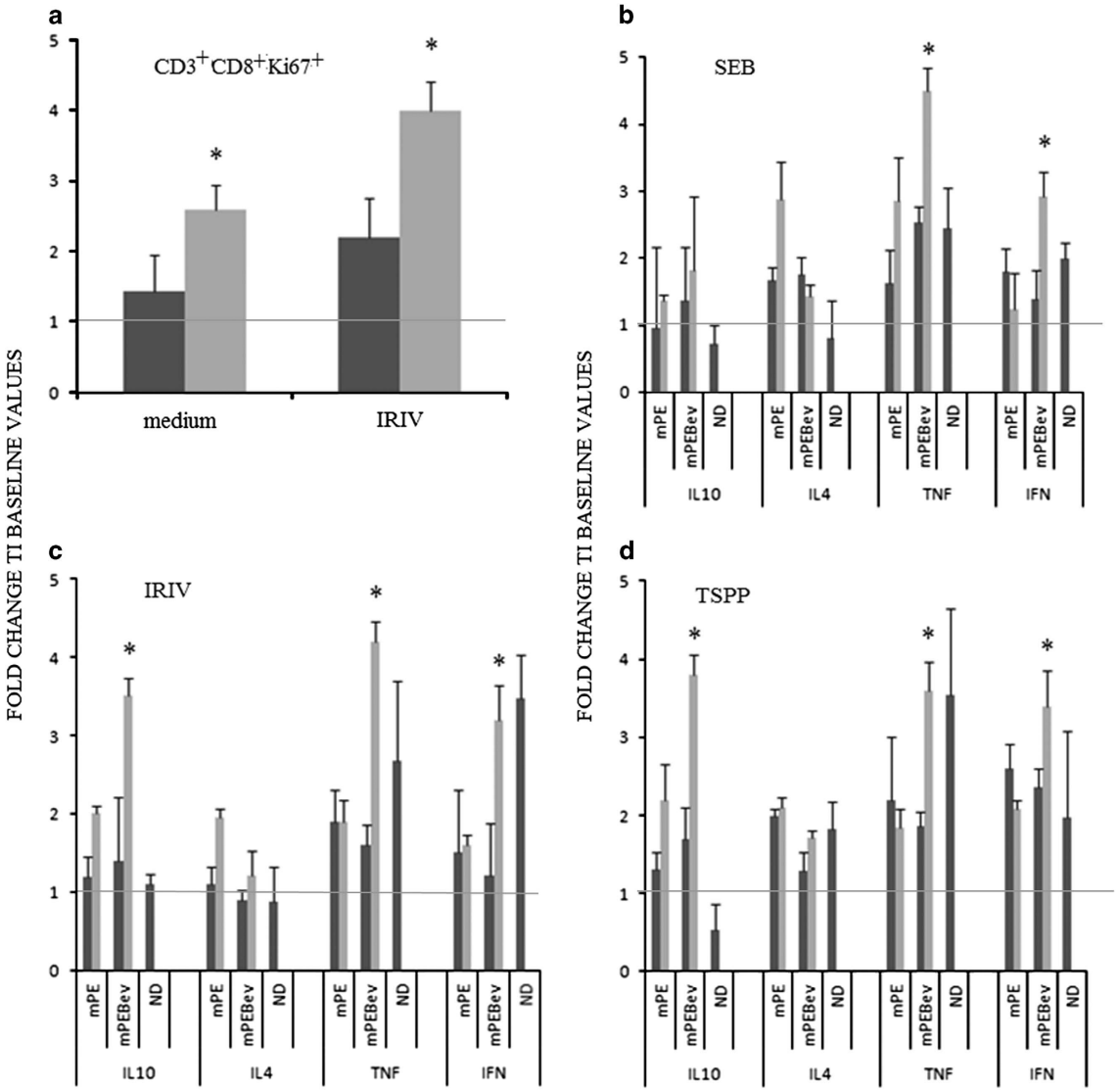

Figure 5. (**a**) A flow cytometric analysis concerning the expression of $CD8^+Ki67^+$ cells in T-cell cultures undergone multiple *in vitro* stimulation with IRIV and derived from the PBMCs of normal donors (ND) or mNSCLC patients isolated at the baseline (■) and after four treatment courses (■) with the mPE doublet alone or combined with bevacizumab (mPEBev). Further panels describe the ELISA dosage of T_h1 (IFNɣ, TNF*α*) and T_h2 (IL4 and IL10) cytokines in the supernatant of T-cell cultures *in vitro* stimulated with SEB (**b**), IRIV (**c**) and TSPP (**d**), and derived from the PBMCs of normal donors (ND) or mNSCLC patients and isolated at the baseline (■) or after four treatment courses (■) with the doublet alone (mPE) or combined with bevacizumab (mPEBev). Results are expressed as fold induction relative to baseline indicated as 1 (± S.E.). Asterisk represents statistical significance to the correspondent baseline values (*$P < 0.05$).

correlate to poor prognosis and serum VEGF levels.[37] Moreover, IL17 promotes angiogenesis by stimulating VEGF production of NSCLC cells via the STAT3/GIV signaling pathway.[38] The results of our study also revealed that bevacizumab combination with the anti-blastic doublet is correlated with a significant increase in activated ($CD8^+CD62L^+$) CTLs, long-term effector memory ($CD8^+CD27^+$) and central-memory ($CD8^+C45RA^-CCR7^+$) CTLs. In addition, our *ex vivo* investigation was on line with these findings; in fact, antigen-specific T-cell proliferation, as well as a greater antigen-specific Th1 response with potential cytotoxic activity, was recorded only in PBMCs derived from patients who had received the mPE doublet plus bevacizumab. On the other hand, the homologs T cells lines derived from mPE group showed a poor antigen-specific proliferative response and a non-cytotoxic, pro-humoral Th_2 response. In our experiments, the antigen-specific IL10 production suggests an immune-response as a possible inhibitory feed-back response to antigen-specific over-stimulation.[36] In the present study, we were unable to identify possible effects of mPEBev on MDICs expression in patients' blood samples; on the contrary, mPEBev regimen was able to increase the percentage of activated and mature myeloid derived DCs, as shown by a significant increase in $CD83^+$ and $CD80^+$-positive cells. The latter findings suggest that VEGF deprivation can improve antigen presentation by promoting DC expression and activation; this, in turn, can induce the expansion of the effector T-cell compartment with long-term memory and high-tumor-specific killing activity and enable to achieve distant lymph-nodes and tumor sites, producing the chemotactic chemokines 19 and 21 recognized by the chemokine receptor (CCR)-7 expressed on the surface of these CTLs.[39,40]

It is commonly accepted that in condition of hypoxia and chronic inflammation, granulocyte produce high levels of VEGF that, in turn, by interacting with the FLT-1/VEGFR1, promotes neo-angiogenesis for tissue repair, and the expansion and maturation

of additional myeloid cells.[41,42] MDICs family is a blood cell lineage population dependent by VEGF, IL10 and IL-13 levels. Once activated, MDICs may exerts a powerful immunological inhibitory activity affecting the activation of both DCs' and antigen-specific CTLs' precursors.[41,42] On this light, we have previously reported that VEGF deprivation, induced by the mPEBev regimen, is associated to a progressive decrease in the number and maturation of neutrophils.[41,42] In the present study, we were unable to demonstrate possible treatment-associated changes in the percentage of $CD14^{-}CD15^{+}CD11b^{+}CD66b^{+}$ MDICs in patients' peripheral blood, mostly due to the significant heterogeneous results obtained in these patients' samples. However, the present finding do not exclude that the inhibitory activity of these cells is repressed by VEGF deprivation, as suggested by the results on DC activation, CTL response and *ex vivo* results on antigen-specific CTLs. Additional experiments are presently ongoing to evaluate the effective role of MDICs deactivation in patients receiving bevacizumab and platinum based doublets. In previous studies, in line with the results of other authors, we have observed that patients receiving mPEBev treatment may develop parenchimal fibrosis and cavitations in lung sites apparently not involved by the tumor and more rarely in lethargic encephalitis.[23–26,43,44] These events can be, at least in part, explained by the occurrence of autoimmunity or of excessive immune-effector-mediated response to subclinical viral infections.[43,44] On the basis of these results, we can hypothesize that the immunological effects associated to bevacizumab administration could, at least theoretically, synergize with chemotherapy in enhancing the final antitumor effect in mNSCLC patients. In this light, it has been proposed that necrosis, massive antigen release and the formation of apoptotic bodies, caused by cytotoxic drugs in tumor tissues, could decrease the levels of immune-response inhibition mediated by PD-1/PD-1 ligand interactions. The latter effect can, in turn, cause a powerful immunological danger signal, thus leading to an increase of efficient antigen-specific CTL response with long-term memory. This observation has represented the bases for the combination of chemotherapy and/or radiotherapy with immune-adjuvant cytokines, active-specific immunotherapy and checkpoint inhibitors, in the treatment of human malignancies.[44–51] Previous results from us and others have already shown preclinical evidence that both chemotherapy and bevacizumab administration may affect MDICs and T_{reg}s' expansion,[50,51] whereas the present study demonstrate that it may also improve DC maturation and enhance CTL response, thus producing a more complex and efficacious antitumor effect. Moreover, the long-term effects of bevacizumab on the effector memory T cells and T_h1 lymphocyte subsets could have a positive impact on patients' survival because the antitumor specific immune-response can be auto-sustained after the end of the treatment.[50,51] In conclusion, bevacizumab immune-modulating effects, together with its anti-angiogenetic properties, could equally contribute to define the ultimate antitumor effects in cancer patients, thus increasing their survival. Our results suggest that the mPEBev regimen promotes the best conditions for an efficient antigen-specific CTL response and makes the mPEBev a potential candidate regimen to be assessed in combination with immune-checkpoint inhibitors in NSCLC patients.

SUBJECTS AND METHODS

Study design

The study protocol code #BEVA2007 was performed in accordance to the good clinical practice guidelines and was approved by the Bioethics Committee of the University of Siena. All patients provided a written informed consent. The inclusion criteria were: histological diagnosis of mNSCLC, performance status (ECOG) from 0 to 2, normal renal and hepatic function, WBC count $>2500/mm^3$, hemoglobin >9 g/dl, platelet cell count $>90\,000/mm^3$ and normal cardiac function. The exclusion criteria were: central tumors with high risk of bleeding (excavated with large necrosis and infiltration of large arterial and venous structures) for bevacizumab use, a history of other severe cardiovascular disease, arrhythmia, second malignant tumors and signs of active infections.

Treatment schedule

All of the patients received every 3 weeks, iv. cisplatinum (30 mg/sqm) on days 1-3, daily oral etoposide (50 mg) on days 1–15 and bevacizumab at 5 mg/kg on the day 3, for a maximum of four consecutive cycles. Subsequently, all patients who did not show a progression of disease, received erlotinib administration (150 mg/die) until progression of disease, starting 1 week after last chemotherapy course.

Biological analysis and blood sampling

Peripheral blood samples (10 ml) were withdrawn at baseline and 1 h before any treatment cycle, for either serum and PBMC isolation. Serum derived from standard peripheral blood centrifugation and PBMCs obtained by Ficoll-Hypaque (Celbio S.P.A., Italy) gradient separation medium, form heparinized blood samples, were immediately frozen and stored as described in previous studies.[52] Lymphocytes, platelets, neutrophils and monocytes were evaluated by hemocytometric cell counts, while their feature was evaluated by microscope analysis. Flow cytometry was perfomed on patients' PBMCs by carrying out standard multicolor immuno-cytoflurimetric analysis with conjugated anti-CD3, CD4, CD8, CD27, CD62L, CD19, CD16, CD56, CD25, FoxP3, CCR7, CD45Ra, CD11b, CD11c, CD14 and CD15, all purchased by eBioscience, USA.

Bio-Plex assay

Blood samples were collected from a peripheral vein at baseline and after 3 treatment courses and kept on ice. Serum was collected by centrifugation (3000 r.p.m. for 10 min at 4 °C), aliquoted and stored at −80 °C until analyzed. A multiplex biometric ELISA-based immunoassay, containing dyed microspheres conjugated with a monoclonal antibody specific for a target protein was used according to the manufacturer's instructions (Bioplex, Bio-Rad Lab., Inc., Hercules, CA, USA). Soluble molecules were measured using either commercially available kits or customized kits for the evaluation of the following cytokines: Interleukin(IL)4, IL8, IL10, IL12, IL17, IFNγ, TNF*α*, VEGF, granulocyte colony-stimulating factor, angiopoietin-2, HGF, PECAM-1, Leptin, PDGF.BB and Follistatin. Each experiment was performed in duplicate using the same procedure described in previous papers.[53] Serum levels of all proteins were determined using a Bio-Plex array reader (Luminex, Austin, TX, USA) that quantifies multiplex immunoassays in a 96-well plate with very small fluid volumes. The analyte concentration was calculated using a standard curve, with software provided by the manufacturer (Bio-Plex Manager Software, Hercules, CA, USA).

In vitro stimulation of patients' PBMC

PBMCs were isolated from four different patients who had received the mPEBev regimen and three patients who had received the mPE treatment. Blood samples taken at baseline and after three treatment courses were seeded in 24-multi-well plate at the final concentration of 10^6 cells/ml in complete medium (AIM-V) with 5% heat inactivated human AB serum. As previously described,[30] PBMCs were *in vitro* stimulated every 15 days with autologous irradiated PBMCs loaded with SEB (1 *μ*g/ml), IRIV (5 *μ*g/ml) or TSPP (10 *μ*g/ml), in complete medium containing IL4 (0.5 ng/ml), granulocyte macrophage colony-stimulating factor (15 ng/ml) for 5 days, and then followed by 10 days of culture in the presence of IL2 (25 UI/ml) before being restimulated with the same modalities.

Flow cytometry was performed on T-cell lines after three IVS with IRIV, whereas cytokine assays were performed by Bioplex analysis on the supernatant T cells after 4 IVS with the specific antigen.

Statistical analysis

The between-mean differences were statistically analyzed using Stat View statistical software (Abacus Concepts, Berkeley, CA). The results were expressed as the mean ± S.D. of four determinations made in three different experiments, and the differences determined using the two-tail Student's *t*-test for paired samples. A *P*-value of 0.05 or less was considered statistically significant.

ACKNOWLEDGEMENTS

The present study has been supported by the Italian Ministry of Education, University and Research (MIUR) with a project (FIRB-Accordi di Programma 2011; RBAP11884M_004) entitled 'Application of High-Throughput Technology Platforms for the Characterization of New Biomarkers and Molecular Targets in Nanovectors for the Diagnosis and Treatment of Human Cancer' and from the Regione Campania (RT 02-Progetto 'Hautville') with a project entitled 'Laboratori Pubblici Progetto Hauteville'.

COMPETING INTERESTS

The authors declare no conflict of interest.

REFERENCES

1 Ettinger DS. Lung Cancer and other pulmonary neoplasms. In: Ettinger DS, Goldman L, Shafer AI. *Goldman's Cecil Medicine*, 24th edn. Elsevier: New York, NY, USA, 2012, pp 1264–1271.
2 Pilkington G, Boland A, Brown T, Oyee J, Bagust A, Dickson R. A systematic review of the clinical effectiveness of first-line chemotherapy for adult patients with locally advanced or metastatic non-small cell lung cancer. *Thorax* 2015; **70**: 359–367.
3 Rajeswaran A, Trojan A, Burnand B, Giannelli M. Efficacy and side effects of cisplatin- and carbolatin-based doublet chemotherapeutic regimens as first line treatment of metastatic non small cell lung carcinoma: a systematic review of randomized controlled trials. *Lung Cancer* 2008; **59**: 1–11.
4 Burotto M, Manasanch EE, Wilkerson J, Fojo T. Gefitinib and erlotinib in metastatic non small cell lung cancer: a meta-analysis of toxicity and efficacy of randomized clinical trials. *Oncologist* 2015; **20**: 400–410.
5 Bayraktar S, Rocha-Lima CM. Molecularly targeted therapies for advanced or metastatic non-small-cell lung carcinoma. *World J Clin Oncol* 2013; **4**: 29–42.
6 Sandler A, Gray R, Perry MC, Brahmer J, Schiller JH, Dowlati A *et al.* Paclitaxel-carboplatin alone or with bevacizumab for non small cell lung cancer. *N Engl J Med* 2006; **355**: 2542–2450.
7 Reck M, von Pawel J, Zatloukal P, Ramlau R, Gorbounova V, Hirsh V *et al.* Phase III trial of cisplatin plus gemcitabine with either placebo or bevacizumab as first line therapy of non squamous non small cell lung cancer: AVAil. *J Clin Oncol* 2009; **27**: 1227–1234.
8 Luke JJ, Ott PA. PD-1 pathway inhibitors: the next generation of immunotherapy for advanced melanoma. *Oncotarget* 2015; **6**: 3479–3492.
9 Sundar R, Cho BC, Brahmer JR, Soo RA. Nivolumab in NSCLC: latest evidence and clinical potential. *Ther Adv Med Oncol* 2015; **7**: 85–96.
10 Boussiotis VA, Chatterjee P. Biochemical signaling of PD-1 on T cells and its functional implications. *Cancer J* 2014; **20**: 265–271.
11 Creelan BC. Update on immune checkpoint inhibitors in lung cancer. *Cancer Control* 2014; **21**: 80–89.
12 Pardoll DM. The blockade of immune check points in cancer immunotherapy. *Nat Rev Cancer* 2012; **12**: 252–264.
13 Brahmer JR, Hammers H, Lipson EJ. Nivolumab: targeting PD-1 to bolster antitumor immunity. *Future Oncol* 2015; **11**: 1307–1326.
14 Alfaro C, Suarez N, Gonzalez A, Solano S, Erro L, Dubrot J *et al.* Influence of bevacizumab, sunitinib and sorafenib as single agents or in combination on the inhibitory effects of VEGF on human dendritic cell differentiation from monocytes. *Br J Cancer* 2009; **100**: 1111–1119.
15 Terme M, Colussi O, Marcheteau E, Tanchot C, Tartour E, Taieb J. Modulation of immunity by antiangiogenic molecules in cancer. *Clin Dev Immunol* 2012; **2012**: 492920.
16 Correale P, Cusi MG, Tagliaferri P. Immunomodulatory properties of anticancer monoclonal antibodies: is the 'magic bullet' still a reliable paradigm? *Immunotherapy* 2011; **3**: 1–4.
17 Agudo J, Ruzo A, Tung N, Salmon H, Leboeuf M, Hashimoto D *et al.* The microRNA-126-VEGFR2 axis controls the innate response to pathogen associated nucleic acids. *Nat Immunol* 2014; **15**: 54–62.
18 Voron T, Marcheteau E, Pernot S, Colussi O, Tartour E, Taieb J *et al.* Control of the immune response by pro-angiogenic factors. *Front Oncol* 2014; **4**: 70.
19 Battinelli EM, Markens BA, Italiano JE. Release of angiogenesis regulatory proteins from plathelet alpha granules: modulation of physiologic and pathologic angiogenesis. *Blood* 2011; **118**: 1359–1369.
20 Koehne P, William C, Strauss E, Schindler R, Eckardt KU, Bührer C. Lack of hypoxic stimulation of VEGF secretion from neutrophils and platelets. *Am J Physiol Heart Circ Physiol* 2000; **279**: H817–H824.
21 Zhang Y, Lu Y, Ma L, Cao X, Xiao J, Chen J *et al.* Activation of vascular endothelial growth factor receptor-3 in macrophages restrains TLR4-NF-κB signaling and protects against endotoxin shock. *Immunity* 2014; **40**: 501–514.
22 Tan KW, Chong SZ, Wong FH. Neutrophils contribute to inflammatory lymphangiogenesis by increasing VEGF-A bioavailability and secreting VEGF-D. *Blood* 2013; **122**: 3666–3677.
23 Correale P, Cerretani D, Remondo C, Martellucci I, Marsili S, La Placa M *et al.* A novel metronomic chemotherapy regimen of weekly platinum and daily oral etoposide in high-risk non-small cell lung cancer patients. *Oncol Rep* 2006; **16**: 133–140.
24 Correale P, Remondo C, Carbone FS, Ricci V, Migali C, Martellucci I *et al.* Dose/dense metronomic chemotherapy with fractioned cisplatin and oral daily etoposide enhances the anti-angiogenic and anti-tumor activity of bevacizumab in advanced non-small-cell-lung cancer patients. *Cancer Biol Ther* 2010; **9**: 685–693.
25 Correale P, Botta C, Basile A, Pagliuchi M, Licchetta A, Martellucci I *et al.* Phase II trial of bevacizumab and dose/dense chemotherapy with cisplatin and metronomic daily oral etoposide in advanced non-small-cell-lung cancer patients. *Cancer Biol Ther* 2011; **12**: 112–118.
26 Correale P, Martellucci I, Pastina P, Botta C, Martino E, Mazza D *et al.* Antitumor and immune-biological activity of a new metronomic chemotherapy with fractioned cisplatin and oral etoposide combined with bevacizumab (mPEBev) followed by erlotinib maintenance in non small cell lung cancer (NSCLC) patients. *J Thorac Oncol* 2013; **8**: S2 (abstract P1.11-028).
27 Botta C, Barbieri V, Ciliberto D, Rossi A, Rocco D, Addeo R *et al.* Systemic inflammatory status at baseline predicts bevacizumab benefit in advanced non-small cell lung cancer patients. *Cancer Biol Ther* 2013; **14**: 469–475.
28 Spaulding AR, Salgado-Pabón W, Koheler PL, Horswill AR, Leung DY, Schlievert PM. Staphilococcal and streptococcal superantigen exotoxins. *Clin Microbiol Rev* 2013; **26**: 422–447.
29 Alam S, Knowlden ZAG, Sangster MY, Sant AJ. CD4 T cell help is limiting and selective during the primary cell response to influenza virus infection. *J Virol* 2014; **88**: 314–324.
30 Correale P, Del Vecchio MT, Cusi MG, Savellini GG, La Placa M, Terrosi C *et al.* 5-fluorouracil-based chemotherapy enhances the antitumor activity of a thymidylate synthase-directed polyepitopic peptide vaccine. *J Natl Cancer Inst* 2005; **97**: 1437–1445.
31 Correale P, Botta C, Martino EC, Ulivieri C, Battaglia G, Carfagno T *et al.* Phase Ib study of poly-epitope peptide vaccination to thymidylate synthase (TSPP) and GOLFIG chemo-immunotherapy for treatment of metastatic colorectal cancer patients. *Oncoimmunology* 2015; **5**: e1101205.
32 Cusi MG, Botta C, Correale P, Rossetti MG, Dreassi E, Guidelli GM *et al.* Phase I trial of thymidylate synthase poly-epitope peptide (TSPP) vaccine in advanced cancer patients. *Cancer Immunol Immunother* 2015; **64**: 1159–1173.
33 Krneta J, Kroll J, Alves F, Prahst C, Sananbenesi F, Dullin C *et al.* Dissociation of angiogenesis and tumorigenesis in follistatin- and activin-expressing tumors. *Cancer Res* 2006; **66**: 5686–5695.
34 Kumar R, Geuna E, Michalarea V, Guardascione M, Naumann U, Lorente D *et al.* The neutrophil-lymphocyte ratio and its utilization for the management of cancer patients in early clinical trials. *Br J Cancer* 2015; **112**: 1157–1165.
35 Grivennikov SI, Greten FR, Karin M. Immunity, inflammation and cancer. *Cell* 2010; **140**: 883–899.
36 Walter MR. The molecular basis of IL-10 function: from receptor structure to the onset of signaling. *Curr Top Microbiol Immunol* 2014; **380**: 191–212.
37 Pan B, Che D, Cao J, Shen J, Jin S, Zhou Y *et al.* Interleukin-17 levels correlate with poor prognosis and vascular endothelial growth factor concentration in the serum of patients with non-small cell lung cancer. *Biomarkers* 2015; **20**: 232–239.
38 Pan B, Shen J, Cao J, Zhou Y, Shang L, Jin S *et al.* Interleukin-17 promotes angiogenesis by stimulating VEGF production of cancer cells via the STAT3/GIV signaling pathway in non-small-cell lung cancer. *Sci Rep* 2015; **5**: 16053.
39 Sallusto F, Geginat J, Lanzavecchia A. Central memory and effector memory T cells subsets: function, generation, and maintenance. *Annu Rev Immunol* 2004; **22**: 745–763.
40 Foster R, Schubel A, Breitfeld D, Kremmer E, Renner-Muller I, Wolf E *et al.* CCR7 coordinates the primary immune-response by establishing functional microenvironments in secondary lymphocid organs. *Cell* 1999; **99**: 23–33.
41 Gabrilovich DI, Ostrand-Rosenberg S, Bronte V. Coordinated regulation of myeloid cells by tumors. *Nat Rev Immunol* 2012; **12**: 253–268.
42 Talmadge JE, Gabrilovich DI. History of myeloid –derived suppressor cells. *Nat Rev Cancer* 2013; **13**: 739–752.
43 Rafailidis PI, Kakisi OK, Vardakas K, Falagas ME. Infectious complications of monoclonal antibodies used in cancer therapy: a systematic review of the evidence from randomized controlled trials. *Cancer* 2007; **109**: 2182–2189.
44 Kang HJ, Park JS, Kim DW, Lee J, Jeong YJ, Choi SM *et al.* Adverse pulmonary reactions associated with the use of monoclonal antibodies in cancer patients. *Respir Med* 2012; **106**: 443–450.
45 Taugourdeau-Raymond S, Rouby F, Default A, Jean-Pastor MJFrench Network of Pharma-covigilance Centers. Bevacizumab-induced serious side-effects: a review of the French pharmacovigilance database. *Eur J Clin Pharmacol* 2012; **68**: 1103–1117.
46 Ramakrishnan R, Assudani D, Nagaraj S, Hunter T, Cho HI, Antonia S *et al.* Chemotherapy enhances tumor cell susceptibility to CTL-mediated killing during cancer immunotherapy in mice. *J Clin Invest* 2010; **120**: 1111–1124.

47 Dalgleish AG. Rationale for combining immunotherapy with chemotherapy. *Immunotherapy* 2015; **7**: 309–316.
48 Zheng Y, Dou Y, Duan L, Cong C, Gao A, Lai Q *et al.* Using chemo-drugs or irradiation to break immune tolerance and facilitate immunotherapy in solid cancer. *Cell Immunol* 2015; **294**: 54–59.
49 Villarreal DO, Wise MC, Walters JN, Reuschel EL, Choi MJ, Obeng-Adjei N *et al.* Alarmin IL-33 acts as an immunoadjuvant for enhancing antigen-specific cell-mediated immunity resulting in potent anti-tumor immunity. *Cancer Res* 2014; **74**: 1789–1800.
50 Bustamante Alvarez JG, González-Cao M, Karachaliou N, Santarpia M, Viteri S, Teixidó C *et al.* Advances in immunotherapy for treatment of lung cancer. *Cancer Biol Med* 2015; **12**: 209–222.
51 Mansfield AS, Nevala WK, Lieser EAT, Leontovich AA, Markovic SN. The immunomodulatory effects of bevacizumab on systemic immunity in patients with metastatic melanoma. *Oncoimmunology* 2013; **2**: e24436.
52 Botta C, Bestoso E, Correale P. Immune-modulating effects of the newest cetuximab-based chemoimmunotherapy regimen in advanced colorectal cancer patients. *J Immunother* 2012; **35**: 440–447.
53 Costantini S, Capone F, Guerriero E, Maio P, Colonna G, Castello G. Serum cytokine levels as putative prognostic markers in the progression of chronic CHC hepatitis leading to cirrhosis. *Eur Cytokine Netw* 2010; **21**: 251–256.

J. Neurovirol. (2016) 22:307–315
DOI 10.1007/s13365-015-0395-2

Toscana virus infects dendritic and endothelial cells opening the way for the central nervous system

Maria Grazia Cusi[1] · **Claudia Gandolfo**[1] · **Chiara Terrosi**[1] · **Gianni Gori Savellini**[1] · **Giuseppe Belmonte**[2] · **Clelia Miracco**[2]

Received: 5 June 2015 / Revised: 6 October 2015 / Accepted: 12 October 2015 / Published online: 28 October 2015

Abstract Toscana virus (TOSV) is a Phlebovirus responsible for human neurological infections in endemic Mediterranean areas. The main viral target is the central nervous system, with viremia as a way of dissemination throughout the host. This study was aimed at understanding the spread of TOSV in the host by identifying the cell population infected by the virus and the vehicle to the organs. In vivo studies provided evidence that endothelial cells are infected by TOSV, indicating their potential role in the diffusion of the virus following viremic spread. These results were further confirmed in vitro. Human peripheral mononuclear blood cells were infected with TOSV; only monocyte-derived dendritic cells were identified as susceptible to TOSV infection. Productive viral replication was then observed in human monocyte-derived dendritic cells (moDCs) and in human endothelial cells by recovery of the virus from a cell supernatant. Interleukin-6 was produced by both cell types upon TOSV infection, mostly by endothelial cells, while moDCs particularly expressed TNF-α, which is known to induce a long-lasting decrease in endothelial cell barrier function. These cells could therefore be implicated in the spread of the virus in the host and in the infection of tissues that are affected by the disease, such as the central nervous system. The identification of in vitro and in vivo TOSV cell targets is an important tool for understanding the pathogenesis of the infection, providing new insight into virus–cell interaction for improved knowledge and control of this viral disease.

Keywords Toscana virus · Target cells · Infection

✉ Maria Grazia Cusi
mariagrazia.cusi@unisi.it

[1] Department of Medical Biotechnologies, University of Siena, V.le Bracci, 1, 53100 Siena, Italy

[2] Department of Medicine, Surgery, and Neurosurgery, Pathological Anatomy Section, University of Siena, V.le Bracci 1, 53100 Siena, Italy

Introduction

Toscana Virus (TOSV), belonging to the *Bunyaviridae* family, has been associated with the occurrence of acute neurological diseases, such as meningitis, meningoencephalitis and encephalitis, in the Mediterranean countries (mainly Italy, Spain and France) during summer months (Valassina et al. 2003a, b; Charrel et al. 2005; Cusi et al. 2010, Sanbonmatsu-Gámez et al. 2009). In the countries where TOSV is present, it is among the most prevalent viruses causing meningitis during the warm season, together with enteroviruses and herpesviruses (Cusi et al. 2010; Charrell et al. 2012). TOSV is transmitted by Phlebotomine sandflies, but its animal reservoir has not yet been identified, although serological studies have found anti-TOSV-specific antibodies in some animal species (Navarro-Marí et al. 2011), indicating that it can also infect these animals. Asymptomatic infection and infection without central nervous system involvement (Charrel et al. 2005) have also been described; thus, the pathogenesis of Toscana virus is still largely unclear (Cusi et al. 2005). Most attention has been focused on the identification of factors involved in the progression of the disease. An intriguing aspect is the understanding of the mechanisms involved in the spread of the virus into the central nervous system (CNS). It has been postulated that arboviruses invade the CNS across the blood–brain barrier either by passive diffusion or by replication in microvascular endothelial cells (Dropulic and Masters 1990; Sahni 2007); consequently, the level of viremia may be critical in determining the chances of the virus passing

into the brain. This study aimed at analysing which cell types can be infected by TOSV after the virus has entered the host. For this purpose, we infected human peripheral blood mononuclear cells (PBMC) in vitro with TOSV in order to identify the cell populations that might be susceptible to the virus. Moreover, we evaluated the ability of the virus to infect in vivo mouse brain microvascular endothelial cells, in order to investigate their role in the viral neuroinvasive process.

Materials and methods

Virus and cells

Vero cells were grown as a monolayer in Dulbecco's modified Eagle's medium (DMEM) (Lonza, Milan, Italy) supplemented with 5 % heat-inactivated foetal calf serum (FCS) (Lonza) and 100 U/mL penicillin/streptomycin (Hyclone Europe, Milan, Italy) at 37 °C. Toscana virus, strain 1812 (TOSV, isolated from the cerebrospinal fluid (CSF) of a patient with meningitis) was propagated on Vero cells as previously described (Cusi et al. 2005). Human humbelical vein endothelial cells (HUVECs) (Cambrex corp., Walkersville, MD) were cultured and subcultured in endothelial basal medium (EBM-2) (Cambrex. Cp) supplemented with 10 % FCS, hydrocortisone (1 mg/ml), human epidermal growth factor (EGF) (0.1 mg/ml) and bovine brain extract (BBE) (1 mg/ml) in 5 % CO2 at 37 °C. PBMCs were isolated from a buffy coat of TOSV seronegative healthy donors, upon informed consent, by Ficoll-Hypaque gradient separation and resuspended in RPMI 1640 medium (Hyclone, Cramligton, UK) supplemented with 10 % FCS (Life Technologies, Milan, Italy) and IL-2 (50 UI/ml) (CHIRON, Emervylle, CA, USA).

Generation of human monocyte-derived dendritic cells

Monocyte-derived dendritic cells (moDCs) were generated by culturing human PBMCs in the presence of granulocyte–macrophage-colony stimulating factor (GM-CSF) (50 ng/ml) and IL-4 (for 0.5 ng/ml) (R & D Minneapolis, MN, USA) for 7 days, as described elsewhere (Bell et al. 1999). To estimate immature monocyte-derived dendritic cells phenotype, cultures were examined for the expression of CD11c and CD83 (Chemicon, Germany) as described below.

TOSV infection of endothelial and dendritic cells in vitro

HUVECs and moDCs were, respectively, seeded in 6-well culture plates at a density of 5×10^5 and 1×10^6 cells per well and incubated at 37 °C in 5 % CO_2 atmosphere. Cells were then infected with TOSV at a multiplicity of infection (MOI) of 1, 3 or 5 and, after 90 min at 37 °C, washed with medium. Twenty-four, 48, 72 and 96 h later, cells were collected and assayed by indirect immunofluorescence assay (IFA). Briefly, cells were spotted on slides and fixed for 10 min at room temperature with cold methanol/acetone. Cells were then incubated for 1 h at 37 °C with anti-TOSV N protein (provided by DIESSE Srl, Siena, Italy; diluted at 1:200). After washing with PBS, fluorescein-labelled anti-mouse IgG (Sigma, Milan, Italy) was added for 1 h at 37 °C. Immunofluorescence was visualised using a Diaplan microscope (Leica Microsystems, Milan, Italy). Infected moDCs were also analysed by cytofluorimetric analysis, as described elsewhere (Lozach et al. 2011). After fixation and permeabilization with phosphate buffered saline (PBS) containing 0.5 % saponin and 2 % FCS, cells were stained with anti-TOSV N protein monoclonal antibody (diluted at 1:50) for 30 min on ice. After two washing steps, cells were incubated with FITC-conjugated anti-mouse IgG (Sigma, Milan, Italy, diluted at 1:100) and anti-hCD4-PE mAb (Sigma, Milan, Italy, diluted at 1:10) or anti-hCD8-PerCy5 mAb (Chemicon, Germany, diluted at 1:10), anti-hCD11c-PE mAb (Chemicon, Germany, diluted at 1:10), anti-hCD14-PE mAb (Chemicon, Germany, diluted at 1:10), anti-hCD19-PE mAb (Chemicon, Germany, diluted at 1:10), or anti CD83 (Chemicon, diluted 1: 50). Stained cells were washed in PBS and analysed using a FACSCalibur with CellQuest software (BD Biosciences, San Jose, CA). The supernatant of infected HUVECs and moDCs was collected 1, 2, 3,and 4 days after infection for virus titration.

TOSV titration

Briefly, the supernatant of infected cells was diluted tenfold and titrated by plaque assay on a 6-well plate of Vero cells and incubated at 37 °C in 5 % CO_2 for 1 h (Hemmersbach-Miller et al. 2004). The medium was then removed, and 3.5 ml of overlay medium containing 3 % purified agar (Oxoid, Milan, Italy) was added. After 5 days, the cell sheet was stained with neutral red, and the viral titre was determined as plaque forming units/ml (PFU/ml). Mock-infected cells were included in each experiment as controls. All experiments were repeated three times.

Cytokine assay

Supernatants of HUVECs and moDCs collected 24, 48, 72 and 96 h after TOSV infection were tested for the presence of interleukin-6 (IL-6) and tumour necrosis factor-α (TNF-α) by ELISArray (SABiosciences Corp. Frederick, MD, USA) following the manufacturer's instructions. To determine interferon-β (IFN-β), the supernatant was assayed at the same time points using the human IFN-β ELISA kit (PBL Interferon Source, Piscataway, NJ, USA) according to the manufacturer's protocol.

Permeability assay

Permeability assays were performed on 24-well plates with polycarbonate filters (3 μm pore and 6 mm diameter (Corning Life Sciences, The Netherlands) coated with HUVECs (5×10^4 cells per cm^2) in 300 μl of complete EBM2 medium (upper compartment) and cultured until confluence (2 days). Lower compartments contained 700 μl of medium. Before the permeability assay, HUVECs were washed with medium and transferred to a new plate.

Cells were then infected in triplicate with TOSV at an MOI of 1 and incubated at 37 °C for 5 h. Human PBMCs (2×10^4), previously isolated as described, were then added to each well coated with infected HUVECs and incubated at 37 °C for 24 h. Finally, FITC-dextran (4 KDa mol wt, Sigma, Milan, Italy) (0.5 mg/ml) was added to the upper chamber of the filter, and after 3 h, the fluorescence intensity of transmigrated FITC-dextran was measured in the upper and lower chambers using a Perkin-Elmer fluorimeter (490-nm excitation, 530 nm emission). Uninfected HUVECs, uninfected HUVECs+ PBMCs and TOSV-infected HUVECs were used as controls. In order to monitor TOSV infections, endothelial cell monolayers in 96-well plates were infected at the same MOI as the Transwell plates. At 24 h post-infection, cells were fixed and tested for the presence of virus by immunofluorescence. The assay was repeated three times. The FITC dextran transmigrated across the membrane was calculated as the ratio of fluorescence units/ml in the upper and lower chambers for all experimental samples. A *t* test for in vitro permeability assay was performed using a SigmaStat (San Jose, California), and *p* values of <0.05 were considered significant.

Animal infection

Four-week-old female BALB/c mice (Charles River, Milan, Italy) were used for TOSV infection. Groups of four mice were subcutaneously (sc.) injected with 200 μl of TOSV 1812 V (3×10^6 PFU/ml) (Cusi et al. 2005). Blood was drawn from mice 24 h and 3 and 6 days after infection for viral genome detection. Mouse blood samples were centrifuged at 1600*g* for 5 min. Plasma was recovered, while the buffy coat and erythrocytes were mixed with an equal volume of phosphate buffered saline and further separated by Ficoll-Hypaque gradient for purifying peripheral blood mononuclear cells. Moreover, pieces of mouse epidermis and brain were removed and processed for histology. Each experiment was repeated three times in order to assess the reproducibility of results. All animal experiments were approved by the local Ethics Committee and carried out in strict compliance with the Institutional Animal Care and Use Committee (IACUC) guidelines and in accordance with the 2010/63/EU Directive (http://eurlex.europa.eu/LexUriServ/LexUriServ.do?uri=OJ:L:2010:276:0033:0079:EN:PDF) of the European Parliament and the Council for the Protection of Animals Used for Scientific Purposes.

Histological and immunohistochemical analysis of tissues

After removal, organs were post-fixed in phosphate buffered 10 % formalin. After fixation, fragments of epidermis and coronal slices of brain were embedded in paraffin. Serial sections from each organ slice were partly stained with haematoxylin and eosin (HE), thionin, Bielschowski and luxol fast blue (Klüver-Barrera) and partly processed for immunohistochemistry or immunofluorescence. A commercial kit (Super Sensitive Bioptica, Milan, Italy) was used to perform immunohistochemistry in order to detect virus antigen distribution and to identify the infected cell types. After deparaffinization, sections were washed in Tris–HCl buffer (pH 7.6) and incubated for 8 min with UltraV Block. After washing, the anti-N TOSV mAb (diluted 1:400) was applied for 1 h, and a secondary biotinylated goat anti-mouse antibody (NeoMarkers, BioOptica, Milan, Italy) was applied for 20 min at room temperature. Sections were washed again and then incubated for 20 min with Streptavidin Alk-Phos or streptavidin-HRP (NeoMarkers) at room temperature. Conjugates were visualised with brown staining, using a diaminobenzidine solution (NeoMarkers) as chromogen, after 8 min incubation. Haematoxylin was used for counterstaining.

In order to colocalize TOSV and endothelial cells, a double immunofluorescence stain was performed in tissue sections treated with mouse FITC-labelled anti-TOSV mAb (DIESSE, srl, diluted 1/200) and rabbit Alexa Fluor 647 labelled anti-mouse CD31 (diluted 1/200; BioLegend, Milan, Italy). The nuclei were counterstained by incubating sections for 10 min with 4,6-diamidino-2-phenylindole (DAPI) as described elsewhere (Tini et al. 2015). Images were acquired and analysed with a Leica AFCTR6500HS microscope (Leica Microsystems, Milan, Italy)

RT-PCR

Separated blood components (plasma, PBMCs) or whole blood of infected mice were subjected to RNA extraction using a total RNA isolation kit (Promega, Mannheim, Germany). Total RNA was amplified by RT-PCR; reverse transcription was performed at 37 °C for 30 s, followed by 35 cycles of amplification (94 °C for 1 min, 52 °C for 30 s and 72 °C for 40 s), as previously described (Cusi et al. 2005).

Statistical analysis

All experiments were carried out in triplicate; mean differences were statistically analysed using Stat View statistical software (Abacus Concepts, Berkeley, CA). Differences of *P* values ≤0.05 were considered significant.

Results

Virus growth in human cells

In this study, we demonstrated that Toscana virus does not infect specific subsets of peripheral blood human mononuclear cells, such as T and B lymphocytes and monocytes, which were negative by flow cytometry (FACS) or immunofluorescence assay (IFA) 2–4 days after in vitro infection (Lozach et al. 2010, 2011). On the contrary, we were able to infect both monocyte-derived DCs and human umbilical vein endothelial cells in vitro, which appeared susceptible to TOSV infection and able to support its replication. Infected cells did not show an evident viral cytophatic effect; however, their supernatant, collected at 1–4 days post-infection, confirmed virus growth when tested for TOSV titration. The virus reached a peak titre at 48 h post-infection and then decreased in both cell types on the following days, as shown in Fig. 1. Endothelial cells were more susceptible to this virus infection than moDCs. Indeed, while HUVECs infected at 1 MOI were positive to TOSV, after 24 h by IFA, no signal was detected in infected moDCs (data not shown). Only a more sensitive cytofluorimetric analysis allowed us to demonstrate that moDCs were TOSV infected after 24 h, but at a very low level (2.7–3.7 %) independently of the MOI used. TOSV-positive moDCs were clearly detectable 48 h post-infection, when higher MOI were used, as previously described by Lozach et al. (2011). Indeed, as shown in Fig. 2, a higher percentage (29.8 %) of infected moDC was observed when an MOI of 5 was used to infect them, indicating that this cell infection is multiplicity dependent. Moreover, infected DCs were activated, as demonstrated by an increase in CD83 at FACS, after TOSV infection (Fig. 2a, b) (Prazma et al. 2007; Prechtel et al. 2007; Prazma and Tedder 2008). These results confirmed that TOSV can infect both endothelial cells and DCs in which the virus is able to replicate, thus providing a model for studying this virus infection.

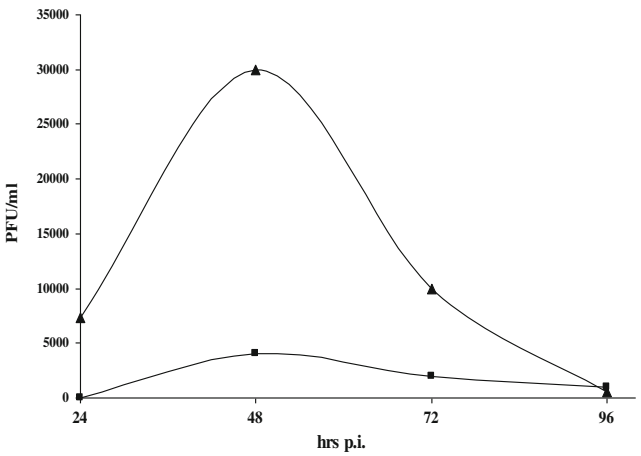

Fig. 1 Titration of TOSV in cell culture supernatant. Cell culture supernatants were collected from HUVECs (—▲—) or moDCs (—■—) infected with TOSV at an MOI of 3 at 24–96 h p.i. for virus titration. Titer values, expressed as PFU/ml, represent the average of at least three independent infections

Effects of PBMCs on the permeability of TOSV-infected endothelial cells

In order to study the effect of TOSV on endothelial permeability, we used a standard cell permeability assay which monitors the passage of FITC-dextran across cell monolayers, and we evaluated the effect of the presence of PBMCs on TOSV-infected endothelial cells. TOV-infected HUVECs did not show a decrease in permeability in comparison to uninfected cells; a similar result was obtained when uninfected cells were added with PBMCs. On the contrary, the addition of PBMCs to endothelial cells, 5 hours after infection, increased the permeability across HUVECs (p=0.01) (Fig. 3).

TOSV detection in infected mice

Previous results were confirmed in vivo by analysing blood cells drawn from mice sc. inoculated with TOSV 1, 3 and 6 days after infection. Blood was centrifuged in order to separate plasma from cells. RT-PCR was performed on each sample to detect the TOSV genome. The virus was revealed only in plasma or in the whole blood samples, 3 and 6 days after mice infection (Fig. 4). No virus was detected in circulating PBMCs, indicating that these cells are not a target for TOSV replication. On the contrary, mouse endothelial cells resulted positive for TOSV infection. Indeed, the histological analysis of skin biopsies drawn from mice sc. inoculated with the virus revealed positivity for TOSV in endothelial cells of the subcutaneous post-capillary venulae (Fig. 5a, g–i). Moreover, in some mice, findings consistent with lymphocytic vasculitis were observed in several venulae, showing a leakage in the endothelium with the elastic lamina partially destroyed by the inflammatory infiltrate (Fig. 5b), mainly represented by CD8+ T lymphocytes (Fig. 5c). However, the arteriolae were less altered or unaffected by this phenomenon. Interestingly, brain sections of sc. infected mice also showed TOSV positivity in the endothelium of venulae, without inflammatory cells, indicating that the virus could reach the central nervous system (Fig. 5d) without causing symptomatology or organ damage in the animal. TOSV positivity of dendritic cells had been previously observed in the same animals (Cusi et al. 2005). Skin and brain tissue of mock-infected mice did not present any positive cells (Fig. 5e–f, l–n). TOSV-infected DCs were also revealed in humans, in particular in a patient infected with TOSV and lymphadenopathy (Ranaldi et al. 2011).

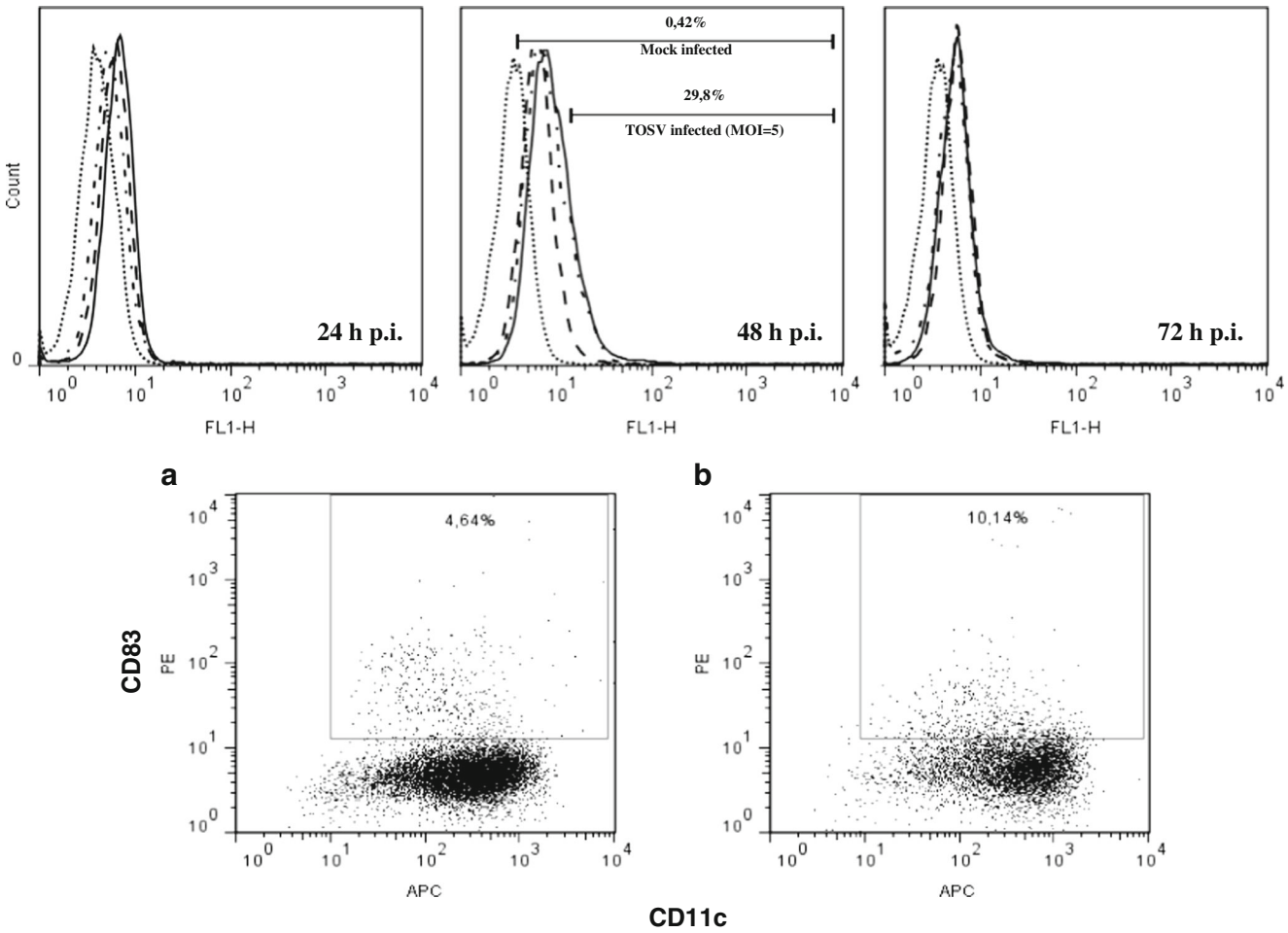

Fig. 2 Quantification of fluorescence in TOSV-infected moDCs by FACS analysis, as described in Experimental procedures. Histograms show uninfected control cells (…) and TOSV-infected cells with 5 MOI (—), 3 MOI (▬▲▬), and 1 MOI (▬■▬) at 24, 48 and 72 h p.i., as indicated. FL1-H is the measurement of fluorescence intensity. Human moDCs were also analysed by immunofluorescence gating for CD11c+ (APC) and CD83+ (PE) cells. **a** Mock-infected moDCs, **b** TOSV-infected moDCs. **c, d** Immunofluorescence assay on HUVECs infected by TOSV (MOI 1) and observed at 24 h p.i. The cells were fixed and stained with anti TOSV mabs (DIESSE)

Cytokine expression following in vitro TOSV infection

Inflammation plays a role in the pathogenesis of some viral diseases (Dionisio et al. 2001; Valassina et al. 2003a, b; Gori Savellini et al. 2011); thus, inflammatory cytokines such as IL-1 b, IL-6 and TNF-α were tested in the supernatant of HUVECs and moDCs after TOSV infection. Among these cytokines, only IL-6, a proinflammatory cytokine with

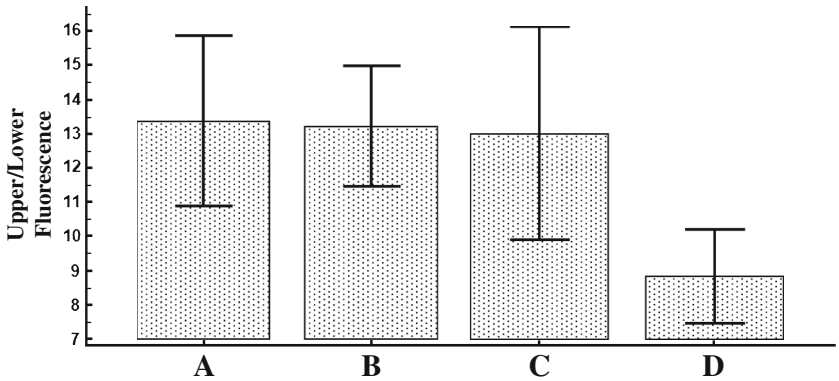

Fig. 3 FITC-dextran permeability assay on HUVECs after TOSV infection. The assay was performed at 24 h p.i. **a** mock-infected HUVECs, **b** TOSV-infected HUVECs, **c** HUVECs+PBMC, **d** TOSV-infected HUVECs+PBMC. FICT-dextran emission was measured and reported as the ratio of the fluorescence units/μl in the upper and lower chamber. The data are representative of three independent experiments

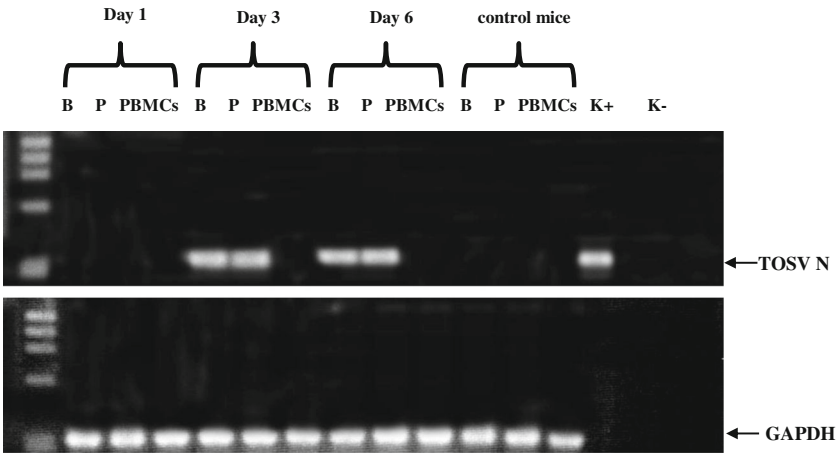

Fig. 4 TOSV detection in infected mice. The presence of TOSV genomic RNA was investigated by RT nested-PCR on whole blood (*B*), plasma (*P*) or peripheral-blood mononuclear cells (PBMCs) samples collected from mice at 1, 3 and 6 days after infection. The same samples drawn from mock-infected mice (control mice) were assayed at the 3rd day p.i. A positive control (K+) and blank (K−) were included in the assay (*upper panel*). All the samples were tested for GAPDH (glyceraldehyde-3-phosphate dehydrogenase) as internal control (*lower panel*)

antiviral effects, was produced by human endothelial cells, reaching a peak (3365±183 pg/ml) at 72 h post-infection. On the contrary, heat-inactivated TOSV was not able to elicit IL-6 synthesis in the same cells. These findings show that this virus is capable of modulating the in vitro production of IL-6, amplifying leukocyte recruitment and thus playing a positive role in vascular inflammatory reactions. However, in addition to IL-6 which was constantly produced during the entire time considered (445±59.11 pg/ml; CI 370–504), MoDcs were able to express the pro-inflammatory cytokine TNF-α, particularly at 96 h (1553±201 pg/ml) after TOSV infection, leading to an enhanced inflammatory response and further activation of antigen presentation.

TOSV-infected cells show an innate antiviral response

In order to determine the presence or absence of an innate immune response to TOSV infection, we performed IFN-β ELISA on supernatants from infected HUVECs and moDCs. HUVECs were able to produce IFN-β at a higher amount at 48 h post-infection (165±1.7 pg/ml), while moDCs produced it at a lower amount in the first 3 days post-infection (7 to 10 pg/ml), confirming that TOSV is an inducer of in vitro IFN-β (Gori Savellini et al. 2011). The UV-inactivated virus was unable to induce IFN-β in the same cells.

Discussion

Since only some subjects infected by TOSV develop a neurological disease (Valassina et al. 2003a, b; Sanbonmatsu-Gámez et al. 2009) and no particular genotype has yet been associated with neurovirulence, it is fundamental to discover the bases of viral pathogenesis in order to understand why clinical manifestation occurs in only a few subjects. Lozach et al. (2011) showed that several Phleboviruses (Bunyaviridae) exploit DC-SIGN to infect dendritic cells. In this study, we have demonstrated that TOSV is able to infect and replicate in moDCs and endothelial cells before entering the bloodstream. It should be noted that infection of DCs is dose dependent and only a high load of virus is able to trigger and induce a productive infection in these cell types. This feature could represent an important factor for determining the development of a serious neurological disease. Moreover, this observed upregulation of CD83, a marker of DC maturation, in TOSV-infected DCs could play an essential role in the initiation of the immune response, regulating innate and adaptive immune responses and mediating the activation of T cells by DCs. Therefore, the role of infected DCs in spreading the virus in the host or activating T cells still needs to be clarified. Furthermore, TOSV is free to move throughout blood and it is not vehiculated by any specific blood mononuclear cell type, as revealed by the absence of the viral genome in blood cell sub-populations and by its presence in plasma of sc. infected mice. Once it has entered the host, TOSV migrates from the skin, where it can infect dendritic cells, towards the draining lymph nodes and, after further replicating in endothelial cells, through the primary viraemia it reaches the spleen (Cusi et al. 2010) finding an ideal location for a secondary replication phase due to the vascular structure of this organ. In most cases, TOSV infection causes mild diseases and innate immunity can resist infection by producing IFN-β, as shown in vitro. However, in some cases, TOSV can enter the central nervous system (CNS) and cause neurological disease through unidentified mechanisms (Dionisio et al. 2001; Valassina et al. 2003a, b; Hemmersbach-Miller et al. 2004; Baldelli et al. 2004; Sanbonmatsu-Gámez et al. 2009). We cannot exclude the role of the innate immune response as a

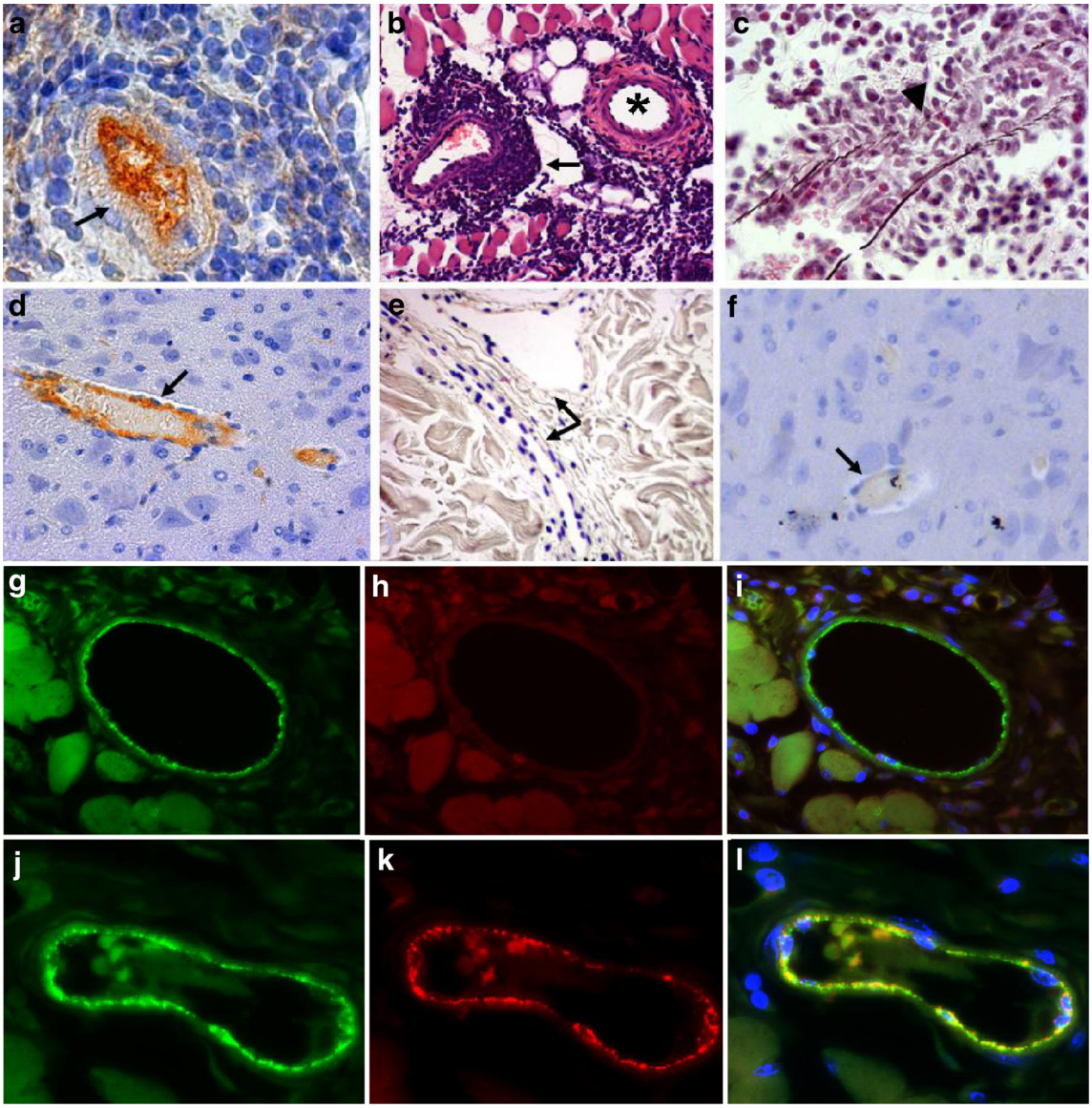

Fig. 5 Immunohistochemistry and IF of tissues of TOSV-inoculated mice. Virus immunohistochemistry of skin (**a**) and brain (**d**) tissues drawn from mice sc. inoculated with TOSV. Brown-stained endothelial cells of cutaneous (**a**) and brain (**d**) venulae (*arrow*), positive for TOSV. Lymphocyte infiltrate of a cutaneous venula wall (**b**, *arrow*). Vasculitis does not affect arteriolae (**b**, the *asterisk* indicates the lumen of an arteriole) and partly destroys venular elastic lamina (**c**, *arrow head*). Skin (**e**) and brain tissue (**f**) of a mock-infected mouse (the *arrows* indicate TOSV-negative vessels). **a**, **d**, **e**, **f** Immunohistochemistry; original magnification (OM): **a**, **d**, **f** ×400; **e** ×200; **b** haematoxylin and eosin; OM ×200; **c** Orcein-Giemsa stain, OM ×200. Immunofluorescence of TOSV and CD31 on endothelial cells of the skin of a sc. infected mouse: positivity to CD31 (**j**) and TOSV (**k**); **l** the merged image shows co-localization of CD31 and TOSV. **g**–**i** IFA performed with the same antibodies on the skin of a negative control mouse (magnification ×630)

co-pathological factor in causing CNS diseases. As already shown for La Crosse Virus, a member of the Bunyaviridae family, on one hand, innate immunity stimulates the anti-viral recognition pathway and inhibits systemic viral replication, but on the other, it activates the same signaling pathway in the CNS, contributing to neuronal cell death (Taylor and Peterson 2014). Thus, the activation of the same pathway at the systemic level and in the CNS results in protective and pathogenetic mechanisms, respectively (Denizot et al. 2012). Although TOSV possesses a non-structural (NSs) protein capable of inhibiting type I IFN, the virus itself is responsible for its induction. We still do not know the contribution of the type I IFN response to the disease pathogenesis in specific tissues after TOSV infection. Although it is not known how well the mouse model mimics the disease in humans, it is still a valid model that provides remarkable insights into different aspects of TOSV infection. We noticed in in vivo experiments that the endothelial cells of brain sections of sc. infected mice can be a target for TOSV few days after infection, without causing vessel damage and neurological signs but indicating

that the virus can reach the central nervous system. However, we do not know how the virus is able to cross the blood brain barrier (BBB) in humans and cause neurological disease. TOSV infection likely exerts changes in the barrier function of the vascular endothelium either directly, by damaging cell adherence, or indirectly, by triggering the release of proinflammatory lymphokines and inducing leukocyte activation (Visseren et al. 1999; Valbuena and Walker 2006; Combes and Grau 2006). It has been shown that inflammatory cell infiltrates, monocytes and particularly CD8+ lymphocytes can be found at the vascular level, such as skin venulae (Fig. 5), altering vascular permeability (Clark 2007). Although TNF-α, which is produced by infected DCs, increases acute phase protein production and acts in synergy with other factors to induce microbicidal activity during phagocytosis (Monaco et al. 2002), it also has the capacity to induce the upregulation of endothelial adhesion molecules, which in turn signal to chemotactic peptides and lipid mediators, then facilitating leukocyte recruitment, which may result in plasma leakage. Thus, TOSV may target these cells, which would have a significant impact on immune modulation. Moreover, we demonstrated a significant increase of IL-6 in the supernatant of infected HUVECs in vitro. It is possible that a local secretion of this cytokine by TOSV-infected endothelial cells may augment the recruitment of leukocytes and activate or damage the same endothelial cells. To confirm this, we have shown that the addition of PBMCs to TOSV-infected HUVECs in vitro caused increased permeability of endothelial cells, suggesting that during this infection, leukocytes play a critical role in mediating endothelial permeability and other cellular mechanisms related to vascular leakage. The presence of a transient rash (Zanelli et al. 2013) in some patients affected by TOSV infection could be explained by these underlying mechanisms.

In this study, we demonstrated that TOSV replication in the endothelium may be important for the maintenance of viremia and it may represent a grow-through mechanism for neuroinvasion. Although host factors, genetic susceptibility and immune status may be involved in controlling the disease, the capability of TOSV to infect and replicate in dendritic cells and, particularly, in human endothelium, represents an important pathway by which the virus can enter the central nervous system.

Acknowledgments We would like to thank Prof. A. De Luca for his helpful suggestions.

Compliance with ethical standards

Conflict of interest The authors, Maria Grazia Cusi, Claudia Gandolfo, Chiara Terrosi, Gianni Gori Savellini, Giuseppe Belmonte and Clelia Miracco, declare that they have no conflict of interest.

References

Baldelli F, Ciufolini MG, Francisci D, Marchi A, Venturi G, Fiorentini C, Luchetta ML, Bruto L, Pauluzzi S (2004) Unusual presentation of life-threatening Toscana virus meningoencephalitis. Clin Infect Dis 38:515–520

Bell D, Young JW, Banchereau J (1999) Dendritic cells. Adv Immunol 72:255–324

Charrel RN, Gallian P, Navarro-Mari JM, Nicoletti L, Papa A, Sánchez-Seco MP, Tenorio A, de Lamballerie X (2005) Emergence of Toscana virus in Europe. Emerg Infect Dis 11:1657–1663

Charrell RN, Bichaud L, De Lamballerie X (2012) Emergence of Toscana virus in the Mediterranean area. World J Virol 1:135–141

Clark IA (2007) The advent of the cytokine storm. Immunol Cell Biol 85: 271–273

Combes V, Grau GE (2006) Cytokines in defence and pathology of the CNS p. 243–267. In: Ransohoff RM, Benveniste EN (eds), Cytokines and the CNS. CRC press

Cusi MG, Gori Savellini G, Terrosi C, Di Genova G, Valassina M, Valentini M, Bartolommei S, Miracco C (2005) Development of a mouse model for the study of Toscana virus pathogenesis. Virology 333:66–73

Cusi MG, Gori Savellini G, Zanelli G (2010) Toscana virus epidemiology: from Italy to beyond. Virol J 4:22–28

Denizot M, Neal JW, Gasque P (2012) Encephalitis due to emerging viruses: CNS innate immunity and potential therapeutic targets. J Infect 65:1–16

Dionisio D, Valassina M, Ciufolini MG, Vivarelli A, Esperti F, Cusi MG, Marchi A, Mazzoli F, Lupi C (2001) Encephalitis without meningitis due to sandfly fever virus serotype Toscana. Clin Infect Dis 32: 1241–1248

Dropulic B, Masters CL (1990) Entry of neurotropic arboviruses into the central nervous system: an in vitro study using mouse brain endothelium. J Infect Dis 161:685–691

Gori Savellini G, Weber F, Terrosi C, Habjan M, Martorelli B, Cusi MG (2011) Toscana virus induces interferon although its NSs protein reveals antagonistic activity. J Gen Virol 92:71–79

Hemmersbach-Miller M, Parola P, Charrel RN, Durand J, Brouqui P (2004) Sandfly fever due to Toscana virus: an emerging infection in southern France. Eur J Intern Med 15:316–317

Lozach PY, Mancini R, Bitto D, Meier R, Oestereich L, Överby AK, Pettersson RF, Helenius A (2010) Entry of Bunyaviruses into mammalian cells. Cell Host Microbe 7:488–499

Lozach PY, Kühbacher A, Meier R, Mancini R, Bitto D, Bouloy M, Helenius A (2011) DC-SIGN as a receptor for Phleboviruses. Cell Host Microbe 10:75–88

Monaco C, Andreakos E, Young S, Feldmann M, Paleolog E (2002) T-cell mediated signaling to vascular endothelium: induction of cytokines, chemokines, and tissue factor. J Leukoc Biol 71:659–668

Navarro-Marí JM, Palop-Borrás B, Pérez-Ruiz M, Sanbonmatsu-Gámez S (2011) Serosurvey study of Toscana virus in domestic animals, Granada, Spain. Vector Borne Zoonotic Dis 11:583–587

Prazma CM, Tedder TF (2008) Dendritic cell CD83: a therapeutic target or innocent bystander? Immunol Lett 115:1–8

Prazma CM, Yazawa N, Fujimoto Y, Fujimoto M, Tedder TF (2007) CD83 expression is a sensitive marker of activation required for B cell and CD4+ T cell longevity in vivo. J Immunol 179:4550–4562

Prechtel AT, Turza NM, Theodoridis AA, Steinkasserer A (2007) CD83 knockdown in monocyte-derived dendritic cells by small interfering RNA leads to a diminished T cell stimulation. J Immunol 178:5454–5464

Ranaldi R, Goteri G, Biagetti S, Cusi MG, Rossini S (2011) Histological description of the lymphadenopathy related to Toscana virus infection. Report of a case. Pathol Res Pract 207:197–201

Sahni SK (2007) Endothelial cell infection and hemostasis. Thromb Res 119:531–549

Sanbonmatsu-Gámez S, Pérez-Ruiz M, Palop-Borrás B, Navarro-Marí JM (2009) Unusual manifestation of Toscana virus infection, Spain. Emerg Infect Dis 15:347–348

Taylor KG, Peterson KE (2014) Innate immune response to La Crosse virus infection. J Nurovirol 20:150–156

Tini P, Belmonte G, Toscano M, Miracco C, Palumbo S, Pastina P, Battaglia G, Nardone V, Butorano MA, Masucci A, Cerase A, Pirtoli L (2015) Combined epidermal growth factor receptor and beclin 1 autophagic protein expression analysis identifies different clinical presentations, responses to chemo- and radiotherapy, and prognosis in glioblastoma. Biomed Res 2015:208076

Valassina M, Cusi MG, Valensin PE (2003a) A Mediterranean arbovirus: the Toscana virus. J Neurovirol 9:577–583

Valassina M, Valentini M, Pugliese A, Valensin PE, Cusi MG (2003b) Serological survey of Toscana virus infections in a high-risk population in Italy. Clin Diagn Lab Immunol 10:483–484

Valbuena G, Walker DH (2006) The endothelium as a target for infections. Annu Rev Pathol 1:171–198

Visseren FL, Verkerk MS, Bouter KP, Diepersloot RJA, Erkelens DW (1999) Interleukin-6 production by endothelial cells after infection with influenza virus and cytomegalovirus. J Lab Clin Med 134:623–630

Zanelli G, Bianco C, Cusi MG (2013) Testicular involvement during Toscana virus infection: an unusual manifestation? Infection 41: 735–736

OncoImmunology

ISSN: (Print) 2162-402X (Online) Journal homepage: http://www.tandfonline.com/loi/koni20

Phase Ib study of poly-epitope peptide vaccination to thymidylate synthase (TSPP) and GOLFIG chemo-immunotherapy for treatment of metastatic colorectal cancer patients

Pierpaolo Correale, Cirino Botta, Elodia Martino, Cristina Ulivieri, Giuseppe Battaglia, Tommaso Carfagno, Maria Grazia Rossetti, Antonella Fioravanti, Giacomo Guidelli, Sara Cheleschi, Claudia Gandolfo, Francesco Carbone, Tatiana Cosima Baldari, Pierfrancesco Tassone, Pierosandro Tagliaferri, Luigi Pirtoli & Maria Grazia Cusi

To cite this article: Pierpaolo Correale, Cirino Botta, Elodia Martino, Cristina Ulivieri, Giuseppe Battaglia, Tommaso Carfagno, Maria Grazia Rossetti, Antonella Fioravanti, Giacomo Guidelli, Sara Cheleschi, Claudia Gandolfo, Francesco Carbone, Tatiana Cosima Baldari, Pierfrancesco Tassone, Pierosandro Tagliaferri, Luigi Pirtoli & Maria Grazia Cusi (2015): Phase Ib study of poly-epitope peptide vaccination to thymidylate synthase (TSPP) and GOLFIG chemo-immunotherapy for treatment of metastatic colorectal cancer patients, OncoImmunology, DOI: 10.1080/2162402X.2015.1101205

To link to this article: http://dx.doi.org/10.1080/2162402X.2015.1101205

Accepted author version posted online: 21 Dec 2015.

Colon cancer TSPP vaccine-based chemo-immunotherapy

Phase Ib study of poly-epitope peptide vaccination to thymidylate synthase (TSPP) and GOLFIG chemo-immunotherapy for treatment of metastatic colorectal cancer patients

Pierpaolo Correale[1,**], Cirino Botta[2], Elodia Martino[1], Cristina Ulivieri[3], Giuseppe Battaglia[1], Tommaso Carfagno[1], Maria Grazia Rossetti[4], Antonella Fioravanti[5], Giacomo Guidelli[5], Sara Cheleschi[5], Claudia Gandolfo[6], Francesco Carbone[7], Tatiana Cosima Baldari[3], Pierfrancesco Tassone[2], Pierosandro Tagliaferri[2,*], Luigi Pirtoli[1], and Maria Grazia Cusi[6]

[1]Unit of Radiotherapy, Catanzaro, Italy

[2]Department of Experimental and Clinical Medicine, "Magna Graecia" University and Medical Oncology Unit, and Medical Oncology Unit, AUO "Materdomini", Catanzaro, Italy

[3]Department of Science of Life, University of Siena, Italy

[4]Unit of Pharmacy, Siena University Hospital; Italy

[5]Unit of Rheumatology, Department of Clinical Medicine and Immunologic Sciences, Catanzaro, Italy

[6]Microbiology Unit, Department of Medical Biotechnology, Italy

[7]Unit of Radiology Department of oncology; Catanzaro, Italy

[*]Corresponding authors: Pierosandro Tagliaferri: Department of Experimental and Clinical Medicine, "Magna Graecia" University and Medical Oncology Unit, and Medical Oncology Unit, AUO "Materdomini", Germaneto, Catanzaro, Italy. Email: Tagliaferri@unicz.it

[**]Corresponding authors: Pierpaolo Correale: Unit of Radiotherapy, Department of oncology, Siena University School of Medicine, Viale Bracci 1, 53100, Siena Italy Phone: ++39-0577585412; Email: correale@unisi.it

Abstract

Thymidylate synthase (TS) is a tumor-associated enzyme critical for DNA replication and main 5'-fluorouracil (5'-FU) target. TSPP/VAC1 is a multi-arm trial phase-Ib trial program aimed to investigate the toxicity and biomodulatory activity of a poly-epitope-peptide vaccine to TS (TSPP) in cancer patients (pts). Here, we present the results of the TSPP/VAC1/arm C trial aimed to evaluate TSPP in combination with chemo-immunotherapy in pretreated metastatic colo-rectal cancer (mCRC) pts. Twenty-nine pts, 14 males and 15 females, received poly-chemotherapy with gemcitabine [1,000 mg/sqm, day-1]; oxaliplatin [80mg/sqm, day-2]; levofolinate [100mg/sqm, days 1-2], bolus/infusional 5'-FU [400mg/800 mg/sqm, days 1-2], sargramostim [50µg, days 3-7/q30] and interleukin-2 [sc. 0.5 MIU twice a day, days 8-14/18-30] [GOLFIG-regimen]. Seventeen pts received sc. TSPP injections at escalating dosage [3 pts, 100µg (DL-1); 3 pts, 200 µg (DL-2) and 11pts, 300 µg (DL-3)] one week after each chemotherapy cycle (concomitant module), while 10 out 12 pts received TSPP (300 µg) after 12 GOLFIG courses [dose level (DL)-0] (sequential module). TSPP MTD was not achieved. Adverse events consisted in swelling/erythema at injection sites (17 cases), G1-2 haematological (16 cases) and gastro-enteric events (12), fever, rhinitis, conjunctivitis, and poly-arthralgia and rise in auto-antibodies [ANA, ENA, c-ANCA, p-ANCA in the DL1-3 pts]. Both treatment-modules showed immunomodulating and antitumor activity (disease-control-rate, DL1-3 and DL0 were 70.6% and 83.3%, respectively) with a better survival recorded in the second group [median OS DL1-3 vs DL0= 8 vs 16 months, P=0.049]. The promising long term survival produced by the sequential treatment module deserves further phase II evaluation.

Key words

Colon cancer, Thymidylate synthase, peptide vaccine, CTLs, epitope peptides, GOLFIG chemo-immunotherapy

Introduction

Active specific immunotherapy (ASI) is a re-emerging anticancer treatment strategy and immune-checkpoint regulator monoclonal antibodies (mAbs) and tumor-associate-antigen (TAA)-specific vaccine formulations are currently under active investigation in cancer pts [1-5]. In the last 15 years, several attempts have been made to combine different therapeutic modalities with ASI in the treatment of solid malignancies in order to improve its antitumor efficacy. Radio- and chemo-immunotherapy have produced promising results in both preclinical and clinical studies [6-11].

We generated and characterized new vaccine constructs able to direct an effective immune-response to molecular structures which are over-expressed in cancer cells and, at the same time, are critical for their growth, survival, and diffusion, as the Epidermal growth Factor Receptor [EGFR], the parathyroid hormone related peptide [PTHrP] and thymidylate synthase [TS] [6-9]. TS, in particular, is a cancer-associated target enzyme, inhibited by several anti-cancer drugs (antimetabolites) such as 5'-fluorouracil [5'-FU], a cytotoxic drug which is a basic component of different regimens for the treatment of colorectal cancer (mCRC) and other common malignancies [10-12]. 5'-FU is a pro-drug, that upon transformation to 5'-FdUMP, binds and permanently inhibits the catalytic site of TS in the presence of levo-folinate. TS is responsible for deoxy-uridine monophosphate (dUMP) methylation to thymidylate, a crucial component for DNA synthesis and repair, whose expression is S phase specific, and is often over-expressed in tumor tissue. TS is a mRNA binding protein which auto-regulates its expression depending on the intracellular levels of metabolites, cofactors, and substrates. Therefore, cancer cell exposure to 5'-FU, by inducing thymidylate depletion, promotes transient TS over-expression within 24/48 hours in the surviving cells. TS-over-expression in tumor tissue, is finally predictive of 5'-FU resistance and poor prognosis in mCRC pts [10-12]. We previously demonstrated that TS is a potential

candidate target for ASI, and identified three TS-derived epitopes with HLA-A(*)02.01 amino-acid anchorage motifs (TS-1, TS-2 and TS-3), recognized by human cytotoxic- T-lymphocytes (CTLs) [8]. We also characterized a 27-mer peptide, designated as TSPP (Thymidylate synthase poly-epitope peptide), which combines the amino-acidic sequences of these peptides [9]. We showed that TSPP elicits a powerful multi-epitope specific CTL response with anti-tumor activity *in vitro* [9,13] and was safe and immunogenic in HHD mice (transgenic for the expression of HLA-A(*)02.01 and human CD8α). In this murine model, TSPP vaccination prevented and/or eradicated tumors after injection of syngeneic EL4/HHD lymphoma cells [9,13]. As an additional finding, TSPP anti-tumor activity, was greatly enhanced when used in combination with 5'-FU-based chemotherapy [9,13]. Indeed, we observed the better results when TSPP immunizations were weekly administered in alternate combination with the GOLF poly-chemotherapy [13], a previously characterized multidrug regimen with gemcitabine (GEM), oxaliplatin (OX), levofolinic acid (LF) and infusional 5'-FU [14,15]. 5'-FdUMP binds TS and promotes its ubiquitination and proteolysis by the proteasome system [12]. TS processing by the proteasomes, in turn, promotes the assembling of class-I HLA/TS-epitope peptides which are subsequently transported to the membrane becoming available for recognition by specific CTL precursors [9,13]. Additionally, thymidine depletion in cancer cells also promotes TS over-expression, thus augmenting the amounts of TS epitopes available for CTL recognition. We already demonstrated that tumor cell exposure to GOLF regimen increases the expression of multiple TAA (like TS, CEA and EGFR), enhances the expression of danger signals and "eat-me" molecules, and induces immunogenicity in colon and breast cancer cell models *in vitro* [9,13, 14,16-19]. These preclinical findings provided a clear rationale to investigate the GOLF regimen in combination with an immune-adjuvant IG-1 cytokine regimen (sc. Interleukin (IL)-2 and sc. Granulocyte-Macrophage colony-stimulating-factor(GM-CSF) (GOLFIG chemo-immunotherapy regimen) in colon cancer pts and successively, in

combination with TSPP based immunotherapy. The GOLFIG regimen has been already evaluated in mCRC pts, resulting safe, with significant immune-modulating effects and powerful antitumor activity [15,20,21]. On these bases, we designed a multi-arm phase Ib trial program (TSPP/VAC-1) to investigate the toxicity and immune-biological activity of TSPP vaccination in cancer pts. Each arm of the program was defined on a dose-finding setting, and aimed to test TSPP vaccination alone (Arm A) or associated with GM-CSF and IL-2 (Arm B) or in combination with the GOLFIG regimen (Arm C). The results obtained in the first two arm trials suggested that TSPP is safe, produces self-limiting auto-immunity signs, is able to generate a TS-specific CTL response with significant rise in serum auto-antibodies (AAbs) such as anti-nuclear Abs (ANA); extractable nuclear antigen Abs (ENA); anti-proteinase-3 anti-neutrophil cytoplasmic Abs (P-ANCA), and anti-myeloperoxidase anti-neutrophil cytoplasmic Abs (C-ANCA)] [22].

In the present study, we report the results concerning the arm C trial of the TSPP/VAC-1 program. This part of the study was planned to enroll pretreated mCRC pts, who received TSPP vaccination concomitantly (alternate weeks) or sequentially (after 12 GOLFIG courses) to the GOLFIG chemo-immunotherapy.

Patient and Methods

The TSPP/VAC-1 is a multi-arm phase Ib trial program designed to test the toxicity and immunological activity of TSPP, a new poly-epitope cancer vaccine to TS, in different therapeutic conditions and in advanced cancer pts. The protocol consisted of three parallel and independent trial arms designed to test TSPP vaccination alone (Arm A) and in combination with immune-adjuvant IG-1 regimen (Arm B) and in combination with GOLFIG chemo-immunotherapy regimen (Arm C). The latter trial arm was reserved to mCRC pts only

and evaluated the effects of peptide vaccination, administered concomitantly with the GOLFIG regimens (DL1-3) and/or sequentially (DL0) after 10/12 courses of this regimen.

Ethical considerations and study design: the study was designed according to good clinical practice (GCP) recommendations, authorized by the Italian National Institute of Health (Istituto Superiore di Sanità) and by the Italian Ministry of Health, approved by the University of Siena Ethical Committee Board (equivalent to Human Subject Committee of Investigational Review Board) and registered with the TSPP/VAC-1 code, Eudract: # 2009-016897-33. This phase Ib study was planned as a dose escalation trial program, in three parallel and independent arms (A, B and C). TSPP dose-escalation was planned according to the Fibonacci's series. The first cohort of pts received 100 µg of peptide (DL1), the second, 200 µg (DL2), and the third 300 µg (DL3), every 21 days. New pts could be enrolled in higher dose level cohorts, only if no Grade IV event were demonstrated in pts treated with lower doses. Pts assigned to the arm A received treatment with vaccine peptide alone, those of arm B received TSPP and sc. GM-CSF (Sargramostim / Leukine®, Berlex, USA) (50 µg days 1-5) and sc. IL-2 (Proleukin®, Novartis, Switzerland) (0.5 MIU bi-daily, days 6-15), while those of arm C/DL1-3 received peptide vaccination seven days after the beginning of the chemo-immunotherapy cycle with gemcitabine 1g/sqm on the day 1, oxaliplatin 85 mg/sqm on the day 2, Levofolinic acid 100 mg/sqm on the days 1 and 2, bolus 5'-FU 400 mg/sqm on days 1 and 2 and infusional 5'-FU 800 mg/sqm on days 1 and 2, every 15 days. These pts also received sc. GM-CSF (50 µg days 3-7) and sc. recombinant (r) IL-2 (Aldesleukine, 0.5 MIU bi-daily on days 8-14 and 17-29). Pts in arm C/DL0 were aimed to receive TSPP vaccination alike arm B, after they had received 12 GOLFIG courses [15, 23].

TSPP Vaccine: TSPP (YMIAHITGLFLDSLGFSTTLGDAHIYL) was synthesized and characterized by good manufacturing practice (GMP) procedures by the American Peptide Ltd (Rockville, MD,USA). The aseptic vial filling process was performed by the Pharmacy of the *Azienda Ospedaliera Universitaria Senese*, which also performed the stability study, endotoxin evaluation and chemical related toxicity analysis of the product. TSPP was dissolved in DMSO (1.5 mg peptide in 1 ml DMSO). The exact peptide dose (100, 200 or 300 µg), was diluted with PBS in a volume of 250 µl, and

then 1:2 diluted with Montanide ISA 720 VG ST (Seppic, Milan, Italy) as adjuvant. The final volume of the vaccine was 500 µl/dose.

Patients: The study-arm-C trial was planned to evaluate the immunological activity and toxicity of TSPP in combination with GOLFIG chemo-immunotherapy, in mCRC pts, who had received at least two standard treatment lines. The primary endpoints of the study were the identification of the maximal tolerated dose (MTD) and most effective biological dose (MEBD) of TSPP peptide, by evaluating the frequency of adverse events per dose level and predefined immune-biological events in three cohorts of three pts each. Evidence of anti-tumor activity was a secondary endpoint. The inclusion criteria were: written informed consent, histological diagnosis of malignant disease, at least two previous chemotherapy lines for advanced disease, measurable disease (according to WHO tumor response criteria), ECOG performance status ≤ 2, normal renal and hepatic functions, white blood cell count ≥ 2,500/mm^3, hemoglobin levels ≥ 9 g/dl, platelet cell count ≥ 100,000/mm^3, and normal heart function. The exclusion criteria were: any major organ failure, unstabilized central nervous system involvement, second malignancies, active infectious disease, major inflammatory and autoimmune rheumatic diseases, and acquired immune-suppression. Treatment allocation was not masked. Standard clinical and laboratory evaluation (clinical history, physical examination, blood count and chemistry, serum dosage of C-reactive protein (CRP), erythrocyte-sedimentation rate (ESR), lactate dehydrogenase (LDH), rheumatoid factor, carcinoembryonic antigen (CEA) and CA19.9 assays, chest x-rays and ultrasound abdominal scans, were performed at baseline and repeated every six weeks. Pts' sera were tested for ANA by IFA, (starting dilution 1:160) (SSA HEp2000, ImmunoConcepts), EliASymphony screening (Thermo Fisher Scientific), and further ELiA tests were performed for single ANA specificities; ANCA; p-ANCA; C-ANCA ENA were tested on Phadia250 instrument; ANCA were measured by indirect immunofluorescence using INOVA substrate. Contrast CT scans were scheduled every three months. Pts enrolled in the arm C/DL1-3

received combined TSPP/GOLFIG treatment for a maximal of 12 cycles, then those who did not progress, received TSPP vaccination every 21 days at the dosage of 300 µg until disease progression, occurrence of unacceptable toxicity, clinical judgment, or withdrawal of consent. Any further treatment decision after disease progression was left to the physician in charge. Adverse events, toxicity and treatment response were evaluated according to WHO classification.

ELISA assays and Multiplex analysis: serum levels of Interferon(IFN)-γ, Tumor necrosis factor (TNF)-α, IL10, IL4, IL12, IL10 and IL17 cytokines were measured using Bio-Plex human cytokine multiplex kits (Bio-Rad Inc., Hercules, CA). The fluorescence intensity of the beads was measured by using the Bio-Plex array reader. Bio-Plex Manager software with five-parametric-curve fitting was used for data analysis. Serum levels of IL6 and IL8 were measured by using human cytokine ELISA kits and analyzed according to the manufacturer's protocol (Bio-Rad Inc., Hercules, CA).

Fluorescence-activated cell sorting analysis of patient peripheral blood mononuclear cells (PBMC): The pts' PBMCs were purified by Ficoll-Hypaque (Celbio S.P.A., Italy) gradient separation of buffy coats of heparinized blood samples and analyzed by Fluorescence-activated cell sorting (FACS) analysis, as described in previous studies [24,25].

PBMC were stained with different pools of labeled monoclonal antibodies (mAbs) (CD4V450, CD45RAPE, CD62LFITC, CCR7PE-Cy7, Pharmingen;CD8PerCPCy 5.5, CD45ROAPC, CD3FITC, CD19FITC, CD14FITC, CD11cAPC, CD16PE, Rat IgG2aFITC, Mouse IgG1, Becton Dickinson, Italy; CD56 APC, Mouse IgG2a APC Immunotools, DE; CD15 PE ABCam, UK; CD25 PE, FoxP3 FITC, eBioscence, UK) and examined by a FACScalibur BD instrument. Ki67 positive cells and T_{reg}s were analyzed after intracellular immune-staining according to the manufacturer's protocol (eBioscience). Cytofluorimetric analysis was carried out by using the FlowJo®software.

Statistical analysis: the statistical analysis was carried out by the GraphPadInstat 3.2 statistical software. The results were expressed as the mean +/- standard deviation (SD) of 4 determinations made in three different experiments, and analyzed by the 2-tail Student's *t*-test. A *p*-value of 0.05 or less was considered statistically significant. Kaplan Meier descriptive statistics was performed by the use of SPSS statistical package.

Results

Demographics, chemo-immunotherapy, peptide vaccination and dose- escalation

Twenty-nine pts with mCRC, 14 males and 15 females, with a good performance status (ECOG 0-1), who had received at least two treatment lines (standard poly-chemotherapy +/- cetuximab and/or bevacizumab) signed an informed consent and were enrolled between May 2011 and July 2013 (Table 1). According to the pre-established platform (see pts and methods), all of them received GOLFIG poly-chemo-immunotherapy. Seventeen pts, received sc. TSPP vaccination at escalating dosage [3 pts entered the DL-1; 3, the DL-2; 11, the DL-3 cohort] on biweekly bases, starting one week after each chemotherapy cycle (concomitant treatment). Twelve pts received GOLFIG chemo-immunotherapy alone (DL0) for 12 courses and then maintenance therapy including TSPP vaccination every 3 weeks. Two of them were excluded from the study, due to early disease progression and decline in performance status. Maintenance therapy included TSPP vaccination [(300 µg on the day 1 every 3 weeks) sc.GM-CSF (50 µg at day, days 1-5 every 3 weeks), sc.rIL2 (0,5 MIU twice at day, days 6-15 every 3 weeks).

Antitumor activity – Within the 17 pts, who received the concomitant TSPP/GOLFIG treatment (DL1-3), we recorded progression of disease (PD) in 9 (52.9%), a partial response (PR) in 3 (17.64%), and stable disease (SD) in 5 (29.4%) subjects, including 4 pts (CLCDL2; SACDL2; BGCDL3; MUCDL3) (23.5%) surviving over 12 months. On the

other hand, in the 12 pts who were enrolled in the sequential treatment group, we recorded 2 PDs occurring before the planned TSPP vaccination, 4 PRs (25%), and 6 SDs (50%). Seven (63.6%) of these pts (SRCDL0, BLDL0, MLDL0, PGDL0, MACDL0, PACDL0, DLCDL0) survived more than 12 months. *(Table 1)*

Although this trial was not designed on a comparative setting in term of antitumor activity, we performed an exploratory descriptive Kaplan Meyer and a Log-Rank test to compare PFS and OS in pts who received concomitant or sequential treatments, finding a better performance in term of OS in the latter group (*Figure 1 A and B*). In our series the Univariate analysis did not find any significant correlation of k-ras mutational status and HLA-$A2^+$ haplotype with either PFS (wt-k-ras vs. k-ras mut status, p:0.063; HLA-$A2^+$ vs HLA.$A2^-$ haplotype, p:0.682) or OS (wt-k-ras vs. k-ras mut status p:0.203; HLA-$A2^+$ vs HLA.$A2^-$ haplotype, p: 0.601) of these pts (*data not shown in figure*).

Toxicity profile

The treatment was safe also in this setting of advanced and largely pre-treated pts. There were no lethal adverse events and there was no statistical correlation between frequency of adverse events and TSPP dosage or absence of concomitant TSPP vaccination (DL0). Similarly, there was no significant difference when the two groups of pts, receiving concomitant (DL1-3) or sequential TSPP/GOLFIG treatment (DL0) were compared. The majority of adverse events were strictly related to the poly-chemotherapy and consisted in moderate (Grade I-II) hematologic (anaemia and thrombocytopenia) and gastro-enteric (mucositis) toxicity. A reaction to oxaliplatin was observed in 4 pts, who continued the treatment without this drug. There was no TSPP dose-dependent difference in adverse event frequency (Table 2). However, it should be underlined that pts who received a concomitant TSPP/GOLFIG treatment showed higher frequency of grade 1-2 asthenia,

fever, poly-arthralgia, and biochemical signs of hypothyroidism (6 cases) (rise in TSH levels) (Table 2).

Twelve out of 17 pts who received concomitant treatment and 8 pts who received TSPP maintenance showed a local reaction at the vaccine injection site, which reflected the occurrence of delayed hypersensitivity with appearance of erythematous reactions with swelling and induration still present 72-96 hours later. TSPP vaccination, therefore, resulting safe and well tolerated did not increase the frequency of grade 3-4 adverse events associated with GOLFIG regimen. Finally, the frequency of adverse events per dose level did not allow to identify a MTD for TSPP (DL0-3) in combination with GOLFIG poly-chemo-immunotherapy. (*Table 2*)

Immunobiological monitoring

Hemocytometric analysis - GOLFIG poly-chemotherapy induced a slight but progressive decline in neutrophil counts, which was not affected by TSPP vaccination (*Table 3*). We also detected a progressive rise in lymphocyte, monocyte and eosinophil counts which, again, was not influenced by concomitant TSPP vaccination. When the hemocytometric monitoring curves of pts in DL1-3 and DL0 groups were compared, we were unable to demonstrate any statistical difference in lymphocyte (P= 0.605), monocyte (P= 0.807) and eosinophil (P= 0.199) count monitoring (*Figure 1 C, D, and E*).

Serologic analysis of systemic inflammatory markers- An analysis of serological inflammatory markers revealed a trend to progressive decline in CRP and an increase in *ESR in both group.* Pts who received the sequential treatment (DL0), however, showed lower levels of inflammatory markers CRP (P= 0.041) and ESR (P< 0.001) at baseline and along the treatment (*Table 3*).

Serologic analysis of auto-antibodies

The serum monitoring of AAbs potentially indicative of autoimmunity, showed a progressive and significant increase in ENA, p-ANCA, and c-ANCA only in the group of pts who received the concomitant treatment (DL1-3) and no change in the other group (DL0). Differences in ANA, ENA, c-ANCA and p-ANCA values between the concomitant and sequential treatment groups resulted statistically significant (P values for ANA and ENA, c-ANCA, p-ANCA value curves were 0.049, 0.0345, 0.0163 and 0.0412, respectively) (*Table 3 and Figure 1 F, G, and H*). Our analysis did not reveal particular changes in other AAbs such as ASMA, ANCA and anti-thyroid Abs.

Flow cytometry

Flow cytometry analysis performed on the peripheral blood of the pts receiving the concomitant and sequential treatment modules did not show differences and changes in the percentages of peripheral CD3+CD4+ (DL1-3 vs DL0 group; P= 0.22) and CD3+CD8+ CTLs (DL1-3 vs DL0 group; P= 0.145). A further analysis of these T cells, similarly, did not show differences in the percentages of CD3+CD4+CD45- memory T cells (DL1-3 vs DL0 group; P= 0.301). Both group of pts receiving the concomitant and sequential treatment module showed an early increase in peripheral $CD4^+CD25^+FoxP3^+$ regulatory-T-cells (*T_{reg}s*) which was lost on the long term (*Figure 2*). There was no difference between the two groups of pts (DL1-3 vs DL0, P= 0.21) suggesting that this effect was related to the presence of GM-CSF and IL-2 in the GOLFIG regimen and not to TSPP administration. The group of pts receiving the concomitant treatment module instead, showed an increase in central memory (CD8+CD45RA-CCR7+) T cells (Tcm), while that receiving the sequential module showed an progressive increase in effector memory T cells (T_{em}) ($CD8^+CD45RA^-CCR7^-$) (*Figure 2 and 3*).

Finally, it was also recorded a trend to increase in peripheral Natural Killer (NK) cells ($CD3^-CD56^+CD16^+$) in both groups of pts, which achieved statistical significance only in the DL0 group. Differences between the two pts' groups were not significant (DL1-3 vs DL0,

P=0.49) (Table 3). The increase in this cell subpopulation seems to be related to the presence of immune-adjuvant cytokines in the GOLFIG regimen and not to the TSPP vaccination.

Cytokine analysis

A cytokine analysis performed on the serum of these pts showed a completely different profile between the two groups of pts receiving concomitant and sequential treatment module. Our analysis showed no changes in TNFα, IL12 levels (*data not shown*), IL6 and IL8 (*Table 3*) while, a significant and progressive increase in IFNɣ and IL-4 was observed in the pts who received the concomitant treatment (DL1-3) (*Figure 2*). In the same group there was also a trend increase in IL10, which did not achieve statistical significance probably, for the small sample of pts. We finally, observed a significant increase in IL17 levels during the maintenance treatment in both group of pts which seems strictly related to the TSPP vaccination (*Figure 2*). The ability of TSPP vaccination to increase the precursors frequency of TSPP specific CTL precursors was demonstrated by IFNɣ ELISPOT assay in the previous study and was not correlated with either dosage of combined treatment [22 and *data not shown*]

Discussion

Our results confirm the safety and immune-modulating activities of TSPP in concomitant and sequential combination with GOLFIG chemo-immunotherapy. The MTD of this peptide could not be identified, while its MEBD was recognized at the dosage of 300 µg which was associated with the highest frequency of biomodulatory effects and longer survival. TSPP vaccination was associated to a high frequency of local immune-reactions at the vaccine injection site, rhinitis, conjunctivitis and poly-arthralgia as shown in the previous study [22]. TSPP vaccination did not increase the frequency and severity of the adverse events

associated with the GOLFIG chemo-immunotherapy, which occurred with the same frequency in the groups of pts who received either the concomitant or the sequential treatment modules. On the whole, the frequency of adverse events was similar to that reported in previous clinical trials investigating the GOLFIG regimen alone in pretreated mCRC pts [15,19,20]. The results of the present study suggest that the TSPP vaccine in combination with GOLFIG poly-chemotherapy is a feasible treatment for pretreated mCRC pts. The sequential treatment appeared to be more active than the concomitant in terms of OS (P= 0.049), and in both cases, it was not affected by k-ras mutational status and HLA-A2 haplotype . These results appear intriguing, although with significant limitation related to the small number of enrolled pts. We have previously demonstrated that the GOLFIG regimen is a very active treatment, that enhances TS specific CTL precursors and promotes an effective anticancer CTL response correlated with the occurrence of autoimmunity and longer survival in mCRC pts [20,21]. These features lead us to believe that the GOLFIG regimen, which combines poly-chemotherapy and immune-adjuvant cytokines, when supported by TSPP vaccination, in addition to a significant reduction of tumor burden, could also promote a mechanism of antigen cascade and cross-presentation triggering an efficient specific immune-response with poly-antigen specificity.

In the present study, TSPP vaccination given concomitantly with GOLFIG treatment was associated with systemic and clinical signs of immune-activation. This assumption was supported by the finding of a coordinate and progressive rise in lymphocytes, monocytes, and appearance of AAbs such as ANA, ENA pANCA e cANCA which are associated with the most common autoimmune-diseases. Consistent with the last finding, we also detected clinical signs of autoimmunity like poly-artharalgia, hypothyroidism, rhinitis, conjunctivitis, and fever in some pts. Some of these events were sporadically observed also in pts who received GOLFIG chemo-immunotherapy alone, as shown in previous studies [20,21,26],

and similarly, in the pts enrolled in the DL0 group of the present trial, prior receiving TSPP vaccination. By comparing the concomitant with sequential treatment groups, we also recorded a significant difference in term of systemic inflammatory status with much higher serum level of CRP e ESR in the first group. This finding could be indicative of chronic inflammation which, in turn, may affect the immunological activity of TSPP vaccination as described in literature [27-31]. The reasons explaining the difference in inflammatory status in the two groups of pts are not clear. It could be either related to an effect of the combined treatment or just to a specific feature of the pts enrolled in the study and deserves to be further investigated with a more homogenous patient population. In line with previous results performed on mCRC pts who had received the GOLFIG regimen, we also detected an increase in T_{reg}s in both patient groups which is lost on the long term. The treatment associated-rise in T_{reg}s, as reported by other authors [32], can be considered as an inhibitory feedback response to an efficient antigen specific immune-reaction in order to avoid dangerous over-reactions and auto-immunity, which mainly occur in a chronic inflammatory status under selective cytokine pressure, or dependent by the IL-2 administration. [27-32]. In both groups of pts, T_{reg} rise was however, lost after the first 10-12 treatment courses, as probably caused by GOLFIG regimen [15,20]. This finding, together with lower systemic inflammatory status, could contribute to explain the more significant antitumor activity of TSPP vaccine in the sequential treatment group (DL0). In fact, these pts received vaccination when the T_{reg} population is exhausted and therefore, unable to affect the immunological activity of TSPP [27, 28, 32]. The results of the immunological analysis, which showed a general treatment-associated increase in peripheral lymphocyte counts, provides a further support to this hypothesis. In this context, there was no difference in the percentages of $CD3^+CD4^+$ or $CD3^+CD8^+$ T cells, however, in the DL0 group we found an increase of the T_{em} subset during TSPP vaccination (started after 12 GOLFIG courses), which was not detected in the concomitant treatment group.

This is a very efficient CTL subset which derives by T_{cm} maturation in the presence of immune-specific micro-environmental conditions (cytokines, chemokines, adhesion molecules, etc) [33-37]. This hypothesis is supported in our pts, by the data concerning the treatment-related increase of IL-17, a cytokine which is able to sustain a local immune-reaction in the tumor site. In our patients, we also detected a treatment-related increase of IL-4 and trend increase of IL-10, which could be related to T_{reg} stimulation and/or of an intrinsic ability of TSPP vaccine to promote a Th2 humoral response as confirmed by a systemic progressive increase of AAbs in these pts. Additionally, we also found a significant increase in IFN-ɣ, a Th1 cytokine, which is strongly involved in the antigen specific CTL response in the DL1-3 group pts. A last consideration concerns the expansion of peripheral NKs in both groups of pts during the first ten treatment courses. This finding, which seems to be sustained by GM-CSF and IL-2 cytokines, both present in the GOLFIG regimen, suggests that this treatment is a valid support to TSPP vaccination. NK cells in fact, together with an innate ability to kill metastatic cancer cells, are also able to produce IFN-ɣ and enhance the antigen presenting ability of peripheral DCs [38]. We can conclude that TSPP-vaccination in combination with the GOLFIG chemo-immunotherapy is safe and immune-biologically active in pretreated mCRC pts. We have also provided preliminary evidence of a promising antitumor effect in both groups of pts receiving either the concomitant or the sequential treatment. The latter group of pts in particular, showed an unexpected PFS and OS median of 7 and 16 months, respectively, which resulted significantly much longer than that reported in other clinical trials investigating newest drugs in pre-treated mCRC pts, which rarely show a median PFS and OS longer of 2 and 6 months, respectively. We believe that our results provide the rationale to design further trials in mCRC pts aimed to investigate the antitumor activity of TSPP vaccine in pts who have received a frontline chemo-immunotherapy line.

Acknowledgement:

This study was supported by the Italian Ministry of Health "Ricerca finalizzata 2010 "RF-2010-2313550 and the "Associazione culturale Federico II", Siena.

We wish to thank the head of nurse team, Dr. G.Fruscoloni; the distinguished nurse specialists M. Bianchi, N. Cicatelli, S. Bacci, D. Graziuso and L. Spito; and the medical staff and residents who offered the best care and management to trial patients.

Finally, we wish to thank all patients and their families who enthusiastically participated to the study.

References

1) Franks HA, Wang Q, Patel PM. New anticancer immunotherapies. Anticancer Res. 2012 Jul;32(7):2439-53. Review.
2) Vaccines for the treatment of non-small cell lung cancer: investigational approaches and clinical experience. Mellstedt H, Vansteenkiste J, Thatcher N. Lung Cancer. 2011 Jul;73(1):11-7. doi: 10.1016/j.lungcan.2011.02.023. Epub 2011 Apr 6. Review.
3) Buonaguro L, Petrizzo A, Tornesello ML, Buonaguro FM. Translating tumor antigens into cancer vaccines. Clin Vaccine Immunol. 2011 Jan;18(1):23-34. doi: 10.1128/CVI.00286-10. Epub 2010 Nov 3. Review.
4) Baxevanis CN, Perez SA, Papamichail M. Cancer immunotherapy. Crit Rev Clin Lab Sci. 2009;46(4):167-89. doi: 10.1080/10408360902937809. Review.
5) Mocellin S, Pilati P, Nitti D. Peptide-based anticancer vaccines: recent advances and future perspectives. Curr Med Chem. 2009;16(36):4779-96. Review.
6) A Scardino, M. Alimandi, P.Correale, S.G. Smith, R.Bei, H.Firat, O.Faure, S. Graf-Dubois, J.Marrocco, S.Chouaib, François A. Lemonnier, A. M. Jackson and K. Kosmatopoulos. A polyepitope DNA vaccine targeted to HER2/ErbB-2 elicits a broad range of human and murine CTL effectors to protect against tumor challenge. Cancer Research, 2007 Jul 15;67(14):7028-36.
7) Francini G, Scardino A, Kosmatopoulos K, Lemonnier FA, Campoccia G, Sabatino M, Pozzessere D, Petrioli R, Lozzi L, Neri P, Fanetti G, Cusi MG, Correale P. High-affinity HLA-A(*)02.01 peptides from parathyroid hormone-related protein generate in vitro and in vivo antitumor CTL response without autoimmune side effects. J Immunol. 2002 Nov 1;169(9):4840-9.
8) Correale P, Sabatino M, Cusi MG, Micheli L, Nencini C, Pozzessere D, Petrioli R, Aquino A, De Vecchis L, Turriziani M, Prete SP, Sanguedolce R, Rausa L, Giorgi G,

Francini G. In vitro generation of cytotoxic T lymphocytes against HLA-A2.1-restricted peptides derived from human thymidylate synthase. J Chemother. 2001 Oct;13(5):519-26.

9) Correale P, Del Vecchio MT, Di Genova G, Savellini GG, La Placa M, Terrosi C, Vestri M, Urso R, Lemonnier F, Aquino A, Bonmassar E, Giorgi G, Francini G, Cusi MG. 5-fluorouracil-based chemotherapy enhances the antitumor activity of a thymidylate synthase-directed polyepitopic peptide vaccine. J Natl Cancer Inst. 2005 Oct 5;97(19):1437-45].

10) Rustum YM. Thymidylate synthase: a critical target in cancer therapy? Front Biosci. 2004 Sep 1;9:2467-73. Review.

11) van der Wilt CL, Peters GJ. New targets for pyrimidine antimetabolites in the treatment of solid tumours. 1: Thymidylate synthase. Pharm World Sci. 1994 Apr 15;16(2):84-103.

12) Ligabue A, Marverti G, Liebl U, Myllykallio H. Transcriptional activation and cell cycle block are the keys for 5-fluorouracil induced up-regulation of human thymidylate synthase expression. PLoS One. 2012;7(10):e47318. doi: 10.1371/journal.pone.0047318. Epub 2012 Oct 9.

13) P. Correale, M. T. Del Vecchio, M. La Placa, F. Montagnani, G. Di Genova, G. Gori Savellini, C. Terrosi, S. Mannucci, G. Giorgi, G. Francini, and M.G.Cusi. Chemotherapeutic drugs may be used to enhance the killing efficacy of human tumor antigen peptide specific CTLs. J. Immunother 2008; 31:132–147

14) Correale P, Cusi MG, Del Vecchio MT, Aquino A, Prete SP, Tsang KY, Micheli L, Nencini C, La Placa M, Montagnani F, Terrosi C, Caraglia M, Formica V, Giorgi G, Bonmassar E, Francini G. Dendritic cell-mediated cross-presentation of antigens derived from colon carcinoma cells exposed to a highly cytotoxic multidrug regimen with gemcitabine, oxaliplatin, 5-fluorouracil, and leucovorin, elicits a powerful human

antigen-specific CTL response with antitumor activity in vitro. J Immunol. 2005 Jul 15;175(2):820-8.

15) Correale P, Cusi MG, Tsang KY, Del Vecchio MT, Marsili S, Placa ML, Intrivici C, Aquino A, Micheli L, Nencini C, Ferrari F, Giorgi G, Bonmassar E, Francini G. Chemo-immunotherapy of metastatic colorectal carcinoma with gemcitabine plus FOLFOX 4 followed by subcutaneous granulocyte macrophage colony-stimulating factor and interleukin-2 induces strong immunologic and antitumor activity in metastatic colon cancer patients. J Clin Oncol. 2005 Dec 10;23(35):8950-8. Epub 2005 Aug 1.

16) P. Correale, A. Aquino, A. Giuliani, M. Pellegrini, L. Micheli M.G. Cusi, C. Nencini, R. Petrioli, S.P. Prete, L. De Vecchis, M. Turriziani, G. Gorgi, E. Bonmassar, and G. Francini. Treatment of colon and breast carcinoma cells with 5-Fluorouracil enhances expression of carcinoembryonic antigen and to HLA-A(*)02.01 restricted, CEA-peptide-specific cytotoxic T cells in vitro. Int J Cancer. 2003 Apr 10;104(4):437-45

17) P. Correale, M.Marra, C.Remondo, C.Migali, F.P.Arcuri, A.Carducci, L.Loiacono, A.Abruzzese, *P.Tagliaferri,* and M.Caraglia. Cytotoxic drugs up-regulate Epidermal Growth Factor Receptor (EGFR) expression in colon cancer cells and enhance their susceptibility to EGFR-targeted Antibody-Dependent-Cell-mediated-Cytotoxicity (ADCC). Eur J Cancer. Jun;46(9):1703-11.2010, IF= 4.454

18) P. Correale, Botta C, Cusi MG, Del Vecchio MT, De Santi M, Gori Savellini G, Bestoso E, Apollinari S, Ginanneschi C, Mannucci S, Marra M, Abruzzese A, Aquino A, Turriziani M, Bonmassar L, Caraglia M, and Tagliaferri P. Cetuximab +/- chemotherapy enhances dendritic cell-mediated phagocytosis of colon cancer cells and ignites a highly efficient colon cancer antigen-specific cytotoxic T-cell response in vitro. Int J Cancer. 2012 Apr 1;130(7):1577-89. doi: 10.1002/ijc.26181. Epub 2011 Aug 16.

19) C. Botta et al., and P.Correale. Cetuximab-based immune-chemotherapy enhances antigen presentation and cytotoxic T cell activity in colorectal cancer patients. J Immunotherapy. 2012 Jun;35(5):440-7.

20) P. Correale, *P.Tagliaferri,* A.Fioravanti, M.T.Del Vecchio, C.Remondo, F.Montagnani, M.S.Rotundo, C.Ginanneschi, I.Martellucci, E.Francini, M.G.Cusi, P.Tassone, and G.Francini. Immunity feedback and clinical outcome in colon cancer patients undergoing chemo-immunotherapy with Gemcitabine + FOLFOX followed by subcutaneous Granulocyte Macrophage-Colony Stimulating Factor and Aldesleukine (GOLFIG-1 trial). Clin.Cancer Res. 2008, 14(13):4192-4199.

21) P. Correale, Botta C, Rotundo MS, Guglielmo A, Conca R, Licchetta A, Pastina P, Bestoso E, Ciliberto D, Cusi MG, Fioravanti A, Guidelli GM, Bianco MT, Misso MT, Martino E, Caraglia M, Tassone P, Mini E, Mantovani G, Ridolfi R, Pirtoli L, and Tagliaferri P. Immune-boost with gemcitabine, oxaliplatin, levofolinate, 5-flurouracil, granulocyte/macrophage colony-stimulating-factor (GM-CSF) and aldesleukine (GOLFIG) enhances progression-free and overall-survival over FOLFOX chemotherapy in metastatic colorectal cancer patients: GOLFIG-2 multi-centric open label randomized phase III trial. J Immunotherapy, 2014 Jan;37(1):26-35.

22) M.G. Cusi, Botta C, Pastina P, Rossetti MG, Dreassi E, Guidelli GM, Fioravanti A, Martino EC, Martorelli B, Pagliuchi M, Basile M, Carbone SF, Ricci V, Micheli L, Tassone P, Tagliaferri P, Pirtoli L, Correale P. Phase I Trial of Thymidylate-synthase poly-epitope peptide (TSPP) vaccine in advanced cancer patients, Cancer Immunol Immunother, 2015 *in press*.

23) P. Correale, G. Campoccia, K. Y. Tsang, L. Micheli, G. Cusi, M. Sabatino, G. Bruni, S. Sestini, R. Petrioli, D. Pozzessere, S. Marsili, G. Fanetti, G. Giorgi, and G. Francini. Recruitment of dendritic cells and enhanced antigen specific immune-reactivity in cancer patients treated with hrGM-CSF (molgramostim) and hr IL-2: results from a Phase Ib Clinical Trial. Eur J Cancer 37 (7):892-902, 2001.

24) Czerkinsky CC, Nilsson LA, Nygren H, Ouchterlony O, Tarkowski A (1983) A solid-phase enzyme-linked immunospot (ELISPOT) assay for enumeration of specific antibody-secreting cells. Journal of immunological methods 65 (1-2):109-121

25) Moodie Z, Price L, Gouttefangeas C, Mander A, Janetzki S, Lower M, Welters MJ, Ottensmeier C, van der Burg SH, Britten CM (2010) Response definition criteria for ELISPOT assays revisited. Cancer immunology, immunotherapy : CII 59 (10):1489-1501. doi:10.1007/s00262-010-0875-4

26) P.Correale, I.Bertoldi, C.Miracco, A.Fioravanti, and G.Francini. Occurrence of discoid lupus erythematousus in a good responder colon carcinoma patient receiving chemo-immunotherapy. J Chemother. 2008 Apr;20(2):278-81. IF= 0.922

27) Mantovani A, Allavena P, Sica A, Balkwill F (2008) Cancer-related inflammation. Nature 454 (7203):436-444. doi:10.1038/nature07205

28) Predina J, Eruslanov E, Judy B, Kapoor V, Cheng G, Wang LC, Sun J, Moon EK, Fridlender ZG, Albelda S, Singhal S (2013) Changes in the local tumor microenvironment in recurrent cancers may explain the failure of vaccines after surgery. Proceedings of the National Academy of Sciences of the United States of America 110 (5):E415-424. doi:10.1073/pnas.1211850110

29) Botta C, Barbieri V, Ciliberto D, Rossi A, Rocco D, Addeo R, Staropoli N, Pastina P, Marvaso G, Martellucci I, Guglielmo A, Pirtoli L, Sperlongano P, Gridelli C, Caraglia M, Tassone P, Tagliaferri P, Correale P (2013) Systemic inflammatory status at baseline predicts bevacizumab benefit in advanced non-small cell lung cancer patients. Cancer biology & therapy 14 (6):469-475. doi:10.4161/cbt.24425

30) Jafri SH, Shi R, Mills G (2013) Advance lung cancer inflammation index (ALI) at diagnosis is a prognostic marker in patients with metastatic non-small cell lung cancer (NSCLC): a retrospective review. BMC cancer 13:158. doi:10.1186/1471-2407-13-158

31) Templeton AJ, McNamara MG, Seruga B, Vera-Badillo FE, Aneja P, Ocana A, Leibowitz-Amit R, Sonpavde G, Knox JJ, Tran B, Tannock IF, Amir E (2014) Prognostic role of

neutrophil-to-lymphocyte ratio in solid tumors: a systematic review and meta-analysis. Journal of the National Cancer Institute 106 (6):dju124. doi:10.1093/jnci/dju124

32) Sakaguchi S, Yamaguchi T, Nomura T, Ono M (2008) Regulatory T cells and immune tolerance. Cell 133 (5):775-787. doi:10.1016/j.cell.2008.05.009

33) Sallusto F, Lanzavecchia A (2009) Heterogeneity of CD4+ memory T cells: functional modules for tailored immunity. European journal of immunology 39 (8):2076-2082. doi:10.1002/eji.200939722

34) Forster R, Schubel A, Breitfeld D, Kremmer E, Renner-Muller I, Wolf E, Lipp M (1999) CCR7 coordinates the primary immune response by establishing functional microenvironments in secondary lymphoid organs. Cell 99 (1):23-33

35) Sallusto F, Geginat J, Lanzavecchia A (2004) Central memory and effector memory T cell subsets: function, generation, and maintenance. Annual review of immunology 22:745-763. doi:10.1146/annurev.immunol.22.012703.104702

36) Correale P, Rotundo MS, Botta C, Del Vecchio MT, Ginanneschi C, Licchetta A, Conca R, Apollinari S, De Luca F, Tassone P, Tagliaferri P (2012) Tumor infiltration by T lymphocytes expressing chemokine receptor 7 (CCR7) is predictive of favorable outcome in patients with advanced colorectal carcinoma. Clinical cancer research : an official journal of the American Association for Cancer Research 18 (3):850-857. doi:10.1158/1078-0432.CCR-10-3186

37) Correale P, Rotundo MS, Botta C, Del Vecchio MT, Tassone P, Tagliaferri P (2012) Tumor infiltration by chemokine receptor 7 (CCR7)(+) T-lymphocytes is a favorable prognostic factor in metastatic colorectal cancer. Oncoimmunology 1 (4):531-532

38) Terrazzano G, Carbone E (2012) NK cells blur the frontier between innate and acquired immunity. Frontiers in immunology 3:400. doi:10.3389/fimmu.2012.00400

Table 1

CODE	Sex	ECOG	Metastatic sites	Previous treatment lines	K-ras	HLA-A2	GOLFIG courses	MANT	Type of response	Overall Serviv al Months
LM/C/DL1	F	2	Peritoneum, lung, liver	2	Mut	A24	6	2	**PD**	**5**
CV/C/DL1	M	1	Peritoneum, lung, liver	6	Mut	A3.24	5	0	**PD**	**4**
BF/C/DL1	M	2	Peritoneum, lung, liver	3	Mut	A11.6	3	0	**PD**	**2**
CL/C/DL2	F	0	Peritoneum, nodes	3	Mut	**A2**	12	1	**PD**	**19**
FA/C/DL2	F	2	Colon, lung, liver	6	Wt	A11.6	11	0	*SD*	*6*
SA/C/DL2	M	0	Lung, liver, nodes	5	Wt	**A2**	10	6	**PR**	**11**
SS/C/DL3	F	0	Brain, lung, liver, nodes	5	Mut	A23.2	12	3	**PR**	**8**
BA/C/DL3	F	1	Colon, lung, liver, nodes	2	Mut	**A2**	11	0	SD	7
SA/C/DL3	F	2	Peritoneum, lung, liver	5	Mut	**A2**	12	0	**PD**	**6**
DA/C/D	F	2	Peritoneum, lung,	4	M		10	0	**PD**	

L3			liver		ut	A1.1 1				**6**
MP/C/D L3	M	1	Peritoneum, lung, liver	6	M ut	**A2**	6	0	*SD*	*14*
PM/C/D L3	M	1	Peritoneum, lung, liver	2	M ut	A11. 2	11	3	*SD*	*9*
MU/C/D L3	F	1	Soft tissue, nodes	2	Wt	A24. 2	12	32	**SD**	**42+**
PA/C/D L3	M	1	Peritoneum, lung, liver	7	Wt	**A2**	11	3	**PR**	**8**
CA/C/D L3	M	2	Peritoneum, lung, liver	3	M ut	NA	6	0	PD	13
BG/C/D L3	F	0	Peritoneum, lung, liver	3	Wt	**A2**	10	8	*SD*	*2*
NR/C/D L3	F	2	Peritoneum, lung, liver	2	m ut	**A2**	3	0	PD	2
SR/C/D L0	M	0	Lung, liver	3	wt	A23. 2	12	5	*SD*	*12*
DG/C/D L0	F	0	Lung, liver	3	wt	A33	10	5	**PR**	*10*
BL/C/D L0	F	0	Lung, liver	2	wt	A3.2 9	10	9	*SD*	**15**
ML/C/D L0	F	0	Peritoneum, lung, liver	2	m ut	**A2**	10	9	*SD*	*8*
VP/C/D L0	M	1	, lung, liver	2	wt	**A2**	7	1	*SD*	*16*
PG/C/D L0	M	1	lung, liver	2	Wt	A24.	9	12	*SD*	**32+**

						3				
SA/C/D L0	M	2	Peritoneum, lung, liver	3	wt	A1.3	7	0	PD	*5*
MA/C/D L0	M	0	lung, liver	2	m ut	A1	9	32	**PR**	**33+**
PA/C/D L0	M	0	lung, liver	2	wt	A3.2 4	11	14	**PR**	**17**
DL/C/D L0	F	0	Peritoneum, lung, liver	3	wt	**A2**	9	4	SD	**13**
VC/C/D L0	M	0	Peritoneum, lung, liver	2	m ut	A23, 2	10	7	**PR**	7
PA/C/D L0	F	1	Peritoneum, lung, liver	3	wt	23.2 6	9	4	SD	**16**

Table 2

	Frequency of adverse events															
ADVERSE EVENTS	**DL0 (11 pts)**				**DL1 (3 pts)**				**DL2 (3 pts)**				**DL3 (12 Pts)**			
	G 1	**G 2**	**G 3**	**G 4**	**G 1**	**G 2**	**G 3**	**G 4**	**G 1**	**G2**	**G 3**	**G 4**	**G 1**	**G 2**	**G 3**	**G 4**
Leukocytopenia	2	4			2					3			5			1
Anemia	4	8				1	2				2		1	5	2	
Thrombocytopenia		2		1			2	1			2		2	1		1
Nausea / Vomit	1	3			1								1	2		
Preaffable pain	1												2	2		
Addominal pain	2									1				3		
Diarrhea	2	1				1							0	0		
Conjunctivitis	1					2			1				1	4		
Cutaneous reaction						1							1	1		
Cough					1	1				1			0	0		
Hiccup													1	1		
Nettle rash													1	1		
Dyspnea	1												1			
Poliarticular syndrome		3								2			1	3		
Infection/ sepsi	2					1						2	2	1		

Fever	1	1			2						2		3	2	1	
Asthenia	1					1				2			3	2	1	
Sensorial Neurotoxicity	3												1			
Transaminase rise	4	1			2									1		
Hypothyroidism	2												3			
Hypotension					1					1						
Hypertension	1						1			1			1	3		
Nether arts edema	3		3		1	2				1			2	2	1	

Table 3 Treatment groups

	DL1-3 (17 pts)				***DL0 (12 pts)***				
	Baseline	**Post 3**	**Post 6**	**Post 12**	**Baseline**	**Post 3**	**Post 6**	**Post 12**	**P**
Neutrophils migl/mm^3	4.7+/-0.7	4.1 +/- 0.75	3.5 +/- 0.2*	2.8+/- 0.2*	4.4+/- 0.4	4.3+/- 0.3	3.0+/0.65*	4.6+/-0.7	0,6
CPR mg/ml	3.5+/-0.9	3.9 +/-1.2	2.3+/0.47	4.5+/- 1.1	2.16+/0.9	1.6 +/- 0.6	1.4 +/-0.6	1.0+/-0.2	**0.041**
ESR mm/h	69.9+/8.3	75.3+/10.4	79.1+/7.5	85.4+/- 11.2	40.7+/7.8	52.8+/- 8.2	56.1 +/9.9	58.1+/11.6	**0.00018**
ANA positive patients	2/17	2/17	6/17	5/17	0/12	0/12	0/12	1/12	**<0.05**
NK % of plotted cells	5.41+/-5	8.3+/-1.2	9.6+/-7.6	8.6+/- 1.9	5.7+/-3.5	10.7+/- 1	11 +/- 4.4*	7.9+/-1.4	0.49
IL6 pg/ml	4.8 +/- 2	6.4 +/- 2	5.5 +/- 1	4.4 +/- 2	1.1+/- 0.6	5.2+/- 2.4	3.1 +/- 1.3	3.5 +/- 0.2	0.09
IL8 pg/ml	36.8 +/- 8	54 +/-18	17+/- 2	13.3 +/-4.4	56.6 +/12.3	62.7+/- 11.3	16 +/-1.1	37.6 +/12.2	0.82

Neutrophils – DL-1-3, baseline vs. 6th vs. 12th course, P<0.01; DL-0, baseline vs. 6th course, P=0.05.

CPR- DL-1-3 values, baseline vs. 6^{th}, P =0,049; DL0 values, baseline vs. 6^{th} vs. 12^{th} course, P<0.05.

NK- DL0 values, baseline vs. 6^{th} course, P=0.04.

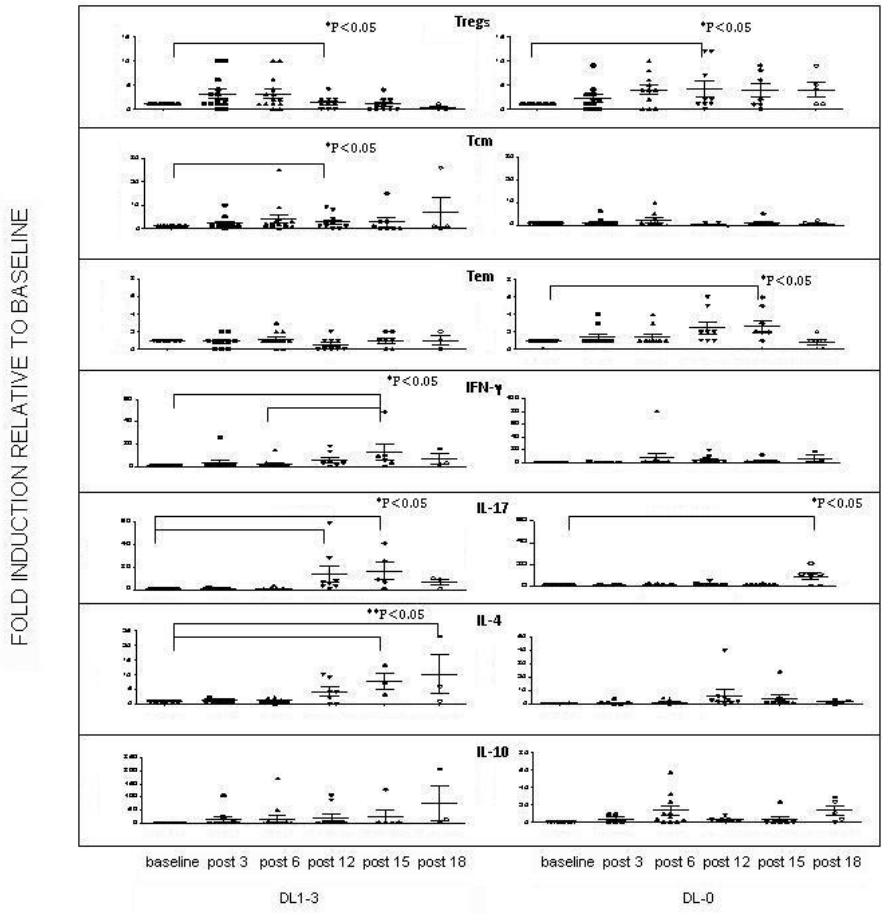

Figure 1 *Kaplan Meyer descriptive for statistics* Panels A-B represent median PFS (A) and OS (B) in pts enrolled in the concomitant (DL1-3) and sequential (DL0) treatment modules. Median PFS, DL1-3 vs. DL0: 3 +/- 0.738 (95%IC: 2.55-5.44) months vs. 7 +/- 0.818 (95%IC:4.64-7.85), P= 0.340; median OS, DL1-3 vs. DL0: 8 +/- 0.038 (95%IC: 6.13-12.69) months vs. 16 +/- 1.67 (95%IC: 10.17-17.05) months; P= 0.049 by log rank test. Panels C-E represent peripheral blood cell counts in mCRC pts enrolled in the TSPP/VAC1 arm-C trial, at baseline and before each treatment course. Lymphocyte counts (C), monocyte counts (D), eosinophil counts (E). Results are expressed a number of cells x 10^2/sqmm +/standard error. Panels F-H represent serum auto-antibodies in mCRC pts enrolled in the TSPP/VAC1 arm-C trial, at baseline and before each treatment course. ENA (F); c-ANCA (G), and p-ANCA (H). Results are expressed as a units/ml +/- standard error. Symbols represent the groups of pts who received TSPP vaccination as concomitant (■) or sequential treatment modules (■). Pts in the DL1-3 group received concomitant TSPP vaccination and GOLFIG chemo-

immunotherapy and then TSPP maintenance starting after 12 courses (Post-12). Pts in the DL0 group received GOLFIG chemo-immunotherapy alone and then TSPP maintenance starting after 12 courses (Post-12). Statistical significance ($P<0.05$) with the co-respective baseline value is represented by an asterisk.

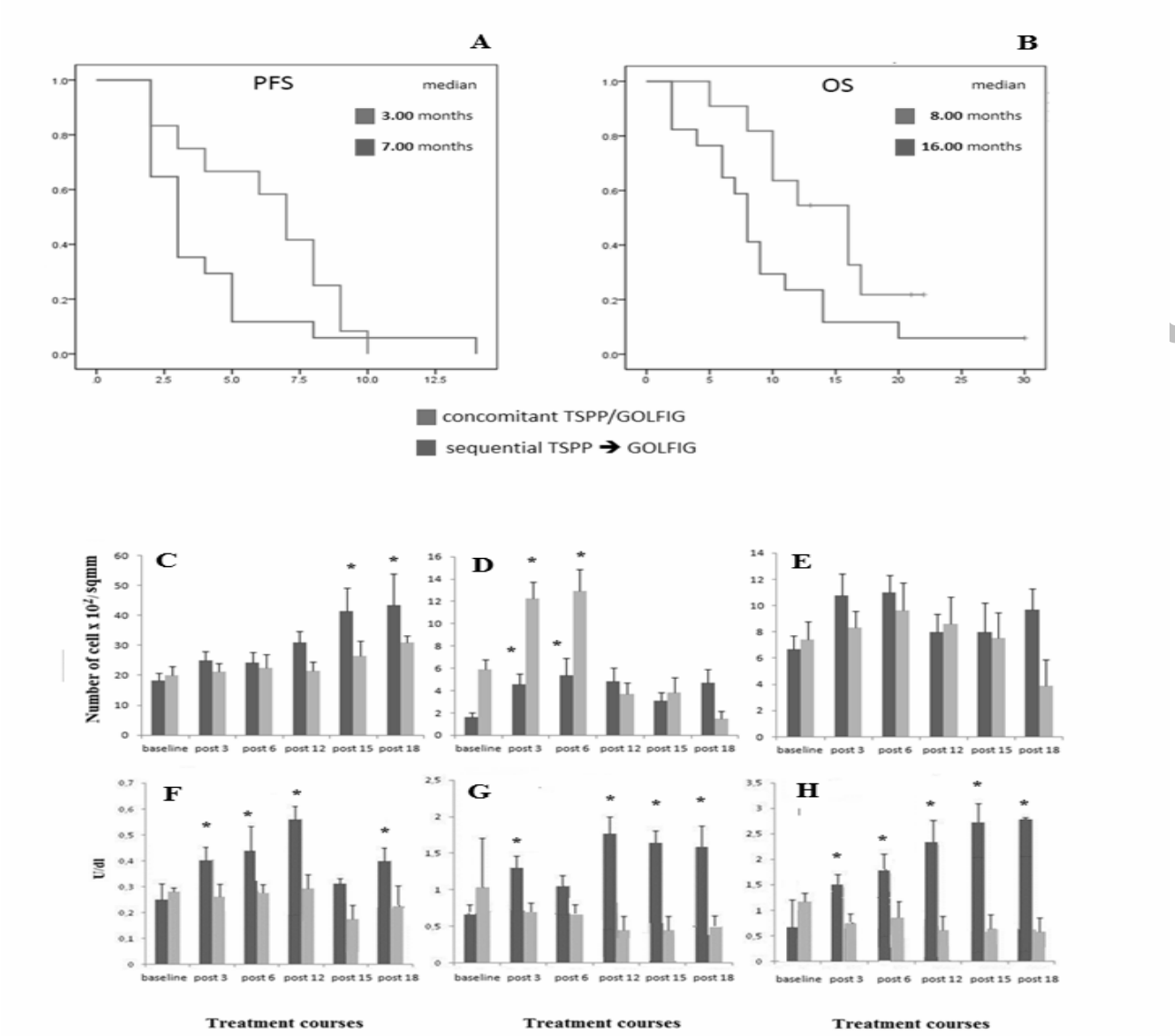

Figure 2 The upper figures (first three rows) represent the fold change modulation relative to baseline values of plotted percentages of peripheral T_{reg}, T_{cm}, T_{em} of the pts enrolled in the trial and who received the concomitant (DL 1-3) (left panels) and sequential (DL-0) treatment modules (right panels). Statistical significance was calculated by performing the one-way Anova analysis of variance, post-test Bonferroni with 95% IC. The bottom figures (last four rows) represent the fold change modulation relative to baseline values of serum level of IFN-γ, IL-17, IL-4 and IL10 of the pts who received the concomitant (DL1-3) (left panels) or the sequential treatment modules (DL0) (right panels). Statistical significance was calculated by

performing the one-way Anova analysis of variance, post-test Bonferroni with 95% IC. Post-3, -6, -12, -15 and -18 represent the number of treatment courses received by the pts. Pts in the DL1-3 group received concomitant TSPP vaccination and GOLFIG chemo-immunotherapy and then TSPP maintenance starting after 12 courses (Post-12). Pts in the DL0 group received GOLFIG chemo-immunotherapy alone and then TSPP maintenance starting after 12 courses (Post-12).

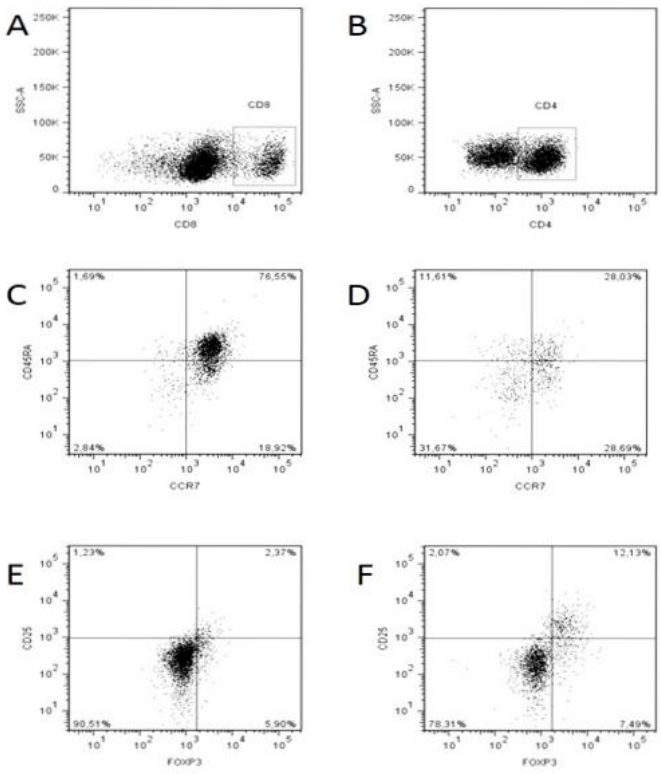

Figure 3 Flow cytometry analysis: Central memory T cells ($T_{CM;}$ $CD45RA^{-}CCR7^{+}$) and effector memory T cells ($T_{EM;}$ $CD45RA^{-}CCR7^{-}$) gated on $CD3^{+}CD8^{+}$ lymphocytes (**A**) of representative patient PBMCs (DL3), isolated at the baseline (C) and after six treatment lines (D) **Regulatory T cells (**T_{reg} **;** $CD25^{+}Foxp3^{+}$) gated on $CD3^{+}CD4^{+}$ lymphocytes **(B)** of representative patient PBMCs, isolated at the baseline (E) and after six treatment lines (F).

Virology 486 (2015) 255–262

Contents lists available at ScienceDirect

Virology

journal homepage: www.elsevier.com/locate/yviro

Truncation of the C-terminal region of Toscana Virus NSs protein is critical for interferon-β antagonism and protein stability

Gianni Gori Savellini, Claudia Gandolfo, Maria Grazia Cusi *

Department of Medical Biotechnologies, Microbiology Section, University of Siena, Italy

ARTICLE INFO

Article history:
Received 20 May 2015
Returned to author for revisions
17 July 2015
Accepted 25 September 2015

Keywords:
Toscana Virus
Non-structural protein
RIG-I
C-terminal deleted protein

ABSTRACT

Toscana Virus (TOSV) is a *Phlebovirus* responsible for central nervous system (CNS) injury in humans. The TOSV non-structural protein (NSs), which interacting with RIG-I leads to its degradation, was analysed in the C terminus fragment in order to identify its functional domains. To this aim, two C-terminal truncated NSs proteins, Δ1C-NSs (aa 1–284) and Δ2C-NSs (aa 1–287) were tested. Only Δ1C-NSs did not present any inhibitory effect on RIG-I and it showed a greater stability than the whole NSs protein. Moreover, the deletion of the TLQ aa sequence interposed between the two ΔC constructs caused a greater accumulation of the protein with a weak inhibitory effect on RIG-I, indicating some involvement of these amino acids in the NSs activity. Nevertheless, all the truncated proteins were still able to interact with RIG-I, suggesting that the domains responsible for RIG-I signaling and RIG-I interaction are mapped on different regions of the protein.

Introduction

Innate immune responses represent the primary defense against virus infections, and the type I interferon (IFN-α/β) system plays one of the most important roles in immunity. Among type I IFNs, IFN-β is secreted by most cells upon viral infection and triggered by two major sensor proteins located in the cytoplasm, RIG-I and MDA-5 (Sato et al., 2000; Yoneyama and Fujita, 2008). However, most viruses have evolved viral proteins capable of overcoming the innate immune response and interfering with the type I IFN response in order to replicate and persist in the host. This antagonizing activity has been observed in several non-structural viral proteins (Haller et al., 2006; Mibayashi et al., 2007; Opitz et al., 2006; Van Knippenberg et al., 2010), by mechanisms which exploit different targets in the IFN signaling pathway. Among the RNA viruses, several members of the *Bunyaviridae* family possess an NSs protein involved in evading innate immune responses in mammalian hosts (Weber et al., 2001; Jääskeläinen et al., 2007; Bridgen et al., 2001; Weber et al., 2002; Blakqori et al., 2007; Léonard et al., 2006). Toscana Virus (TOSV) is an arthropod-borne virus of the *Phlebovirus* genus of the *Bunyaviridae* family. Like all bunyaviruses, it is an enveloped virus containing a tri-segmented, single strand negative-sense RNA genome: the large (L), the medium (M) and the small (S) segment coding for the structural proteins (L, Gc, Gn, and N) and two non-structural proteins (NSm and NSs). In most cases, TOSV infection consists of a mild disease with a favorable outcome, but some severe cases of CNS infections have been reported in the literature (Kuhn et al., 2005; Bartels and Heckmann, 2012). TOSV is considered an emerging pathogen and the major etiologic agent of aseptic meningitis and encephalitis in the Mediterranean area (Braito et al., 1997; Valassina et al., 1998, 2000; Echevarria et al., 2003; Calisher et al., 1987; Charrel et al., 2005; Dobler et al., 1997; Ehrnst et al., 1985; Eitrem et al., 1991; Endris and Perkins, 1987; Hukić and Salimović-Besić, 2009; Sonderegger et al., 2009; Epelboin et al., 2008; Bahri et al., 2010; Papa et al., 2010). The pathological mechanisms of TOSV infection are still unclear. Previous data have shown that Toscana Virus, conversely to other phleboviruses, such as Rift Valley Fever Virus (RVFV) and Punta Toro Virus (PTV) (Billecocq et al., 2004; Mendenhall et al., 2009; Kalveram et al., 2011), triggers IFN-β production after infection, although expressing a non-structural NSs protein with IFN-β antagonistic properties (Gori Savellini et al., 2011). It was demonstrated that TOSV NSs, when transiently over-expressed in mammalian cells, exerted its inhibitory effect on the host innate immunity by interacting with RIG-I and mediating its degradation. The mechanisms by which TOSV NSs controls RIG-I activity are still largely unknown. A hypothetical mechanism is based on the activation of cellular proteases after NSs-RIG-I interaction and formation of a protein complex that leads to its degradation. In fact, the MG-132 proteasome inhibitor could revert NSs induced RIG-I degradation, as previously described (Gori Savellini et al., 2013). In the present study, we have more thoroughly investigated the function of TOSV NSs, with respect to RIG-I down-regulation and IFN-β inhibition. Deleted forms of NSs protein were generated in an attempt to identify the protein domain (s) involved in functional properties which could be important for

* Correspondence to: Department of Medical Biotechnologies, University of Siena, V.le Bracci, 1 53100 Siena, Italy. Fax: +39 577 233870.
E-mail address: cusi@unisi.it (M.G. Cusi).

http://dx.doi.org/10.1016/j.virol.2015.09.021
0042-6822/

understanding the pathogenesis of TOSV infection in humans. For this purpose, we constructed two C-truncated forms of NSs protein that were more stable than the whole protein. Moreover, a short sequence (TQL) at the C-terminus of NSs was identified as an important element showing a partial inhibitory activity on RIG-I. In fact, ΔTLQ-NSs was shown to be much less active in mediating RIG-I degradation, although it bound RIG-I CARDs, as observed by co-immunoprecipitation assay. These findings suggest that functional sites and interacting domain (s) are located in different regions of the NSs protein.

Results

C-terminal region of TOSV NSs retains functions involved in RIG-I degradation

Previous results showed that TOSV NSs protein is poorly expressed during viral replication in cell cultures and its role during the infection is largely unknown. However, when transiently over-expressed by transfection, the NSs counteracts IFN-β production by interacting with RIG-I and mediating its degradation (Gori Savellini et al., 2011, 2013). A C-terminal deleted NSs protein (aa 1–277) was tested in a previous study, showing that it had no inhibitory effect on IFN-β promoter activation and that it was able to retain the ability to interact with RIG-I (Gori Savellini et al., 2013). In the present study, we decided to analyse more thoroughly the sequence(s) involved in this function. Thus, to better characterise the TOSV NSs protein and its role in the IFN-β pathway, carboxyl-terminal deleted forms of NSs protein were tested. After a preliminary screening of some deleted forms of multiples of ten amino acids from the C-terminal of NSs, we analysed the two closer C-truncated forms of NSs, Δ1C-NSs (aa 1–284) and Δ2C-NSs (aa 1–287) (Fig. 1A) which appeared to show a different behavior vs RIG-I. As shown in Fig. 1B, the over-expression of Δ2C-NSs, lacking the 29 C-terminal aa, led to RIG-I degradation (Relative Density 0.45), just as that which occurred with the wild-type NSs protein (Relative

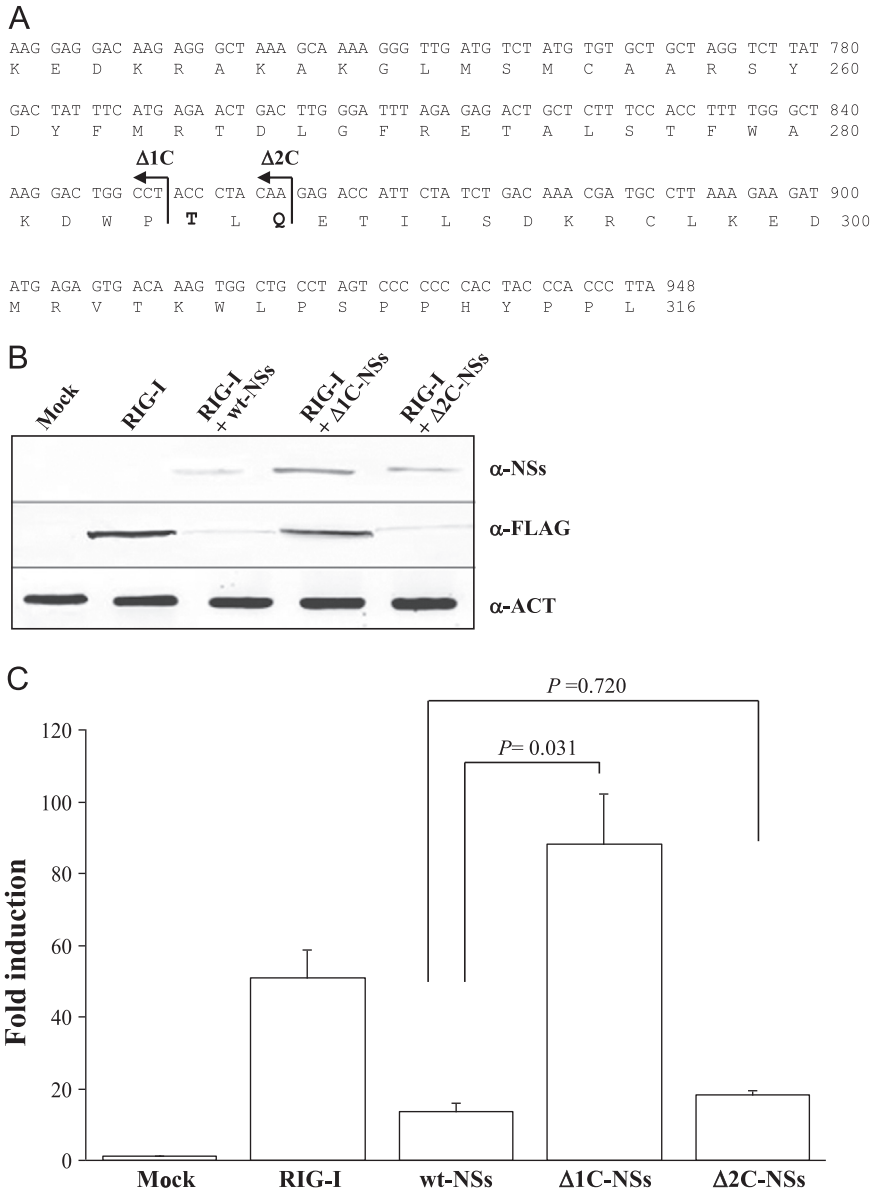

Fig. 1. The involvement of TOSV NSs C-terminal region on RIG-I degradation and IFN-β inhibition was demonstrated by generating deleted NSs proteins: Δ1C-NSs (aa 1–284) and Δ2C-NSs (aa 1–287) (A). The behavior of these deleted NSs forms was investigated by immunoblot on lysates of cells transfected with FLAG-RIG-I, alone or in combination with wt-NSs, Δ1C-NSs or Δ2C-NSs. Specific proteins were detected by using anti-FLAG M2, anti-NSs and anti-actin antibodies (B). Densitometric analysis was performed on reactive protein bands. These results were further confirmed by measuring the RIG-I-mediated IFN-β promoter activation in a Luciferase reporter assay (C). Results are shown as the mean value of Luciferase activities normalized with respect to *Renilla* luciferase values collected in at least three independent experiments ± standard deviation.

Density 0.42). On the contrary, the Δ1C-NSs, lacking the 32 C-terminal aa, significantly lost its degrading activity on RIG-I (Relative Density 0.91) upon co-transfection of cells with the respective plasmids (Fig. 1B). These results were further confirmed by Luciferase reporter assay, showing that Δ2C-NSs inhibited the IFN-β promoter upon poly(I:C) stimulation ($p=0.72$), like the wild-type viral protein, while Δ1 C-NSs had completely lost its inhibitory effect on RIG-I mediated IFN-β promoter activation ($p=0.031$) (Fig. 1C).

Since the two C-terminus deleted forms showed a different behavior, we hypothesized that the amino acid sequence, TLQ (aa 285–287), interposed between the two constructs, could be responsible for the functional effect. Thus, we analysed the effect of point mutations in the sequence coding for this amino acid triplet.

Generation of NSs with mutated TLQ sequence

The fundamental role of the TLQ selected peptide was first demonstrated by its deletion in the wt-NSs protein, analyzing RIG-I protein accumulation in cells by immunofluorescence and immunoblotting. The resulting ΔTLQ-NSs protein showed properties similar to Δ1C-NSs, indicating that this sequence could have an important role in the activation of RIG-I signaling. As shown in Fig. 2A, a significant increase of RIG-I positive cells was observed in RIG-I and ΔTLQ-NSs co-transfected cells, compared to those expressing RIG-I in combination with wt-NSs ($p<0.001$). Moreover, RIG-I was not degraded as shown by immunoblot and densitometric analysis, when Lenti-X 293T cells where co-transfected with ΔTLQ-NSs (Relative Density 0.8) (Fig. 2B). It appeared that this string of amino acids could be involved in the RIG-I degradation process. Moreover, IFN-β promoter induction was restored upon poly(I:C) stimulation of RIG-I and ΔTLQ-NSs transfected cells, as shown by luciferase assay (Fig. 2C). To better understand TLQ function, we substituted the two polar amino acids, T (aa 285) and Q (aa 287) of the triplet, with G, a non polar amino acid, in order to evaluate the consequences of these amino acid substitutions. We found that both changes could be partly responsible for RIG-I degradation. In fact, these amino acid substitutions led to an increase in the number of RIG-I positive cells (Fig. 3B) as also shown by western blot. In fact, cells transfected by T/Q mutated NSs showed a similar profile ($p=0.59$). Moreover, the fold induction of IFN-β promoter activity was significantly higher in cells co-transfected with RIG-I and Q_{285}/G or T_{287}/G NSs compared to RIG-I and wt-NSs ($p=0.02$) (Fig. 3C).

Deletion alters NSs protein stability

We also evaluated the expression levels of the deleted NSs forms described above. By counting fluorescent cells or by semi-quantitative immunoblotting, differences in cytoplasmic accumulation of NSs protein were observed. By immunofluorescence, an increased cytoplasmic accumulation of Δ1C-NSs was noticed compared to the wt and Δ2C-NSs proteins, indicating that the last 32aa at the C-terminus could influence the stability of the entire protein (Fig. 4A). The high number of cells expressing Δ1C-NSs reflected the high amount of protein detected by immunoblot (Fig. 4A). To better understand the role of TLQ sequence on NSs stability, NSs variants fused with Firefly Luciferase (FF-Luc) were generated. These FF-Luc NSs proteins retaining their functional activity on RIG-I (data not shown) were tested for their stability by measuring luciferase activity in transfected, cycloheximide (CHX)-treated cells. A significant decrease in Luciferase activity, in parallel with NSs disappearance, was detected in Δ2C-NSs and wt-NSs lysates 4 h after CHX treatment ($p<0.001$) (Fig. 4B). On the contrary, Δ1C-NSs was able to maintain Luciferase activity up to 6 h after CHX treatment of the cells, thus confirming its stability, further validated by immunoblotting (Fig. 4B). These data support the hypothesis that the TLQ sequence could be involved in NSs protein stability. Moreover, an mRNA quantitation analysis of the

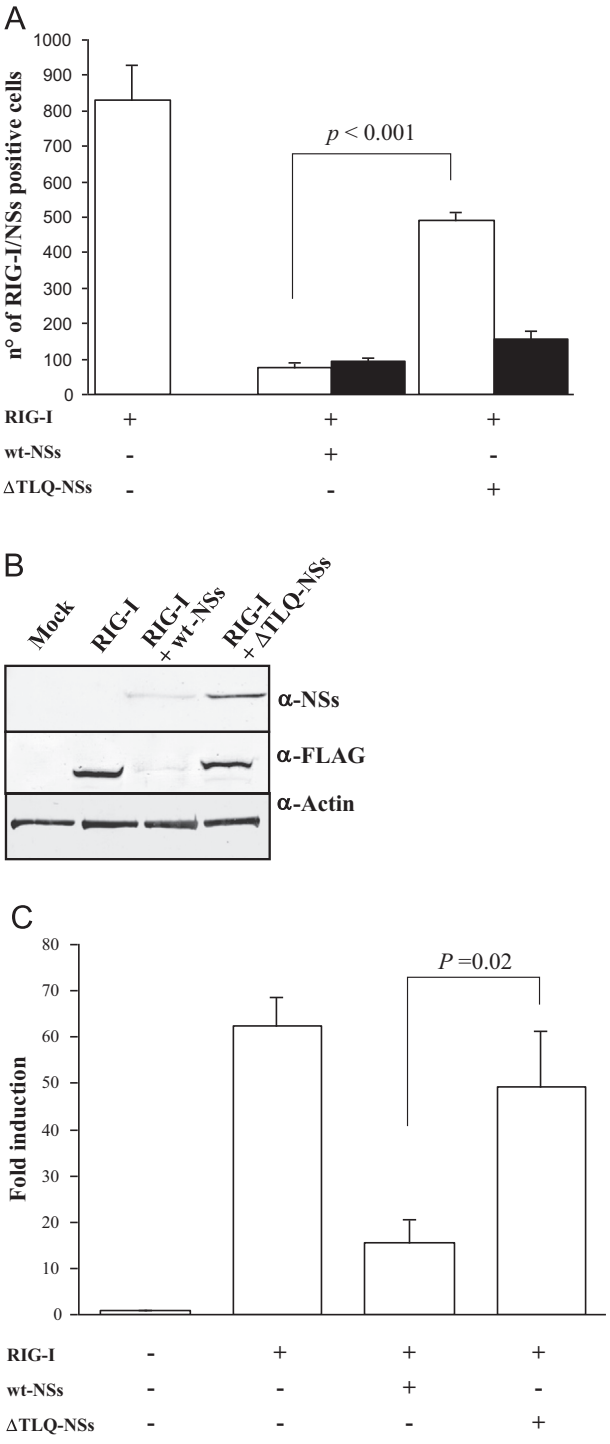

Fig. 2. The fundamental role of the TLQ peptide (285–287 aa) of the TOSV NSs protein was investigated in Lenti-X 293T cells transfected with FLAG-RIG-I alone or in combination with wt-NSs or ΔTLQ-NSs coding plasmids. Transfected cells were collected and tested by immunofluorescence with anti-FLAG M2 and anti-His antibodies. RIG-I (□) and NSs (■) positive cells were counted (A). Graph bars represent mean results from different experiments ± standard deviation. Quantitative analysis of cytoplasmic RIG-I in the presence of wt-NSs or ΔTLQ-NSs was performed by immunoblotting with anti-FLAG M2 antibody (B) and densitometric evaluation. Loading control was represented by actin detection (α-ACT) and NSs expression was evaluated by using anti-NSs antibody. The ability of TLQ deletion to abolish NSs RIG-I degradation activity and an IFN-β antagonistic effect was further investigated by Luciferase reporter assay (C), evaluating the activation of the IFN-β promoter. Luciferase activities were measured in each sample and results were reported as the mean value ± standard deviation, of normalised data from three independent experiments.

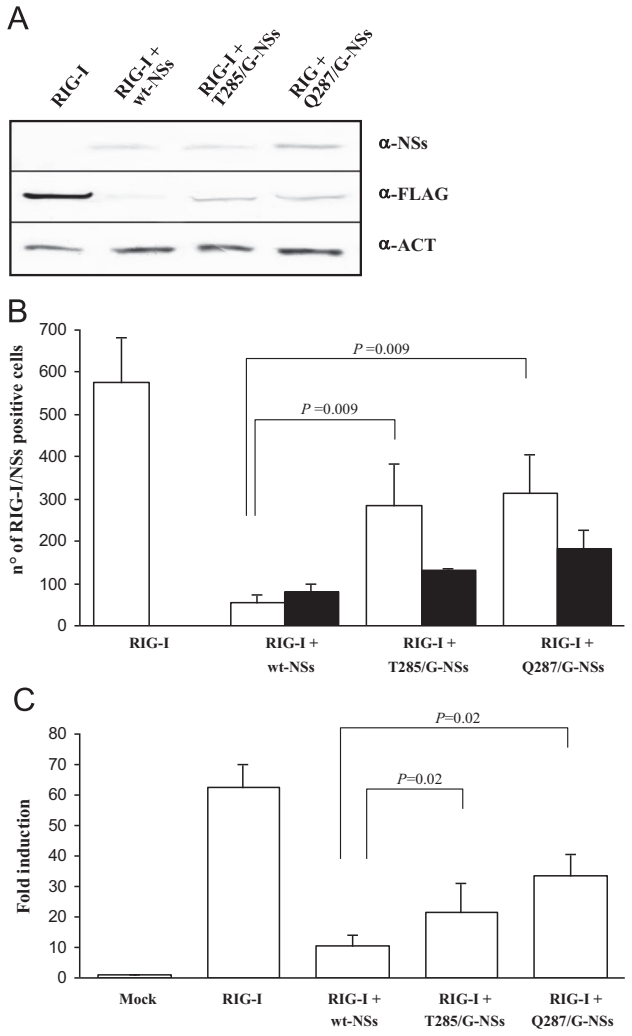

Fig. 3. The effect of T_{285}/G and/or Q_{287}/G point mutations on NSs protein activity was investigated in Lenti-X 293T cells transfected with RIG-I and NSs plasmids. The cellular levels of RIG-I in the presence of different NSs forms were analysed by immunoblotting with anti-FLAG M2 antibodies. NSs expression was confirmed by anti-NSs antibody. Loading control was represented by actin (α-ACT) detection (A). Cells were collected and also tested by indirect immunofluorescence with anti-FLAG M2 and anti-His, counting RIG-I (□) and NSs (■) positive cells, respectively (B). Error bars represent the standard deviation of the mean value obtained in at least three independent experiments. The ability of NSs mutants to revert the protein inhibitory effects on RIG-I-mediated IFN-β signaling was further investigated by Luciferase reporter assay, evaluating the activation of the IFN-β promoter in the presence of wt or mutated NSs proteins (C). Luciferase activities were measured in each sample and results were reported as the mean value. Error bars show standard deviations in the *Renilla* Luciferase normalized data from at least three independent experiments.

NSs protein forms did not reveal any significant difference, indicating that the different amount of protein present in the cells was due to a greater stability and cytoplasmic accumulation of the Δ1C-NSs protein itself and not to a higher mRNA expression (data not shown).

Interaction of C-deleted forms of NSs with RIG-I

Previous results showed that TOSV NSs may exhibit its inhibitory effects on the host innate immune response by interacting with RIG-I, in particular with the CARD domains (Gori Savellini et al., 2013). In this study, we more thoroughly investigated the RIG-I interaction properties of deleted NSs proteins in order to identify which NSs domain is involved in the interaction and whether this is associated to its inhibitory activity. C-deleted NSs proteins were tested for their ability to bind the RIG-I CARDs (RIG-IN) by co-immunoprecipitation (Co-IP). As shown in Fig. 5, all the recombinant NSs proteins were able to bind the RIG-IN protein, as previously tested (Gori Savellini et al., 2013) indicating that the C-terminal region of the NSs does not appear essential for RIG-I binding. These results suggest that it is likely that the NSs domain interacting with RIG-I is different from that involved in the inhibition/degradation of RIG-I.

Discussion

Among *Phleboviruses*, some show different levels of pathogenicity; some can cause fatal disease, and others can even cause asymptomatic illness. The non-structural protein, expressed by the small segment of the RNA genome (Giorgi et al., 1991; Bishop, 1986), is considered an important virulence factor, having the activity shared with other members of the *Bunyaviridae* family, to inhibit IFN induction through different pathways (Billecocq et al., 2004; Habjan et al., 2009; Ikegami et al., 2009; Le May et al., 2004, 2008; Léonard et al., 2006; Thomas et al., 2004). The mechanisms by which TOSV NSs can block IFN induction in cells are not completely clear, however, we previously demonstrated that when NSs is over-expressed, it is able to antagonize IFN-β response by targeting RIG-I for degradation (Gori Savellini et al., 2013). Moreover, we recognized the involvement of the C-terminus of the NSs protein in this activity. For this reason, aiming at identifying the sequence(s) responsible for NSs functional properties, two C-terminus truncated forms of NSs, Δ1C-NSs and Δ2C-NSs, were synthesized and tested for their stability and involvement in RIG-I degradation activity. We found that a 32 aa deletion at the C-terminus (Δ1C-NSs) conferred greater stability to the protein itself, as demonstrated by pulse-chase experiments and reporter gene assay. A higher Luciferase activity was detected several hours after cycloheximide treatment of cells expressing Firefly Luciferase fused Δ1C-NSs, in agreement with a longer life-time of the truncated NSs protein. No increase of specific mRNA was detected, indicating that the higher amount of recombinant NSs was due to a greater stability of the protein. On the contrary, Δ2C-NSs resulted less stable than Δ1C-NSs, suggesting that the interposed TLQ sequence might play a crucial role in this function. In fact, by the prediction of disordered sequences (http://prdos.hgc.jp/cgi-bin/top.cgi), the C-terminus of NSs contains intrinsically disordered regions. Usually, disordered proteins are present in relatively low levels and for short periods of time compared to structured proteins (Babu et al., 2011). Moreover, these regions frequently interact with their targets with relatively high specificity and low affinity, suggesting that they can associate rapidly and initiate a signaling process and at the same time dissociate easily when the task is accomplished. In this study, however, the deletion of the predicted disordered sequence, corresponding to the last 16–17 aa at the C-terminus of the protein which was not even present in the Δ2C-NSs construct, neither increased protein stability nor contrasted with RIG-I degradation. Only the further deletion of the TLQ triplet allowed a change in NSs behavior. A similar result was obtained when one of the polar amino acids T or Q was mutated, indicating that these amino acids might have an important effect on the protein function. A prediction analysis (http://elm.eu.org) of conserved domains in the NSs sequence identified the TLQ peptide as part of a TRAF2-ligand motif, which is associated with proteins involved in signal transduction, particularly those mediating RIG-I/MAVS/TRAFs signaling pathways. Thus, we can speculate that this functional domain, present in the NSs protein, could be partly involved in its inhibitory properties versus the IFN-β mediated immune response.

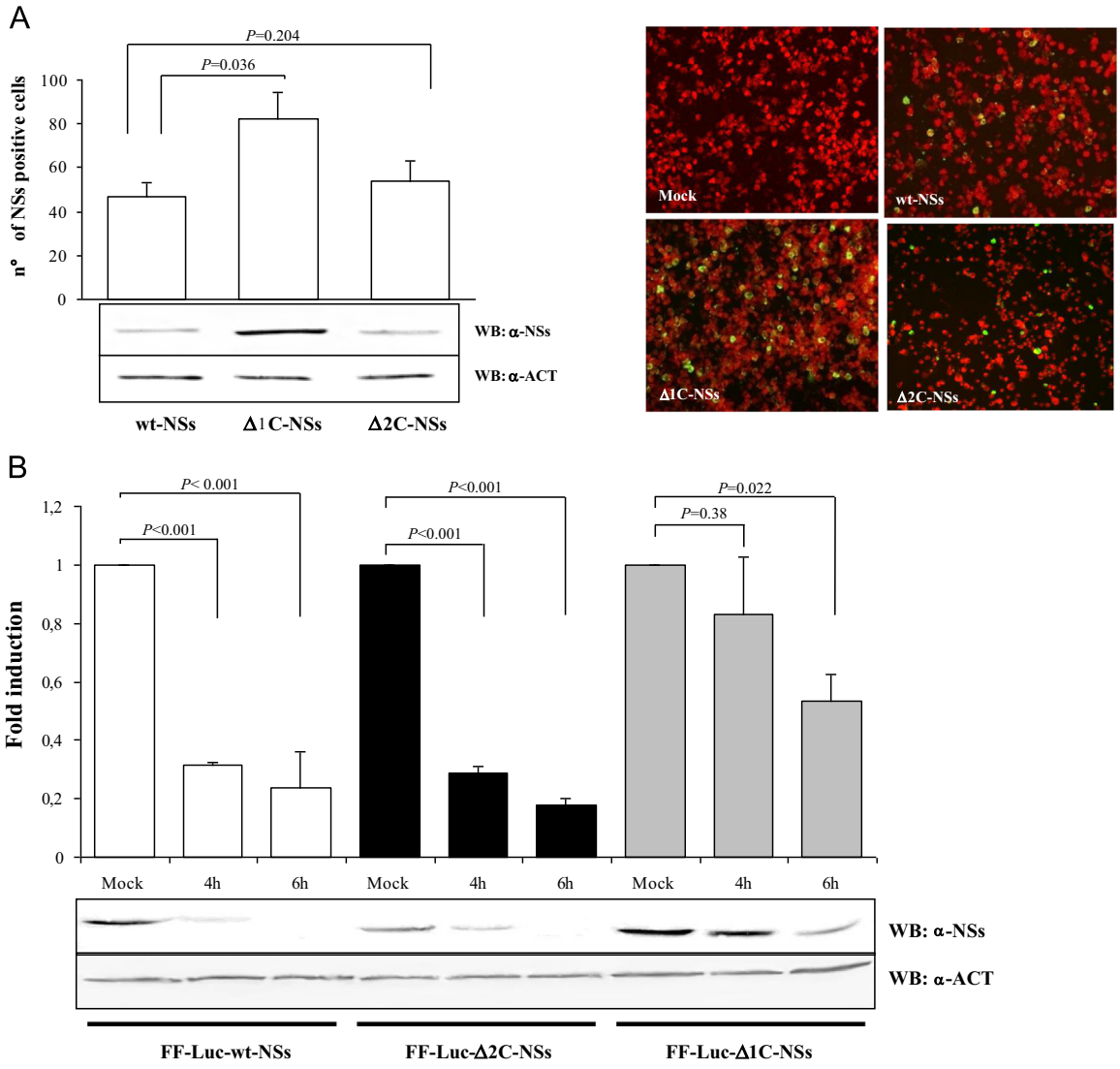

Fig. 4. The stability of TOSV NSs protein was investigated by immunofluorescence or immunoblot. Lenti-X 293T cells were transfected with full-length NSs, Δ1C-NSs or Δ2C-NSs expressing plasmids. Forty-eight hours post-transfection, cells were collected and assayed for indirect immunofluorescence with anti-6xHis antibody. The fluorescence was analysed with a Diaplan microscope and NSs positive cells were counted (A). The error bars represent the standard deviation from the mean values obtained in independent experiments. A representative immunofluorescence picture of FITC-stained NSs positive cells is shown in (A), right panel (magnification 40 ×). The same samples were lysed and equal amounts of cell extracts (50 μg) were subjected to immunoblot with anti-NSs antibodies or anti-actin (α-ACT) as a control. Quantitative assessment of deleted NSs stability was determined by pulse-chase experiments and reporter gene assay. Lenti-X 293T cells were transfected with FF-Luc NSs fusion constructs and *Renilla* Luciferase as an internal control. Transfected cells were mock-treated or treated with cycloheximide and collected at 4 h and 6 h. Luciferase activities were measured and results were reported as the mean value. Error bars show the standard deviation of the *Renilla* Luciferase normalized data from at least three independent experiments (B).

Nevertheless, the deleted forms of NSs were still able to bind RIG-I, as demonstrated by immunoprecipitation assay using RIG-IN, indicating that the domain(s) responsible for this interaction is/are not located in the C-terminus of the viral protein. Taken together, these results indicate that the 32 aa at the NSs C-terminus may be critical for suppressing an IFN expression response in host cells and for conferring greater stability to the NSs protein. Moreover, the TLQ triplet might have a relevant involvement in the IFN-β inhibition activity mediated by NSs, since its deletion or the mutation of T/Q could suppress the inhibitory effect of NSs. We do not know whether this triplet is involved in addressing the protein itself to the proteasome or whether it targets RIG –I to the proteasome. However, since cell treatment with MG 132 further increased the accumulation of Δ1CNSs in the cytoplasm (data not shown), it seems that other domains not located in the C-terminal sequence might be potential targets for ubiquitylation and degradation of NSs. This triplet might affect the biological function of NSs, probably due to the lack of conformational domains. In fact, ΔTLQ, as well as the T/Q mutated forms were able to partially restore RIG-I activity (Figs. 2 and 3C). It is noteworthy that Rift Valley Fever (RVFV), although it belongs to the same genus of TOSV, has an NSs protein whose conformational integrity is important for its stability, because truncation of NSs causes mis-folding and mis-localization of the protein, abolishing its biological functions (Head et al., 2012; Indran et al., 2013). Consequently, it appears that the non-structural protein of these phylogenetically close viruses appears to have a "joint" factor of virulence, but the mechanisms by which it carries out its activities are different and they merit exploration in order to counteract the pathogenicity of these viruses and to prevent infection.

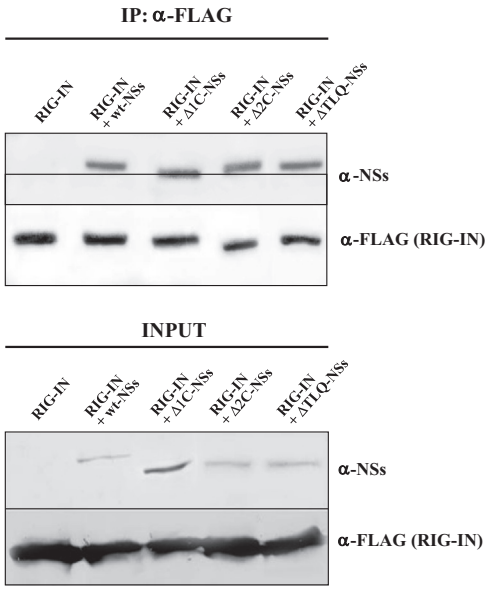

Fig. 5. Co-immunoprecipitation (Co-IP) assay. Lenti-X 293T cells were co-transfected with FLAG-tagged RIG-I CARDs (RIG-IN) along with 6xHis-tagged wild-type (wt) or Δ1C-; Δ2C- or ΔTLQ- deleted TOSV NSs. Clarified lysates were subjected to Co-IP by using anti-FLAG M2 magnetic beads. The presence of either RIG-IN and NSs proteins in the immune-precipitated complex was revealed by immunoblot with anti-FLAG M2 or anti-NSs antibodies, respectively. In the lower panel, 20% of the whole cell lysates were analysed to confirm NSs and RIG-IN expression (input).

Materials and methods

Cells, viruses and chemicals

Vero (ATCC CCL-81) cells and human embryonic kidney Lenti-X 293T cells (Clontech, Milan, Italy) were grown as a monolayer in Dulbecco's modified Eagle's medium (DMEM) (Lonza, Milan, Italy) supplemented with 100 U/mL penicillin/streptomycin (Hyclone Europe, Milan, Italy) and 5% or 10% heat-inactivated fetal calf serum (FCS) (Lonza), respectively, at 37 °C. Toscana Virus (TOSV), strain 1812, was isolated from a clinical specimen, plaque-purified and propagated on Vero cells (Gori Savellini et al., 2008). Transfections were performed using SuperFect Transfection Reagent (Qiagen, Milan, Italy) following the manufacturer's instruction. The MG-132 proteasome inhibitor was purchased from Sigma-Aldrich (Milan, Italy).

Plasmids

Viral RNA was extracted from a cell culture supernatant of TOSV-infected Vero cells by using a QIAamp viral RNA mini kit (Qiagen). The NSs coding gene (GenBank Accession no. EU327772 nt 57–1007) was amplified by reverse transcriptase-polymerase chain reaction (RT-PCR) from purified viral RNA with NSs BamHI sense (nt 1–15) 5′-GGATCCACACAAAGACCTCCC-3′ and NSs XhoI antisense (nt 993–1017) 5′-CTCGAGTCATAAGGGTGGGTA-3′ primers (Sigma-Aldrich). The reaction was carried out using the SuperScript III One-Step RT-PCR with Platinum Taq (Invitrogen) by one cycle of reverse transcription at 50 °C for 30 min and at 94 °C for 2 min followed by 40 cycles of PCR (1 min at 94 °C; 30 s at 60 °C; 1 min at 72 °C). The gene was cloned in pcDNA4HisMax-A plasmid (Invitrogen) at the BamHI-XhoI unique sites of the polylinker in frame with the 6xHis tag. C-terminal deleted NSs protein expression plasmids were generated by cloning the nt 1–852 (Δ1C-NSs) and 1–861 (Δ2C-NSs) ORFs in pcDNA4HisMax-A plasmid, as 6xHis fusion proteins, Firefly Luciferase fused versions of the deleted NSs proteins were generated by cloning the FF-Luc gene at the BamHI site of the constructs above described. The TLQ deleted NSs coding gene was generated by using overlapping primers in PCR. T285/G and Q287/G NSs mutants were generated by QuikChange II XL Site-Directed Mutagenesis (Agilent Technologies, Milan, Italy). The correct constructs were confirmed by sequencing. The reporter plasmid encoding Firefly Luciferase downstream the complete interferon-beta promoter (p125-Luc) and the plasmid coding the RIG-I CARD domains (RIG-IN) were kindly provided by Prof. Takashi Fujita (Tokyo Metropolitan Institute of Medical Science, Tokyo, Japan) (Yoneyama et al., 1996). The human RIG-I expression plasmid fused with the FLAG tag was kindly provided by Prof. A. García-Sastre (Mount Sinai School of Medicine, New York) (Mibayashi et al., 2007). The *Renilla* Luciferase reporter plasmid was purchased from Promega (Promega, Milan, Italy).

Transient expression of NSs and RIG-I

Lenti-X 293T cells were seeded in a 24-wells culture plate at a density of 2×10^5 cells per well and incubated at 37 °C in 5% CO_2 atmosphere. Cell monolayers were transfected with 0.5 μg of wild-type (wt) or deleted NSs expressing plasmids, and 0.05 μg of FLAG-RIG-I plasmid by using SuperFect Transfection reagent (Qiagen), as suggested by the manufacturer. Where indicated, 36 h post-transfections cells were treated-or mock-treated with 2.5 μM MG-132 for an additional 12 hours. Cells were collected and assayed for indirect immunofluorescence (IFA). Briefly, cells were spotted on slide and fixed for 10 min at room temperature with cold methanol/acetone. Cells were then incubated for 1 h at 37 °C with mouse anti-6xHis antibody (GE Healthcare, Milan, Italy) or with mouse anti-Flag M2 polyclonal serum (Agilent Technologies) (1:500 dilution). After washing with PBS containing 0.05% Tween-20 (PBS-T), fluorescein-labeled anti-mouse IgG (Sigma-Aldrich) was added for 30 min. at 37 °C. Immunofluorescence was visualized by a Diaplan microscope (Leica Microsystems, Milan, Italy). RIG-I and NSs positive cells were counted.

Luciferase reporter assay

2×10^5 Lenti-X 293T cells were seeded in 24-well plates and allowed to grow at 37 °C in 5% CO_2 atmosphere. The next day, cell monolayers were transfected with indicated plasmids by using SuperFect Transfection Reagent following the manufacturer's instructions. Briefly, 0.2 μg of p125-Luc, 0.050 μg of RIG-I and, where indicated, 0.5 μg of NSs expressing plasmids were used for co-trasfensfection. The total DNA amount was kept constant with empty plasmid. All cells were co-transfected with 20 ng of *Renilla* Luciferase reporter plasmid (pRL-SV40) (Promega) to normalize results. Thirty-six hours post-transfection, cells were stimulated with 0.1 μg of poly(I:C) by transfection. Twelve hours later, cells were collected, lysed and luciferase activities were measured with dual Luciferase reporter assay reagent (Promega), according to the manufacturer's instructions. Cell lysates were analysed by immunoblotting to detect RIG-I and NSs proteins.

Pulse-chase analysis and NSs stability

Lenti-X 293T cells were seeded in 24-well plates and transfected, in triplicate, with the FF-Luc-NSs or the two FF-Luc-deleted NSs expressing plasmids, along with 20 ng of *Renilla* Luciferase reporter plasmid (pRL-SV40) (Promega) to normalize results. Forty-two hours after transfection, cells were mock-treated or treated with 100 μg/ml of cycloheximide (CHX) (Sigma-Aldrich, Milan, Italy). Samples were collected 4 h and 6 h post-CHX treatment. Lysates were prepared according to Dual-Luciferase reporter assay (Promega) and Luciferase activities were measured. Relative

FF-Luc values were normalized with respect to the *Renilla* luciferase activity and fold induction of each sample was calculated with respect to the corresponding mock-treated sample.

Immunoprecipitation

Cells transfected with RIG-IN, alone or in combination with wt-NSs or deleted/mutated NSs plasmids, were subjected to co-immunoprecipitation (Co-IP). Cellular pellets were resuspended in lysis buffer consisting of 50 mM Tris–HCl [pH 7.5]; 150 mM NaCl: 1 mM EDTA and 1% Triton X-100 supplemented with a complete protease inhibitor cocktail (Roche, Milan, Italy). After clarification by centrifugation, extracts were incubated for 3 hours at room temperature with anti-FLAG M2 magnetic beads (Sigma-Aldrich). Beads were extensively washed with lysis buffer, resuspended in 20 μl of denaturing loading buffer and assayed by sodium dodecyl sulphate (SDS)-polyacrylamide gel electrophoresis (PAGE) and western blotting in order to identify the precipitated proteins.

Western blot analyses

Lysates from Luciferase reporter gene assay were analysed by immunoblotting for RIG-I and NSs protein expression. Protein concentration was determined by BCA assay (Pierce, Milan, Italy). Fifty μg of total proteins were separated by SDS-PAGE and transferred to NitroBind nitrocellulose membranes (Santa Cruz Biotechnology, Heidelberg, Germany). After blocking with 5% non-fat dry milk, the filters were incubated O/N at room temperature with anti-Flag M2 (1:2000) or anti-NSs (1:200) antibodies. After being washed three times with PBS-T, membranes were incubated with horseradish peroxidise (HRP)-conjugated secondary antibody (Santa Cruz Biotecnology). After extensive washes, the immune-complexes were developed with ECL western blotting substrate (Pierce). Quantitative comparison among samples was performed by densitometric analysis using the ImageJ software (http://imagej.nih.gov/ij). Results were expressed as a fold-change value of test samples compared to the reference samples, upon normalization with relative actin values.

Relative quantification of NSs mRNA by real-time PCR

Total RNA was extracted from Lenti-X 293T cells transfected with different NSs recombinant plasmids using the RNeasy Mini Kit (Qiagen) and treated with DNaseI (Promega). A real time PCR assay was performed for quantitation of NSs mRNA using 100 ng of RNA of each sample and the AgPath-ID One-Step RT-PCR kit (Applied Biosystems, Monza, Italy), in ABI Prism 7000 Sequence Detection System (Applied Biosystems). The reaction consisted of reverse transcription at 50 °C for 30 min, an initial denaturation step at 95 °C for 10 min followed by 45 PCR cycles (95 °C for 20 sec; 60 °C 30 sec). Primers and labeled probe for Toscana Virus NSs, strain 1812 (GenBank Accession no. EU327772.1) were: NSs forward 5′-TGATCTCCCAGGAAATGACA-3′ (nt: 558–577); NSs reverse 5′-CATCAGATGGGTGTCTCTGG-3′ (nt: 631-650); NSs probe 5′-FAM-CACCCGTGCTGCTTGGACC-TAMRA-3′ (nt: 597–615). A human β-actin Probe dye VIC-MGB (Applied Biosystems) was used for housekeeping gene quantification. To quantify the products, a normalization algorithm was used. Each sampling point was run in triplicate and the relative quantifications of IFN-β and RIG-I were determined. The Ct values of positive amplicons were analysed using the ΔΔCt method (Livak and Schmittgen, 2001) to get the relative fold increase of the deleted or mutated NSs genes calibrated to the housekeeping gene and normalized with the wt-NSs expressing cells control.

Statistics

The mean differences were statistically analyzed using Stat View statistical software (Abacus Concepts, Berkeley, CA). p Values were calculated by Mann Whitney test. A probability (p) value of less than 0.05 was considered statistically significant.

References

Babu, M.M., van der Lee, R., de Groot, N.S., Gsponer, J., 2011. Intrinsically disordered proteins: regulation and disease. Curr. Opin. Struct. Biol. 21, 432–440.

Bahri, O., Fazaa, O., Ben Alaya-Bouafif, N., Bouloy, M., Triki, H., Bouattour, A., 2010. Role of Toscana virus in meningo-encephalitis in Tunisia. Pathol. Biol. 59, 125–127.

Bartels, S., Heckmann, J.G., 2012. Lethal encephalitis caused by Toscana virus in an elderly patient. J. Neurol. 259, 175–177.

Billecocq, A., Spiegel, M., Vialat, P., Kohl, A., Weber, F., Bouloy, M., Haller, O., 2004. NSs protein of Rift Valley fever virus blocks interferon production by inhibiting host gene transcription. J. Virol. 78, 9798–9806.

Bishop, D.H., 1986. Ambisense RNA viruses: positive and negative polarities combined in RNA virus genomes. Microbiol. Sci. 3, 183–187.

Blakqori, G., Delhaye, S., Habjan, M., Blair, C.D., Sánchez-Vargas, I., Olson, K.E., Attarzadeh-Yazdi, G., Fragkoudis, R., Kohl, A., et al., 2007. La Crosse bunyavirus nonstructural protein NSs serves to suppress the type I interferon system of mammalian hosts. J. Virol. 81, 4991–4999.

Braito, A., Corbisiero, R., Corradini, S., Marchi, B., Sancasciani, N., Fiorentini, C., Ciufolini, M.G., 1997. Evidence of Toscana virus infections without central nervous system involvement: a serological study. Eur. J. Epidemiol. 13, 761–764.

Bridgen, A.M., Weber, F., Fazakerley, J.K., Elliott, R.M., 2001. Bunyamvera bunyavirus non-structural protein NSs is nonessential gene product that contributes to the viral pathogenesis. Proc. Natl. Acad. Sci. USA 98, 664–669.

Calisher, C.H., Weinberg, A.N., Muth, D.J., Lazuick, I.S., 1987. Toscana virus infection in United States citizen returning from Italy. Lancet 1, 165–166.

Charrel, R.N., Gallian, P., Navarro-Mari, J.M., Nicoletti, L., Papa, A., Sánchez-Seco, M. P., Tenorio, A., de Lamballerie, X., 2005. Emergence of Toscana virus in Europe. Emerg. Infect. Dis. 11, 1657–1663.

Dobler, G., Treib, J., Haass, A., Frösner, G., Woesner, R., Schimrigk, K., 1997. Toscana virus infection in German travellers returning from the mediterranean. Infection 25, 325.

Echevarria, J.M., de Ory, F., Guisasola, M.E., Sanchez-Seco, M.P., Tenorio, A., Lozano, A., Cordoba, J., Gobernado, M., 2003. Acute meningitis due to Toscana virus infection among patients from both the Spanish Mediterranean region and the region of Madrid. J. Clin. Virol. 26, 79–84.

Ehrnst, A., Peters, C.J., Niklasson, B., Svedmyr, A., Holmgren, B., 1985. Neurovirulent Toscana virus (a sandfly fever virus) in Swedish man after visit to Portugal. Lancet 1, 1212–1213.

Eitrem, R., Niklasson, B., Weiland, O., 1991. Sandfly fever among Swedish tourists. Scand. J. Infect. Dis. 23, 451–457.

Endris, R.G., Perkins, P.V., 1987. Transmission of Toscana virus by sandflies in Italy. Lancet 1, 808–809.

Epelboin, L., Hausfater, P., Schuffenecker, I., Riou, B., Zeller, H., Bricaire, F., Bossi, P., 2008. Meningoencephalitis due to Toscana virus in a French traveler returning from central Italy. J. Travel. Med. 15, 361–363.

Giorgi, C., Accardi, L., Nicoletti, L., Gro, M.C., Takehara, K., Hilditch, C., Morikawa, S., Bishop, D.H., 1991. Sequences and coding strategies of the S RNAs of Toscana and Rift Valley fever viruses compared to those of Punta Toro, Sicilian Sandfly fever, and Uukuniemi viruses. Virology 180, 738–753.

Gori Savellini, G., Di Genova, G., Terrosi, C., Di Bonito, P., Giorgi, C., Valentini, M., Docquier, J.D., Cusi, M.G., 2008. Immunization with Toscana virus N-Gc proteins protects mice against virus challenge. Virology 375, 521–528.

Gori Savellini, G., Valentini, M., Cusi, M.G., 2013. Toscana virus NSs protein inhibits the induction of type I interferon by interacting with RIG-I. J. Virol. 87, 6660–6667.

Gori Savellini, G., Weber, F., Terrosi, C., Habjan, M., Martorelli, B., Cusi, M.G., 2011. Toscana virus induces interferon although its NSs protein reveals antagonistic activity. J. Gen. Virol. 92, 71–79.

Habjan, M., Pichlmair, A., Elliott, R.M., Overby, A.K., Glatter, T., Gstaiger, M., Superti-Furga, G., Unger, H., Weber, F., 2009. NSs protein of Rift Valley Fever Virus induces the specific degradation of the double-stranded RNA-dependent protein kinase. J. Virol. 83, 4365–4375.

Haller, O., Kochs, G., Weber, F., 2006. The interferon response circuit: induction and suppression by pathogenic viruses. Virology 344, 119–130.

Head, J.A., Kalveram, B., Ikegami, T., 2012. Functional analysis of Rift Valley fever virus NSs encoding a partial truncation. PLoS One 7, e45730.

Hukić, M., Salimović-Besić, I., 2009. Sandfly-Pappataci fever in Bosnia and Herzegovina: the new-old disease. Bosn. J. Basic Med. Sci. 9, 39–43.

Ikegami, T., Narayanan, K., Won, S., Kamitani, W., Peters, C.J., Makino, S., 2009. Rift Valley fever virus NSs protein promotes post-transcriptional downregulation of protein kinase PKR and inhibits eIF2alpha phosphorylation. PLoS Pathog. 5, e1000287.

Indran, S.V., Lihoradova, O.A., Phoenix, I., Lokugamage, N., Kalveram, B., Head, J.A., Tigabu, B., Smith, J.K., Zhang, L., Juelich, T.L., et al., 2013. Rift Valley fever virus

MP-12 vaccine encoding Toscana virus NSs retains neuroinvasiveness in mice. J. Gen. Virol. 94, 1441–1450.
Jääskeläinen, K.M., Kaukinen, P., Minskaya, E.S., Plyusnina, A., Vapalahti, O., Elliott, R.M., Weber, F., Vaheri, A., Plyusnin, A., 2007. Tula and Puumala hantavirus NSs ORFs are functional and the products inhibit activation of the interferon-beta promoter. J. Med. Virol. 79, 1527–1536.
Kalveram, B., Lihoradova, O., Ikegami, T., 2011. NSs protein of rift valley fever virus promotes posttranslational downregulation of the TFIIH subunit p62. J. Virol. 88, 6234–6243.
Kuhn, J., Bewermeyer, H., Hartmann-Klosterkoetter, U., Emmerich, P., Schilling, S., Valassina, M., 2005. Toscana virus causing severe meningoencephalitis in an elderly traveler. J. Neurol. Neurosurg. Psychiatry 76, 1605–1606.
Le May, N., Dubaele, S., Proietti De Santis, L., Billecocq, A., Bouloy, M., Egly, J.M., 2004. TFIIH transcription factor, a target for the Rift Valley hemorrhagic fever virus. Cell 20, 541–550.
Le May, N., Mansuroglu, Z., Léger, P., Josse, T., Blot, G., Billecocq, A., Flick, R., Jacob, Y., Bonnefoy, E., et al., 2008. A SAP30 complex inhibits IFN-beta expression in Rift Valley fever virus infected cells. PLoS Pathog. 4, e13.
Léonard, V.H., Kohl, A., Hart, T.J., Elliott, R.M., 2006. Interaction of Bunyamwera Orthobunyavirus NSs protein with mediator protein MED8: a mechanism for inhibiting the interferon response. J. Virol. 80, 9667–9675.
Livak, K.J., Schmittgen, T.D., 2001. Analysis of relative gene expression data using real-time quantitative PCR and the $2-\Delta\Delta$ CT method. Methods 25, 402–408.
Mendenhall, M., Wong, M.H., Skirpstunas, R., Morrey, J.D., Gowen, B.B., 2009. Punta Toro virus (Bunyaviridae, Phlebovirus) infection in mice: strain differences in pathogenesis and host interferon response. Virology 395, 143–151.
Mibayashi, M., Martinez-Sobrido, L., Loo, Y.M., Cardenas, W.B., Gale Jr., M., Garcia-Sastre, A., 2007. Inhibition of retinoic acid-inducible gene I-madiatwed induction of beta interferon by the NS1 protein of influenza A virus. J. Virol. 81, 514–524.
Opitz, B., Rejaibi, A., Dauber, B., Eckhard, J., Vinzing, M., Schmeck, B., Hippenstiel, S., Suttorp, N., Wolff, T., 2006. INFbeta induction by influenza A virus is mediated by RIG-I which is regulated by the viral NS1 protein. Cell. Microbiol. 9, 930–938.
Papa, A., Andriotis, V., Tzilianos, M., 2010. Prevalence of Toscana virus antibodies in residents of two Ionian islands, Greece. Travel Med. Infect. Dis. 8, 302–304.
Sato, M., Suemori, H., Hata, N., Asagiri, M., Ogasawera, K., Nakao, K., Nakaya, T., Katsuki, M., Noguchi, S., Tanaka, N., et al., 2000. Distinct and essential roles of transcription factors IRF-3 and IRF-7 in response to viruses for IFN-alpha/beta gene induction. Immunity 13, 539–548.
Sonderegger, B., Hachler, H., Dobler, G., Frei, M., 2009. Imported aseptic meningitis due to Toscana virus acquired on the island of Elba, Italy. Euro Surveill. 14, 19079.
Thomas, D., Blakqori, G., Wagner, V., Banholzer, M., Kessler, N., Elliott, R.M., Haller, O., Weber, F., 2004. Inhibition of RNA polymerase II phosphorylation by a viral interferon antagonist. J. Biol. Chem. 23, 31471–31477.
Valassina, M., Cuppone, A.M., Bianchi, S., Santini, L., Cusi, M.G., 1998. Evidence of Toscana virus variants circulating in Tuscany, Italy, during the summers of 1995 to 1997. J. Clin. Microbiol. 36, 2103–2104.
Valassina, M., Meacci, F., Valensin, P.E., Cusi, M.G., 2000. Detection of neurotropic viruses circulating in Tuscany: the incisive role of Toscana virus. J. Med. Virol. 60, 86–90.
Van Knippenberg, I., Calton-Smith, C., Eliott, R.M., 2010. The N-terminus of Bunyamvera orthobunyavirus NSs protein is essential for interferon antagonism. J. Gen. Virol. 91, 2002–2006.
Weber, F., Bridgen, A., Fazakerley, J.K., Streitenfeld, H., Kessler, N., Randall, R.E., Elliott, R.M., 2002. Bunyamwera bunyavirus nonstructural protein NSs counteracts the induction of alpha/beta interferon. J. Virol. 76, 7949–7955.
Weber, F., Dunn, E.F., Bridgen, A., Elliott, R.M., 2001. The Bunyamvera virus nonstructural protein NSs inhibits viral RNA synthesis in a minireplicon system. Virology 281, 67–74.
Yoneyama, M., Suhara, W., Fukuhara, Y., Sato, M., Ozato, K., Fujita, T., 1996. Autocrine amplification of type I interferon gene expression mediated by interferon stimulated gene factor 3 (ISGF3). J. Biochem. 120, 160–169.
Yoneyama, M., Fujita, T., 2008. RNA recognition and signal transduction by RIG-like receptors. Immunity 227, 54–65.

Phase I trial of thymidylate synthase poly-epitope peptide (TSPP) vaccine in advanced cancer patients

Maria Grazia Cusi, Cirino Botta, Pierpaolo Pastina, Maria Grazia Rossetti, Elena Dreassi, Giacomo Maria Guidelli, Antonella Fioravanti, et

Cancer Immunology, Immunotherapy

ISSN 0340-7004

Cancer Immunol Immunother
DOI 10.1007/s00262-015-1711-7

Springer

Cancer Immunol Immunother
DOI 10.1007/s00262-015-1711-7

ORIGINAL ARTICLE

Phase I trial of thymidylate synthase poly-epitope peptide (TSPP) vaccine in advanced cancer patients

Maria Grazia Cusi[1] · Cirino Botta[2] · Pierpaolo Pastina[3] · Maria Grazia Rossetti[4] · Elena Dreassi[5] · Giacomo Maria Guidelli[6] · Antonella Fioravanti[6] · Elodia Claudia Martino[3] · Claudia Gandolfo[1] · Marco Pagliuchi[7] · Assunta Basile[7] · Salvatore Francesco Carbone[8] · Veronica Ricci[8] · Lucia Micheli[9] · Pierfrancesco Tassone[2] · Pierosandro Tagliaferri[2] · Luigi Pirtoli[3] · Pierpaolo Correale[3]

Received: 26 May 2014 / Accepted: 5 May 2015

Abstract Thymidylate synthase (TS) poly-epitope peptide (TSPP) is a 27-mer peptide vaccine containing the amino acidic sequences of three epitopes with HLA-A2.1-binding motifs of TS, an enzyme overexpressed in cancer cells, which plays a crucial role in DNA repair and replication. Based on the results of preclinical studies, we designed a phase Ib trial (TSPP/VAC1) to investigate, in a dose escalation setting, the safety and the biological activity of TSPP vaccination alone (arm A) or in combination with GM-CSF and IL-2 (arm B) in cancer patients. Twenty-one pretreated metastatic cancer patients, with a good performance status (ECOG $\leq$ 1) and no severe organ failure or immunological disease, were enrolled in the study (12 in arm A, nine in arm B) between April 2011 and January 2012, with a median follow-up of 28 months. TSPP resulted safe, and its maximal tolerated dose was not achieved. No grade 4 toxicity was observed. The most common adverse events were grade 2 dermatological reactions to the vaccine injection, cough, rhinitis, fever, poly-arthralgia, gastroenteric symptoms and, to a lesser extent, moderate hypertension and hypothyroidism. We detected a significant rise in auto-antibodies and TS-epitope-specific CTL precursors. Furthermore, TSPP showed antitumor activity in this group of pretreated patients; indeed, we recorded one partial response and seven disease stabilizations (SD) in arm A, and three SD in arm B. Taken together, our findings provide the framework for the evaluation of the TSPP antitumor activity in further disease-oriented clinical trials.

Keywords Cancer vaccine · Phase Ib trial · CTLs · Immune response · Immunotherapy

Abbreviations

5-FU	5-fluorouracil
ANA	Antinuclear antibodies

Maria Grazia Cusi and Cirino Botta have equally contributed to this work.

Electronic supplementary material The online version of this article (doi:10.1007/s00262-015-1711-7) contains supplementary material, which is available to authorized users.

✉ Cirino Botta
cirino.botta@gmail.com

✉ Pierpaolo Correale
correale@unisi.it

[1] Department of Medical Biotechnologies, Siena University, Siena, Italy

[2] Department of Experimental and Clinical Medicine, Catanzaro "Magna Graecia" University and Medical Oncology Unit, Catanzaro, Italy

[3] Unit of Radiotherapy, Department of Medical, Surgical Sciences and Neurosciences, Siena University, Viale Bracci 11, 53100 Siena, Italy

[4] Unit of Pharmacy, Siena University Hospital, Siena, Italy

[5] Department of Biotechnology, Chemistry and Pharmacy, Siena University, Siena, Italy

[6] Unit of Rheumatology, Siena University Hospital, Siena, Italy

[7] Unit of Psychology, Siena University Hospital, Siena, Italy

[8] Unit of Radiology, Siena University Hospital, Siena, Italy

[9] Department of Medical, Surgical Sciences, Neurosciences Siena University, Siena, Italy

Published online: 02 June 2015

ANCA	Anti-neutrophil cytoplasmic antibodies
APC	Antigen-presenting cell
ASMA	Anti-smooth muscle antibodies
CEA	Carcinoembryonic antigen
CRP	C-reactive protein
CTL	Cytotoxic T lymphocyte
DC	Dendritic cell
DMSO	Dimethyl sulfoxide
ECOG	Eastern Cooperative Oncology Group
ELISA	Enzyme-linked immune absorbance assay
ELISPOT	Enzyme-linked immunospot assay
ENA	Extractable nuclear antigen antibodies
ESR	Erythrocyte sedimentation rate
FACS	Fluorescence-activated cell sorting
GCP	Good clinical practice
GM-CSF	Granulocyte–macrophage colony-stimulating factor
GMP	Good manufacturing practice
IVS	In vitro stimulation
LDH	Lactate dehydrogenase
mAb	Monoclonal antibody
MEBD	Most effective biological dose
MPX	Myeloperoxidase
MTD	Maximal tolerated dose
NK	Natural killer
NSCLC	Non-small cell lung cancer
OS	Overall survival
PBMCs	Peripheral blood mononuclear cells
PD	Progressive disease
PFS	Progression-free survival
PHA	Phytohemagglutinin
PR	Partial response
QoL	Quality of life
RECIST	Response evaluation criteria in solid tumors
RSV	Respiratory syncytial virus
SD	Stable disease
TAA	Tumor-associated antigens
T_{cm}	Central memory T cell
T_{em}	Effector memory T cell
T_{reg}	Regulatory T cell
TS	Thymidylate synthase
TSPP	Thymidylate synthase poly-epitope peptide

Introduction

Peptide vaccine-based immunotherapy is emerging as an investigational therapeutic strategy for human cancer [1–5]. It relies on the concept that synthetic tumor-associated antigen (TAA)-derived peptides may be recognized by cytotoxic T lymphocyte (CTL) precursors and used to generate a specific antitumor immune response [5–8]. Different well-known TAAs play critical functions in tumor cell proliferation and survival, and their loss, under selective pressure exerted by antigen-specific CTLs, might impair tumor progression. Thymidylate synthase (TS) is a 36-kDa enzyme commonly overexpressed by cancer cells that play an essential role for thymidylate synthesis, which is crucial for DNA synthesis and repair [9–11]. During the normal cell cycle, the TS expression is restricted at the beginning of S phase, and its synthesis is under control of genes involved in cell cycle progression, often deregulated in cancer cells [9, 10]. Additionally, TS has self-regulatory properties, and intracellular metabolites, cofactors and substrates can modulate its expression. Indeed, tumor cell exposure to anticancer drugs such as pemetrexed or 5′-fluorouracil (5′-FU), which act by inhibiting TS activity, generates a rapid positive feedback which leads to enzyme overexpression [9]. Tumor cells with high intracellular levels of TS become resistant to 5′-FU representing a major cause of 5′-FU treatment failure [9, 10]. TS overexpression in tumor tissues has been investigated and recognized as a marker of poor prognosis in colon and gastric cancer patients [10]. On this basis, we carried out a preclinical characterization of a novel immunogenic 27-mer poly-epitope peptide, designated as TSPP (thymidylate synthase poly-epitope peptide). This peptide was synthesized by assembling amino acidic sequences of three known CTL-specific TS-epitopes (TS-1; TS-2 and TS-3) with HLA-A2.1 anchorage motifs, and it was found to be immunogenic with an efficient antitumor T cell response in vitro [12, 13]. Indeed, preclinical findings revealed that TSPP-sensitized CTLs were able to kill HLA-A2.1$^+$target cells pulsed with the three single TS-epitopes, and HLA-A2.1$^+$human breast and colon carcinoma cells in vitro [12]. Furthermore, CTL toxicity was higher against tumor cells previously exposed to sublethal doses of 5′-FU which enhanced TS expression [12]. TSPP immunological and antitumor activity was also demonstrated in HLA-A(*)02.01/human-CD8α transgenic (HHD) mice [12] inoculated with syngeneic lymphoma EL4/HHD cells, showing antitumor effects in both preventive and therapeutic studies, with additive interaction with 5′FU-based chemotherapy. Pathology studies showed that TSPP vaccination ±5′-FU-based chemotherapy was associated with enhanced CTL ($CD3^+CD8^+$) tumor infiltration, decline in regulatory T cells (T_{reg}s) ($CD4^+CD25^+FoxP3^+$) and disappearance of TS-overexpressing tumor cells, as compared to controls. The latter finding, in particular, suggested that TSPP vaccination could potentially restore tumor cell sensitivity to 5-FU [12, 14]. This phase Ib trial evaluated the safety and biological activity of TSPP administered alone or in combination with an immune-adjuvant regimen (IG-1) containing granulocyte–macrophage colony-stimulating factor (GM-CSF) and interleukin (IL)-2 [15], in advanced cancer patients. The rationale to combine TSPP with IG-1 regimen derived from preclinical in vitro findings [12, 14, 16, 17] and previous clinical studies, where the IG-1 regimen

alone [15] or in combination with 5′FU-based chemotherapy was found to be safe, able to generate activated dendritic cells (DCs) and to promote an efficient antigen-specific T cell response [18, 19].

Patients, materials and methods

TSPP vaccine

TSPP (YMIAHITGLFLDSLGFSTTLGDAHIYL) was synthesized and characterized according to the good manufacturing practice (GMP) procedures by the American Peptide (USA) and aseptically vialed by the Pharmacy of the "*Azienda Ospedaliera Universitaria Senese" (Siena, Italy*), which also performed the stability study, endotoxin evaluation and chemical-related toxicity analysis. TSPP (100, 200 or 300 μg), dissolved in dimethyl sulfoxide (DMSO) (1.5 mg peptide in 2 ml DMSO), was suspended in 250 μl of PBS and then diluted (1:2 ratio) with Montanide ISA 720 VG ST (Seppic, Milan, Italy) in a final injection volume of 500 μl. DMSO was approved for clinical use, and its dosage was within the safety limits [20].

Ethical considerations and study design

This trial was designed according to good clinical practice (GCP) recommendations and authorized by the Italian National Institute of Health (*Istituto Superiore di Sanità*) and by the Italian Ministry of Health, and approved by the University of Siena Ethical Committee (equivalent to Human Subject Committee of Investigational Review Board); the trial has been registered with the TSPP/VAC-1 code, Eudract: #2009-016897-33. TSPP/VAC-1 was a phase IB trial, planned on dose escalation setting and subdivided in two parallel and independent arms (A and B) with unmasked treatment allocation; patients were consequently enrolled in arm A (nine patients in three doses) and then in arm B (nine patients in three doses). Three additional patients, according to the trial protocol, were enrolled in the highest dose level of arm A after the end of arm B enrollment. Patients were grouped into three doses following a standard dose escalation using a Fibonacci series (*n*, 2*n* and 3*n*) [21].

The first cohort of patients received three-weekly subcutaneous (sc) injections of 100 μg of peptide [dose level (DL)1)], the second one, 200 μg (DL2), and the third one, 300 μg (DL3). New patients could be enrolled in higher-dose cohorts only if no grade 3/4 events had been recorded in lower-dose cohorts. Patients in arm A received peptide vaccination alone, while those in arm B received peptide vaccination (day 3/q21) combined with the IG-1 regimen [GM-CSF (Sagramostim/Leukine®, Berlex, USA) (50 μg days 1–5) and IL-2 (Aldesleukine, Proleukin®, Novartis, Switzerland) (0.5 MIU bi-daily, days 6–15)].

The study was designed to investigate the toxicity and biological activity of TSPP. Its primary endpoint was the definition of TSPP maximal tolerated dose (MTD) and most effective biological dose (MEBD). Evaluation of antitumor activity was a secondary endpoint.

Eligibility and outcome measures

The inclusion criteria were as follows: written informed consent, histological diagnosis of malignant disease, at least two previous treatments for advanced disease, clinical and imaging-confirmed progressive disease, ECOG performance status ≤1, no major organ or hematological impairment. The exclusion criteria were as follows: second malignancies, active infectious disease and acquired immunosuppression.

Standard clinical (clinical history, physical examination) and laboratory evaluation [blood cell counts and chemistry and carcinoembryonic antigen (CEA) monitoring] were performed prior to each TSPP injection. Chest X-rays, ultrasound abdominal scans and computerized tomography (CT) scans were carried out at baseline and after 3 months (or at the appearance of clinical signs of progression) to evaluate treatment response (complete response, CR; partial response, PR; disease stabilization, SD; progressive disease, PD) according to the RECIST criteria. Patients remained on treatment until disease progression, occurrence of unacceptable toxicity, clinical judgment or withdrawal of consent. Progression-free survival (PFS) was measured as the time elapsed between enrollment and PD or death, while overall survival (OS) was measured as the time elapsed between enrollment and death. A quality-of-life (QoL) evaluation test, a psychometric analysis designed to measure the patients' compliance to the treatment and to detect subjective reactions to potential side effects, symptoms and changes in social interaction was performed at each immunization.

Serum inflammatory and autoimmune markers

Patient serum was withdrawn prior to each TSPP vaccination and immediately frozen. Serum levels of C-reactive protein (CRP), erythrocyte sedimentation rate (ESR), lactate dehydrogenase (LDH) and rheumatoid factor were included in the routine blood chemistry analysis. Serum myeloperoxidase (MPX) was evaluated by enzyme-linked immune absorbance assay (ELISA) (Calbiochem, Milan, Italy), antinuclear antibodies (ANA) by indirect fluorescence antibody (SSA HEp2000, ImmunoConcepts) through EliA™ Symphony screening (Thermo Fisher Scientific); further EliA tests were performed for single

ANA specificities; anti-neutrophil cytoplasmic antibodies (ANCA) to proteinase-3 (p-ANCA), ANCA to MPX (c-ANCA) and extractable nuclear antigen antibodies (ENA) were tested on Phadia250 instrument; ANCA and anti-smooth muscle antibodies (ASMA) were evaluated by indirect immunofluorescence using INOVA substrate. The presence of TS and TSPP peptide-specific antibodies in the patients' serum was evaluated by ELISA on flat-bottom microtiter plates coated with 100 μl/well of rTS (5 μg/ml) or TSPP peptide (5 μg/ml) diluted in coating buffer (0.05 M NaHCO3/Na2CO3, pH 9.6). Anti-human IgG peroxidase- conjugated antibodies (Sigma, Milan, Italy) were added to each well. Colorimetric conversion of the substrate (tetramethylbenzidine, TMB) was measured at 450 nm in a microplate spectrophotometer. Sera were considered positive if showing an optical density at least twice the background represented by a pool of sera of healthy 1-year-old children. A positive control was represented by an anti-TS mAb (Chemicon, DE).

Blood samples

Peripheral blood was collected from patients at baseline and prior each TSPP vaccination. Peripheral blood mononuclear cells (PBMCs) were isolated by density gradient centrifugation using Ficoll-Hypaque (Celbio S.P.A., Italy), re-suspended in FBS with 10 % DMSO, and immediately stored in nitrogen liquid, as described elsewhere [22, 23]. Viability of the thawed cells, assessed by trypan blue stain before each experiment, was greater than 90 %. Plasma samples were also collected by centrifugation and stored at −80 °C.

Cytokine multiplex analysis

Serum levels of interferon (IFN)-γ, tumor necrosis factor (TNF)-α, IL10, IL4, IL12(p70) and IL17 cytokines were measured at baseline and 20 days after the third vaccination using Bio-Plex human cytokine multiplex kits (Bio-Rad Inc., Hercules, CA). The Beads' fluorescence intensity was measured and analyzed by using the Bio-Plex array reader and the provided manager software with five-parametric-curve fittings.

Fluorescence-activated cell sorting (FACS) analysis

PBMCs were analyzed by FACS analysis (BD FACSCanto II flow cytometer, CA, USA) as described in previous studies [19, 22] after staining with different combinations of conjugated monoclonal antibodies (mAbs) (CD4-V450, CD45RA-PE, CD62L-FITC, CCR7-PE-Cy7, Pharmingen; CD8-PerCPCy 5.5, CD45Ra-APC, CD3-FITC, CD19-FITC, CD16-PE, Rat IgG2a-FITC, Mouse IgG1, Becton–Dickinson, Italy; CD56-APC, Mouse IgG2a-APC Immune-tools, DE; CD25-PE, FoxP3-FITC, eBioscence, UK). T_{reg}s were analyzed after FoxP3 intracellular staining according to the manufacturer guidelines (eBioscience). Statistical analysis was carried out by using the FlowJo® software.

ELISPOT analysis

IFN-γ ELISPOT (Enzyme-Linked ImmunoSPOT) assays were performed according to the provider guidelines (U-Cytech Bioscience CM-Utrech TCH the Netherlands #CT230-PB2, Human IFN-γ ELISPOT KIT) [24] and the results evaluated by an ELISPOT reader (A.EL.VIS Gmbh, Hannover, Germany; ELISPOT analysis software V 5.1, Roxio creator 2009 License #13413). The assay, as described in previous studies [12, 13, 22], evaluates a T cell response in TSPP-sensitized PBMCs withdrawn at baseline and before the fourth and sixth TSPP vaccination. Briefly, TSPP-sensitized PBMCs were co-cultured with autologous DCs (1:5, DC/lymphocyte ratio) loaded with 10 μg/ml of the following antigen peptides: recombinant TS (rTS), TS1, TS2, TS3 and TSPP, and Respiratory Syncytial Virus (RSV) antigen (Meridian, Bioscience, Milan, IT).

To enhance the frequency and the detectability of TSPP-specific T cell precursors in the assays, patients' PBMCs were sensitized to this peptide by two in vitro stimulations (IVS) prior to carrying out the assay. Each IVS consisted of a 5-day PBMCs' co-incubation with TSPP peptide-loaded autologous DCs, followed by 10-day culture in rIL-2 (10 IU/ml)-enriched medium [12, 22].

Dendritic cells used for the ELISPOT assay and IVS were generated as described in previous studies [12, 22]. In each assay, fresh AIM-V medium with 5 % AB human serum (medium) was used as negative background control; Respiratory Syncytial Virus Antigen peptide (RSV) was used as an irrelevant antigen peptide control, while PHA was used as an unspecific positive control.

Results were expressed as the mean number of spot-forming units (spots) per 10^6 cells. According to Moodie et al. [25], we considered a cytokine response as positive if 40 spots/10^6 cells were detected and the mean number of spots/10^6 cells was at least twofold higher than that in the negative control wells [26]. Differences in response between time points were assessed by comparing spot number averages by using a paired Student's *T* test.

Statistical analysis

Statistical analysis was carried out by using GraphPadInstat PRISM 3.2 statistical software. The results were analyzed by performing the Student's *t* test (two-tailed), which was paired when used to evaluate variable modulation during the treatment in the same patients, and unpaired when used to compare intergroup differences.

Results

Patients' characteristics

Twenty-one patients, whose baseline characteristics are summarized in Table 1, were enrolled in the TSPP/VAC1 trial between April 2011 and January 2012, with a median follow-up of 28 (±2.94) months. Twelve patients, six males and six females, with a median age of 57 years (range 46–70), were enrolled in arm A, and nine, five males and four females, with a median age of 65 years (range 56–76) in arm B. Eighteen patients enrolled in the study had previously received multiple treatment lines and presented clinical and imaging-confirmed PD. Three patients had received one previous chemotherapy line only, due to the lack of a standard second-line treatment (MA/A/DL3, gallbladder carcinoma; RV/B/DL1, gastric cancer) or to the refuse of a further chemotherapy regimen (AR/A/DL3, NSCLC). In agreement with ethical committee, we decided to offer to these patients the possibility to be enrolled in this trial.

Patients enrolled in arm A received TSPP vaccination every 3 weeks, while those enrolled in arm B received TSPP vaccination (on day 3) and immune-adjuvant cytokines according to IG-1 regimen [15]. Patients in both arms were subdivided into three cohorts, receiving escalating TSPP doses. A code, composed by name initials, enrollment arm (A or B) and DL (1, 2 or 3), was assigned to each patient. The study was not restricted to patients with a HLA-A2.1 haplotype. This decision was based on the knowledge that TSPP processing by antigen-presenting cells (APCs) produces multiple cryptic epitopes potentially able to bind different class I HLA molecules (as indicated by a HLA-binding prediction algorithm), with the potential of producing an immune response in 90 % of the human individuals ([12] and personal communication). HLA typing was, however, mandatory, and nine out 21 patients (seven in arm A and two in arm B) showed a HLA-A2.1^{+} haplotype.

Adverse events and clinical monitoring

No treatment-related death or life-threatening toxicity occurred during treatment. The most frequent adverse events included grade 1–2 hypersensitivity and skin reactions at the site of vaccine injection, rhinitis, cough, vomiting, diarrhea, fever and diffuse arthralgia (Table 1). Five patients, under treatment with angiotensin-converting enzyme inhibitors showed a grade 1–2 arterial hypertension episode, while other five presented slight hypothyroidism. A bacterial infection, with complete recovery upon antibiotic treatment, was diagnosed in four patients (two in arm a: one in DL2 and one in DL3; and two in arm B: one in DL1 and one in DL2). A patient in arm A (AR/A/DL3) presented an *ab ingestis* pneumonia due to previous lung surgery and refused to continue the vaccination program after he received the second vaccine dose. Finally, a NSCLC patient (OA/A/DL2) with irradiated brain metastases showed progressive cognitive impairment and a reversible episode of narcolepsy (fifth vaccine course). This patient received corticosteroid treatment and was withdrawn from the study.

TSPP vaccination resulted safe; there was no statistical correlation between frequency of adverse events and TSPP dose level; thus, we were unable to identify the MTD. However, it was observed a greater discomfort in arm B patients as evaluated by the quality-of-life (QoL) test [27]. Indeed, average QoL score in arm A, showed a late improvement [average QoL score 60.4 (±14.88) at baseline vs. 62.96 (±21.91), after three treatment courses, vs. 76.2 (±10.60) after six treatment courses (score at Baseline vs. sixth treatment course; $p = 0.045$)], while a score decrease was observed in arm B [average QoL score 60.4 (±27.55) at baseline vs. 59.37 (±26.67), after three treatment courses, vs. 50 (±31.43) after six treatment courses (score at Baseline vs. sixth treatment course; $p = 0.06$)]. This finding could be related to either effects of cytokine administration, or different tumor-type distributions in the two arms, or different responses to vaccine treatment.

Blood cell counts and serologic analysis

An initial increase in neutrophil counts was observed; no change in lymphocyte, basophil, and platelet counts, and a slight and progressive reduction in monocyte and eosinophil counts were recorded in arm A. Progressive increase in neutrophil and eosinophil counts, no change in lymphocyte, basophil and platelet counts and again a decline in monocyte counts were, instead, observed in arm B (Fig. 1). Monitoring of systemic inflammatory markers showed an opposite trend for CRP and ESR in the two arms (Fig. 1); indeed, both were found to decrease in arm A and to increase in arm B. Serum levels of MPX, a protein released during neutrophil and monocyte degranulation, which reflects tissue damage and inflammation [28], showed significant rise in both arms (arm A: values at baseline vs. third and vs. sixth treatment course = 1600 vs. 3000 vs. 2700 U/ml, $p < 0.05$; arm B: values at baseline vs. third and vs. sixth treatment course = 1800 vs. 1700 vs. 6000 U/ml, $p < 0.05$) (Fig. 1). Serum LDH levels finally showed a significant reduction in both arms with no inter-arm difference (data not shown).

The research of specific IgGs commonly associated with autoimmune disease revealed a progressive increase in

Table 1 Patients characteristics, adverse events and response

ID	Age/sex	HLA	Site of primary tumor	Metastatic sites	Previous treatments (number)	Vaccinations (number)	Adverse events (grading)	Clinical response	PFS/OS
Arm A									
MF/A/DL1	48/F	A2	Colorectal cancer	Liver, lung	11	3	Erythema (G1), cough (G1), rhinitis (G2), hypertension (G2)	SD	5/6
RA/A/DL1	59/F	A2	Colorectal cancer	Abdomen, nodes	7	3	Erythema (G1), rhinitis (G2), diarrhea (G2), hypothyroidism (G1)	PD	3/3
AS/A/DL1	56/M	A2	Colorectal cancer	Liver, lung	3	3	Hypertension (G2)	PD	4/4
LV/A/DL2	70/M	A11	Colorectal cancer	Lung, nodes	7	6	Erythema (G2), headache (G2), vomiting (G2), fever (G1)	SD	7/30+
OA/A/DL2	53/M	A1	NSCLC	Brain, bone, liver, lung	3	5	Erythema (G2), cough (G2), rhinitis (G2)	SD	5/9
SG/A/DL2	46/M	A25	Colorectal cancer	Abdomen, nodes	4	6	Erythema (G1), hives (G2), fever (G2)	SD	7/16
ZS/A/DL3	70/F	A2	Colorectal cancer	Nodes, adrenal	3	32	Arthritis (G2), diarrhea (G2)	SD	30 +/30+
MA/A/DL3	54/F	A23	Gallbladder Carcinoma	Peritoneum, nodes	1	28	Erythema (G2), hives (G2), edema (G2), coughing (G2), rhinitis (G2)	PR	24/29+
CM/A/DL3	70/F	A2	Breast cancer	Lung, skin, pleura	3	12	Erythema (G1), hives (G2), arthritis (G2), diarrhea (G2), hypertension (G2)	SD	4/15
AR/A/DL3	66/M	A2	NSCLC	Lung, nodes	1	2	Erythema (G1), Infection (G2), cough (G2), rhinitis (G2) hypothyroidism (G2)	PD	3/7
PN/A/DL3	61/F	A1	Colorectal cancer	Lung, bone	3	3	Erythema (G1), cough (G2), rhinitis (G2) hypothyroidism (G2)	SD	4/8
SN/A/DL3	51/M	A2	Colorectal cancer	Liver, lung	3	3	Fever (G2), infection (G2), hypertension (G2)	PD	3/3
Arm B									
PL/B/DL1	63/F	A1	NSCLC	Lung, nodes	4	5	Hypothyroidism (G2), asthenia (G2), vomiting (G2)	SD	5/6
RV/B/DL1	76/M	A2	Gastric cancer	Liver, peritoneum	1	3	Fever (G2)	PD	2/3

Table 1 continued

ID	Age/sex	HLA	Site of primary tumor	Metastatic sites	Previous treatments (number)	Vaccinations (number)	Adverse events (grading)	Clinical response	PFS/OS
PG/B/DL1	62/M	A26	NSCLC	Brain, lung, nodes	3	3	Coughing (G2), fever (G2)	SD	3/5
GL/B/DL2	42/F	A24	Colorectal cancer	Liver, abdomen	3	3	No	PD	3/4
PP/B/DL2	70/F	A2	Colorectal cancer	Lung, liver, peritoneum	5	3	Fever (G1), vomiting (G2)	PD	3/4
FG/B/DL2	81/M	A24	Colorectal cancer	Peritoneum, nodes	3	3	Erythema (G1), hives (G2), hypothyroidism (G2), diarrhea (G2)	PD	3/5
SF/B/DL3	73/F	A24	NSCLC	Liver, abdomen	3	15	Hypertension (G2), cough (G2), rhinitis (G2), diarrhea (G2), vomiting (G2)	SD	13/16
MM/B/DL3	56/M	A1	Colorectal cancer	Lung, liver, peritoneum	4	3	Headache (G2), cough (G1)	PD	3/7
BA/B/DL3	50/F	A30	NSCLC	Peritoneum, nodes	2	3	Vomiting (G2), depression (G2)	PD	3/9

The enrollment code was composed by patient's initials/arm of enrollment (A or B)/dose level (DL). *NSCLC* non-small cell lung cancer, *SD* stable disease, *PR* partial response, *PD* progression disease

the mean serum level of ENA, c-ANCA and p-ANCA in both arms (Fig. 1). We also detected the presence of ANA (Ab titer: 1/640; normal value titer: 1/160) in five patients of arm A and four patients of arm B, after three treatment courses, and the occurrence of ASMA in a good responder patient of arm A, after six TSPP immunizations (ZS/A/DL3). Only two patients, ZS/A/DL3 and MA/A/DL3 produced IgGs reacting with TSPP after 13 treatment courses.

Taken together, these data suggest that TSPP vaccination is associated with the occurrence of serological signs of autoimmunity with rise in multiple autoantibodies. However, the finding of a progressive and parallel rise in neutrophils, eosinophils, CRP, ESR and MPX in arm B [differences among arm A and arm B patients for these parameters were statistically significant ($p < 0.05$)] suggests that the use of TSPP in combination with immune-adjuvant cytokines compared with TSPP alone ignites a stronger systemic inflammatory response in cancer patients.

Analysis of lymphocyte subpopulations

A FACS analysis of patients' PBMCs did not show any significant treatment-related changes of $CD3^+CD4^+$ and $CD3^+CD8^+$ lymphocytes, $CD3^+CD4^+CD45Ra^-$ (memory) T cells, effector memory ($CD8^+CD45Ra^-CCR7^-$) T cells (T_{em}s) or activated CTLs ($CD3^+CD8^+CD62L^+$Tcells) in either arms (data not shown). Furthermore, we observed a significant increase in central memory ($CD8^+CD45Ra^-CCR7^+$; baseline vs. third course values, $p = 0.048$) T cells (T_{cm}s) and natural killer cells (NK, $CD3^-CD16^+CD56^+$; baseline vs. third course values, $p = 0.05$) in arm A patients (Fig. 2). For what concerns possible changes in immunosuppressive blood cell lineages, we found a significant treatment-related increase in regulatory $CD4^+CD25^+FoxP3^+$T cells (T_{reg}s) ($p = 0.035$) in arm B patients (Fig. 2).

Cytokine analysis

The baseline serum levels of TNF-α, and IFN-γ, IL12(p70), IL17A, IL10 and IL4 in the enrolled patients resulted very heterogeneous. We then evaluated modulations in cytokine levels after three treatment courses. There was no treatment-related change in the serum levels of IL10 and IL4 (Th2 cytokines) in both treatment arms (Fig. 3). On the other hands, patients in arm A showed a slight decline in TNFα, and no change in IFN-γ, IL12 and IL17, while those in arm B, showed a significant increase in IFN-γ, IL12(p70) [Th1 cytokines], and IL17 ($p < 0.05$). Again these results suggest effective engagement of an inflammatory response associated with TSPP and IG cytokine treatment.

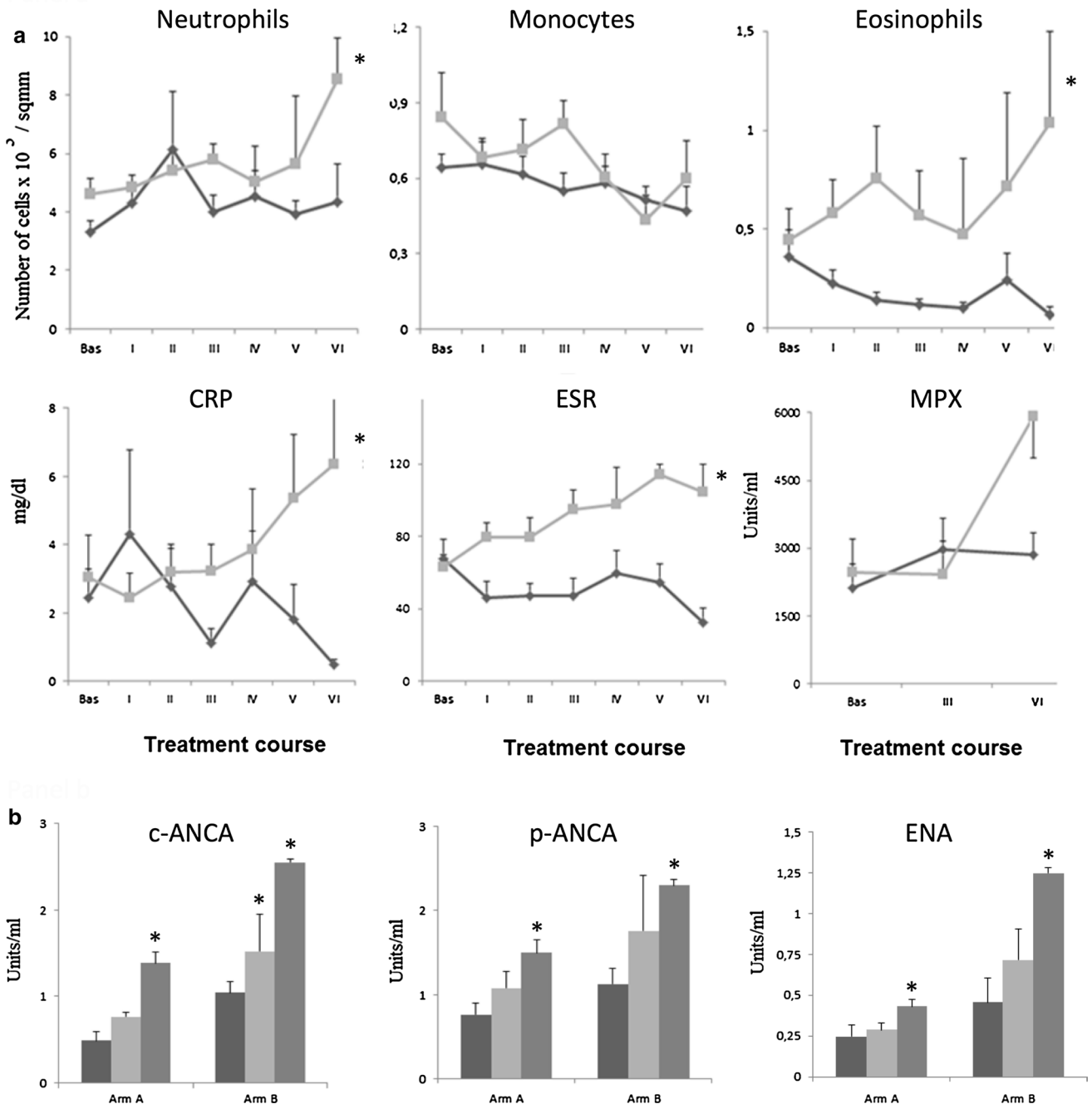

Fig. 1 **a** Peripheral blood cell counts, serum inflammation markers in cancer patients enrolled in the TSPP/VAC1 trial arm A (*diamond*) and arm B (*dark gray square*), at baseline and before each treatment course. *Asterisk* represents statistical significance when arm A and arm B values were compared ($p < 0.05$). *CRP* C-reactive protein, *ESR* erythrocyte sedimentation ratio, *MPX* myeloperoxidase. **b** Serological evaluation of c-ANCA, p-ANCA and ENA immunoglobulins in peripheral blood samples of patients enrolled in arms A and B at baseline (*black square*) and after the third (*light gray square*) and sixth (*dark gray square*) treatment course (±Standard error). *Asterisks* indicate statistical significance of post-treatment versus baseline values ($p < 0.05$)

TS specific CTL precursors

IFN-γ ELISpot analysis performed on patients' TSPP-sensitized PBMCs revealed a treatment-associated T cell response to either rTS or TSPP peptide (Fig. 3) in both arms. When performed in HLA-A2.1$^+$ patients, this analysis showed a treatment-associated CTL response only to the TS-1 and TS-3 epitopes (Fig. 3). The small sample of evaluated patients which just includes four patients in arm A and two patients in arm B could have

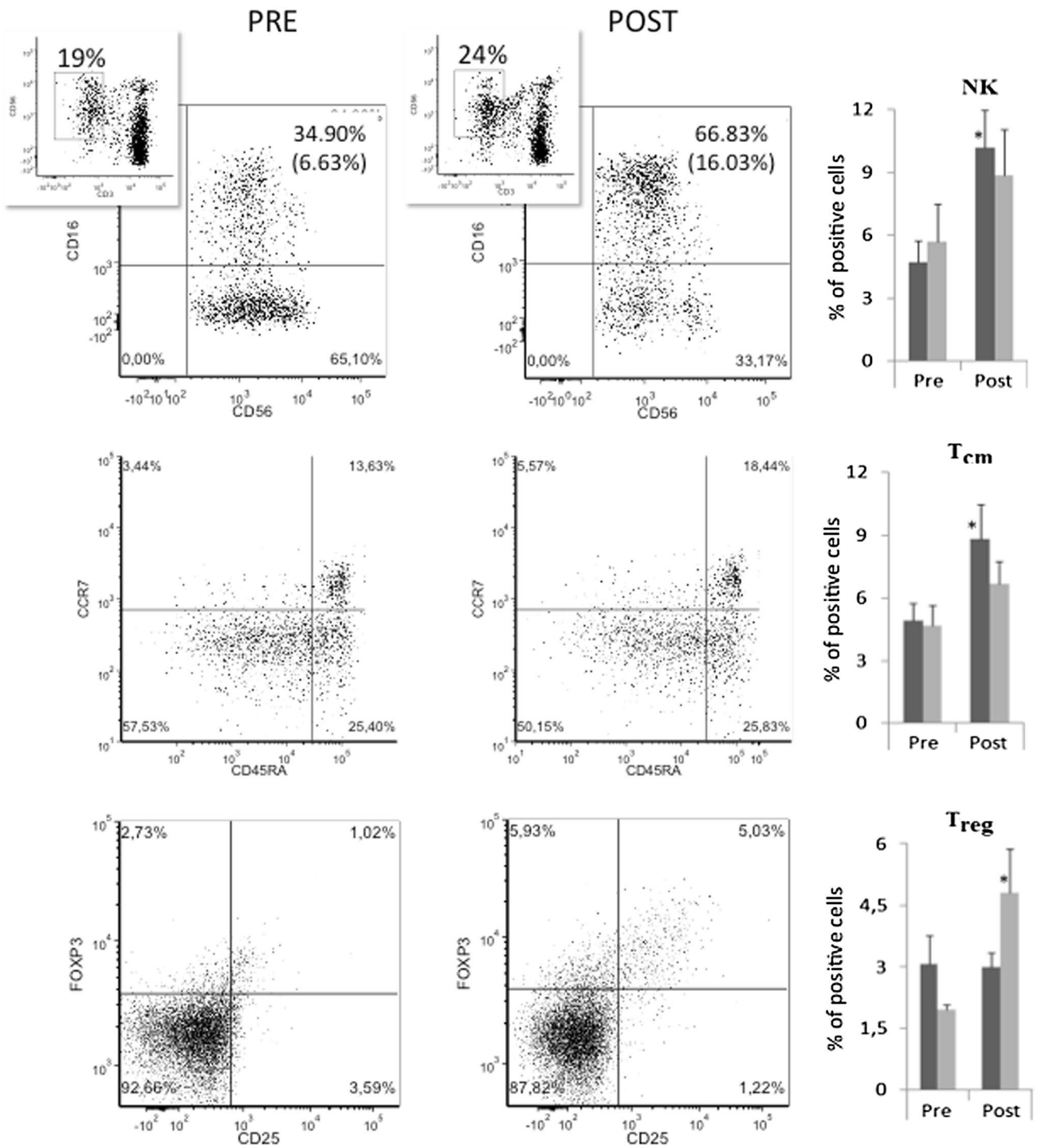

Fig. 2 Baseline (pre) and post-TSPP vaccination (20 days after the third vaccination) (post) flow cytometric analysis of PBMCs from patients enrolled in arm A (*black square*) and B (*gray square*). *NK* natural killer cells ($CD3^{-}CD56^{dim}CD16^{+}$), T_{cm}s central memory T cells ($CD3^{+}CD8^{+}CD45RA^{-}CCR7^{+}$), T_{reg}*s* regulatory T cells ($CD3^{+}CD4^{+}CD25^{+}FoxP3^{+}$). *Asterisks* indicate statistical significance of post-treatment versus baseline values ($p < 0.05$)

affected the sensitivity of this assay. Our test did not record any change when complete AIM-V medium with 5 % human AB serum (background), PHA (positive control) or RSV (negative antigen peptide control) were used to stimulate patients' TSPP-sensitized PBMCs in vitro (Fig. 3).

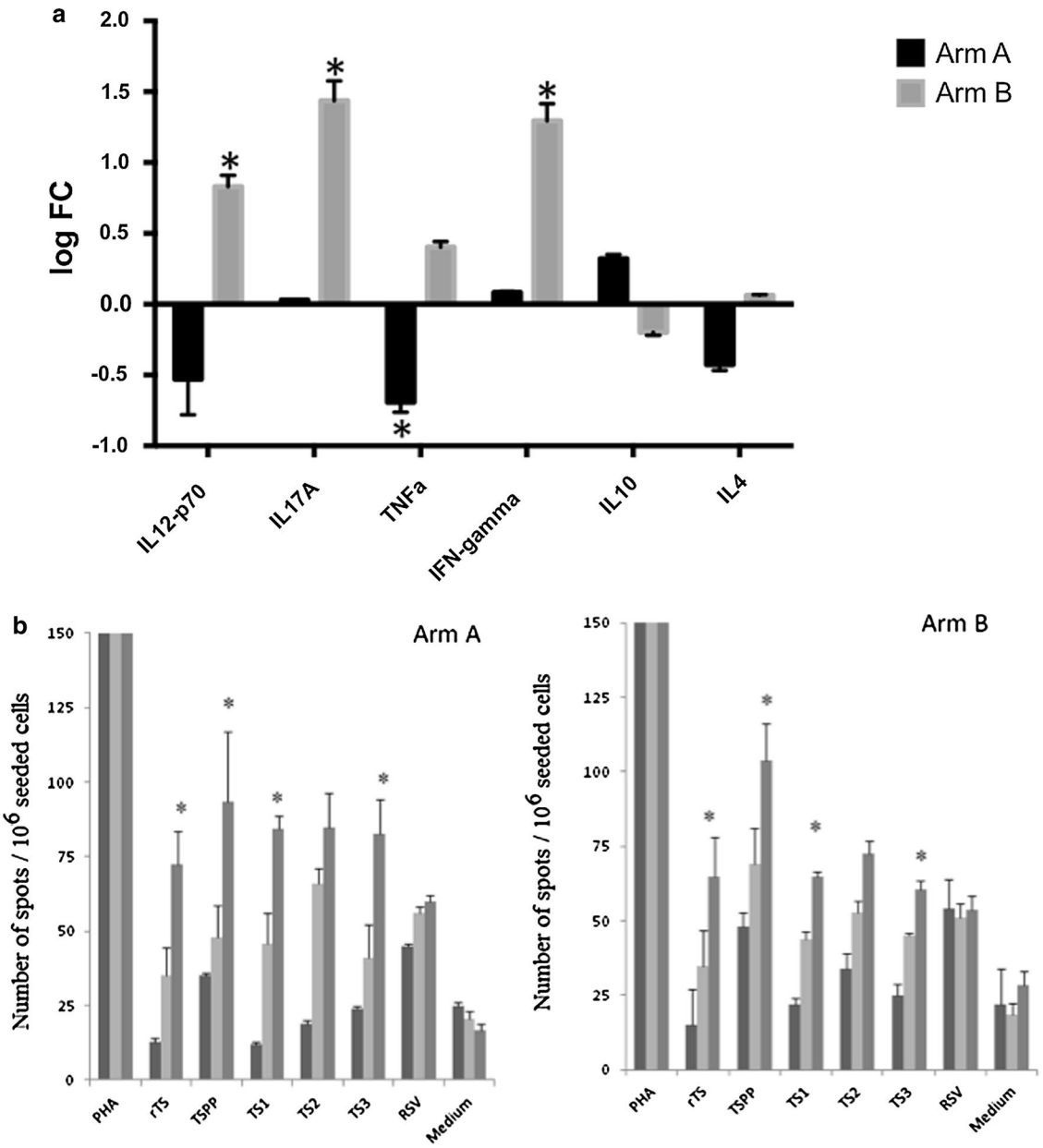

Fig. 3 **a** Represents fold-change (FC) modulation (baseline vs. 20 days after the third vaccination) in serum level of TNFα, IFNγ, IL12, IL17, IL10 and IL4 of the patients enrolled in arms A and B (±Standard error). **b** Shows a gamma-interferon ELISPot assay performed on the PBMCs isolated at baseline (*light gray square*) and after three treatment courses (20 days after the last vaccination) (*dark gray square*), from patients enrolled in arm A and arm B of the trial. PBMCs derived from two different normal donors (*solid lines*) were used as a control group. Results are expressed as average of the number of spots × 10^6 cells per group ± Standard error. PHA, phytohemagglutinin; rTS, recombinant thymidylate synthase; RSV, respiratory syncytial virus antigen peptide; TS1, TS2, TS3, thymidylate synthase epitopes 1, 2 and 3; TSPP, thymidylate synthase polyepitope peptide

Antitumor activity

A PR and a SD were, respectively, recorded in one and seven cases in arm A (on a total of 12 patients), while a SD was recorded in three out nine patients in arm B (Table 1; Fig. 4). Nine patients, three in arm A (AS/A/DL1, SN/A/DL3 and AR/A/DL3) and six in arm B (RV/B/DL1, FG/B/DL1, GL/B/DL2, PP/B/DL2, BA/B/DL3 and MM/B/DL3) discontinued the treatment because of rapid PD or refuse. Mean PFS was 6.4 (95 % CI 3.66–9.2) months in arm A and 3.69 (95 % CI 1.55–5.82) months in arm B, while mean OS was 10.98 (95 % CI 7.56–14.4)

months in arm A and 5.9 (95 % CI 4.11–7.69) months in arm B. Six patients in arm A (50 %) and one patient in arm B (11 %) survived more than 12 months (Table 1); in particular, two patients in arm A had a PFS of more than 20 months.

Correlations between antitumor activity and inflammatory status

We further evaluated correlations between survival and inflammatory parameters in arms A and B. We found that patients in arm A surviving more than 10 months (median of the group) presented a low inflammatory status at baseline, with a significant lower serum CRP level, ESR and neutrophil-to-lymphocyte ratio (NLR) and a significant higher lymphocyte count. Furthermore, lymphocyte count at baseline linearly correlated with patients' survival (Fig. 5). Conversely, in arm B, none of such parameters was found to correlate with patients' survival (Supplementary Fig. 1). These preliminary findings are in line with the current idea that inflammatory status at baseline (or induced by the exogenous administration of pro-inflammatory cytokines) may impair the capability of patient's immune system to mount an effective response against cancer [29].

Discussion

In this phase I study, TSPP vaccine-based immunotherapy demonstrated to be relatively safe and did not affect patients' quality of life as shown by our psychometric monitoring, thus fulfilling the primary endpoint of our trial. There were no G4 adverse events, while the most common (grades 1 and 2) side effects were local reactions to vaccine injections, acute inflammatory disease-related symptoms and/or self-limiting autoimmune reactions. Immune monitoring revealed direct and indirect signs of TSPP-dependent immune activation/autoimmunity (changes in peripheral blood cell lineages, serum inflammatory markers and specific cytokine production) in both arms, a finding in line with the results of other authors, who reported similar effects in different immunotherapy trials [30–34]. Indeed, the occurrence of autoimmunity and/or inflammatory disease following a specific immune-treatment appears to be consequent to active and complex immunological phenomena occurring in the tumor microenvironment [35]. These events can cause tissue damage, acute inflammation, antigen release/cross-presentation, which in turn trigger a process of antigen cascade with the final result of a more efficient multi-antigen-specific response [19, 22, 31, 33, 36]. Furthermore, the occurrence of autoimmunity following

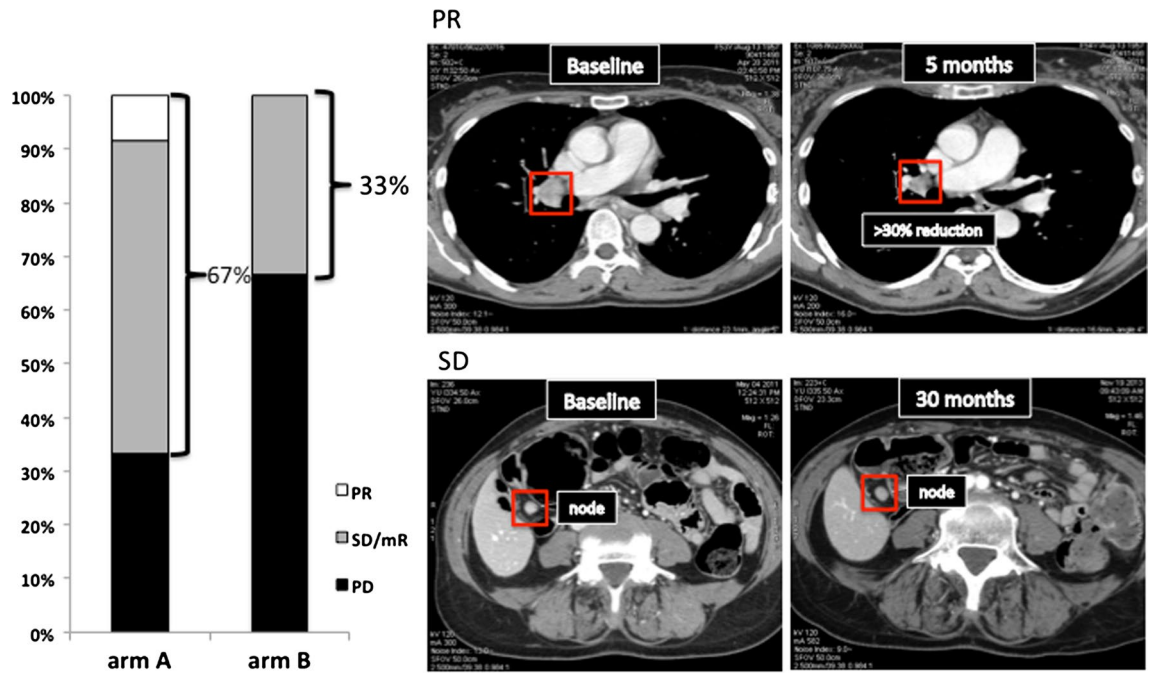

Fig. 4 TSPP vaccination activity in terms of clinical responses. The two representative TC scans included in this picture showed the PR obtained in the patient affected by gallbladder carcinoma (MA/A/DL3) and an impressive 30-month disease stabilization in a patient affected by metastatic colorectal cancer (ZS/A/DL3)

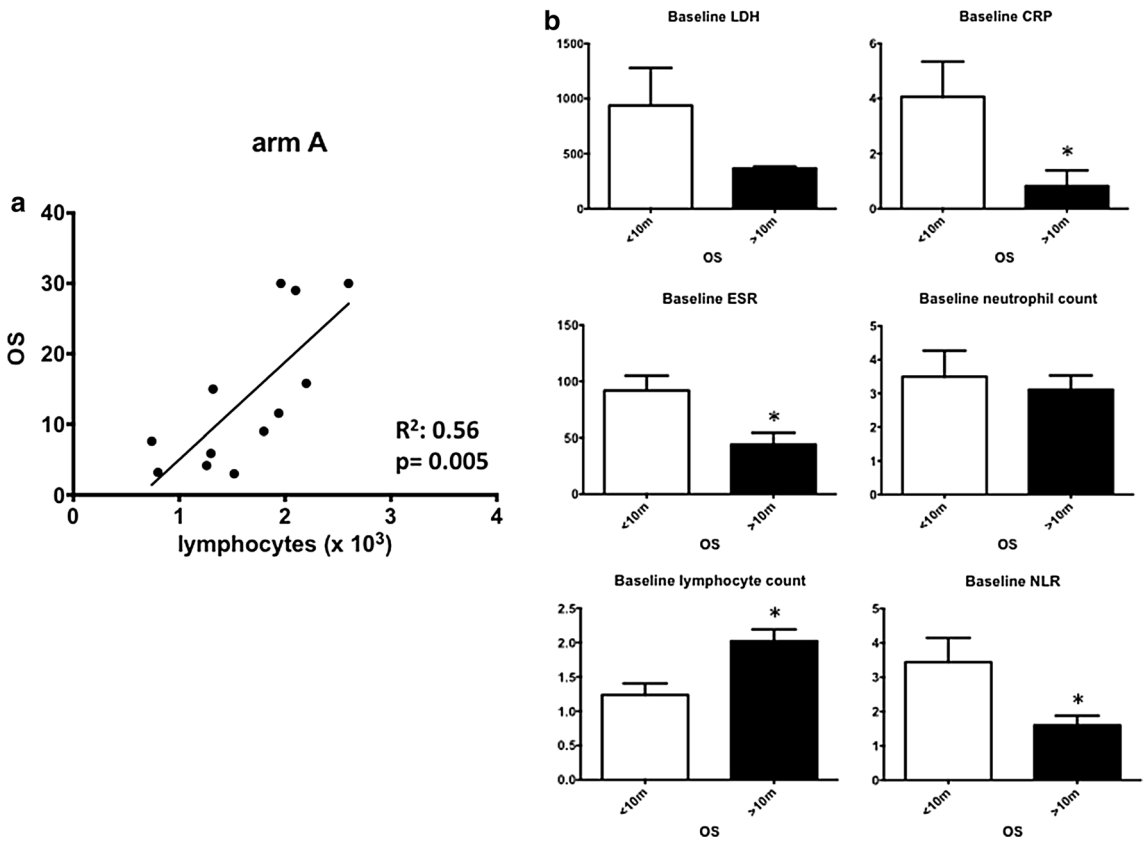

Fig. 5 Correlation analysis performed in arm A to evaluate the association between baseline inflammatory status and survival after vaccination. **a** Shows the linear correlation between baseline lymphocyte count and patients' OS. **b** Evidences the differences between different baseline clinical laboratory parameters associated with inflammation in patients surviving more or less than 10 months (median OS of the group)

patient immunotherapy revealed to be a strong favorable outcome and prolonged survival predictor in different clinical trials [19, 31, 33].

IFN-γ ELISpot assays further confirmed the immunological activity of TSPP vaccination on patients CTL precursors. Indeed, the treatment was associated with a significant ex vivo T cell response to rTS, TSPP and TS1 and TS3 epitopes in patients' PBMCs, with no significant differences between the two treatment arms. However, in spite of immune activation, we found different results, in terms of outcome, between patients enrolled in arm A and B. Specifically, the outcome of patients who received TSPP vaccine alone was found to be greatly influenced by the baseline inflammatory status; indeed, patients with low inflammatory status at baseline experienced the longest survival. Conversely, the administration of pro-inflammatory cytokines appeared to exacerbate patients' systemic inflammation, in spite of their baseline status, with a potential detrimental effect on the therapeutic activity of TSPP vaccination.

Several studies in this field demonstrated that a systemic chronic inflammatory status with high neutrophil counts at baseline is predictive of poor prognosis in patients with different malignant disease [37–39] and in a recent phase III chemo-immunotherapeutic trial on metastatic colorectal cancer patients we observed that patients with low baseline neutrophil counts presented a survival advantage over those with high baseline neutrophil counts [40].

In our opinion, these results underline the dual and conflicting role of GM-CSF in both improving immune response, through eliciting DC maturation [41], and inducing immune suppression, by generating and mobilizing immune-suppressive populations such as myeloid-derived suppressor cells [42]. Such counterbalancing effects may indeed rely on patients' systemic inflammatory status and tumor microenvironment. As a further observation, in arm B, the treatment-associated increase in systemic inflammation markers was coupled with an uncoordinated Th1/Th2/Th17 cytokine response. In this setting, the ability of Th1 cells to promote an efficient CTL response to cancer cells may be mostly counteracted by an enhanced presence of Th17 [43]. This important point, however, is presently under active investigation by our group, and further studies

are needed to elucidate the potential predictive/prognostic role of the chronic inflammatory response on OS in vaccine patients. Furthermore, in this trial, we cannot exclude that part of the above-reported biological events are related to a higher frequency of NSCLC patients in arm B compared to arm A. Further differences in the two arms were also recorded in terms of specific T cell response. Indeed, we found a significant increase in T_{cm}s and NK cells with cytotoxic phenotype in arm A and a significant increase in T_{reg}s in arm B patients. T_{cm} lymphocytes represent a fresh source of CTLs expressing the CCR7 receptor, a surface molecule which allows them to follow the gradient of their ligands, the chemotactic chemokines (CCL) 19 and 21, produced by inflammatory cells in lymph nodes and tumor sites [44] where these cells may differentiate in highly cytotoxic effector cells or acquire long-lasting memory [45]. We have recently shown that their overexpression in the primary tumor is strongly predictive of favorable prognosis in metastatic colorectal cancer patients [46, 47]. The T_{reg}s rise observed in patients on arm B could instead be dependent on the presence of IL-2 in the combined TSPP/IG-1 cytokine treatment arm [48]. Even though antitumor activity was a secondary endpoint of this trial, we recorded a disease control rate (PR + SD) of 66.7 % (*t* 12) in arm A and 33.3 % (three out nine) in arm B, with two patients (two in arm A and one in arm B) who remained free of progression for more than 12 months, and two additional patients (in arm A) who showed a survival longer than 12 months.

Taking account that the majority of these patients presented multiple metastatic sites and that they had received multiple treatment lines prior to receiving TSPP vaccination, we can consider our results encouraging in terms of antitumor activity. Additionally, the finding that patients experiencing the longest survival also presented a low baseline inflammatory status leads us to believe that the pharmacological modulation of systemic inflammatory response could be a promising candidate approach to improve anticancer immunotherapy.

In conclusion, the findings of this clinical study suggest that the TSPP vaccine is safe (its MTD could not be reached in both arms) and is associated with both bio-modulatory and antitumor activity. The immunological analysis showed that TSPP vaccination induces effects with potential anti-tumor activity at the dosage of 2–300 μg (MEBD), while the addition of GM-CSF and IL2 does not provide any clinical or immunological advantages. These results offer the rationale to investigate TSPP anti-tumor activity in disease-oriented phase II trials.

Acknowledgments This study was supported by grants from the Italian Ministry of Scientific and Technological Research [MURST ex 40 %], the Ministry of Health (Bando Ricerca Finalizzata N° RF-2010-231355), and the "Associazione Culturale Federico II di Siena", Italy. We wish to thank the head of the nurse team, Dr. Guido Fruscoloni; our distinguished nurse specialists Marco Bianchi, Erika Bindi, Nicola Cicatelli and Laura Spito, and the medical staff who offered the best care and management to the trial patients. Finally, we wish to thank all the patients and families who participated to the study.

Conflict of interest The authors declare that they have no conflict of interest.

Ethical standards All patients gave their informed consent prior to be enrolled in the study.

References

1. Baxevanis CN, Perez SA, Papamichail M (2009) Cancer immunotherapy. Crit Rev Clin Lab Sci 46(4):167–189. doi:10.1080/10408360902937809
2. Buonaguro L, Petrizzo A, Tornesello ML, Buonaguro FM (2011) Translating tumor antigens into cancer vaccines. Clin Vaccine Immunol 18(1):23–34. doi:10.1128/CVI.00286-10
3. Franks HA, Wang Q, Patel PM (2012) New anticancer immunotherapies. Anticancer Res 32(7):2439–2453
4. Mellstedt H, Vansteenkiste J, Thatcher N (2011) Vaccines for the treatment of non-small cell lung cancer: investigational approaches and clinical experience. Lung Cancer 73(1):11–17. doi:10.1016/j.lungcan.2011.02.023
5. Mocellin S, Pilati P, Nitti D (2009) Peptide-based anticancer vaccines: recent advances and future perspectives. Curr Med Chem 16(36):4779–4796
6. Pardoll DM (1994) Tumour antigens. A new look for the 1990s. Nature 369(6479):357. doi:10.1038/369357a0
7. Boon T, van der Bruggen P (1996) Human tumor antigens recognized by T lymphocytes. J Exp Med 183(3):725–729
8. Nijman HW, Houbiers JG, Vierboom MP, van der Burg SH, Drijfhout JW, DAmaro J, Kenemans P, Melief CJ, Kast WM (1993) Identification of peptide sequences that potentially trigger HLA-A2.1-restricted cytotoxic T lymphocytes. Eur J Immunol 23(6):1215–1219. doi:10.1002/eji.1830230603
9. Ligabue A, Marverti G, Liebl U, Myllykallio H (2012) Transcriptional activation and cell cycle block are the keys for 5-fluorouracil induced up-regulation of human thymidylate synthase expression. Plos One 7(10):e47318. doi:10.1371/journal.pone.0047318
10. Rustum YM (2004) Thymidylate synthase: a critical target in cancer therapy? Front Biosci 9:2467–2473
11. van der Wilt CL, Peters GJ (1994) New targets for pyrimidine antimetabolites in the treatment of solid tumours. 1: thymidylate synthase. Pharm World Sci 16(2):84–103
12. Correale P, Del Vecchio MT, Di Genova G, Savellini GG, La Placa M, Terrosi C, Vestri M, Urso R, Lemonnier F, Aquino A, Bonmassar E, Giorgi G, Francini G, Cusi MG (2005) 5-fluorouracil-based chemotherapy enhances the antitumor activity of a thymidylate synthase-directed polyepitopic peptide vaccine. J Natl Cancer Inst 97(19):1437–1445. doi:10.1093/jnci/dji188
13. Correale P, Sabatino M, Cusi MG, Micheli L, Nencini C, Pozzessere D, Petrioli R, Aquino A, De Vecchis L, Turriziani M, Prete SP, Sanguedolce R, Rausa L, Giorgi G, Francini G (2001) In vitro generation of cytotoxic T lymphocytes against HLA-A2.1-restricted peptides derived from human thymidylate synthase. J Chemother 13(5):519–526. doi:10.1179/joc.2001.13.5.519

14. Correale P, Del Vecchio MT, La Placa M, Montagnani F, Di Genova G, Savellini GG, Terrosi C, Mannucci S, Giorgi G, Francini G, Cusi MG (2008) Chemotherapeutic drugs may be used to enhance the killing efficacy of human tumor antigen peptide-specific CTLs. J Immunother 31(2):132–147. doi:10.1097/CJI.0b013e31815b69c8
15. Correale P, Campoccia G, Tsang KY, Micheli L, Cusi MG, Sabatino M, Bruni G, Sestini S, Petrioli R, Pozzessere D, Marsili S, Fanetti G, Giorgi G, Francini G (2001) Recruitment of dendritic cells and enhanced antigen-specific immune reactivity in cancer patients treated with hr-GM-CSF (Molgramostim) and hr-IL-2. Results from a phase Ib clinical trial. Eur J Cancer 37(7):892–902
16. Correale P, Cusi MG, Del Vecchio MT, Aquino A, Prete SP, Tsang KY, Micheli L, Nencini C, La Placa M, Montagnani F, Terrosi C, Caraglia M, Formica V, Giorgi G, Bonmassar E, Francini G (2005) Dendritic cell-mediated cross-presentation of antigens derived from colon carcinoma cells exposed to a highly cytotoxic multidrug regimen with gemcitabine, oxaliplatin, 5-fluorouracil, and leucovorin, elicits a powerful human antigen-specific CTL response with antitumor activity in vitro. J Immunol 175(2):820–828
17. Francini G, Scardino A, Kosmatopoulos K, Lemonnier FA, Campoccia G, Sabatino M, Pozzessere D, Petrioli R, Lozzi L, Neri P, Fanetti G, Cusi MG, Correale P (2002) High-affinity HLA-A(*)02.01 peptides from parathyroid hormone-related protein generate in vitro and in vivo antitumor CTL response without autoimmune side effects. J Immunol 169(9):4840–4849
18. Correale P, Cusi MG, Tsang KY, Del Vecchio MT, Marsili S, Placa ML, Intrivici C, Aquino A, Micheli L, Nencini C, Ferrari F, Giorgi G, Bonmassar E, Francini G (2005) Chemo-immunotherapy of metastatic colorectal carcinoma with gemcitabine plus FOLFOX 4 followed by subcutaneous granulocyte macrophage colony-stimulating factor and interleukin-2 induces strong immunologic and antitumor activity in metastatic colon cancer patients. J Clin Oncol 23(35):8950–8958. doi:10.1200/JCO.2005.12.147
19. Correale P, Tagliaferri P, Fioravanti A, Del Vecchio MT, Remondo C, Montagnani F, Rotundo MS, Ginanneschi C, Martellucci I, Francini E, Cusi MG, Tassone P, Francini G (2008) Immunity feedback and clinical outcome in colon cancer patients undergoing chemoimmunotherapy with gemcitabine + FOLFOX followed by subcutaneous granulocyte macrophage colony-stimulating factor and aldesleukin (GOLFIG-1 Trial). Clin Cancer Res 14(13):4192–4199. doi:10.1158/1078-0432.CCR-07-5278
20. Santos NC, Figueira-Coelho J, Martins-Silva J, Saldanha C (2003) Multidisciplinary utilization of dimethyl sulfoxide: pharmacological, cellular, and molecular aspects. Biochem Pharmacol 65(7):1035–1041
21. Omura GA (2003) Modified fibonacci search. J Clin Oncol 21(16):3177. doi:10.1200/JCO.2003.99.058
22. Botta C, Bestoso E, Apollinari S, Cusi MG, Pastina P, Abbruzzese A, Sperlongano P, Misso G, Caraglia M, Tassone P, Tagliaferri P, Correale P (2012) Immune-modulating effects of the newest cetuximab-based chemoimmunotherapy regimen in advanced colorectal cancer patients. J Immunother 35(5):440–447. doi:10.1097/CJI.0b013e31825943aa
23. Boyum A (1968) A one-stage procedure for isolation of granulocytes and lymphocytes from human blood. General sedimentation properties of white blood cells in a 1g gravity field. Scand J Clin Lab Investig Suppl 97:51–76
24. Czerkinsky CC, Nilsson LA, Nygren H, Ouchterlony O, Tarkowski A (1983) A solid-phase enzyme-linked immunospot (ELISPOT) assay for enumeration of specific antibody-secreting cells. J Immunol Methods 65(1–2):109–121
25. Moodie Z, Price L, Gouttefangeas C, Mander A, Janetzki S, Lower M, Welters MJ, Ottensmeier C, van der Burg SH, Britten CM (2010) Response definition criteria for ELISPOT assays revisited. Cancer Immunol Immun 59(10):1489–1501. doi:10.1007/s00262-010-0875-4
26. Morse MA, Chaudhry A, Gabitzsch ES, Hobeika AC, Osada T, Clay TM, Amalfitano A, Burnett BK, Devi GR, Hsu DS, Xu Y, Balcaitis S, Dua R, Nguyen S, Balint JP Jr, Jones FR, Lyerly HK (2013) Novel adenoviral vector induces T-cell responses despite anti-adenoviral neutralizing antibodies in colorectal cancer patients. Cancer Immunol Immun 62(8):1293–1301. doi:10.1007/s00262-013-1400-3
27. Groenvold M, Klee MC, Sprangers MA, Aaronson NK (1997) Validation of the EORTC QLQ-C30 quality of life questionnaire through combined qualitative and quantitative assessment of patient-observer agreement. J Clin Epidemiol 50(4):441–450
28. Mika D, Guruvayoorappan C (2011) Myeloperoxidase: the yin and yang in tumour progression. J Exp Ther Oncol 9(2):93–100
29. Grivennikov SI, Greten FR, Karin M (2010) Immunity, inflammation, and cancer. Cell 140(6):883–899. doi:10.1016/j.cell.2010.01.025
30. Amos SM, Duong CP, Westwood JA, Ritchie DS, Junghans RP, Darcy PK, Kershaw MH (2011) Autoimmunity associated with immunotherapy of cancer. Blood 118(3):499–509. doi:10.1182/blood-2011-01-325266
31. Calderwood SK, Stevenson MA, Murshid A (2012) Heat shock proteins, autoimmunity, and cancer treatment. Autoimmune Dis 2012:486069. doi:10.1155/2012/486069
32. Finn OJ (2012) Immuno-oncology: understanding the function and dysfunction of the immune system in cancer. Ann Oncol 23(Suppl 8):viii6–viii9. doi:10.1093/annonc/mds256
33. Jensen-Jarolim E, Singer J (2011) Cancer vaccines inducing antibody production: more pros than cons. Expert Rev Vaccines 10(9):1281–1289. doi:10.1586/erv.11.105
34. Mantovani A, Allavena P, Sica A, Balkwill F (2008) Cancer-related inflammation. Nature 454(7203):436–444. doi:10.1038/nature07205
35. Predina J, Eruslanov E, Judy B, Kapoor V, Cheng G, Wang LC, Sun J, Moon EK, Fridlender ZG, Albelda S, Singhal S (2013) Changes in the local tumor microenvironment in recurrent cancers may explain the failure of vaccines after surgery. Proc Natl Acad Sci USA 110(5):E415–E424. doi:10.1073/pnas.1211850110
36. Gandhi AK, Shi T, Li M, Jungnelius U, Romano A, Tabernero J, Siena S, Schafer PH, Chopra R (2013) Immunomodulatory effects in a phase II study of lenalidomide combined with cetuximab in refractory KRAS-mutant metastatic colorectal cancer patients. Plos One 8(11):e80437. doi:10.1371/journal.pone.0080437
37. Botta C, Barbieri V, Ciliberto D, Rossi A, Rocco D, Addeo R, Staropoli N, Pastina P, Marvaso G, Martellucci I, Guglielmo A, Pirtoli L, Sperlongano P, Gridelli C, Caraglia M, Tassone P, Tagliaferri P, Correale P (2013) Systemic inflammatory status at baseline predicts bevacizumab benefit in advanced non-small cell lung cancer patients. Cancer Biol Ther 14(6):469–475. doi:10.4161/cbt.24425
38. Jafri SH, Shi R, Mills G (2013) Advance lung cancer inflammation index (ALI) at diagnosis is a prognostic marker in patients with metastatic non-small cell lung cancer (NSCLC): a retrospective review. BMC Cancer 13:158. doi:10.1186/1471-2407-13-158
39. Templeton AJ, McNamara MG, Seruga B, Vera-Badillo FE, Aneja P, Ocana A, Leibowitz-Amit R, Sonpavde G, Knox JJ, Tran B, Tannock IF, Amir E (2014) Prognostic role of neutrophil-to-lymphocyte ratio in solid tumors: a systematic review and

meta-analysis. J Natl Cancer Inst 106(6):dju124. doi:10.1093/jnci/dju124
40. Correale P, Botta C, Rotundo MS, Guglielmo A, Conca R, Licchetta A, Pastina P, Bestoso E, Ciliberto D, Cusi MG, Fioravanti A, Guidelli GM, Bianco MT, Misso G, Martino E, Caraglia M, Tassone P, Mini E, Mantovani G, Ridolfi R, Pirtoli L, Tagliaferri P (2014) Gemcitabine, oxaliplatin, levofolinate, 5-fluorouracil, granulocyte-macrophage colony-stimulating factor, and interleukin-2 (GOLFIG) versus FOLFOX chemotherapy in metastatic colorectal cancer patients: the GOLFIG-2 multicentric open-label randomized phase III trial. J Immunother 37(1):26–35. doi:10.1097/CJI.0000000000000004
41. Zhan Y, Xu Y, Lew AM (2012) The regulation of the development and function of dendritic cell subsets by GM-CSF: more than a hematopoietic growth factor. Mol Immunol 52(1):30–37. doi:10.1016/j.molimm.2012.04.009
42. Botta C, Gulla A, Correale P, Tagliaferri P, Tassone P (2014) Myeloid-derived suppressor cells in multiple myeloma: pre-clinical research and translational opportunities. Front Oncol 4:348. doi:10.3389/fonc.2014.00348
43. Sallusto F, Lanzavecchia A (2009) Heterogeneity of CD4+ memory T cells: functional modules for tailored immunity. Eur J Immunol 39(8):2076–2082. doi:10.1002/eji.200939722
44. Forster R, Schubel A, Breitfeld D, Kremmer E, Renner-Muller I, Wolf E, Lipp M (1999) CCR7 coordinates the primary immune response by establishing functional microenvironments in secondary lymphoid organs. Cell 99(1):23–33
45. Sallusto F, Geginat J, Lanzavecchia A (2004) Central memory and effector memory T cell subsets: function, generation, and maintenance. Annu Rev Immunol 22:745–763. doi:10.1146/annurev.immunol.22.012703.104702
46. Correale P, Rotundo MS, Botta C, Del Vecchio MT, Ginanneschi C, Licchetta A, Conca R, Apollinari S, De Luca F, Tassone P, Tagliaferri P (2012) Tumor infiltration by T lymphocytes expressing chemokine receptor 7 (CCR7) is predictive of favorable outcome in patients with advanced colorectal carcinoma. Clin Cancer Res 18(3):850–857. doi:10.1158/1078-0432.CCR-10-3186
47. Correale P, Rotundo MS, Botta C, Del Vecchio MT, Tassone P, Tagliaferri P (2012) Tumor infiltration by chemokine receptor 7 (CCR7)(+) T-lymphocytes is a favorable prognostic factor in metastatic colorectal cancer. Oncoimmunology 1(4):531–532
48. Sakaguchi S, Yamaguchi T, Nomura T, Ono M (2008) Regulatory T cells and immune tolerance. Cell 133(5):775–787. doi:10.1016/j.cell.2008.05.009

VECTOR-BORNE AND ZOONOTIC DISEASES
Volume 13, Number 5, 2013

DOI: 10.1089/vbz.2011.0945

Seroprevalence of Antibodies to Sandfly Fever Sicilian Virus in a Sample Population in Tuscany, Italy

Maria Grazia Cusi, Claudia Gandolfo, Melissa Valentini, and Gianni Gori Savellini

Abstract

Toscana virus is the main phlebovirus circulating in Tuscany during the warm season, thus, a seroprevalence study was performed in the same area to estimate the antibody prevalence rates for sandfly fever Sicilian virus (SFSV) that is endemic in the Mediterranean countries. The low seroprevalence observed in this study shows that this virus does not play an important role in the etiology of febrile illness in central Italy.

Key Words: Toscana virus—Tuscany—Sandfly fever Sicilian virus—Phleboviruses.

Introduction

Sandfly fever viruses cause human illness and are transmitted by sandfly vectors (*Phlebotomus* spp.). Phleboviruses, in particular, the Sandfly Naples (SFNV), Sandfly Sicilian (SFSV), and Toscana (TOSV) viruses circulate in the Mediterranean basin (Izri et al. 2008, Calamusa et al. 2012, Ergünay et al. 2011, Guler et al. 2012). In endemic areas, these infections occur during the warm season, in parallel with the highest activity of sandfly vectors. TOSV has been considered the etiologic agent of acute meningitis, meningoencephalitis, or encephalitis. Naples and Sicilian serotype viruses are the etiologic agents of a usually mild, self-limited disease characterized by fever, myalgia, headache, and muscle and joint pain, and patients generally recover within a week. SFSV, which is specially transmitted by *Phlebotomus papatasi* (Karabatos 1985) was discovered in Italy (Palermo, Sicily) where it affected Allied Army troops in World War II after landings in Sicily in 1943. In Italy, *P. papatasi* is scarce, but it was abundant before dichlorodiphenyltrichloroethane (DDT) was used in the 1940s, and it may have been substituted by other vectors belonging to the subgenus *Larroussius* for SFSV transmission.

More recently, 37 cases of SFSV infection were recorded in Swedish tourists returning from Cyprus between 1986 and 1989 (Eitrem et al. 1990), and an outbreak affecting 286 Greek soldiers stationed in Cyprus occurred in 2002 (Konstantinou et al. 2007). This virus and SFSV-like viruses are now circulating in Italy, Egypt, Cyprus, Iran, Israel, Algeria, Tunisia, and Pakistan (Depaquit et al. 2012). A recent seroepidemiological study conducted on a population sample in Sicily showed that 9.2% of the subjects were positive for SFSV immunoglobulin G (IgG), and this percentage was about 2-fold higher in subjects over the age of 64 (15.9%) compared to the youngest (7%) (Calamusa et al. 2012). It seems likely that the oldest subjects were heavily exposed to *P. papatasi*, the main SFSV vector, when they were young, after which the sandfly was markedly suppressed by the extensive use of DDT (Calamusa et al. 2012).

Data for SFSV seroprevalence in northern and central Italy are lacking, thus our aim was to investigate the seroepidemiology of SFSV in Tuscany, where TOSV is widely diffused. All consecutive serum samples ($n = 365$) submitted to the laboratory of "S. Maria delle Scotte" Hospital in Siena during the winter season 2011, collected from people of different ages for pathologies not related to neurological forms, were included in the study. They were divided into 3 groups of subjects by age: (1) Aged 0–20 years ($n = 104$, median age, 12 years); (2) aged 21–60 years ($n = 120$, median age, 41 years); and (3) aged >60 years ($n = 141$, median age, 74 years). The tested population was composed of 195 males and 170 females. All patients in the study lived in Siena or its suburbs. Sera were analyzed for the presence of specific anti-SFSV IgM and IgG antibodies by indirect immunofluorescence assay (EuroImmun, Germany). None of the serum was positive for IgM, but 4 samples (1.09 %) were IgG positive to SFSV (Table 1).

A comparison of these data with that observed in Sicily showed that the virus is not circulating in Tuscany, whereas it is still present in Sicily, where seropositivity to SFSV has been recorded in the analyzed population (Calamusa et al. 2012). We could hypothesize that the virus is not present in central Italy or that its vector is not circulating in the area considered in this study. Currently, phlebotomine sandflies are the main

Department of Biotechnology, Microbiology Section, University of Siena, Italy.

Table 1. Seroprevalence of SFSV Antibodies in People Living in Siena

Subjects	*SFSV positive*	*SFSV negative*
Group 1 (0–20 years)	0	104
Group 2 (21–60 years)	0	120
Group 3 (>60 years)	4	137

vector of Toscana virus, which is widely diffuse in central Italy, and it is possible that *P. papatasi*, the vector of SFSV, is less diffuse among the species of the Phlebotomidae family, due to the past use of insecticides; however, this feature does not justify the low seroprevalence rate, because other sandflies have been recognized as vectors for the SFSV (Cusi et al. 2010, Moureau et al. 2010). The 4 patients that resulted positive for SFSV IgG were over 70 years old; thus, we do not know whether they acquired the infection outside Tuscany or if their seropositivity dates back to their youth when the virus might have been circulating in central Italy.

SFSV-like viruses are diffuse in the Mediterranean basin and some recent reports have described the presence of these new viruses by serological analyses on the human population (Izri et al. 2008, Ergünay et al. 2011, Calamusa et al. 2012, Guler et al. 2012). The results obtained in Tuscany are in line with those observed in the south of France, where SFSV does not appear to be circulating (Bichaud et al. 2011). The seroprevalence to TOSV in central Italy and Tuscany is quite high (20–21%) (Terrosi et al. 2009); thus, it was interesting to analyze the seroprevalence of another sandfly virus transmitted by the same vectors in the same area. This study shows that SFSV is not endemic in Tuscany and, unlike Sicily, seroprevalence is rather low, confirming that this virus does not play an important role in the etiology of febrile illness in central Italy during the warmest months of the year.

Acknowledgments

This study was funded by Fondazione Carlo Denegri Onlus.

Author Disclosure Statement

No competing financial interests exist.

References

Bichaud L, Piarroux RP, Izri A, Ninove L, et al. Low seroprevalence of sandfly fever Sicilian virus antibodies in humans, Marseille, France. Clin Microbiol Infect 2011; 17:1189–1190.

Calamusa G, Valenti RM, Vitale F, Mammina C, et al. Seroprevalence of and risk factors for Toscana and Sicilian virus infection in a sample population of Sicily (Italy). J Infect 2012; 64:212–217.

Cusi MG, Gori Savellini G, Zanelli G. Toscana virus epidemiology: From Italy to beyond. Open Virol J 2010; 22:22–28.

Depaquit J, Grandadam M, Fouque F, Andry PE, et al. Arthropod-borne viruses transmitted by Phlebotomine sanflies in Europe: A review. Euro Surveill 2010; 15:pii=19507.

Eitrem R, Vene S, Niklasson B. Incidence of sandfly fever among Swedish United Nations soldiers on Cyprus during 1985. Am J Trop Med Hyg 1990; 43:207–211.

Ergünay K, Saygan MB, Aydoğan S, Lo MM, et al. Sandfly fever virus activity in central/northern Anatolia, Turkey: first report of Toscana virus infections. Clin Microbiol Infect 2011; 17:575–581.

Guler S, Guler E, Caglayik DY, Kokoglu OF, et al. A sandfly fever virus outbreak in the East Mediterranean region of Turkey. Int J Infect Dis 2012; 16:244–246.

Izri A, Temmam S, Moureau G, Hamrioui B, et al. Sandfly fever Sicilian virus, Algeria. Emerg Infect Dis 2008: 14:795–797.

Karabatos N, eds. *International Catalogue of Arboviruses Including Certain Viruses and Vertebrates*, 3rd ed. San Antonio, TX: Am J Trop Med Hyg, 1985.

Konstantinou GN, Papa A, Antoniadis A. Sandfly-fever outbreak in Cyprus: are phleboviruses still a health problem? Travel Med Infect Dis 2007; 12:192–194.

Moureau G, Bichaud L, Salez N, Ninove L, et al. Molecular and serological evidence for the presence of novel phleboviruses in sandflies from Northern Algeria. Open Virol J 2010; 4:15–21.

Terrosi C, Olivieri R, Bianco C, Cellesi C, et al. Age-dependent seroprevalence of Toscana virus in central Italy and correlation with the clinical profile. Clin Vaccine Immunol 2009; 16:1251–1252.

Address correspondence to:
Maria Grazia Cusi, PhD
Department of Biotechnology
Section of Microbiology
Policlinico S. Maria alle Scotte -V.le Bracci, 1
53100 Siena
Italy

E-mail: mariagrazia.cusi@unisi.it

Activities carried out during PhD course

1° year

Educational activities:

- Courses: “Valorizzazione dei risultati della ricerca e della proprietà intellettuale” and “Conoscenza dei sistemi di ricerca Europei”.
- Life Technologies training course on Ion Torrent sequencing. Siena

Seminary:

- “Qualità degli animali da esperimento: Tecniche di allevamento e qualità microbiologica”, organized by Organismo per il benessere degli animali. Siena
- “Gestione di colonie murine geneticamente modificate e moderne tecnologie riproduttive”, organized by Organismo per il benessere degli animali. Siena

Training event:

- Modulo 1, Legislazione Nazionale, organized by Organismo per il benessere degli animali. Siena

Work esperiences:

Training at Institute for Research in Biomedicine (IRB), Bellinzona Switzerland), concerning the production of human monoclonal antibodies from blood mononuclear cells.

2° year

Educational activities:

- Corso di formazione per lavoratori con verifica dell'apprendimento in materia di Salute e Sicurezza nei luoghi di lavoro. Area scientifica- Rischio Alto. Università degli Sudi di Siena.

Conferences:

- "La sperimentazione sugli animali nella ricerca scientifica. Finalità, limiti, alternative", Accademia dei Lincei, Roma.
- XVI International Conference on Negative Strand Viruses.Università di Siena

3° year

Seminar:

- "Functional and structural proprierties of proteins: Theory and Practice", EU- sponsored Erasmus course. UniversitàdegliStudi di Siena.
- "Design of proteins able to bind specifically to single-stranded or structured RNAs in order to investigate the non-coding RNA world,organized in the frame of Erasmus+ Annual Post-Graduate Course on Functional and Structural Properties of Proteins."UniversitàdegliStudi di Siena.
- "Farmaco Veterinario/ Anestesia Generale/ Anestesia con Isofluorano". Università degli Studi di Siena.

Pubblications:

- Wiegand M., Gori-Savellini G., Gandolfo C., Papa G., Kaufmann C., Felder E., Ginori A., Disanto M., Spina D., and Cusi M. G."Respiratory syncytial virus (RSV) vaccine vectored by a stable chimeric and replication-deficient Sendai virus protects mice without inducing enhanced disease". Sumitted to J. Virol. 2016.
- Martino E. C., Misso G., Pastina P., Costantini S., Vanni F., Gandolfo C., Botta C., Capone F., Lombardi A., Pirtoli L., Tassone P., Ulivieri C., Tagliaferri P., Cusi M. G., Caraglia M., and Correale P., "Immune-modulating effects of bevacizumab in metastatic non-small-cell lung cancer patients.," *Cell death Discov.*, vol. 2, p. 16025, Oct. 2016.
- Cusi M. G., Gandolfo C., Terrosi C., Gori Savellini G., Belmonte G., and Miracco C., "Toscana virus infects dendritic and endothelial cells opening the way for the central nervous system.," *J. Neurovirol.*, vol. 22, no. 3, pp. 307–315, Jun. 2016.
- Correale P., Botta C., Martino E. C., Ulivieri C., Battaglia G., Carfagno T., Rossetti M. G.,.Fioravanti A, Guidelli G. M., Cheleschi S., Gandolfo C., CarboneF.,.BaldariT. C, TassoneP., TagliaferriP., PirtoliL., and CusiM. G., "Phase Ib study of poly-epitope peptide vaccination to thymidylate synthase (TSPP) and GOLFIG chemo-immunotherapy for treatment of metastatic colorectal cancer patients.," *Oncoimmunology*, vol. 5, no. 4, p. e1101205, Dec. 2015.
- Gori Savellini G., Gandolfo C., and Cusi M. G., "Truncation of the C-terminal region of Toscana Virus NSs protein is critical for interferon-beta antagonism and protein stability.," *Virology*, vol. 486, pp. 255–262, Dec. 2015.
- Cusi M. G., Botta C., Pastina P., Rossetti M. G., Dreassi E., Guidelli G. M., Fioravanti A., Martino E. C., Gandolfo C., Pagliuchi M., Basile A., Carbone S. F., Ricci V., Micheli L., Tassone P., Tagliaferri P., Pirtoli L., and Correale P., "Phase I trial of thymidylate synthase poly-epitope peptide (TSPP) vaccine in advanced cancer patients.," *Cancer Immunol. Immunother.*, vol. 64, no. 9, pp. 1159–1173, Sep. 2015.
- Cusi M. G., Gandolfo C., Valentini M., and. Savellini G. G, "Seroprevalence of antibodies to sandfly fever Sicilian virus in a sample population in Tuscany, Italy.," *Vector Borne Zoonotic Dis.*, vol. 13, no. 5, pp. 345–346, May 2013.

Congress Presentation

Sierologia dell'infezione da EBV: confronti tra sistemi automatizzati. Maria grazia Cusi, Claudia Gandolfo, Stefania Cresti, Marcello Valassina. XLV Congresso Nazionale AMCLI. Rimini, 6-9 Novembre 2016.